Stem Cells International

Stem Cells in Cartilage Diseases and Repair 2018

Lead Guest Editor: Jianying Zhang
Guest Editors: Shiwu Dong, Wesley Sivak, Hui Bin Sun, and Peng Chang

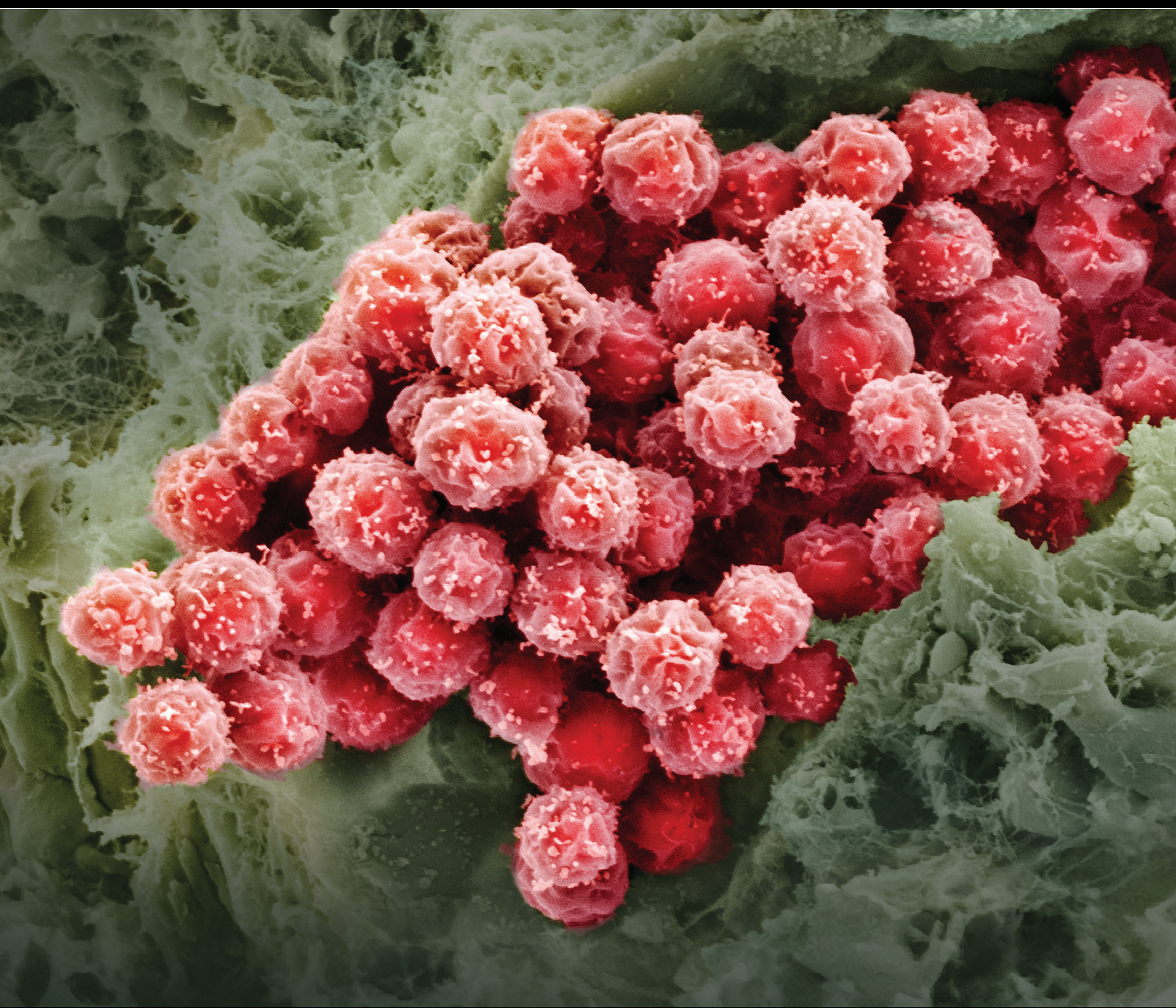

Stem Cells in Cartilage Diseases and Repair 2018

Stem Cells International

Stem Cells in Cartilage Diseases and Repair 2018

Lead Guest Editor: Jianying Zhang
Guest Editors: Shiwu Dong, Wesley Sivak, Hui Bin Sun, and Peng Chang

Editorial Board

Contents

Hindawi
Stem Cells International
Volume 2018, Article ID 3672890, 2 pages
https://doi.org/10.1155/2018/3672890

Editorial

Stem Cells in Cartilage Diseases and Repair 2018

Jianying Zhang,[1] **Shiwu Dong**,[2] **Wesley N. Sivak**,[1] **Hui Bin Sun**,[3] **and Peng Chang**[4]

[1]*University of Pittsburgh School of Medicine, Pittsburgh, PA, USA*
[2]*Third Military Medical University, Chongqing, China*
[3]*Albert Einstein College of Medicine, New York, NY, USA*
[4]*General Hospital of Shenyang Military Command, Shenyang, China*

Correspondence should be addressed to Jianying Zhang; jianying@pitt.edu and Wesley N. Sivak; sivakwn2@upmc.edu

Received 2 July 2018; Accepted 5 July 2018; Published 24 July 2018

Cartilage is a resilient and smooth elastic tissue that is not hard and rigid as bone but stiffer and less flexible than soft tissues such as muscle, ligament, and tendon. Cartilage is one of the critical tissues found in human and animal bodies including rib cage, ear, nose, bronchial tubes, intervertebral discs, meniscus, elbow, knee, ankle, and the joints between bones [1].

Cartilage plays an important role in the life of human and animals. Healthy cartilage at the joints helps the body move by allowing the bones to glide over each other and protects bones from rubbing against each other. Stress concentration at the joint site is a key issue that can cause cartilage problems such as inflammation, damage, tears, and injuries. Cartilage disorders affect millions of people worldwide. However, the damaged cartilage has little ability for repairing itself due to the lack of blood supply, nerves, and lymphangion [1].

The aim of this special issue is to understand the role of the stem cells in cartilage diseases and regeneration. It has been demonstrated that stem cells play a critical role in tissue regeneration.

For more efficient repair of cartilage, the regenerative medicine provides a variety of trials. Among these, using autologous stem cells to regenerate autologous cartilage is the gold standard in the cartilage tissue engineering. This special issue has focused on the effect of stem cells in cartilage injuries and regenerations. Generally, bone marrow (BM) was the most commonly used source of mesenchymal stem cells (MSCs) [2]. However, low tissue volume and low cell volume have limited the BMSC applications. Searching new stem cell source is a great challenge in tissue engineering and regenerative medicine. Adipose-derived mesenchymal stem cells (ADMSCs) have been used for damaged cartilage regeneration due to adipose tissue that can provide an abundant source of ADMSCs autologously and does not pose the ethical, tumorigenic, or immunogenic risk as presented by pluripotent stem cells. These factors have made adipose tissue a more desirable source of stem cells. S. L. Francis et al. have reviewed several ADSC isolation techniques in this special issue. They developed a rapid one-step isolation protocol that can isolate ADSCs from adipose tissue in 85 min. The authors suggest using this one-step isolation protocol in the context of a surgical procedure.

A novel stem cell population has been isolated from human urine [3]. Human urine-derived stem cells (hUSCs) have several advantages. Firstly, hUSCs show robust proliferation ability and have the capacity for multipotent differentiation [4]. Secondly, hUSCs can be accessed via a simple, noninvasive, and low-cost approach, and thus, surgical procedures are avoided [5]. Importantly, hUSCs isolated from autologous urine have no immune responses or rejection. In this special issue, we would like to introduce an interesting researcher article authored by L. Chen et al. They have demonstrated that human urine-derived stem cells (hUSCs) can be differentiated into chondrocytes *in vitro* and enhanced wounded rabbit knee joint healing *in vivo*.

In this special issue, the potential of synovium-derived stem cells (SMSCs) to regenerate cartilage has been investigated by H. Schmal et al. They tested the effect of SMSCs on chondrogenic differentiation *in vitro* and implanted a SMSC-containing collagen matrix into osteochondral defect

of rabbit condyle *in vivo*. SMSC is available in a high quantity, and the isolation procedure does not lead to significant donor site morbidity. The cellular characteristics of SMSC suggest their suitability for cartilage regeneration protocols based on their chondrogenic phenotype including its maintenance after several cell culture passages and their excellent ability to form extracellular matrix [6].

In the current issue, a 3D culture model has been developed for nucleus pulposus (NP) regeneration by Y. Gan et al. They studied the biological effect of a relatively wide magnitude of the dynamic compression (5–20%) on encapsulated MSCs. The underlying mechanotransduction mechanism of transient receptor potential vanilloid 4 (TRPV4) was also investigated.

This special issue also introduces more interesting articles about the effect of environment or stem cell niche on inducing chondrogenic differentiation of stem cells *in vitro* and enhancing cartilage formation *in vivo*. The effect of link protein N-terminal peptide (LPP) as a potential stimulating factor on cartilage stem cells has been studied by R. He et al. The influence of hypoxia-mimetic agent cobalt chloride on chondrogenesis of human MSCs has been investigated by G. Teti et al. in this special issue.

A review article authored by N. K. Dubey et al. provides an excellent summary of the current status of stem cell therapies in osteoarthritis (OA) pathophysiology. The relationships among stem cell types, protein productions, growth factors, cartilage diseases, and cartilage regeneration were outlined and discussed in this review article. In addition, the role of infrapatellar fat pad- (IFP-) derived stem cells in cartilage formation was also described. Furthermore, the effect of exosomes in mediating cellular communication between stem cells and chondrocytes was also summarized in this review article. Finally, the authors indicated the current research limitations of stem cell therapies for cartilage repair including the lack of universal donor cells and the inefficient of reprogrammable approaches to induce stem cell differentiation into cartilage tissue. These limitations will be overcome by genetic modification and gene-editing techniques.

We hope the articles published in this special issue can help researchers comprehend the regulatory mechanism of chondrogenesis and find more useful approaches for enhancing cartilage regeneration and repair.

Jianying Zhang
Shiwu Dong
Wesley N. Sivak
Hui Bin Sun
Peng Chang

References

[1] A. J. Sophia Fox, A. Bedi, and S. A. Rodeo, "The basic science of articular cartilage: structure, composition, and function," *Sports Health*, vol. 1, no. 6, pp. 461–468, 2009.

[2] G. Sheng, "The developmental basis of mesenchymal stem/stromal cells (MSCs)," *BMC Developmental Biology*, vol. 15, no. 1, p. 44, 2015.

[3] Y. Zhang, E. McNeill, H. Tian et al., "Urine derived cells are a potential source for urological tissue reconstruction," *The Journal of Urology*, vol. 180, no. 5, pp. 2226–2233, 2008.

[4] J. J. Guan, X. Niu, F. X. Gong et al., "Biological characteristics of human-urine-derived stem cells: potential for cell-based therapy in neurology," *Tissue Engineering. Part A*, vol. 20, no. 13-14, pp. 1794–17806, 2014.

[5] S. Bharadwaj, G. Liu, Y. Shi et al., "Multipotential differentiation of human urine-derived stem cells: potential for therapeutic applications in urology," *Stem Cells*, vol. 31, no. 9, pp. 1840–1856, 2013.

[6] E. J. Kubosch, E. Heidt, P. Niemeyer, A. Bernstein, N. P. Sudkamp, and H. Schmal, "In-vitro chondrogenic potential of synovial stem cells and chondrocytes allocated for autologous chondrocyte implantation—a comparison: synovial stem cells as an alternative cell source for autologous chondrocyte implantation," *International Orthopaedics*, vol. 41, no. 5, pp. 991–998, 2017.

Hindawi
Stem Cells International
Volume 2018, Article ID 2791632, 10 pages
https://doi.org/10.1155/2018/2791632

Research Article

Intra-Articular Injection of Alginate-Microencapsulated Adipose Tissue-Derived Mesenchymal Stem Cells for the Treatment of Osteoarthritis in Rabbits

Seongjae Choi,[1] **Jun-Hyung Kim**,[1] **Jeongho Ha**,[1] **Bo-Ing Jeong**,[2] **Yun Chan Jung**,[2] **Geun-Shik Lee**,[1] **Heung-Myong Woo**,[1] **and Byung-Jae Kang**[1]

[1]*College of Veterinary Medicine and Institute of Veterinary Science, Kangwon National University, Chuncheon 24341, Republic of Korea*
[2]*KPC, Gwangju 12773, Republic of Korea*

Correspondence should be addressed to Byung-Jae Kang; bjkang@kangwon.ac.kr

Received 14 December 2017; Revised 17 April 2018; Accepted 20 May 2018; Published 26 June 2018

Academic Editor: Peng Chang

We investigated the effects of intra-articular injections of alginate-microencapsulated adipose tissue-derived mesenchymal stem cells (ASCs) during osteoarthritis (OA) development in a rabbit model of anterior cruciate ligament transection (ACLT). We induced OA in mature New Zealand white rabbits by bilateral ACLT. Stifle joints were categorised into four groups according to intra-articular injection materials. Alginate microbeads and microencapsulated ASCs were prepared using the vibrational nozzle technology. Two weeks after ACLT, the rabbits received three consecutive weekly intra-articular injections of 0.9% NaCl, alginate microbeads, ASCs, or microencapsulated ASCs, into each joint. Nine weeks after ACLT, we euthanised the rabbits and collected bilateral femoral condyles for macroscopic, histological, and immunohistochemical analyses. Macroscopic evaluation using the modified OA Research Society International (OARSI) score and total cartilage damage score showed that cartilage degradation on the femoral condyle was relatively low in the microencapsulated-ASC group. Histological analysis of the lateral femoral condyles indicated that microencapsulated ASCs had significant chondroprotective effects. Immunohistochemically, the expression of MMP-13 after the articular cartilage damage was relatively low in the microencapsulated-ASC-treated stifle joints. During the development of experimental OA, as compared to ASCs alone, intra-articular injection of microencapsulated ASCs significantly decreased the progression and extent of OA.

1. Introduction

Degenerative joint disease or osteoarthritis (OA) of the knee is the most common form of arthritis and reduces quality of life by causing pain, stiffness, and physical disability [1]. OA is characterised by progressive deterioration of cartilage and destruction of the extracellular matrix owing to an impaired anabolic and/or catabolic balance [2, 3]. Articular cartilage has lower capacity for self-repair [4]. It is challenging to enhance regeneration of hyaline cartilage tissue [5]. Many clinical treatments have been used for OA management [6]. These treatments include nonsteroidal anti-inflammatory drugs, platelet-rich plasma, analgesics, hyaluronic acid, mevastatin, and mesenchymal stem cells (MSCs) [7–11]. Although many treatments with MSCs have been developed, adipose tissue-derived mesenchymal stem cells (ASCs) have several advantages. In humans, intra-articular injection of ASCs improves the functioning and reduces pain and cartilage defects of the knee joint [11]. In addition, ASCs can be more easily cultured and obtained in vastly greater quantities—by less aggressive methods—than MSCs can [12–14].

Systemic or local stem cell-based therapies represent a growing field of treatment of OA, resulting in repair of articular cartilage [15]. Nonetheless, studies have increasingly revealed poor viability and a low survival rate of the transplanted stem cells at the disease-affected site [16, 17]. Recent research has therefore focused on enhancing cell viability at a local site affected by the disease and on treatments involving

the paracrine effect of MSCs [18–21]. Most therapeutic effects of MSCs are thought to act in a paracrine manner by promoting angiogenesis, tissue regeneration, and production of soluble anti-inflammatory factors [16, 22, 23]. Alginate-microencapsulated cells provide a mechanical barrier that acts as an artificial extracellular matrix, increasing cell viability and allowing for a release of stem cell-produced growth factors and anti-inflammatory factors into surrounding injured tissue [24].

We investigated the effects of periodic intra-articular injection of alginate-microencapsulated ASCs on OA in a rabbit model of anterior cruciate ligament transection (ACLT). We hypothesised that the microencapsulated ASCs would reduce OA progression more effectively than ASCs alone would.

2. Materials and Methods

2.1. Animals. Fifteen adult New Zealand white rabbits (weighing 3.0–3.5 kg, 25–30 weeks old, male) with closed epiphyses were used in this study. Eleven rabbits were allocated to the OA model and four rabbits to allogeneic-ASC harvesting. The animal care and research protocol was reviewed and approved by the Institutional Animal Care and Use Committee of Kangwon National University (KW-170315-1).

2.2. The Rabbit Model of ACLT. Eleven rabbits were anesthetised via intramuscular injection of tiletamine-zolazepam (20 mg/kg; Zoletil 50, Virbac, Seoul, Korea) and xylazine hydrochloride (5 mg/kg; Rompun, Bayer Korea, Seoul, Korea). Intravenous ketoprofen (3 mg/kg; SCD Pharm, Seoul, Korea) was given for preemptive analgesia. Intravenous cefazolin (22 mg/kg; Chong Kun Dang Pharmaceutical, Seoul, Korea) was administered (to prevent infection) at the time of the surgical procedure and once every 24 h for 3 d postoperatively. When the rabbits were under anesthesia, electric clippers were employed to shear the hair overlying each stifle joint, and a sterile surgical operation was carried out to obtain subcutaneous adipose tissue. After the patellar tendon was dislocated laterally, the anterior cruciate ligament of bilateral hind limbs was transected completely with a No. 11 scalpel blade. After suturing, 10 cranial draw motions provoked joint stimulation, and ACLT was completely confirmed. The rabbits were closely monitored for infection and other complications and were allowed to rest in a cage without immobilisation.

2.3. ASC Isolation and Culture. Rabbit ASCs were isolated by the collagenase perfusion technique according to previously described methods [22, 25, 26]. Approximately 5 g of fat collected from the posterior cervical subcutaneous adipose tissue of four rabbits was mixed and washed with phosphate-buffered saline (PBS). The adipose tissue was cut into strips during 10 min incubation in collagenase I (Thermo Fisher Scientific, Waltham, MA, USA) in a 6-well plate. Collagenase was dissolved in PBS so that its concentration would be 0.1% in 25 mL and was used to digest adipose tissue at 37°C for 90 min in a water bath. The mixture was shaken every 10 min during the digestion period. Immediately after the reaction was finished, 25 mL of high-glucose Dulbecco's modified Eagle's medium (DMEM, Invitrogen, Carlsbad, CA, USA) was added to neutralise the collagenase activity. The resulting solution was filtered through a 100 μm cell strainer. The filtrate was centrifuged at 1500 ×g for 6 min at 25°C, and the supernatant was removed. Next, a pellet of ASCs was seeded in cell culture dishes and cultured under standard conditions in high-glucose DMEM supplemented with 10% of foetal bovine serum (FBS, Invitrogen, Carlsbad, CA, USA) and 1% of an antibiotic-antimycotic solution (Thermo Fisher Scientific, Waltham, MA, USA). The medium was replaced at 48 h intervals until the cells became confluent. After the cells reached 90% confluence, they were harvested with 0.25% trypsin ethylenediaminetetraacetic acid (EDTA; Welgene, Gyeongsan-si, Korea) and stored in liquid nitrogen or subcultured. When cell density was ~2.5×10^4 cells/cm^2, passaging of ASCs was performed. The cryopreserved ASCs were used up to passage 5.

2.4. Preparation of Alginate Microbeads. A 1.2% sodium alginate solution served as the polymer. A sterile filtered isotonic 1.8% sodium alginate solution (Büchi Labortechnik AG, Flawil, Switzerland) was diluted to 1.2% concentration with sterile normal saline. The 1.2% sodium alginate solution was prepared in syringes. Alginate microbeads were produced by the vibrational nozzle technology by means of a Büchi Encapsulator B-395 Pro (Büchi Labortechnik AG, Flawil, Switzerland) at the parameters previously reported for preparation of alginate microbeads suitable for passing through a 23-gauge needle: nozzle size, 120 μm; frequency, 1000 Hz; flow rate, 23 mL/min; and electrode potential, 1000 V [21]. The gelling solution was prepared in 100 mM calcium chloride. Alginate droplets were gelled in 100 mM calcium chloride for 30 min. The finished alginate microbeads were filtered through a 40 μm cell strainer and washed in PBS. The morphology and size of the alginate microbeads were analysed under a light microscope.

2.5. Preparation of Alginate-Microencapsulated ASCs. An alginate solution containing ASCs was prepared by mixing the 1.2% sodium alginate solution with ASCs at a concentration of 10^7 cells/mL. This suspension was subjected to microencapsulation and was then filtered under optimised processing parameters. Next, the microencapsulated ASCs were washed in 1x PBS, and the size and shape of the microcapsules containing ASCs were analysed by bright-field microscopy.

2.6. The Study Scheme. Rabbits were injected every week for 3 weeks with a material according to an experimental group, starting at 2 weeks after the ACLT. At 9 weeks after ACLT, all the rabbits were euthanised, and stifle joint samples were collected and evaluated (Figure 1(a)).

2.7. Intra-Articular Injections of Materials. Before intra-articular injection of any material, each rabbit was anesthetised with an intramuscular injection of 10 mg/kg tiletamine-zolazepam (Zoletil 50, Virbac, Seoul, Korea) and 5 mg/kg xylazine hydrochloride (Rompun, Bayer Korea, Seoul, Korea). A 1 mL plastic syringe was loaded with one of the materials in 0.5 mL of 0.9% NaCl, with or without the cell

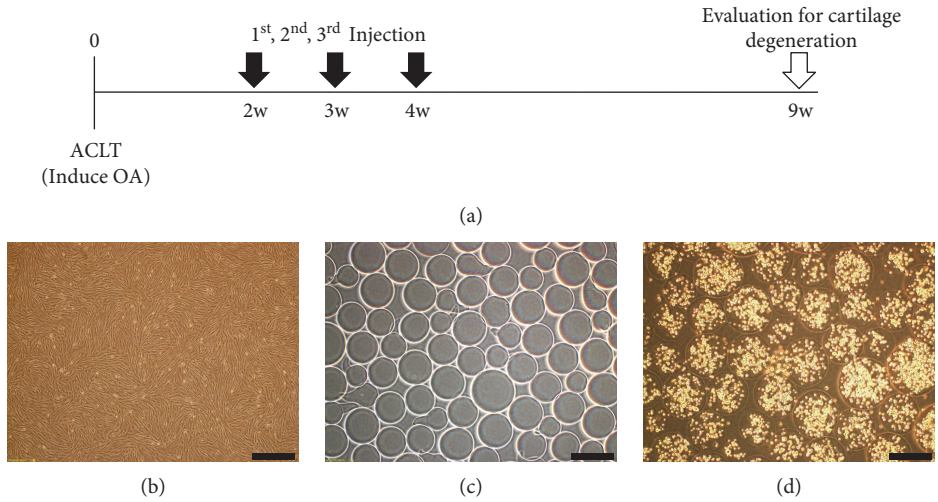

Figure 1: The scheme of the study on intra-articular injection with a material according to experimental groups and microscopic appearance. (a) The study scheme for intra-articular injection of a material according to an experimental group. (b) A light-microscopy image of ASCs having spindle-shaped morphology. (c) A light-microscopy image of alginate microbeads in the absence of cells. (d) Light-microscopic appearance of microencapsulated ASCs at the time of implantation, with 300–400 cells within each 400–500 μm capsule. Scale bar = 500 μm.

suspension; to this syringe, a 21-gauge hypodermic needle was then attached.

For matched-pair analysis, 11 rabbits (22 knees) were used. At 2, 3, and 4 weeks after ACLT, in five rabbits, ASCs were injected into the left stifle joint, and microencapsulated ASCs were injected into the right stifle joint, via the medial approach. In six rabbits, 0.9% NaCl was injected into the left stifle joint, and alginate microbeads were injected into the right stifle joint, via the medial approach. Each rabbit was held down for 5 min to allow for attachment of the injected materials to the synovium.

2.8. Macroscopic Analysis. Eleven rabbits were euthanised at 9 weeks after ACLT, by intravenous injection of a potassium chloride overdose. Both femoral condyles were carefully collected to avoid damage to any cartilage surfaces. The articular surfaces of the joints were stained with India ink (American MasterTech, Lodi, CA, USA) for macroscopic examination and were studied regarding fibrillation and erosion [27]. The cartilage surface was painted with India ink twice, and we rinsed the cartilage with PBS each time; the ink was applied 3 min after the rinsing. Macroscopic pictures were taken using a Sony digital camera (Sony, Tokyo, Japan).

The macroscopic OA score was calculated by summing the medial and lateral condyle scores and by means of the modified version of the Osteoarthritis Research Society International (OARSI) scoring system (Supplementary Table 1) [28].

To determine the total cartilage damage score (TCDS), femoral condyles were graded based on ink retention; quantification of a defect region in femoral condyles was conducted in ImageJ (NIH, Bethesda, MD, USA): image analysis software. The TCDS was calculated by adding cartilage damage scores (CDSs) of the medial and lateral femoral condyles. These CDSs were calculated by multiplying the percentage of the damaged articular cartilage area of each condyle by an ink retention-based grade (grade 1, intact surface: surface normal in appearance and not retaining India ink; grade 2, fibrillation: surface retains India ink as elongated specks or light grey or black patches; and grade 3, erosion: loss of exposed cartilage). CDSs ranged from 0 to 300 (0 = no cartilage damage; 300 = complete exposure of subchondral bone). TCDSs were computed via the following equations [29]:

$$\begin{aligned} \text{CDS} &= [\%_{\text{area}} \times \text{ink retention grade}_{\text{area}}], \\ \text{TCDS} &= \text{CDS}_{\text{medial femoral condyle}} + \text{CDS}_{\text{lateral femoral condoyle}}. \end{aligned} \quad (1)$$

The macroscopic OA score and TCDS were determined by two veterinarians, one of whom was blinded to the injection material.

2.9. Histological Analysis. For the histological examination, both distal femoral cartilages were fixed in a 10% neutral buffered formalin solution (Thermo Fisher Scientific, Waltham, MA, USA) after macroscopic analysis. The specimens were decalcified in a 4% EDTA solution and embedded in paraffin. Paraffin-embedded sections were cut to a thickness of 4 μm in the parasagittal plane. The sections were made through the most severely degenerated area. All the samples were mounted onto slides and stained with haematoxylin and eosin for general pathological observations. In addition, all the samples were stained with Safranin-O and counterstained with fast green so that OARSI scores could be determined. One histopathological section per condyle was independently evaluated under a light microscope (Olympus Optical Co., Tokyo, Japan) by two veterinarians who were blinded to the group distribution. Articular cartilage changes were evaluated according to the OARSI guidelines for evaluation of rabbit tissues [28, 30]. The OA score was an index of the combined grade and stage as seen in a microscopic

section (score = grade × stage). The grade represented one of six levels: surface intact, discontinuity, vertical fissures, erosion, denudation, or deformation. The stage was assigned on the basis of the horizontal extent of the involved cartilage surface defect of the underlying OA grade. Stage 1 represents less than 10% involvement, stage 2 means 10–25% involvement, stage 3 denotes 25–50% involvement, and stage 4 represents more than 50% involvement.

2.10. Immunohistochemical (IHC) Analysis. From each block, serial sections were cut to 4 μm thickness and mounted onto gelatin-coated slides for improved attachment. The slides were deparaffinised in xylene and next washed in ethanol (100%, followed by 95%) and PBS. Articular cartilage IHC analysis was performed manually by means of a mouse anti-human MMP-13 monoclonal antibody (1 : 20; Thermo Fisher Scientific, Waltham, MA, USA). For antigen retrieval, the sections were incubated and then processed in an autoclave for 5 min at 95°C using 0.1% sodium citrate buffer (pH 6.0). After that, the slides were rinsed three times with PBS and were incubated with the peroxidase-conjugated polymer of the DAKO Real Envision/HRP rabbit/mouse/kit (REAL EnVision Detection System K5007, DAKO, Copenhagen, Denmark) for 30 min, again rinsed three times with PBS, and incubated with DABb from the kit for 5 min, according to the manufacturer's instructions. Finally, nuclei were counterstained with haematoxylin for 30 s, blued under tap water, washed in ethanol, and cover-slipped. A semiquantitative analysis was performed on the cartilage of lateral femoral condyles. Immunoreactive cells and normal cells were counted in the articular surface regions as cells per square millimetre. IHC values, as a percentage of cells positive for MMP-13, were determined for a complete assessment of protein expression, with a maximum score of 100%. The assay was conducted by two blinded investigators [31].

2.11. Statistical Analysis. This analysis was performed in Prism 5.00 (GraphPad Software Inc., San Diego, CA, USA). The results are presented as mean ± standard deviation (SD). Statistical significance was assessed by the Kruskal-Wallis test followed by the Mann–Whitney post hoc test (to compare the groups). Data with $P < 0.05$ were considered significant for all tests.

3. Results

3.1. Morphological Confirmation of ASCs, Alginate Microbeads, and Alginate-Microencapsulated ASCs. Using a light microscope, we confirmed that ASCs were spindle-shaped (Figure 1(b)). Alginate microbeads and microcapsules containing ASCs were also confirmed by light microscopy to have a mostly normal spherical shape. We determined differences in bead diameter between alginate microbeads and microcapsules containing ASCs. The alginate microbeads were 250–300 μm in diameter, and the microcapsules containing ASCs were 400–500 μm in diameter. Each microcapsule containing ASCs included 300–400 cells, and the number of contained cells varied according to the bead diameter (Figures 1(c) and 1(d)).

3.2. Macroscopic Analysis. After gross visual inspection, all stifle joints showed complete transection of the anterior cruciate ligament and severe erosion or fissure in both medial and lateral femoral condyles. There were more extensive lesions in medial condyles than in lateral condyles. The grade of the bilateral condyles was "erosion" in the control and alginate microbead groups. Meanwhile, the grade of medial condyles was erosion, and the grade of lateral condyles was "fissure" in the ASC group and in the microencapsulated-ASC group. In addition, the areas of damaged cartilage in the microencapsulated-ASC group appeared to be significantly smaller than those in the other groups. Figure 2(a) presents examples of a condyle typical of each group, stained with India ink. Significant decreases in the macroscopic OA score were observed in the microencapsulated-ASC group (13.5 ± 0.94) and the ASC group (16.9 ± 2.86) compared with the control group (21.58 ± 2.11). Besides, the macroscopic OA score in the microencapsulated-ASC group was significantly lower than that in the ASC group. Nonetheless, there were no significant differences between the control and alginate microbead groups (20.33 ± 4.48) (Figure 2(b)). Significant decreases in the TCDS were observed in the microencapsulated-ASC group (26.6 ± 5.59) relative to the control group (50.17 ± 15.89), alginate microbead group (71.33 ± 23.99), and ASC group (41 ± 3.08) (Figure 2(c)). The lower macroscopic OA score and TCDS in the microencapsulated-ASC group indicated significantly less damage to the cartilage surface.

3.3. Histological Analysis. This evaluation of stifle joints showed more specific differences in lateral condyles (Figure 3(a)). Medial condyle cartilage surfaces showed mostly denudation or deformation, and there were no significant differences among the groups. In lateral condyles, there was no significant difference in the OARSI OA score between the control group (15.88 ± 4.50) and the other groups except for the microencapsulated-ASC group (4.35 ± 3.04) (Figure 3(b)). In the control group and alginate microbead group (12.96 ± 9.14), the lateral articular surface showed denudation or deformation. Although not reaching statistical significance, more favourable scores for the articular surface were observed in the microencapsulated-ASC group than in the ASC group (7.3 ± 5.34).

3.4. IHC Analysis. The expression of MMP-13 was semiquantitatively analysed by IHC staining, using samples prepared at 9 weeks after ACLT. IHC analysis of stifle joints revealed more specific differences in the lateral condyle (Figure 4(a)).

The proportion of MMP-13-positive cells was significantly lower in the microencapsulated-ASC group (17.2 ± 2.77) than in the other groups, including the ASC group (22.6 ± 2.30). There was no significant difference between the control group (31 ± 5.14) and the alginate microbead group (38.17 ± 8.73) (Figure 4(b)).

4. Discussion

Many strategies for preventing cartilage degeneration and OA have been developed and clinically tested. The

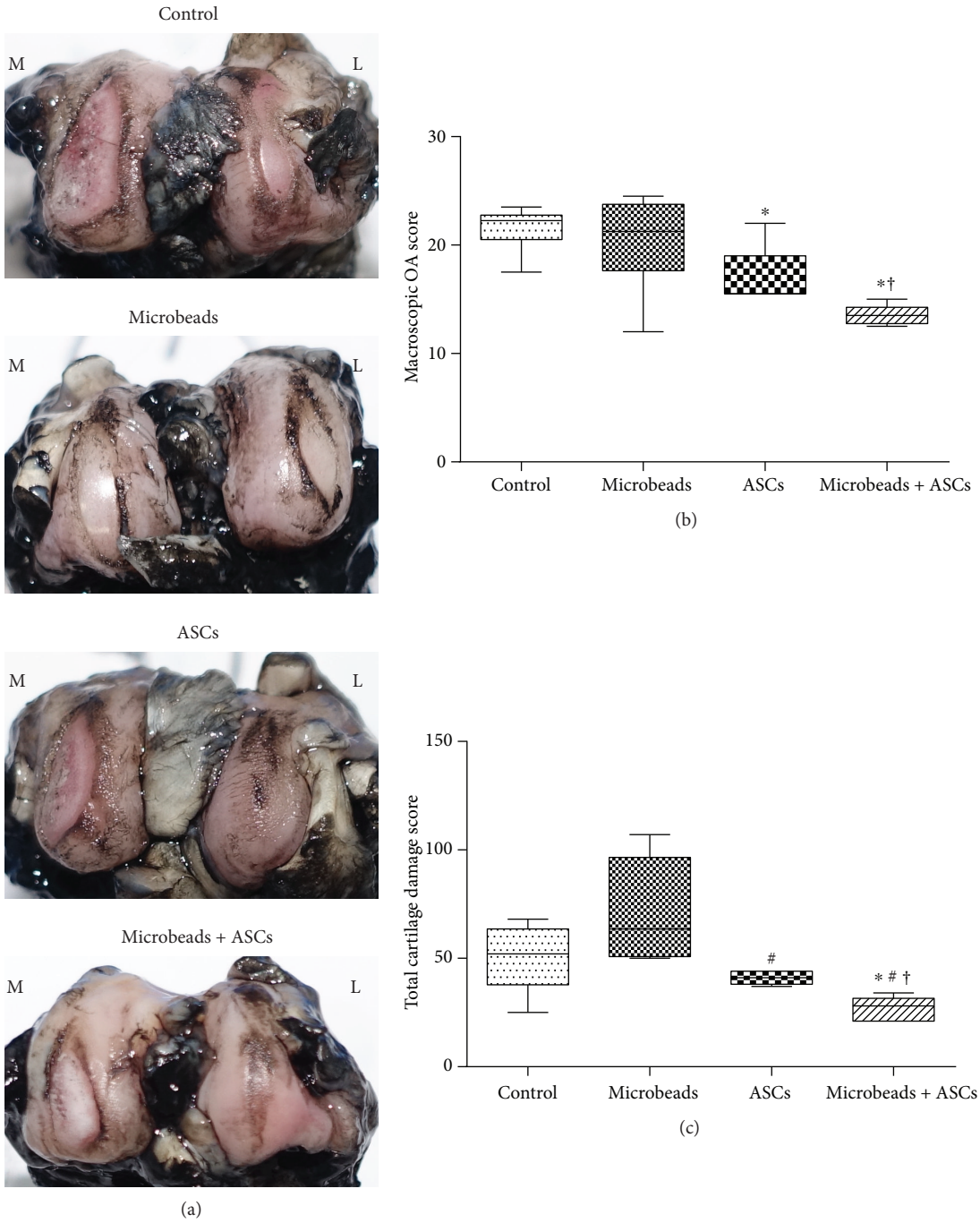

Figure 2: Macroscopic analysis of femoral condyles at 9 weeks after ACLT. (a) A representative specimen of a condyle (from each group) stained with India ink to identify any fibrillation and erosion. (b) The macroscopic OA score. (c) The TCDS. *A significant difference from the control group ($P < 0.05$). #A significant difference from the alginate microbead group ($P < 0.05$). †A significant difference from the ASC group ($P < 0.05$).

nonimmunogenic effectiveness and potent immunosuppressive activity of MSCs have been reported, and allogeneic MSCs can be used safely in OA without immunosuppressive medication [32, 33]. To enhance their effect, to improve MSC viability, and to prolong the survival of MSCs in a harsh microenvironment, MSCs can be combined with traditional treatments, such as injection of hyaluronic acid [34, 35]. Recently, stem cells were reported to disappear by day 7 after intra-articular injection; periodic injection was found to be more effective. Nevertheless, this method requires many cells and repeated injections [36–38]. If the cell viability were increased, it would be possible to further increase the therapeutic effect, while reducing the frequency and size of MSC injections, and this approach may be more cost-effective. When scaffolds and stem cells are applied to bone defects, the therapeutic effect can be increased by augmenting the

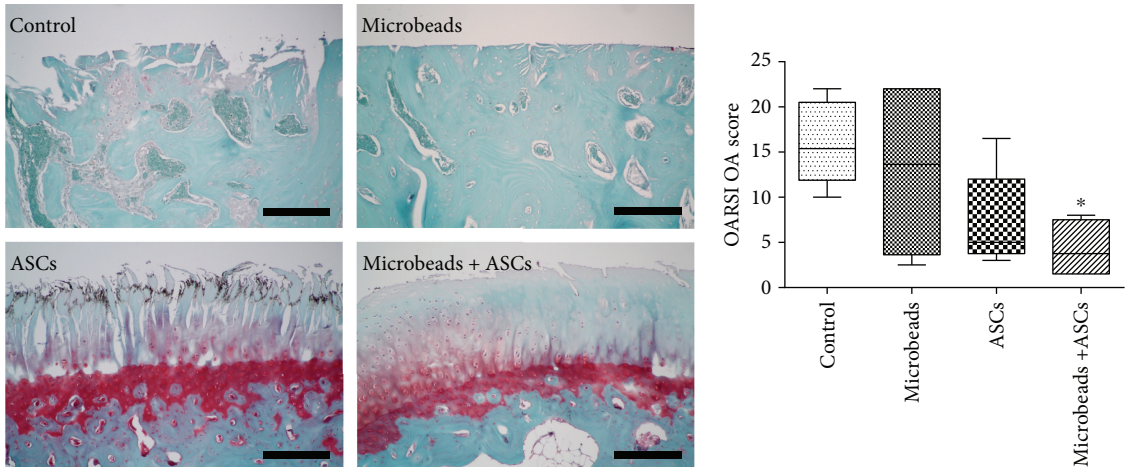

Figure 3: Histological analysis of femoral lateral condyles. (a) A representative specimen of a lateral condyle from each group stained with Safranin-O and counterstained with fast green. (b) The OARSI score of OA. *A significant difference from the control group ($P < 0.05$). Scale bar = 200 μm.

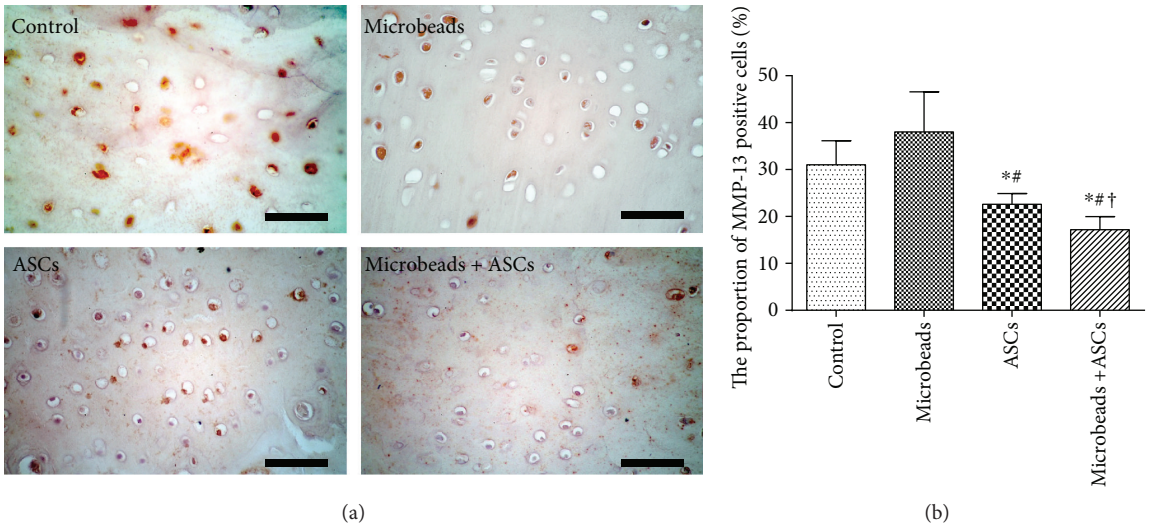

Figure 4: IHC analysis for MMP-13 in cartilage. (a) A representative specimen from each group evaluated for MMP-13 in a femoral lateral condyle. (b) The proportion of MMP-13-positive cells. *A significant difference from the control group ($P < 0.05$). #A significant difference from the alginate microbead group ($P < 0.05$). †A significant difference from the ASC group ($P < 0.05$). Scale bar = 100 μm.

differentiation potential of MSCs [39]. On the other hand, such scaffolds have not been employed within joints and have been applied invasively. Recently, it was reported that microencapsulation of cells in alginate is a noninvasive and novel method of increasing the viability of cells for joint injection [21]. To increase cell viability, it is most important to protect the injected cells from the host's immune response. One method of protection is to encapsulate cells within a semipermeable system [40] such as alginate. Alginate is a natural biopolymer extracted from brown algae and is known to be biocompatible, relatively nontoxic, and inexpensive [24, 41, 42].

ASCs were recently reported to exert paracrine action, which indirectly stimulates the secretion of bioactive factors such as cytokines and growth factors [31, 43]. The three-dimensional gel-sphere scaffold of alginate microbeads is a porous structure that allows for diffusion of oxygen and nutrients and for the transport of metabolites [24]. These structural features of alginate microbeads may facilitate the paracrine activity of ASCs used in stem cell therapy.

In this study, we performed three periodic injections, since 2 weeks after ACLT, for the treatment of OA. It has been demonstrated that degenerative changes can be observed in early OA at 4 weeks after ACLT [44]. In acute OA, we thought that the stem cells injected at 2, 3, and 4 weeks after the ACLT would not have a direct therapeutic effect (e.g., cartilage regeneration) because the joint damage would not have advanced sufficiently. Nevertheless, if

progressive damage of articular cartilage occurred since the 4 weeks after ACLT, the ASCs would be effective in suppressing OA progression via paracrine action rather than via articular cartilage regeneration. In other studies, cells injected into joints have been found to survive for ~7 d [36–38]. Although the present study did not experimentally determine how long microencapsulated ASCs survive in joints, it has been reported elsewhere that subcutaneously injected microencapsulated cells show more viability *in vivo* than do cells directly injected without microencapsulation [18, 21]. On the basis of previous studies, we expected that alginate microencapsulation might prolong the survival of stem cells in joints and improve OA treatment efficacy by prolonging the paracrine activity.

Macroscopic analysis was performed at 9 weeks after ACLT because all signs of OA were present during the 8–12 weeks after ACLT [44]. When the tibial plateau was observed, OA lesions in this area were mild or moderate. This is a phenomenon that takes place in the ACLT model in rabbits, in agreement with a study by Mero et al. [45]. Given that the lesion is mild or moderate, the tibial plateau appears to be an unreasonable indicator for assessing cartilage degeneration. In addition, there were no differences among the groups in the gross evaluation. Furthermore, acute lesions with ACLT have the greatest effect on the femoral condyle, and some studies also indicate that the femoral condyle is a good indicator of cartilage degeneration [44]. For this reason, we focused on lesions on the femoral condyle.

Stifle joints are often used in OA models. Load distribution and gait mechanics of stifle joints vary depending on animal species. Unlike other animals, rabbits tend to be loaded on the lateral aspect of the stifle joint [46]. Mild early arthritic changes begin to appear from the 4th week after ACLT, and severe cartilage degeneration first occurs in the lateral femoral condyle, followed by the medial femoral condyle and meniscus [45]. Therefore, the lateral compartment in the stifle joint of a rabbit is the site for confirming early cartilage changes [47]. In the lateral femoral condyle, where early cartilage degeneration took place, cartilage damage was significantly lower in the microencapsulated-ASC group than in the other groups. Nonetheless, we grossly evaluated the meniscus, and the damage had already occurred. In addition, when the meniscus was assessed by the grading method of Adams et al. [48], there was no significant difference among the experimental groups. This finding suggests that early administration of microencapsulated ASCs may have prevented or delayed cartilage damage on the lateral femoral condyle, and this damage represents early joint lesions. In contrast, microencapsulated ASCs did not prevent or slow down the damage to the medial femoral condyle and meniscus damage that later developed during OA progression. It is expected that microencapsulated ASCs will survive longer than ASCs alone will, but early repeated administration will not prevent cartilage damage for long periods after administration. Therefore, additional administration after 4 weeks or shortening the harvest time may prevent the damage to the meniscus and to the medial femoral condyle.

India ink staining was performed, and there was an advantage that could be confirmed more visually. There was no significant difference between the control group and the alginate microbead group, implying that alginate microbeads did not afford additional antiarthritis effects. We interpret the differing results between the microencapsulated-ASC group and the ASC group as indicative of a delay in arthritis progression. Various studies suggest that alginate microencapsulation can increase the viability of stem cells and prolong their secretion of therapeutic cytokines [49]. Accordingly, macroscopic evaluation showed that cartilage degeneration significantly decreased in the microencapsulated-ASC group. By contrast, histological evaluation revealed no significant difference in the medial-condyle defects among all the groups, because of the extent of damage. In addition, the microencapsulated-ASC group showed a significant difference in lateral joints only in comparison with the control group. The alginate microbead group manifested large variation in results. Nonetheless, because alginate microbeads are biocompatible, these results do not appear to be due to the characteristics of alginate microbeads. The variation in the results can be assumed to be caused by insufficient sample size and limitations of the model of experimentally induced OA. If the harvest time had been slightly earlier, we may have observed great differences in the OA progression. Further studies on injection timing and frequency in acute and chronic OA should indicate how microencapsulated ASCs can be applied more efficaciously.

The degree of damage to hyaline cartilage can be assessed by IHC staining regarding upregulation of MMP-13, a proven matrix-degrading enzyme in articular cartilage [50]. As previously reported, the hyaline cartilage matrix is composed of type II collagen and the proteoglycan macromolecule aggrecan. When type II collagen is damaged by OA, matrix-degrading enzymes including MMP-1, MMP-8, and MMP-13 are upregulated [51, 52].

In this study, to confirm the effect of microencapsulated ASCs, we identified only MMP-13 expression via IHC analysis. The MMP-13-positive cell ratio was significantly lower in the microencapsulated-ASC group when compared to all the other groups. These results suggest that microencapsulation may increase the paracrine action exerted by ASCs. Assays of additional enzymes and factors, such as collagenase-generated cleavage neoepitope of type II collagen, which has been identified as a sensitive OA biomarker [53, 54], may confirm the influence of microencapsulation on ASCs.

In humans, the effect of arthritis treatment has been found to depend on the dose of stem cells injected. A high-dose group shows clinical, radiological, and arthroscopic results that are more favourable than those from groups receiving a low or medium dose [11]. These data indicate that a sufficient number of MSCs should be delivered to the disease-affected site for the best results. The importance of the cell dose has been raised by several authors [55–57]. Some have reported that injection of 10^7 MSCs leads to complete healing of scars in rats [55], whereas others have demonstrated that insufficient numbers of applied MSCs yield inferior results [58]. It is expected that alginate microencapsulation will increase the viability of stem cells in joints. Over the course of repeated injections, the number of surviving cells in the microencapsulated-ASC group should be higher than that

in the ASC group. This viability may presumably mean that microencapsulated ASCs are more effective than ASCs in the treatment of arthritis.

The limitations of this study are as follows: it is necessary to study the long-term cartilage protection effect because it reflects the short-term cartilage protection activity in the early stages of OA. There is also a need to study potential complications over long periods. In addition, viability of alginate-microencapsulated cells has already been investigated, and in vivo studies have shown that injected alginate-microencapsulated cells are superior to free cells in terms of survival and retention [21]. Nevertheless, because the present study did not investigate the degradation kinetics of alginate microbeads within joints, it is necessary to study microcapsule degradation duration in joints to evaluate the effect in a joint before clinical application. Finally, many types of codelivery strategies are currently being developed and discussed [59, 60]. Therefore, it is necessary to demonstrate that when compared with other codelivery strategies, alginate microbeads ensure higher viability and retention of cells.

5. Conclusions

Microencapsulated ASCs slowed the progression of OA and decreased its extent, more so than did free ASCs. Alginate-based microencapsulation may increase ASC viability within the knee joint. To our knowledge, this study is the first to employ alginate-based scaffolding for improving the efficacy of ASC-based treatment of arthritis.

Conflicts of Interest

The authors state that there are no competing interests.

Acknowledgments

This work was supported by the Basic Science Research Program through the National Research Foundation of Korea (NRF), funded by the Ministry of Science, ICT and Future Planning (Grant no. NRF-2015R1C1A1A01051759).

Supplementary Materials

The Modified Osteoarthritis Research Society International (OARSI) scoring system for assessment of macroscopic changes in articular cartilage using India ink. *(Supplementary Materials)*

References

[1] R. C. Lawrence, D. T. Felson, C. G. Helmick et al., "Estimates of the prevalence of arthritis and other rheumatic conditions in the United States: part II," *Arthritis & Rheumatology*, vol. 58, no. 1, pp. 26–35, 2008.

[2] R. F. Loeser, S. R. Goldring, C. R. Scanzello, and M. B. Goldring, "Osteoarthritis: a disease of the joint as an organ," *Arthritis & Rheumatology*, vol. 64, no. 6, pp. 1697–1707, 2012.

[3] M. B. Goldring, "Chondrogenesis, chondrocyte differentiation, and articular cartilage metabolism in health and osteoarthritis," *Therapeutic Advances in Musculoskeletal Disease*, vol. 4, no. 4, pp. 269–285, 2012.

[4] B. O. Diekman and F. Guilak, "Stem cell-based therapies for osteoarthritis: challenges and opportunities," *Current Opinion in Rheumatology*, vol. 25, no. 1, pp. 119–126, 2013.

[5] S. Wakitani, T. Goto, S. J. Pineda et al., "Mesenchymal cell-based repair of large, full-thickness defects of articular cartilage," *The Journal of Bone and Joint Surgery-American Volume*, vol. 76, no. 4, pp. 579–592, 1994.

[6] W. Zhang, G. Nuki, R. W. Moskowitz et al., "OARSI recommendations for the management of hip and knee osteoarthritis: part III: changes in evidence following systematic cumulative update of research published through January 2009," *Osteoarthritis and Cartilage*, vol. 18, no. 4, pp. 476–499, 2010.

[7] G. H. Lo, M. LaValley, T. McAlindon, and D. T. Felson, "Intra-articular hyaluronic acid in treatment of knee osteoarthritis: a meta-analysis," *Journal of the American Medical Association*, vol. 290, no. 23, pp. 3115–3121, 2003.

[8] M. E. Farkouh, H. Kirshner, R. A. Harrington et al., "Comparison of lumiracoxib with naproxen and ibuprofen in the therapeutic arthritis research and gastrointestinal event trial (TARGET), cardiovascular outcomes: randomised controlled trial," *The Lancet*, vol. 364, no. 9435, pp. 675–684, 2004.

[9] N. Tammachote, S. Kanitnate, T. Yakumpor, and P. Panichkul, "Intra-articular, single-shot Hylan G-F 20 hyaluronic acid injection compared with corticosteroid in knee osteoarthritis: a double-blind, randomized controlled trial," *The Journal of Bone and Joint Surgery*, vol. 98, no. 11, pp. 885–892, 2016.

[10] G. Filardo, B. Di Matteo, A. Di Martino et al., "Platelet-rich plasma intra-articular knee injections show no superiority versus viscosupplementation: a randomized controlled trial," *The American Journal of Sports Medicine*, vol. 43, no. 7, pp. 1575–1582, 2015.

[11] C. H. Jo, Y. G. Lee, W. H. Shin et al., "Intra-articular injection of mesenchymal stem cells for the treatment of osteoarthritis of the knee: a proof-of-concept clinical trial," *Stem Cells*, vol. 32, no. 5, pp. 1254–1266, 2014.

[12] G. F. Muschler, H. Nitto, C. A. Boehm, and K. A. Easley, "Age- and gender-related changes in the cellularity of human bone marrow and the prevalence of osteoblastic progenitors," *Journal of Orthopaedic Research*, vol. 19, no. 1, pp. 117–125, 2001.

[13] A. Banfi, G. Bianchi, M. Galotto, R. Cancedda, and R. Quarto, "Bone marrow stromal damage after chemo/radiotherapy: occurrence, consequences and possibilities of treatment," *Leukemia & Lymphoma*, vol. 42, no. 5, pp. 863–870, 2001.

[14] D. Minteer, K. G. Marra, and J. P. Rubin, "Adipose-derived mesenchymal stem cells: biology and potential applications," in *Mesenchymal stem cells - basics and clinical application I*, pp. 59–71, Springer, 2012.

[15] J. M. Murphy, D. J. Fink, E. B. Hunziker, and F. P. Barry, "Stem cell therapy in a caprine model of osteoarthritis," *Arthritis & Rheumatology*, vol. 48, no. 12, pp. 3464–3474, 2003.

[16] I. Linero and O. Chaparro, "Paracrine effect of mesenchymal stem cells derived from human adipose tissue in bone regeneration," *PLoS One*, vol. 9, no. 9, article e107001, 2014.

[17] C. Toma, W. R. Wagner, S. Bowry, A. Schwartz, and F. Villanueva, "Fate of culture-expanded mesenchymal stem cells in the microvasculature: in vivo observations of cell kinetics," *Circulation Research*, vol. 104, no. 3, pp. 398–402, 2009.

[18] R. D. Levit, N. Landazuri, E. A. Phelps et al., "Cellular encapsulation enhances cardiac repair," *Journal of the American Heart Association*, vol. 2, no. 5, article e000367, 2013.

[19] M. Serra, C. Correia, R. Malpique et al., "Microencapsulation technology: a powerful tool for integrating expansion and cryopreservation of human embryonic stem cells," *PLoS One*, vol. 6, no. 8, article e23212, 2011.

[20] L. Chen, E. E. Tredget, P. Y. G. Wu, and Y. Wu, "Paracrine factors of mesenchymal stem cells recruit macrophages and endothelial lineage cells and enhance wound healing," *PLoS One*, vol. 3, no. 4, article e1886, 2008.

[21] E. KOH, Y. C. JUNG, H.-M. WOO, and B.-J. KANG, "Injectable alginate-microencapsulated canine adipose tissue-derived mesenchymal stem cells for enhanced viable cell retention," *Journal of Veterinary Medical Science*, vol. 79, no. 3, pp. 492–501, 2017.

[22] K. Kuroda, T. Kabata, K. Hayashi et al., "The paracrine effect of adipose-derived stem cells inhibits osteoarthritis progression," *BMC Musculoskeletal Disorders*, vol. 16, no. 1, p. 236, 2015.

[23] D. J. Whitworth and T. A. Banks, "Stem cell therapies for treating osteoarthritis: prescient or premature?," *The Veterinary Journal*, vol. 202, no. 3, pp. 416–424, 2014.

[24] J. Sun and H. Tan, "Alginate-based biomaterials for regenerative medicine applications," *Materials*, vol. 6, no. 4, pp. 1285–1309, 2013.

[25] B.-J. Kang, H.-H. Ryu, S. S. Park et al., "Comparing the osteogenic potential of canine mesenchymal stem cells derived from adipose tissues, bone marrow, umbilical cord blood, and Wharton's jelly for treating bone defects," *Journal of Veterinary Science*, vol. 13, no. 3, pp. 299–310, 2012.

[26] S. Suganuma, K. Tada, K. Hayashi et al., "Uncultured adipose-derived regenerative cells promote peripheral nerve regeneration," *Journal of Orthopaedic Science*, vol. 18, no. 1, pp. 145–151, 2013.

[27] G. Meachim, "Light microscopy of Indian ink preparations of fibrillated cartilage," *Annals of the Rheumatic Diseases*, vol. 31, no. 6, pp. 457–464, 1972.

[28] S. Laverty, C. A. Girard, J. M. Williams, E. B. Hunziker, and K. P. H. Pritzker, "The OARSI histopathology initiative–recommendations for histological assessments of osteoarthritis in the rabbit," *Osteoarthritis and Cartilage*, vol. 18, pp. S53–S65, 2010.

[29] M. Freire, J. Brown, I. D. Robertson et al., "Meniscal mineralization in domestic cats," *Veterinary Surgery*, vol. 39, no. 5, pp. 545–552, 2010.

[30] K. P. H. Pritzker, S. Gay, S. A. Jimenez et al., "Osteoarthritis cartilage histopathology: grading and staging," *Osteoarthritis and Cartilage*, vol. 14, no. 1, pp. 13–29, 2006.

[31] G. Desando, C. Cavallo, F. Sartoni et al., "Intra-articular delivery of adipose derived stromal cells attenuates osteoarthritis progression in an experimental rabbit model," *Arthritis Research & Therapy*, vol. 15, no. 1, p. R22, 2013.

[32] M. Gutiérrez-Fernández, B. Rodríguez-Frutos, J. Ramos-Cejudo et al., "Comparison between xenogeneic and allogeneic adipose mesenchymal stem cells in the treatment of acute cerebral infarct: proof of concept in rats," *Journal of Translational Medicine*, vol. 13, no. 1, p. 46, 2015.

[33] S. Y. Tsai, Y. C. Huang, L. L. Chueh, L. S. Yeh, and C. S. Lin, "Intra-articular transplantation of porcine adipose-derived stem cells for the treatment of canine osteoarthritis: a pilot study," *World Journal of Transplantation*, vol. 4, no. 3, pp. 196–205, 2014.

[34] P.-Y. Chen, L. L. H. Huang, and H.-J. Hsieh, "Hyaluronan preserves the proliferation and differentiation potentials of long-term cultured murine adipose-derived stromal cells," *Biochemical and Biophysical Research Communications*, vol. 360, no. 1, pp. 1–6, 2007.

[35] A. M. Altman, F. J. Abdul Khalek, M. Seidensticker et al., "Human tissue-resident stem cells combined with hyaluronic acid gel provide fibrovascular-integrated soft-tissue augmentation in a murine photoaged skin model," *Plastic and Reconstructive Surgery*, vol. 125, no. 1, pp. 63–73, 2010.

[36] N. Ozeki, T. Muneta, H. Koga et al., "Not single but periodic injections of synovial mesenchymal stem cells maintain viable cells in knees and inhibit osteoarthritis progression in rats," *Osteoarthritis and Cartilage*, vol. 24, no. 6, pp. 1061–1070, 2016.

[37] M. ter Huurne, R. Schelbergen, R. Blattes et al., "Antiinflammatory and chondroprotective effects of intraarticular injection of adipose-derived stem cells in experimental osteoarthritis," *Arthritis & Rheumatology*, vol. 64, no. 11, pp. 3604–3613, 2012.

[38] M. Horie, H. Choi, R. H. Lee et al., "Intra-articular injection of human mesenchymal stem cells (MSCs) promote rat meniscal regeneration by being activated to express Indian hedgehog that enhances expression of type II collagen," *Osteoarthritis and Cartilage*, vol. 20, no. 10, pp. 1197–1207, 2012.

[39] X. He, Y. Liu, X. Yuan, and L. Lu, "Enhanced healing of rat calvarial defects with MSCs loaded on BMP-2 releasing chitosan/alginate/hydroxyapatite scaffolds," *PLoS One*, vol. 9, no. 8, article e104061, 2014.

[40] G. Luca, M. Calvitti, C. Nastruzzi et al., "Encapsulation, in vitro characterization, and in vivo biocompatibility of Sertoli cells in alginate-based microcapsules," *Tissue Engineering*, vol. 13, no. 3, pp. 641–648, 2007.

[41] A. Bhat, A. I. Hoch, M. L. Decaris, and J. K. Leach, "Alginate hydrogels containing cell-interactive beads for bone formation," *The FASEB Journal*, vol. 27, no. 12, pp. 4844–4852, 2013.

[42] L. Gasperini, J. F. Mano, and R. L. Reis, "Natural polymers for the microencapsulation of cells," *Journal of the Royal Society Interface*, vol. 11, no. 100, article 20140817, 2014.

[43] Y. S. Kim, Y. J. Choi, and Y. G. Koh, "Mesenchymal stem cell implantation in knee osteoarthritis: an assessment of the factors influencing clinical outcomes," *The American Journal of Sports Medicine*, vol. 43, no. 9, pp. 2293–2301, 2015.

[44] M. Yoshioka, R. D. Coutts, D. Amiel, and S. A. Hacker, "Characterization of a model of osteoarthritis in the rabbit knee," *Osteoarthritis and Cartilage*, vol. 4, no. 2, pp. 87–98, 1996.

[45] A. Mero, M. Campisi, M. Favero et al., "A hyaluronic acid–salmon calcitonin conjugate for the local treatment of osteoarthritis: Chondro-protective effect in a rabbit model of early OA," *Journal of Controlled Release*, vol. 187, pp. 30–38, 2014.

[46] A. Bendele, "Animal models of osteoarthritis," *Journal of Musculoskeletal and Neuronal Interactions*, vol. 1, no. 4, pp. 363–376, 2001.

[47] E. Teeple, G. D. Jay, K. A. Elsaid, and B. C. Fleming, "Animal models of osteoarthritis: challenges of model selection and analysis," *The AAPS Journal*, vol. 15, no. 2, pp. 438–446, 2013.

[48] M. E. Adams, M. E. J. Billingham, and H. Muir, "The glycosaminoglycans in menisci in experimental and natural

osteoarthritis," *Arthritis & Rheumatology*, vol. 26, no. 1, pp. 69–76, 1983.

[49] Y.-H. Chang, H.-W. Liu, K.-C. Wu, and D.-C. Ding, "Mesenchymal stem cells and their clinical applications in osteoarthritis," *Cell Transplantation*, vol. 25, no. 5, pp. 937–950, 2016.

[50] M.-P. Hellio le Graverand, J. Eggerer, P. Sciore et al., "Matrix metalloproteinase-13 expression in rabbit knee joint connective tissues: influence of maturation and response to injury," *Matrix Biology*, vol. 19, no. 5, pp. 431–441, 2000.

[51] R. L. Smith, "Degradative enzymes in osteoarthritis," *Frontiers in Bioscience*, vol. 4, no. 4, pp. D704–D712, 1999.

[52] R. C. Billinghurst, L. Dahlberg, M. Ionescu et al., "Enhanced cleavage of type II collagen by collagenases in osteoarthritic articular cartilage," *The Journal of Clinical Investigation*, vol. 99, no. 7, pp. 1534–1545, 1997.

[53] Q. Chu, M. Lopez, K. Hayashi et al., "Elevation of a collagenase generated type II collagen neoepitope and proteoglycan epitopes in synovial fluid following induction of joint instability in the dog," *Osteoarthritis and Cartilage*, vol. 10, no. 8, pp. 662–669, 2002.

[54] J. R. Matyas, L. Atley, M. Ionescu, D. R. Eyre, and A. R. Poole, "Analysis of cartilage biomarkers in the early phases of canine experimental osteoarthritis," *Arthritis & Rheumatology*, vol. 50, no. 2, pp. 543–552, 2004.

[55] M. Agung, M. Ochi, S. Yanada et al., "Mobilization of bone marrow-derived mesenchymal stem cells into the injured tissues after intraarticular injection and their contribution to tissue regeneration," *Knee Surgery, Sports Traumatology, Arthroscopy*, vol. 14, no. 12, pp. 1307–1314, 2006.

[56] H. Koga, T. Muneta, T. Nagase et al., "Comparison of mesenchymal tissues-derived stem cells for in vivo chondrogenesis: suitable conditions for cell therapy of cartilage defects in rabbit," *Cell and Tissue Research*, vol. 333, no. 2, pp. 207–215, 2008.

[57] Y. Qi, G. Feng, and W. Yan, "Mesenchymal stem cell-based treatment for cartilage defects in osteoarthritis," *Molecular Biology Reports*, vol. 39, no. 5, pp. 5683–5689, 2012.

[58] J. C. Fernandes, J. Martel-Pelletier, and J. Pelletier, "The role of cytokines in osteoarthritis pathophysiology," *Biorheology*, vol. 39, no. 1-2, pp. 237–246, 2002.

[59] H. Kang, J. Peng, S. Lu et al., "In vivo cartilage repair using adipose-derived stem cell-loaded decellularized cartilage ECM scaffolds," *Journal of Tissue Engineering and Regenerative Medicine*, vol. 8, no. 6, pp. 442–453, 2014.

[60] Y. S. Kim, Y. J. Choi, D. S. Suh et al., "Mesenchymal stem cell implantation in osteoarthritic knees: is fibrin glue effective as a scaffold?," *The American Journal of Sports Medicine*, vol. 43, no. 1, pp. 176–185, 2015.

Hindawi
Stem Cells International
Volume 2018, Article ID 4142031, 12 pages
https://doi.org/10.1155/2018/4142031

Research Article

Comparison of Regenerative Tissue Quality following Matrix-Associated Cell Implantation Using Amplified Chondrocytes Compared to Synovium-Derived Stem Cells in a Rabbit Model for Cartilage Lesions

Hagen Schmal,[1,2] **Justyna M. Kowal**,[3] **Moustapha Kassem**,[3] **Michael Seidenstuecker**,[1] **Anke Bernstein**,[1] **Katharina Böttiger**,[1] **Tanshiyue Xiong**,[1] **Norbert P. Südkamp**,[1] **and Eva J. Kubosch**[1]

[1]*Department of Orthopedics and Trauma Surgery, Medical Center-Albert-Ludwigs-University of Freiburg, Faculty of Medicine, Albert-Ludwigs-University of Freiburg, Freiburg, Germany*
[2]*Department of Orthopaedics and Traumatology, Odense University Hospital and Department of Clinical Research, University of Southern Denmark, Odense, Denmark*
[3]*Molecular Endocrinology & Stem Cell Research Unit (KMEB), Department of Endocrinology and Metabolism, Odense University Hospital and University of Southern Denmark, Odense, Denmark*

Correspondence should be addressed to Hagen Schmal; hagen.schmal@freenet.de

Received 27 November 2017; Accepted 5 March 2018; Published 19 April 2018

Academic Editor: Shiwu Dong

Known problems of the autologous chondrocyte implantation motivate the search for cellular alternatives. The aim of the study was to test the potential of synovium-derived stem cells (SMSC) to regenerate cartilage using a matrix-associated implantation. In an osteochondral defect model of the medial femoral condyle in a rabbit, a collagen membrane was seeded with either culture-expanded allogenic chondrocytes or SMSC and then transplanted into the lesion. A tailored piece synovium served as a control. Rabbit SMSC formed typical cartilage in vitro. Macroscopic evaluation of defect healing and the thickness of the regenerated tissue did not reveal a significant difference between the intervention groups. However, instantaneous and shear modulus, reflecting the biomechanical strength of the repair tissue, was superior in the implantation group using allogenic chondrocytes ($p < 0.05$). This correlated with a more chondrogenic structure and higher proteoglycan expression, resulting in a lower OARSI score ($p < 0.05$). The repair tissue of all groups expressed comparable amounts of the collagen types I, II, and X. Cartilage regeneration following matrix-associated implantation using allogenic undifferentiated synovium-derived stem cells in a defect model in rabbits showed similar macroscopic results and collagen composition compared to amplified chondrocytes; however, biomechanical characteristics and histological scoring were inferior.

1. Introduction

Articular cartilage defects often result in pain, loss of function, and finally osteoarthritis (OA), which cause a significant impact to the public health system in every developed country, where OA currently affects one in eight individuals [1]. Autologous chondrocyte implantation is a cellular therapy, which has successfully been employed to treat large, isolated, full thickness cartilage defects [2]. Several disadvantages such as the need for two surgical procedures and a significant donor site morbidity underline the need for modifications of the procedure. Furthermore, typical complications such as formation of hypertrophic regenerative cartilage, disturbed bonding of repair cartilage, insufficient biomechanical resistance of the newly formed cartilage, and delamination [3] drive the search for alternative techniques. Mesenchymal (stromal) stem cells, particularly synovium-derived mesenchymal stem cells (SMSC), represent a promising alternative

cell source. This was concluded from their marker profile expressed on the cell surface [4, 5], indicating a chondrogenic phenotype, and their natural ability to form cartilage especially in the vicinity of chondrocytes [6]. Furthermore, the formation of hypertrophic differentiation was significantly less pronounced compared to that formed by bone marrow mesenchymal stem cells [7, 8].

SMSC is available in a high quantity and their procurement does not lead to significant donor site morbidity. The cellular characteristics of SMSC suggest their suitability for cartilage regeneration protocols based on their chondrogenic phenotype [5] including its maintenance after several cell culture passages and their excellent ability to form extracellular matrix [9]; however, how SMSC should be applied to cartilage defects to reach best repair quality needs to be determined.

Following this clinical paradigm, in the present study, we hypothesized that undifferentiated SCMC can repair cartilage lesions in a rabbit model of medial condyle full-thickness lesions just as efficient as allogenic culture-expanded chondrocytes. By using an allogenic transplantation approach, the study design is relevant to clinical application and mimics an off-the-shelf protocol [10]. The primary outcome criterion was biomechanical stability, the secondary outcome criterion the histological evaluation of repair quality. Explorative outcomes were the immunohistological evaluation of the expression of the collagen types I, II, and X, markers for chondrocyte differentiation and hypertrophy.

2. Methods

2.1. Cell Preparation. We followed the methods of Kubosch et al. [6].

Two animals were sacrificed 3 months before the experiments and the knees dissected totally removing the cartilage from the tibia and femur. At the same time, the knee synovia was prepared. The cartilage was cut into small pieces, washed, and transferred into DMEM F-12 10% (Lonza BioWhittaker, Basel, Switzerland), fetal calf serum (FCS), 1% penicillin/streptomycin (P/S) (Invitrogen, Karlsruhe, Germany), 0.5% gentamycin and 3% collagenase CLS type II (Biochrom, Berlin, Germany). Minced cartilaginous tissue was then enzymatically digested during the next 16 hours on a shaking incubator at 37°C with 200 rpm. Subsequently, the released chondrocytes were centrifuged, washed, and seeded in expansion medium DMEM F-12 supplemented with 10% FCS, 1% P/S, and 0.5% gentamycin. Expansion of chondrocytes was performed by seeding them on coated T-flasks with a density of 2500–5000 cells/cm^2. The cells were frozen after reaching confluence. Thawed cells were grown and used when reaching a log phase of growth (passage 2). Similarly, the synovial tissue was cut into small pieces, washed, and transferred into DMEM F-12 medium with 10% FCS (Biochrom, Berlin, Germany), 1% penicillin/streptomycin (P/S) (Invitrogen, Karlsruhe, Germany), 0.5% gentamycin (Biochrom, Berlin, Germany), and 3% collagenase P (Roche, Mannheim, Germany). The suspension was digested during the next four hours on a shaking incubator (200 rpm) at 37°C. Subsequently, the released cells were centrifuged, washed, and seeded in expansion medium DMEM F-12 (10% FCS, 1% P/S, and 0.5% gentamycin). SMSC were seeded on coated T-flasks with a density of 2500–5000 cells/cm^2 for expansion. The cells were frozen after reaching confluence. Thawed cells were grown and used when reaching a log phase of growth (passage 2). Both SMSC and chondrocytes were amplified, growth synchronized, and used for the animal experiments at passage 2.

2.2. Characterization of Rabbit Synovium-Derived Mesenchymal Stem Cells (SMSC)

2.2.1. Chondrogenic Differentiation. Rabbit SMSC were distributed in 15 ml polypropylene tubes using 250,000 cells per 500 μl medium (DMEM high glucose) supplemented with 10% FBS, 1% penicillin/streptomycin, 10% ITS (mixture of insulin, human transferrin, and sodium selenite from Corning, NY, USA), 1% sodium pyruvate (Thermo Fisher Scientific, MA, USA), 100 nM dexamethasone (Sigma-Aldrich, Brøndby, Denmark), 10 ng/ml TGFβ3 (PeproTech, NJ, USA), and 50 µg/ml vitamin C (Sigma-Aldrich). In order to facilitate aggregate formation, the cells were gently centrifuged using 500g for 5 min. Chondrogenic media were changed every 2-3 days for 21 days, and cells were cultured in 37°C and 5% CO_2.

2.2.2. Osteogenic Differentiation. Rabbit SMSC were plated in density of 20,000 cells/cm^2 in standard DMEM (low glucose) media and cultured until they reached 80–90% confluency. After 24 h, rabbit SMSC were exposed to osteogenic media described by Lee et al. [11], which contained DMEM (5.5 mM glucose), 10% FBS, 1% penicillin/streptomycin, 10 mM β-glycerophosphate (Calbiochem-Merck, Darmstadt, Germany), 100 nM dexamethasone, and 50 μg/ml vitamin C (Sigma-Aldrich). Osteogenic media were changed every 2-3 days for 21 days, and cells were cultured in 37°C and 5% CO_2.

(1) Alkaline Phosphatase (ALP) Activity and Cell Viability. ALP activity was measured at day 21 of osteogenic differentiation and normalized to cell viability. In order to asses cell viability, the cells were incubated with 20 μl of CellTiter-Blue reagent (Promega, Mannheim, Germany) and 100 μl media in 37°C for 1 h. After 1 h, the fluorescent intensity was measured ($560_{ex}/590_{em}$) in FluoStar Omega microplate reader (BMG Labtech, Birkerød, Denmark). Subsequently, the cells were washed with Tris-buffered saline and fixed with a mixture of 3.7% formaldehyde and 90% ethanol for 30 seconds at room temperature. After that, the cells were incubated with ALP substrate, 1 mg/ml p-nitrophenyl phosphate in 50 mM $NaHCO_3$ (pH = 9.6) and 1 mM $MgCl_2$ at 37°C for 20 min. The reaction was stopped by adding 3 M NaOH. Absorbance was measured at 405 nm using the FluoStar Omega microplate reader.

(2) Alizarin Red Staining. In order to assess matrix mineralization, after 21 days of osteogenic differentiation, rabbit SMSC were stained with Alizarin Red. Briefly, the cells were washed with PBS and fixed with 70% iced-cold ethanol for

1 h at −20°C. Subsequently, the cells were washed with H_2O and stained with Alizarin Red solution (Sigma) pH = 4.2 for 10 min. After staining, the cells were washed with PBS for 5 min in order to remove unbound dye.

2.2.3. Adipogenic Differentiation. For adipogenic differentiation, rabbit SMSC were plated in a density of 30,000 cells/cm^2 in standard DMEM (low glucose) media and cultured until the cells reached 100% confluency. Subsequently, the media were replaced by adipogenic media adapted from Lee et al. [11], which contained DMEM (25 mM glucose), 10% FBS, 1% penicillin/streptomycin, 500 μM IBMX (3-isobutyl-1-methylxanthine, Gibco, Herlev, Denmark), 1 μM dexamethasone, 200 μM indomethacin, and 10 μg/ml insulin (Sigma, Brøndby, Denmark). Adipogenic media were changed every 2-3 days for 21 days, and cells were cultured in 37°C and 5% CO_2.

(1) Oil Red O Staining. After 21 days of adipogenic differentiation, rabbit SMSC were stained with Oil Red O in order to assess adipocyte formation. Briefly, the cells were washed with PBS and fixed with 4% paraformaldehyde at room temperature for 10 min. Subsequently, the cells were washed with 3% isopropanol and incubated with 25 mg Oil Red O (Sigma) in 5 ml of 60% isopropanol and 3.35 ml H_2O for 1 h.

2.3. RNA Isolation and Quantitative PCR. Total RNA was isolated from the cells using TRIzol® reagent (Invitrogen, Tastrup, Denmark) according to manufacturer's protocol. After 21 days of differentiation, the samples were dissociated in TRIzol using the gentleMACS Dissociator (Miltenyi Biotec, Lund, Sweden). cDNA was synthetized from 1 μg of total RNA using a RevertAid H Minus First Strand cDNA Synthesis Kit (Thermo Scientific, MA, USA). Primers were designed using Primer-BLAST software. Primer sequences are described in Table 1 (Supplementary Figures available here). Real-time PCR was performed in the StepOnePlus Real-Time PCR System (Applied Biosystems) using Fast SYBR® Green Mix (Applied Biosystems, Foster City, CA, USA). Each sample was run in triplicates. The results were calculated using ΔCt method. The data are presented as $2^{-\Delta\Delta Ct}$, giving the relative expression change between day 0 and day 21.

2.4. Certification. The regional board for animal protection approved the experiments with the decision from 9 March 2013 with additional modifications at 21 August and 11 September 2015 (G-13/75).

2.5. Anesthesia. The rabbits received ketamine (35 mg/kg) combined with medetomidine (0.25 mg/kg) by intramuscular injection. During the surgery, Ringer's solution (10 ml/kg/h) was given through an intravenous access in the marginal ear vein. Anesthesia was supplemented with 0.5–2% isoflurane (double facemask with spontaneous ventilation, $FiO_2 > 0.4$). Heart rate and blood oxygen saturation were monitored. Prior to surgery and 3 days after, the rabbits received carprofen, a nonsteroidal anti-inflammatory drug (4 mg/kg s.c.) as an analgesic and Baytril (enrofloxacin) 2.5% (0.4 ml/kg) as an antibiotic.

Table 1: Macroscopic evaluation.

Defect	Group	ICRS grading	p (versus others)	Area	p (versus others)
Synovium	1	2.2 ± 0.4	n.s.	96.8 ± 10.2	n.s.
ACI-SMSC	2	2.7 ± 0.8	n.s.	83.3 ± 30.3	n.s.
ACI-CHDR	3	2.7 ± 0.8	n.s.	79.2 ± 24.6	n.s.

2.6. Operation. Female New Zealand white rabbits were obtained from Charles River (Sulzfeld, Germany). The animals were kept applying specific pathogen-free conditions and controlled room temperature. Acclimatization lasted 14 days. The animals were housed in cages with unrestricted water and food supply and a typical day/night rhythm. By the time of operation, the animals had reached a bodyweight of approximately 3.5 to 4.2 kg with closed growth plates. After shaving and disinfection, both knee joints were opened by a central skin cut and a medial parapatellar arthrotomy. Following this, the patella was laterally displaced. Hereafter, the Hoffa fat pad with the synovium was partially resected, and full-thickness cartilage lesions were prepared in the central medial femoral condyle using a drill with a 3.5 mm diameter and a stop at 2 mm depth. Attention was paid on an exact vertical angle for the drilling direction. Considering an average cartilage height of 0.5 mm (Figure 1(a)), the subchondral bone plate was opened. The defects of the control group were covered with a synovium flap, matching the prepared lesion size, and fixed with compression and fibrin glue (Baxter, Unterschleißheim, Germany). For the groups treated with cells, matching flaps of a bilayered collagen type I/III scaffold (Chondro-Gide, Geistlich, Pharma AG, Wolhusen, Switzerland) were prepared, passively seeded with cells (porous side, 400,000 cells per defect; 15 min adhesion time) and fixed as described for the synovium flaps. For inoculation, a cell suspension of 40,000,000 cells/ml was prepared and 10 μl dropped on the tailored scaffold. After transplant fixation, the patella was relocated and the joint moved followed by a visual control of the correct transplant location. Hereafter, the arthrotomy and the skin were sutured separately. Wounds were sealed using an aluminium spray.

We compared 4 groups (synovium flap, nontreated uninjured cartilage, transplantation of amplified chondrocytes, or SMSC) and included 6 operated knees in each group (12 rabbits). The knees were randomly assigned to each group by using a random number generator. The animals were sacrificed after 6 weeks and the knees explanted and first biomechanically tested. After this, specimens were histologically analyzed. In a pilot study comparing the implantation of a collagen scaffold with and without chondrocytes, significant differences were found after 3, 6, 12, and 24 weeks (Oliver Huwert, unpublished data). The differences, however, declined from 7 to 5.4 points on a summary scale, evaluating macroscopic and histological scoring (Supplementary Figure 1). This was probably caused by the natural repair capacity of cartilage defects in rabbits and forced the focus on the 6-week time point.

2.7. Clinical Evaluation of Rabbits. The rabbits mobilized themselves immediately after weaning with full-weight

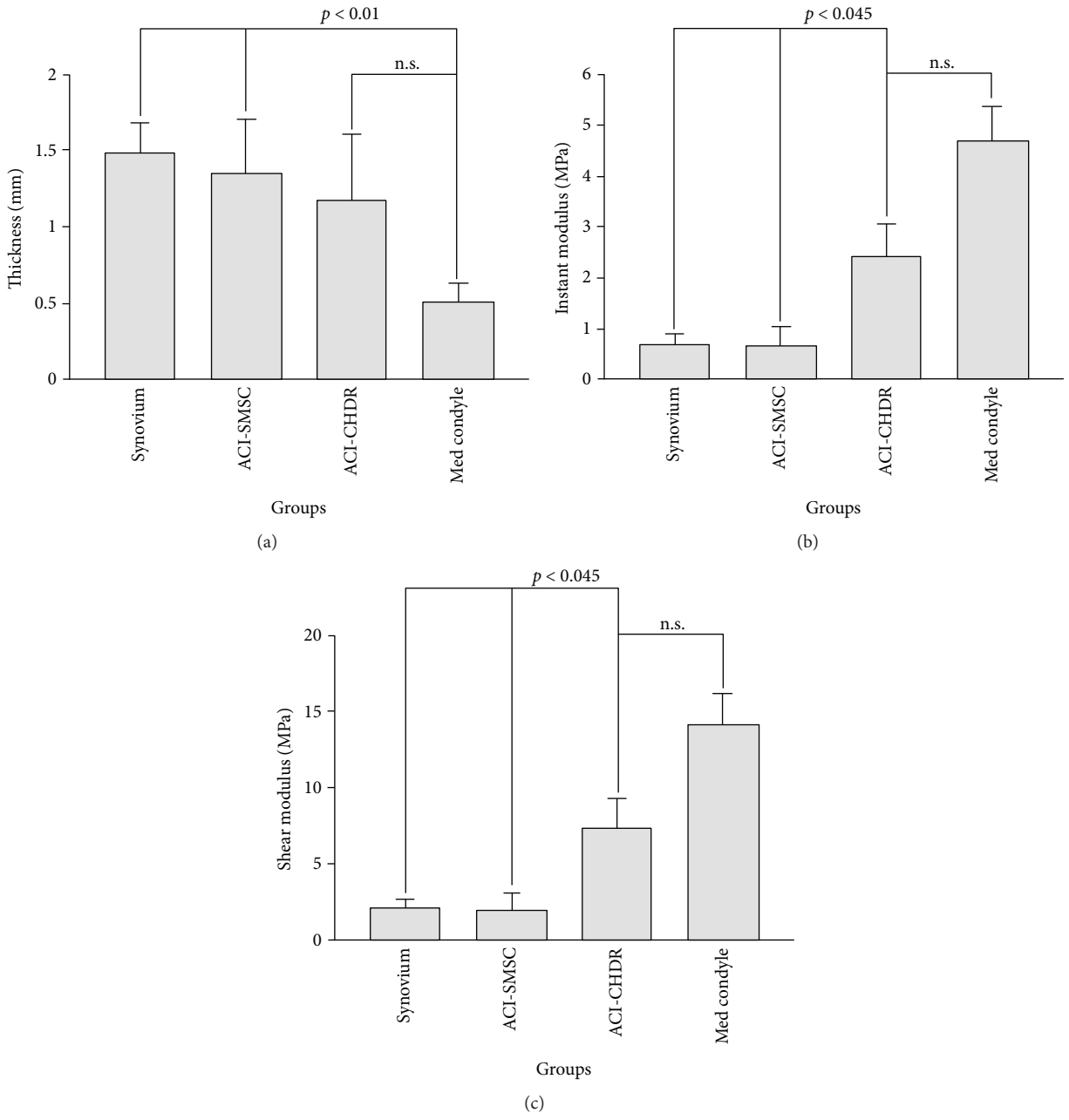

Figure 1: (a) Cartilage thickness. The cartilage thickness differs not significantly between the groups but is higher than normal caused by the technique of defect preparation (n.s.: not significant). (b) Instantaneous or instant modulus. The instant modulus is significantly higher in the group treated with amplified chondrocytes compared to the other intervention groups (n.s.: not significant). (c) Shear modulus. The shear modulus reached significantly higher values in the group treated with amplified chondrocytes compared to the other intervention groups (n.s.: not significant).

bearing. They had no clinical signs of pain. They were closely observed one week until wound healing and had no signs of infection. The rabbits did not limp longer than 2-3 days having soon normal, species-specific moving patterns.

2.8. Biomechanical Evaluation. To define mechanical parameters, the multiaxial testing unit Mach-1 Model V500css (Biomomentum, Montreal, Canada) for automated normal alignment and indentation mapping with a multiple-axis load cell by Honeywell Mod. 34 (Honeywell, New Jersey, USA), a Newport Motion Controller ESP 301 (Newport, Irvine, USA), and an indenter with spherical geometry of 1 mm diameter was employed. For the biomechanical investigations, 10 different positions on the sample were examined. The positions were selected at the mapping module of Mach-1 Software (Biomomentum, Montreal). Five positions were selected on the healthy part of the sample (left condyle in Supplementary Figure 4A), and five positions were selected on the defective part of the sample (right condyle in Supplementary Figure 4A). To avoid dehydration of the

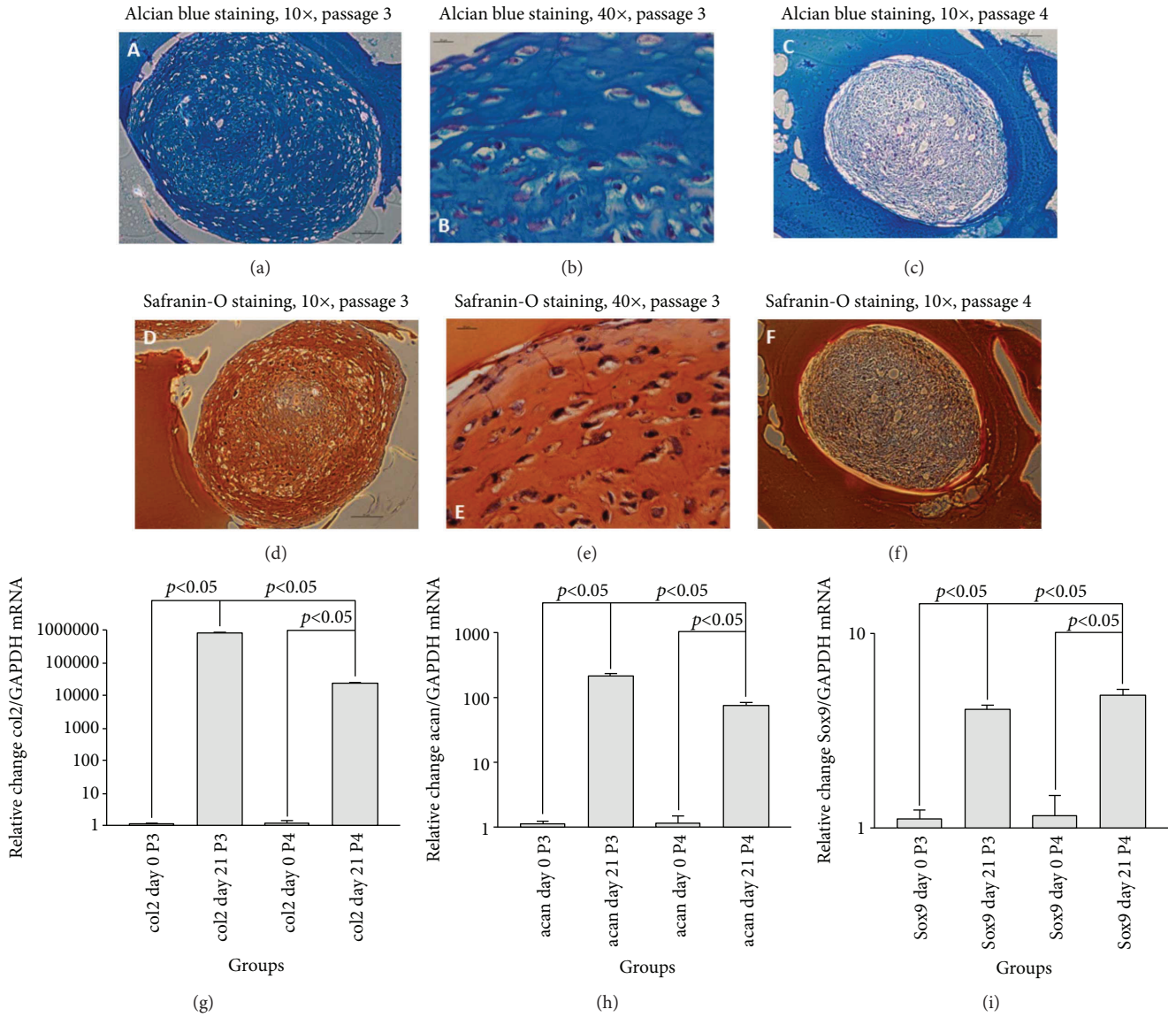

Figure 2: Rabbit SMSC have the ability to undergo chondrogenic differentiation in vitro in a pellet culture. Staining with Alcian blue (upper row) and Safranin-O (lower row) indicates a successful production of glycosaminoglycans after 21 days. Chondrogenic differentiation capacity declined remarkably with a further passage. Specimens were embedded in gelatin before staining. Quantitative PCR revealed mRNA formation of typical cartilage markers such as collagen type II (g), Aggrecan (h), and Sox9 (i) in both passage 3 and 4 ($n = 3$, $p < 0.05$).

cartilage during the measurements, the sample was moisturized several times with phosphate-buffered saline (PBS).

2.8.1. Automated Indentation Mapping. For the automated indentation mapping, the following parameters were set in Mach-1 Motion: z-contact velocity of 0.5 mm/s, a contact criteria of 0.1015 N, and a scanning grid of 0.5 mm. The indentation amplitude was set to 0.2 mm and the indentation velocity to 0.2 mm/s. The relaxation time was set to 5 s.

2.8.2. Automated Thickness Mapping. Thickness was mapped with the needle technique [12] by replacing the spherical indenter with a $27G \times 3/4''$ intradermal needle (B. Braun, Melsungen, Germany). The following parameters were input into the Mach-1 Motion Software: stage velocity of 0.5 mm/s; contact criteria of 4 N, and stage repositioning of 2x load resolution. The needle on the mechanical tester was directed vertically towards the sample at a constant speed until the cartilage surface was penetrated and the needle stopped at the subchondral bone edge.

2.8.3. Data Processing. The findings were analyzed using the software Mach-1 Analysis Version 4.1.0.17 (Biomomentum, Montreal) and Origin 9.1 Professional (Origin Lab, Northampton, USA). The evaluation methods used were according to Sim et al. [13]. Using automated thickness mapping results, the cartilage thickness was calculated at each position from the difference between the vertical position of the surface (where the load starts to increase) and the position of the cartilage/bone interface (corresponding to the first inflection point in the displacement/force curve) (see

Supplementary Figure 4B). The instantaneous modulus (IM or instant or Young's modulus) at each position was obtained by fitting the load-displacement curve (with corresponding thickness and effective Poisson ratio of 0.5) to an elastic model for indentation [14] (see following equation).

$$\mathrm{IM} = \frac{P}{H} \cdot \frac{1-\nu^2}{2ak \cdot ((a/h)\nu)}, \quad (1)$$

with P = load, H = indentation depth, a = radius of the contact region, ν = Poisson's ratio, and k = correction factor dependent on a/h and ν.

The shear modulus (G) is calculated as follows:

$$G = \frac{E}{2(1+\nu)}. \quad (2)$$

An example for a typical strain-relaxation curve is provided in the Supplementary Material (Figure 4C).

2.9. Histology. After biomechanical testing, specimens were fixed in 4% buffered formaldehyde solution. A thin-section technique facilitated the preparation of the slides. The longitudinally sectioned specimens were decalcified with ethylenediamine-tetra-acetic acid, dehydrated with ethanol, degreased with xylene substitute (Histoclear®), and then embedded in paraffin. The sections were made using a rotary microtome (HM 340E, Microm, Thermo Fisher Scientific Inc., Waltham, MA, USA). They were stained with hematoxylin-eosin and Safranin-O. The image analysis of the sections was done utilizing a light microscope (KS300, Carl Zeiss Ltd., Oberkochen, Germany) associated with a picture analysis unit (Axioplan, Carl Zeiss Vision Ltd., Oberkochen, Germany). Representative slides were selected and blindly evaluated by two different examiners, determining the OARSI score [15]. The average and the median were calculated and used for statistical group comparisons.

2.10. Immunohistology. For collagen type I, type II, and type X immunohistochemistry, sections were incubated for 30 min with 5% normal goat serum, followed by incubation with a 1 : 50 monoclonal mouse anticollagen type I antibody (MAB3391, Clone 5D8-G9, Chemicon, Hofheim, Germany), a 1 : 50 monoclonal mouse anticollagen type II antibody (MAB8887, Clone 6B3, Chemicon), or a 1 : 500 monoclonal mouse anticollagen type X antibody (Clone COL-10, C7974, Sigma, Taufkirchen, Germany) for 2 h, three washings with PBS, and incubation with a biotin-labelled goat antimouse immunoglobulin for 30 min (Acris, Herford, Germany). Afterwards, sections were incubated with avidin for 30 min and with 3-amino-9-ethylcarbazole (AEC) substrate for 10 min. Representative slides were selected, blinded, and evaluated by two different examiners, determining the Remmele-Stegner Score [16] and comparing positive and negative stains. The average and the median were calculated and used for statistical group comparisons.

2.11. Statistics. All values were expressed as mean ± standard error of the mean. Regarding the scores and all numerical values (if $n < 5$), statistical significance was tested nonparametrically primarily using the Mann–Whitney U test. Multiple comparisons were calculated using a post hoc statistics with the Kruskall-Wallis H test. Probability distributions of samples with $n \geq 5$ were analyzed by a Kolmogorov–Smirnov test. Normally distributed samples were then compared using a t-test, otherwise the samples were nonparametrically compared as indicated. Statistical significance was defined as $p < 0.05$.

3. Results

3.1. Cell Characterization. Rabbit synovial mesenchymal stem cells (SMSC) differentiated readily into chondrocytes in pellet culture after 3 weeks. Alcian blue staining of glycosaminoglycans of the pellets is shown in Figures 2(a) and 2(b). Similar staining pattern of cartilage by Safranin-O was observed (Figures 2(d) and 2(e)). The cells exhibited a partially fibroblast-like phenotype. Chondrogenic differentiation capacity declined remarkably after one further passage of the cells (Figures 2(c) and 2(f)).

Furthermore, quantitative RT-PCR revealed overexpression of cartilage mRNA markers during chondrocyte differentiation of SMSC. As seen in Figures 2(g)–2(i), collagen type II (col2), Aggrecan (acan), and Sox9 mRNA were significantly induced, and this was observed in both p3 and p4 cells. However, the response was lower in p4 compared to p3 cells.

Osteogenic differentiation of SMSC was evidenced by typical morphological changes (Supplementary Figures 2A and 2B). Alizarin Red staining visualized the formation of mineralized extracellular matrix. However, both the intensity of Alizarin Red stain and the lack of alkaline phosphatase expression indicated a limited capacity for osteoblastic differentiation (Supplementary Figures 2C and 2E). Quantitative RT-PCR analysis corroborated this finding, showing marginally increased collagen type I (col1) and osteocalcin (OCN) mRNA expression after 21 days (Supplementary Figure 2D). Similar to adipocyte differentiation, passage 4 cells had very limited osteoblastic differentiation capacity.

Rabbit SMSC were also able to differentiate in adipocytes, demonstrated by an Oil Red O stain (Supplementary Figures 3A and 3B). Adipocyte's differentiation was associated with accumulation of small lipid droplets and the induction of adipogenic genes such as PPARG (peroxisome proliferator-activated receptor gamma) and AN (adiponectin) (Supplementary Figure 3C). Together with a decreasing proliferation rate, p4 cells almost lost their adipogenic differentiation capacity (data not shown).

3.2. Gross Evaluation. The evaluation of the macroscopic degree of recovery using the ICRS subscore for defect filling [17] showed successful healing of the medial condyle lesions reaching values ranging below 3. We did not observe differences between the intervention groups (Table 1). All knees of the control group without intervention had naturally no cartilage damage (ICRS subscore = 0). The results are not separately reported, because there was no area of healing or lesion. Furthermore, the percentage of surface in the lesion containing repair tissue corresponding with the

adjacent natural cartilage was evaluated as "area of healing." Most of the surface was covered by repair tissue, but we did not detect differences between the groups evaluated 6 weeks postinjury (Table 1).

The evaluation of the macroscopic degree of healing using the ICRS score and the area of healing did not show differences between the groups after 6 weeks. Each group was statistically compared to every other group; the results are indicated by n.s. (not significant).

3.3. Biomechanical Evaluation

3.3.1. Thickness. The thickness of the uninjured reference cartilage of the medial femoral condyle was 0.50 ± 0.12 mm. There were no statistically significant differences between the cartilage thickness obtained in the intervention groups: 1.47 ± 0.20 mm for the synovium group, 1.35 ± 0.36 mm for transplanted SMSC, and 1.17 ± 0.44 mm for transplanted amplified chondrocytes (Figure 1(a)). The comparison between the uninjured control and each of the synovium group or the SMSC group revealed significant statistical differences ($p < 0.01$); however, the direct statistical comparison of the chondrocyte and the control group failed to reach significance ($p = 0.06$).

3.3.2. Instantaneous or Instant Modulus (IM). The instantaneous or instant modulus describes mechanical stress resistance of cartilage and correlates with osteoarthritic changes [13]. Normal cartilage is predicted to have high IM values, correlating with the instant modulus that was highest in the uninjured control group reaching 4.69 ± 0.68 MPa. There were no statistically significant differences between the groups with a transplanted piece of synovium (1.48 ± 0.20 MPa) and transplanted SMSC (1.35 ± 0.358 MPa, $p = 0.85$). However, both groups had a lower instant modulus than the control group ($p < 0.001$) and the group with transplanted amplified chondrocytes (2.42 ± 0.66 MPa, $p < 0.05$). Although numerically lower, the instant modulus of the chondrocyte group was not significantly different from the control group without defect ($p = 0.06$, Figure 2(b)).

3.4. Shear Modulus. The collagen content influences the shear modulus, which describes the material's response to shear stress and provides a functional measure of cartilage health [18]. The pattern of this analysis resembles the instant modulus. The shear modulus was highest in the uninjured control group reaching 14.09 ± 2.05 MPa. There was no statistically significant difference between the group with a transplanted piece of synovium (2.06 ± 0.63 MPa) and transplanted SMSC (1.90 ± 1.16, $p = 0.85$). However, both groups had a lower instant modulus than the control group ($p < 0.001$) and the group with transplanted amplified chondrocytes (7.27 ± 1.97 MPa, $p < 0.05$). Although numerically lower, the instant modulus of the chondrocyte group did not statistically significantly differ from the control group without a lesion ($p = 0.06$, Figure 2(c)).

3.5. Histological Evaluation. For qualitative histological evaluation of the regenerated tissue, the specimens were stained by HE and Safranin-O (Figure 3(a)). The stains confirmed uniform defect preparation and defect filling as well as the expression of glycosaminoglycans. The bonding at defect edges had partially a very high quality independent of the intervention group. The defects were slightly conically shaped, corresponding with the drill, which was used for defect preparation. There were no signs of immunological reactions against the implanted material evidenced by the absence of macrophages or giant cells.

The OARSI score was employed to obtain quantitative comparison. All uninjured cartilage areas had no sign of osteoarthritis (OARSI score = 0), which was significantly better than the scores of all intervention groups. The lowest scores were observed following treatment with amplified chondrocytes reaching 4.88 ± 1.43 points, compared to 8.11 ± 3.84 points ($p < 0.05$) in the synovium group and 8.71 ± 4.19 points ($p = 0.05$) in defects treated with amplified SMSC. Only the comparison with the synovium group reached statistical significance level (Figure 3(b)).

3.6. Immunohistology. The quantitative evaluation of the collagen type I, II, and X expression using the Remmele-Stegner Score did not show differences between the intervention groups after 6 weeks (Table 2), but all collagen types were expressed in the different types of original or regenerative cartilage tissue.

The evaluation of the collagen type I, II, and X expression quantified using the Remmele-Stegner Score did not show differences between the groups after 6 weeks. Each group was statistically compared for each examined collagen to every other group (n.s. (not significant)).

The levels of staining quality and intensity were comparable for collagen types I and II and lower for collagen type X in the intervention groups. Figure 4 shows representative slides for collagen types I (a), II (b), and X (c), comparing the staining of the specific antibodies with their isotype controls.

4. Discussion

The main finding of this study is that rabbit synovium-derived stromal (mesenchymal) stem cells (SMSC) can differentiate into the adipogenic, osteogenic, and chondrogenic lineage in vitro; however, SMSC are most suitable to form cartilage. Undifferentiated SMSC are eligible for matrix-associated implantation in a defect model in rabbits; however, the gained biomechanical stability of the regenerated cartilage and its quality, evaluated by a validated histological osteoarthritis score, was lesser compared to the current standard protocol utilizing amplified chondrocytes.

Numerous studies have highlighted the chondrogenic phenotype of SMSC [5, 6], which indicate an extraordinary suitability for natural [19] and surgically induced cartilage repair purposes [10, 20]. This was supported by findings in pathological processes, showing that synovial chondrogenesis leads to synovial chondromatosis [21]. A direct comparison of mesenchymal stem cells of different origin pointed out significant differences and a superiority of SMSC for cartilage formation [22]. This data is in line with our findings, demonstrating formation of high-quality cartilage with expression of

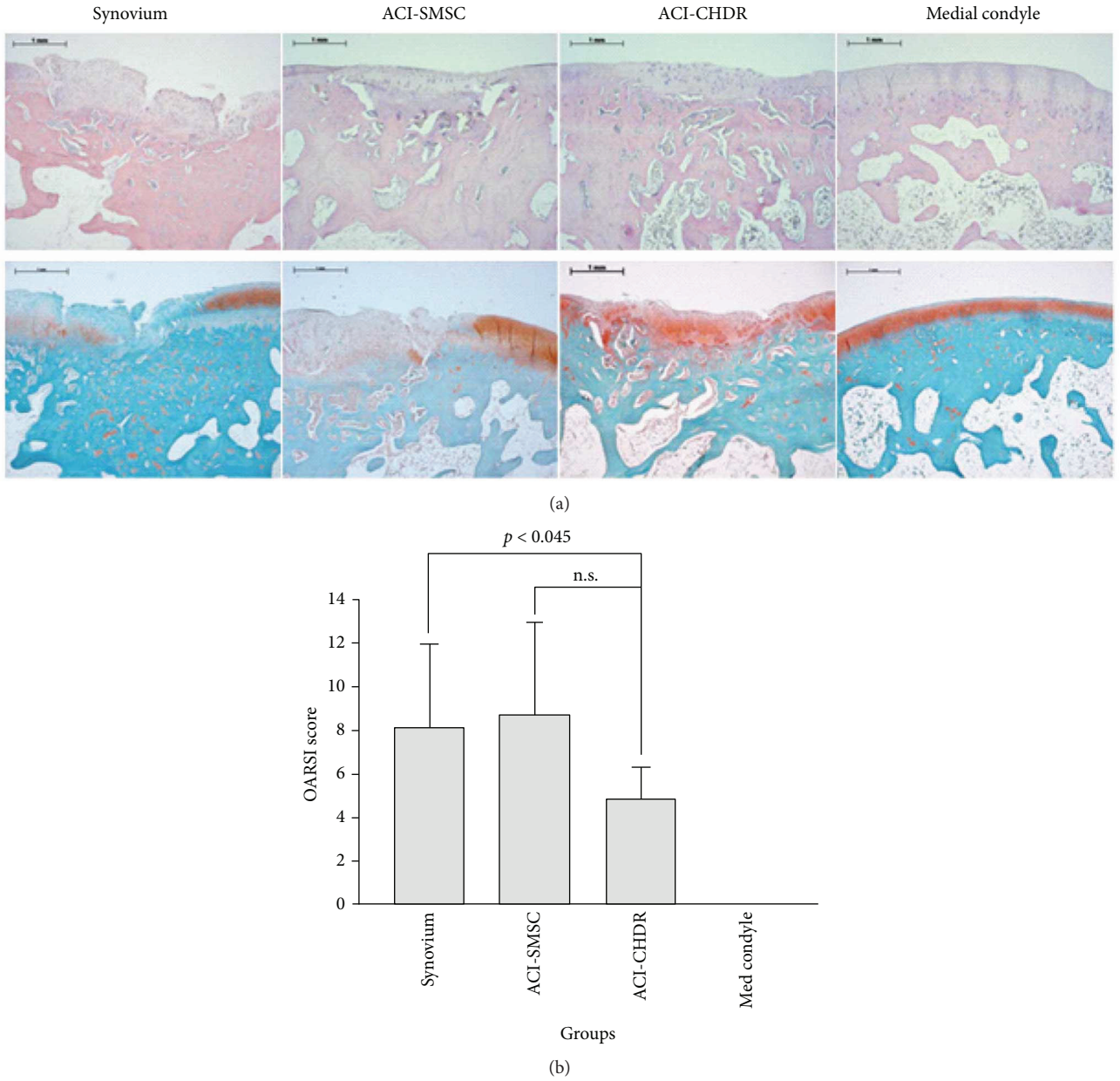

Figure 3: (a) HE (upper row) and Safranin-O (lower row) staining of the medial condyle showing the defect region with regenerative tissue following the different interventions. The red color indicates the presence of glycosaminoglycans. (b) The OARSI score is lower in the lesions treated with amplified chondrocytes compared to negative controls (n.s.: not significant).

glycosaminoglycans and collagen type II using rabbit SMSC. In contrast, the ability for adipogenic and osteogenic differentiation of these cells was limited. Lee et al. described similar findings and subjoined that the expression of certain surface markers, such as CD29 and CD90, differs between mesenchymal stem cells of human and rabbit origin and that they vary regarding their phenotype [11]. Despite this, different in vivo models demonstrated comparable functioning and success for rabbit SMSC applications [10, 11]. Beyond that, these cells supported successful cartilage regeneration in animal models of other species [20, 23] and in clinical applications in humans. SMSC were for instance successfully used for arthroscopically assisted cartilage repair resulting in improved MRI features, histology, and clinical outcome [24]. However, the study included only 10 patients without standardized follow-up and control group. By demonstrating that a single injection of SMSC was ineffective, but weekly injections in rat knees had significant chondroprotective effects, Ozeki et al. pointed out that the modus of application possesses a decisive influence on treatment attainment [25]. Pei et al. demonstrated the successful usage of SMSC seeded into nonwoven polyglycolic acid mesh in combination with a synthetic bone substitute to repair osteochondral defects in rabbit knee joints [10]. However, the cells were first treated in an incubator 1 month before implantation using a growth factor cocktail. Thereafter, the implants were biochemically,

Table 2: Quantitation of immunostaining using the Remmele-Stegner Score.

Defect	Collagen type I	p	Collagen type II	p	Collagen type X	p
Synovium	6.1 ± 1.7	n.s.	6.1 ± 3.2	n.s.	1.8 ± 2.9	n.s.
ACI-SMSC	5.5 ± 1.6	n.s.	4.8 ± 2.8	n.s.	2.2 ± 1.6	n.s.
ACI-CHDR	5.1 ± 0.9	n.s.	4.0 ± 1.3	n.s.	2.6 ± 2.1	n.s.

biomechanically, and histologically characterized, showing that the maturation prior to implantation improved the construct. The basis for the design of the presented study was the need for easy-to-use protocols for clinical applications. Therefore, the procedure was the same as a standard protocol for the autologous chondrocyte implantation, in which the chondrocytes were substituted with SMSC. Otherwise, the cells had the same starting conditions regarding passage, origin from the same rabbit, allogenic transplantation, and viability. The chondrocytes, currently the "gold standard," served at the same time as a control. Based on the very promising in vitro data of our own experiments and the results published by other groups regarding their chondrogenic predifferentiation, we expected to see similar results, when the in vitro predifferentiation, which was to date applied by all other groups, was omitted [10]. This approach should avoid another characteristic problem of preformed constructs, the failure of sufficient boundary integration as observed by Fujie et al. [26]. A successful testing of this procedure would also be the prerequisite for a possible one-step protocol, which truly would improve the perspectives of this method. However, the undifferentiated SMSC failed to show the same efficiency in cartilage repair as chondrocytes. Although the height of the regenerated tissue in the defect was larger than that in all the intervention groups compared to natural cartilage, the biomechanical stress resistance was lower. Since the prepared defect was 2 mm and therefore larger than the natural cartilage height, this difference is obvious and similar between the intervention groups. The measured height of the regenerated tissue correlated with the defect depth, which indirectly confirmed the uniform configuration of the lesions. Neither gross evaluation nor regeneration height differed in the intervention groups, which directly leads to the conclusion that the actual relevant parameter for the quality evaluation of regenerative tissue is the instantaneous and the shear modulus, reflecting the biomechanical stress resistance. Similarly, this was described by an analysis using scaffold-free tissue-engineered constructs utilizing SMSC [27], which exhibited compressive properties similar to uninjured cartilage. However, also in this study, the constructs lacked the typical zonal configuration of mature cartilage, having inferior surface stiffness and water retention capacity. The lack of a directional differentiation environment may have caused this. Therefore, the biomechanics could possibly be improved significantly when combining SMSC in a scaffold with growth factors, inducing chondrogenic differentiation such as TGFβ.

The collagen types I, II, and X characterize fibrocartilage and chondrocyte dedifferentiation, typical hyaline cartilage, and cartilage hypertrophy, respectively [28]. Although all collagen types were expressed without statistically significant differences between the intervention groups, differences were found comparing the level of collagen types. Whereas the quantity and quality for staining of collagen types I and II equaled each other, the level of collagen type X expression was least. This is a typical pattern for early cartilage repair [29], especially when the regeneration is associated with partial fibrocartilage formation.

Possible explanations for the less effectivity in cartilage defect healing are the original differentiation capacity of the synovial cells used. Caused by the anatomical conditions of a rabbit with very small dimensions, it is difficult to separate synovium from the rest of the surrounding tissue such as the Hoffa fat pad. By this, other types of mesenchymal stem cells derived from fat tissue or CD44+CD34− adventitial nonendothelial progenitor cells might have been mixed in the implanted stem cell population and have influenced the resulting cartilage-forming abilities [30]. The cells were also not labeled for later tracing purposes. Furthermore, the reported outcomes reflect only short-term results. The 6 weeks might simply have been not long enough to allow chondrogenic differentiation in vivo and adequate cartilage formation. However, an in vitro study using a transwell coculture has demonstrated that already after 7 days, SMSC could differentiate into chondrocytes forming typical chondron-like structures without applying biomechanical stimulation [6]. Moreover, biomechanical stimulation is expected to significantly support cartilage formation [31].

There are several possibilities to improve the results following SMSC transplantation. First, the cells could be predifferentiated during the amplification phase as shown before [10]. However, this complicates the preparation process prior to implantation and therefore challenges the production process. Furthermore, a different scaffold could be used, providing biomechanical characteristics or/and a growth factor-releasing mechanism, supporting spontaneous chondrogenic differentiation [32]. The study does not address the influence of time, which could lead to further maturation of the regenerative tissue under the influence of the natural environment. Furthermore, other groups have tested injection techniques of SMSC, showing successful treatment of osteoarthritis or cartilage lesions [20, 25, 33]. However, the functioning mechanism of this approach remains uncertain, because it is not clear whether the cells are enriched in the lesion and how the cells act.

5. Conclusion

Synovium-derived stem cells (SMSC) demonstrated a high chondrogenic potential in vitro. When used for matrix-associated implantation in a defect model in rabbits, undifferentiated SMSC showed macroscopic and immunohistological repair results comparable to the current standard utilizing amplified chondrocytes. However, biomechanical resistance and histological scoring were inferior. Considering the large evidence for the potential of SMSC in cartilage regeneration, the search for alternative protocols and conditions should continue. Furthermore, the study suggests that allogenic implantation is possible for both mesenchymal stem cells

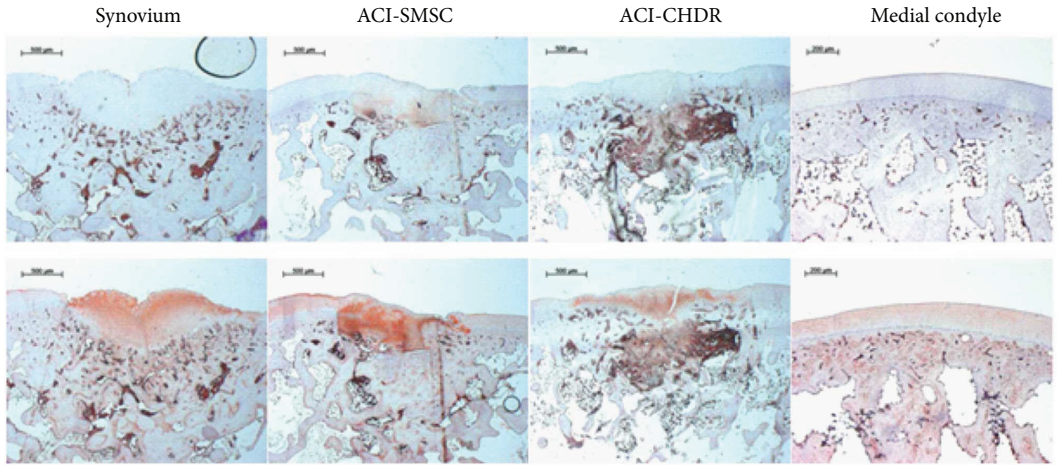

(a)

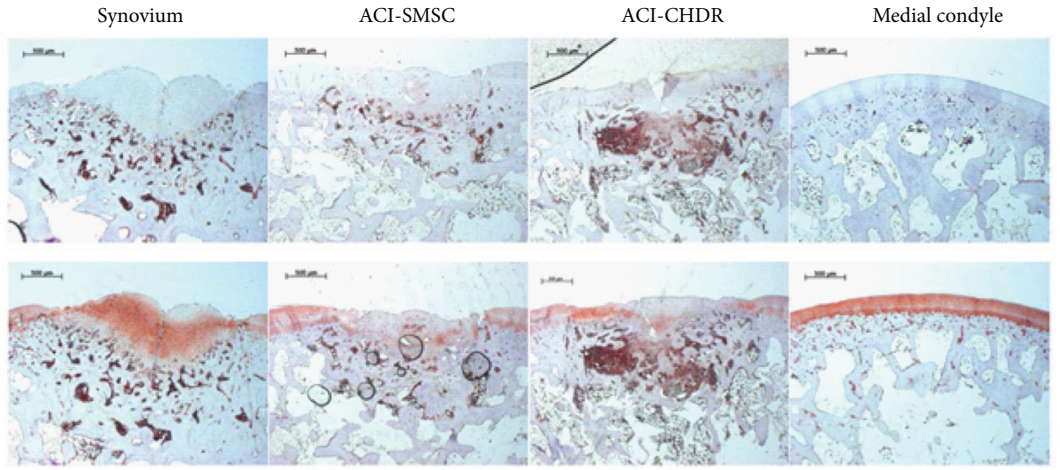

(b)

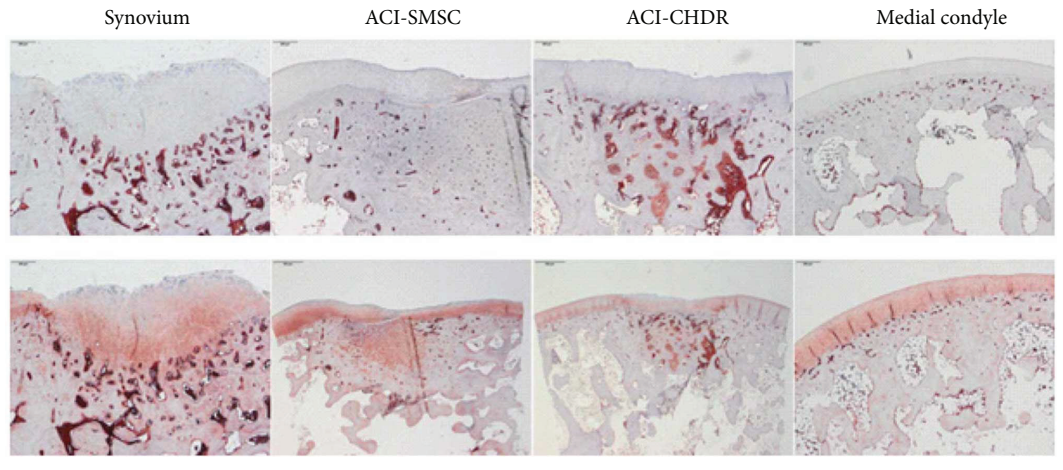

(c)

Figure 4: (a) Collagen type I staining of the medial condyle showing the defect region with regenerative tissue following the different interventions. The slides of the upper row were stained with an isotype control antibody; the slides of the lower row were stained using the specific antibody. Red color indicates positive staining. (b) Collagen type II staining of the medial condyle showing the defect region with regenerative tissue following the different interventions. The slides of the upper row were stained with an isotype control antibody; the slides of the lower row were stained using the specific antibody. Red color indicates positive staining. (c) Collagen type X staining of the medial condyle showing the defect region with regenerative tissue following the different interventions. The slides of the upper row were stained with an isotype control antibody; the slides of the lower row were stained using the specific antibody. Red color indicates positive staining.

and chondrocytes, offering a significant simplification of the matrix-associated cell implantation.

Disclosure

An earlier version of this work was presented as a poster at ECM Meeting Abstracts 2017.

Conflicts of Interest

The authors declare that no competing interests exist.

Authors' Contributions

Hagen Schmal was responsible for the study's conception and design, contributed to the analysis and interpretation of the data, is the corresponding author, obtained funding, carried out the surgeries, coordinated the collaborations of the different research groups, and was responsible for writing the manuscript and for obtaining final approval for the submitted article. Justyna M. Kowal was responsible for the in vitro characterization of SMSC including qPCR and histology, supported the interpretation of the results, contributed to the conception of the study, and approved the final version of the article. Moustapha Kassem was responsible for coordinating the work in the cell lab, supported the interpretation of the results and writing the article, contributed to the conception of the study, and approved the final version of the article. Michael Seidenstuecker was responsible for the biomechanical tests, supported the interpretation of the results and writing the article, contributed to the conception of the study, and approved the final version of the article. Anke Bernstein was involved in the conception, supported the animal experiments, coordinated the lab work regarding biomechanical testing and histology, supported this with her expertise, had significant input in the interpretation of data, and approved the final version of the article. Katharina Böttiger supervised the animal experiments and was responsible for anesthesiology and aftercare of the rabbits, contributed to the conception of the study, supported the specimen preparation for the histological and biomechanical analysis, and approved the final version of the article. Tanshiyue Xiong carried out the immunohistology, supported the specimen preparation, and approved the final version of the article. Eva J. Kubosch contributed decisively to the conception and design of this study and the analysis and interpretation of the data, obtained funding, was responsible for the local coordination, participated in the operations, supported the specimen preparation for the histological and biomechanical analysis, drafted parts of the article, revised the article, and finally approved the submitted article.

Acknowledgments

The study was supported by a grant of the German Division of the AOTrauma (2015) and the Research Commission of the University of Freiburg Medical School (1072/15). The publication costs were provided by the Open Access Fund of the University of Southern Denmark, Odense.

Supplementary Materials

Supplementary Table 1: the used primer sequences. Supplementary Figures 4A–4C: a more detailed description of the biomechanical analysis. Supplementary Figure 2: osteogenic differentiation of rabbit SMSC. Supplementary Figure 3: a description of adipogenic differentiation of rabbit SMSC. *(Supplementary Materials)*

References

[1] C. A. Emery, E. M. Roos, E. Verhagen et al., "OARSI clinical trials recommendations: design and conduct of clinical trials for primary prevention of osteoarthritis by joint injury prevention in sport and recreation," *Osteoarthritis and Cartilage*, vol. 23, no. 5, pp. 815–825, 2015.

[2] P. Niemeyer, G. Salzmann, M. Feucht et al., "First-generation versus second-generation autologous chondrocyte implantation for treatment of cartilage defects of the knee: a matched-pair analysis on long-term clinical outcome," *International Orthopaedics*, vol. 38, no. 10, pp. 2065–2070, 2014.

[3] P. Niemeyer, J. M. Pestka, P. C. Kreuz et al., "Characteristic complications after autologous chondrocyte implantation for cartilage defects of the knee joint," *The American Journal of Sports Medicine*, vol. 36, no. 11, pp. 2091–2099, 2017.

[4] D. D. Campbell and M. Pei, "Surface markers for chondrogenic determination: a highlight of synovium-derived stem cells," *Cell*, vol. 1, no. 4, pp. 1107–1120, 2012.

[5] E. J. Kubosch, E. Heidt, P. Niemeyer, A. Bernstein, N. P. Südkamp, and H. Schmal, "In-vitro chondrogenic potential of synovial stem cells and chondrocytes allocated for autologous chondrocyte implantation - a comparison," *International Orthopaedics*, vol. 41, no. 5, pp. 991–998, 2017.

[6] E. J. Kubosch, E. Heidt, A. Bernstein, K. Böttiger, and H. Schmal, "The trans-well coculture of human synovial mesenchymal stem cells with chondrocytes leads to self-organization, chondrogenic differentiation, and secretion of TGFβ," *Stem Cell Research & Therapy*, vol. 7, no. 1, p. 64, 2016.

[7] T. Kurth, E. Hedbom, N. Shintani et al., "Chondrogenic potential of human synovial mesenchymal stem cells in alginate," *Osteoarthritis and Cartilage*, vol. 15, no. 10, pp. 1178–1189, 2007.

[8] B. A. Jones and M. Pei, "Synovium-derived stem cells: a tissue-specific stem cell for cartilage engineering and regeneration," *Tissue Engineering Part B: Reviews*, vol. 18, no. 4, pp. 301–311, 2012.

[9] H. Yoshimura, T. Muneta, A. Nimura, A. Yokoyama, H. Koga, and I. Sekiya, "Comparison of rat mesenchymal stem cells derived from bone marrow, synovium, periosteum, adipose tissue, and muscle," *Cell and Tissue Research*, vol. 327, no. 3, pp. 449–462, 2007.

[10] M. Pei, F. He, B. M. Boyce, and V. L. Kish, "Repair of full-thickness femoral condyle cartilage defects using allogeneic synovial cell-engineered tissue constructs," *Osteoarthritis and Cartilage*, vol. 17, no. 6, pp. 714–722, 2009.

[11] T.-H. Lee, Y.-H. Huang, N.-K. Chang et al., "Characterization and spinal fusion effect of rabbit mesenchymal stem cells," *BMC Research Notes*, vol. 6, no. 1, p. 528, 2013.

[12] J. S. Jurvelin, T. Räsänen, P. Kolmonens, and T. Lyyra, "Comparison of optical, needle probe and ultrasonic techniques for the measurement of articular cartilage thickness," *Journal of Biomechanics*, vol. 28, no. 2, pp. 231–235, 1995.

[13] S. Sim, A. Chevrier, M. Garon et al., "Electromechanical probe and automated indentation maps are sensitive techniques in assessing early degenerated human articular cartilage," *Journal of Orthopaedic Research*, vol. 35, no. 4, pp. 858–867, 2017.

[14] W. C. Hayes, L. M. Keer, G. Herrmann, and L. F. Mockros, "A mathematical analysis for indentation tests of articular cartilage," *Journal of Biomechanics*, vol. 5, no. 5, pp. 541–551, 1972.

[15] K. P. H. Pritzker, S. Gay, S. A. Jimenez et al., "Osteoarthritis cartilage histopathology: grading and staging," *Osteoarthritis and Cartilage*, vol. 14, no. 1, pp. 13–29, 2006.

[16] W. Remmele and H. E. Stegner, "Recommendation for uniform definition of an immunoreactive score (IRS) for immunohistochemical estrogen receptor detection (ER-ICA) in breast cancer tissue," *Pathologe*, vol. 8, no. 3, pp. 138–140, 1987.

[17] L. Goebel, P. Orth, A. Müller et al., "Experimental scoring systems for macroscopic articular cartilage repair correlate with the MOCART score assessed by a high-field MRI at 9.4 T–comparative evaluation of five macroscopic scoring systems in a large animal cartilage defect model," *Osteoarthritis and Cartilage*, vol. 20, no. 9, pp. 1046–1055, 2012.

[18] J.-P. Berteau, M. Oyen, and S. J. Shefelbine, "Permeability and shear modulus of articular cartilage in growing mice," *Biomechanics and Modeling in Mechanobiology*, vol. 15, no. 1, pp. 205–212, 2016.

[19] C. H. Lee, J. L. Cook, A. Mendelson, E. K. Moioli, H. Yao, and J. J. Mao, "Regeneration of the articular surface of the rabbit synovial joint by cell homing: a proof of concept study," *The Lancet*, vol. 376, no. 9739, pp. 440–448, 2010.

[20] M. Pei, F. He, J. Li, J. E. Tidwell, A. C. Jones, and E. B. McDonough, "Repair of large animal partial-thickness cartilage defects through intraarticular injection of matrix-rejuvenated synovium-derived stem cells," *Tissue Engineering Part A*, vol. 19, no. 9-10, pp. 1144–1154, 2013.

[21] K. Nishimura, L. A. Solchaga, A. I. Caplan, J. U. Yoo, V. M. Goldberg, and B. Johnstone, "Chondroprogenitor cells of synovial tissue," *Arthritis and Rheumatism*, vol. 42, no. 12, pp. 2631–2637, 1999.

[22] Y. Sakaguchi, I. Sekiya, K. Yagishita, and T. Muneta, "Comparison of human stem cells derived from various mesenchymal tissues: superiority of synovium as a cell source," *Arthritis and Rheumatism*, vol. 52, no. 8, pp. 2521–2529, 2005.

[23] J. Mak, C. L. Jablonski, C. A. Leonard et al., "Intra-articular injection of synovial mesenchymal stem cells improves cartilage repair in a mouse injury model," *Scientific Reports*, vol. 6, no. 1, article 23076, 2016.

[24] I. Sekiya, T. Muneta, M. Horie, and H. Koga, "Arthroscopic transplantation of synovial stem cells improves clinical outcomes in knees with cartilage defects," *Clinical Orthopaedics*, vol. 473, no. 7, pp. 2316–2326, 2015.

[25] N. Ozeki, T. Muneta, H. Koga et al., "Not single but periodic injections of synovial mesenchymal stem cells maintain viable cells in knees and inhibit osteoarthritis progression in rats," *Osteoarthritis and Cartilage*, vol. 24, no. 6, pp. 1061–1070, 2016.

[26] H. Fujie, R. Nansai, W. Ando et al., "Zone-specific integrated cartilage repair using a scaffold-free tissue engineered construct derived from allogenic synovial mesenchymal stem cells: biomechanical and histological assessments," *Journal of Biomechanics*, vol. 48, no. 15, pp. 4101–4108, 2015.

[27] K. Shimomura, W. Ando, Y. Moriguchi et al., "Next generation mesenchymal stem cell (MSC)-based cartilage repair using scaffold-free tissue engineered constructs generated with synovial mesenchymal stem cells," *Cartilage*, vol. 6, 2_Supplement, pp. 13S–29S, 2015.

[28] A. T. Mehlhorn, P. Niemeyer, K. Kaschte et al., "Differential effects of BMP-2 and TGF-β1 on chondrogenic differentiation of adipose derived stem cells," *Cell Proliferation*, vol. 40, no. 6, pp. 809–823, 2007.

[29] S. Choi, G. M. Kim, Y. H. Maeng et al., "Autologous bone marrow cell stimulation and allogenic chondrocyte implantation for the repair of full-thickness articular cartilage defects in a rabbit model," *Cartilage*, article 194760351770122, 2017.

[30] C.-S. Lin and T. F. Lue, "Defining vascular stem cells," *Stem Cells and Development*, vol. 22, no. 7, pp. 1018–1026, 2013.

[31] C. McKee, Y. Hong, D. Yao, and G. R. Chaudhry, "Compression induced chondrogenic differentiation of embryonic stem cells in three-dimensional polydimethylsiloxane scaffolds," *Tissue Engineering Part A*, vol. 23, no. 9-10, pp. 426–435, 2017.

[32] M. Morille, K. Toupet, C. N. Montero-Menei, C. Jorgensen, and D. Noël, "PLGA-based microcarriers induce mesenchymal stem cell chondrogenesis and stimulate cartilage repair in osteoarthritis," *Biomaterials*, vol. 88, pp. 60–69, 2016.

[33] D. Hatsushika, T. Muneta, T. Nakamura et al., "Repetitive allogeneic intraarticular injections of synovial mesenchymal stem cells promote meniscus regeneration in a porcine massive meniscus defect model," *Osteoarthritis and Cartilage*, vol. 22, no. 7, pp. 941–950, 2014.

Hindawi
Stem Cells International
Volume 2018, Article ID 7061898, 12 pages
https://doi.org/10.1155/2018/7061898

Research Article

Low Magnitude of Compression Enhances Biosynthesis of Mesenchymal Stem Cells towards Nucleus Pulposus Cells via the TRPV4-Dependent Pathway

Yibo Gan,[1,2] **Bing Tu**,[1] **Pei Li**,[3] **Jixing Ye**,[1] **Chen Zhao**,[1] **Lei Luo**,[1] **Chengmin Zhang**,[1] **Zetong Zhang**,[1] **Linyong Zhu**,[4] **and Qiang Zhou**[1]

[1]*National & Regional United Engineering Laboratory of Tissue Engineering, Department of Orthopedics, Southwest Hospital, Third Military Medical University (Army Medical University), 29 Gao Tan Yan Street, Shapingba District, Chongqing 400038, China*
[2]*Institute of Rocket Force Medicine, State Key Laboratory of Trauma, Burns and Combined Injury, Third Military Medical University (Army Medical University), 30 Gao Tan Yan Street, Shapingba District, Chongqing 400038, China*
[3]*Department of Orthopedic Surgery, No.89 Hospital of PLA, Weifang, 261026 Shandong, China*
[4]*Key Laboratory for Advanced Materials, Institute of Fine Chemicals, East China University of Science and Technology, 130 Meilong Road, Shanghai 200237, China*

Correspondence should be addressed to Qiang Zhou; zq_tlh@163.com

Received 8 January 2018; Accepted 28 February 2018; Published 17 April 2018

Academic Editor: Peng Chang

Mesenchymal stem cell- (MSC-) based therapy is regarded as a promising tissue engineering strategy to achieve nucleus pulposus (NP) regeneration for the treatment of intervertebral disc degeneration (IDD). However, it is still a challenge to promote the biosynthesis of MSC to meet the requirement of NP regeneration. The purpose of this study was to optimize the compressive magnitude to enhance the extracellular matrix (ECM) deposition towards discogenesis of MSCs. Thus, we constructed a 3D culture model for MSCs to bear different magnitudes of compression for 7 days (5%, 10%, and 20% at the frequency of 1.0 Hz for 8 hours/day) using an intelligent and mechanically active bioreactor. Then, the underlying mechanotransduction mechanism of transient receptor potential vanilloid 4 (TRPV4) was further explored. The MSC-encapsulated hybrids were evaluated by Live/Dead staining, biochemical content assay, real-time PCR, Western blot, histological, and immunohistochemical analysis. The results showed that low-magnitude compression promoted anabolic response where high-magnitude compression induced the catabolic response for the 3D-cultured MSCs. The anabolic effect of low-magnitude compression could be inhibited by inhibiting TRPV4. Meanwhile, the activation of TRPV4 enhanced the biosynthesis analogous to low-magnitude compression. These findings demonstrate that low-magnitude compression promoted the anabolic response of ECM deposition towards discogenesis for the 3D-cultured MSCs and the TRPV4 channel plays a key role on mechanical signal transduction for low-magnitude compressive loading. Further understanding of this mechanism may provide insights into the development of new therapies for MSC-based NP regeneration.

1. Introduction

Intervertebral disc degeneration (IDD) has become a severe socioeconomic issue that attracts public attention in recent years. With the fastening of aging society, increasing number of people are influenced by lower back pain, neck pain, and reduced labor ability caused by IDD [1]. However, current treatments, including bed rest, exercise, physical therapy, and surgery, could only relieve the symptom but not remove the etiology of IDD, which cannot stop the development of IDD progression [2]. Therefore, there is an urgent need to find an effective treatment targeting the etiology of IDD.

Nucleus pulposus (NP), the central hydrated jelly-like tissue of the intervertebral disc (IVD), plays a core role in the process of IDD [3]. With the degeneration of the NP, the dehydrated NP lose its ability to exert the hydrostatic

pressure within the IVD. Thus, the physiological tensile stress on outer annulus fibrosis (AF) is converted to the non-physiological compressive stress. The change would accelerate the degeneration of AF and eventually lead to disc herniation. Therefore, repairing the degenerated NP is the key to the treatment of IDD. However, there is still no way to repair the NP because it lacks the capabilities of self-renewal and self-regeneration. Therefore, tissue engineering technology, particularly stem cell-based strategy to renew the NP, is the hot spot of current research for the treatment of IDD [4].

In recent years, research showed that mesenchymal stem cells (MSCs) have great potential in the field of NP regeneration [5]. MSC has shown several advantages as seed cells such as wide-range sources, easy accessibility, and ability of orientable differentiation, which makes it one of potential ideal cell source for NP regeneration. Previously, we successfully established a codelivery system of a dextran/gelatin hydrogel with TGF-β3-loaded PLGA nanoparticles that induced MSCs into discogenesis cells in situ [6]. Hiyama et al. recently reported that MSC-based tissue engineering strategy could be applied to repair the degenerated disc in canine [7]. These studies have shown the promising prospect to construct a tissue-engineered NP. A previous study has shown that a functional tissue-engineered NP needs to realize matrix deposition for encapsulated cells, which is the foundation of a repaired disc to bear mechanical loading [8]. However, the biosynthesis of MSC is relatively insufficient to meet the requirement even though we have proved that they could express the discogenesis phenotype with suitable orientation induction [6]. Thus, it is particularly important to find effective stimulation to enhance the biosynthesis of MSC.

Mechanical loading is one of the most effective external stimulations that significantly influence the cell fate [9]. Recent study has shown that the biosynthesis of the nucleus pulposus cells could be strengthened by proper magnitude of compressive loading when the disc was ex vivo cultured in a bioreactor [10]. Wang et al. also found that the expression of some critical genes which targets extracellular matrix (ECM) could be regulated with certain magnitude of compression [11]. However, whether could mechanical compression be applied to enhance the biosynthesis of MSC towards discogenesis is still indistinct. It is worth noting that the IVD is a load-bearing tissue *in vivo* and the mechanical stimulation is an ever-present external physical condition. If the proper magnitude of mechanical loading could be distinguished to boost the MSC biosynthesis, the function of the regenerative NP and subsequently the repaired IVD could be continuously restored using surgical technique.

In this study, the MSCs encapsulated in hydrogel were properly discogenesis induced with the previous 3D culture system. The biological effect of a relatively wide magnitude of the dynamic compression (5–20%) on encapsulated MSCs was studied using an intelligent and mechanically active bioreactor. The overall objective of this study was to investigate the potential of dynamic compression on the enhancement of the NP-like biosynthesis for MSCs. To achieve this, we first evaluated the cell viability of 3D-cultured MSCs under different magnitudes of dynamic compression. Second, we investigated the ECM deposition profile of 3D-cultured MSCs under the same mechanical environment. Finally, we further explored the underlying mechanism of its mechanical effect on the biosynthesis of MSCs.

2. Materials and Methods

2.1. Preparation of the TGF-β3-PLGANPs. The TGF-β3-loaded PLGANPs were prepared as previously described [6]. Briefly, 10 μg of TGF-β3 (PeproTech, USA) was dissolved in 0.1 mL of distilled water. Thereafter, PLGA (50,50, Sigma-Aldrich, USA) was dissolved in dichloromethane (Sigma-Aldrich, USA). Later, the TGF-β3 was added to the PLGA solution and treated with ultrasonic in an ice bath. Then, the emulsion was added to 1% polyvinyl alcohol (PVA, Sigma-Aldrich, USA) aqueous solution to treat with ultrasonic. The obtained emulsion was transferred into PVA aqueous solution and stirred. Then, the solid particles were collected and washed with deionized water.

2.2. Isolation and Culture of Mouse MSCs. All the animal experiments followed the guidelines of the local Animal Ethics Committee (SYXK (YU) 2012-0012) of the Third Military Medical University. As a previous study [12], bone marrow-derived MSCs were collected from 6-week-old Balb/c mouse after euthanasia. The bone marrow was harvested by blushing the femurs and tibiae with the complete culture medium consisting of Dulbecco's modified Eagle's medium (DMEM, HyClone, USA), 10% fetal bovine serum (FBS, Gibco, USA), and 1% penicillin/streptomycin (Gibco, USA). Using density gradient centrifugation, the MSCs were isolated from the bone marrow and cultured in culture dishes (Corning, USA). The adherent cells were collected by trypsinization (0.05% trypsin-EDTA, Gibco, USA) after 5 days. The medium was changed every 3 days.

2.3. Establishment of the 3D Culture System for the MSCs. 4A-PEG-acr (Mw 10,000, Jemkem Technology, China), oxidative dextran (Mw 100,000), and amino-modified gelatin were synthesized using previously described procedures [13]. The achieved solution was dialyzed by dialysis membrane (JingKeHongDa Biotechnology Co., China) in distilled water for 4 times per day to eliminate by-products. Finally, the mixture was lyophilized and cryopreserved. The IPN hydrogels were prepared as previously described [14]. Briefly, dextran, gelatin, and PEG solutions in PBS were mixed as the mass ratio of 5 : 3 : 2 to achieve a final polymer concentration of 10% while I2959 (Sigma-Aldrich, USA) concentration was 0.1%. Then, the P4 MSCs were premixed with precursor solutions at a density of 1×107 cells/mL. Then, the cell polymer mixture was injected into a cylindrical mold ($\varnothing = 5$ mm, height = 5 mm) for 1 min at 37°C to form the first network, followed by exposure to 365 nm UV light (5 W, UVATA, China) for 1 min to construct the second network. Then, the cell-encapsulated hydrogel was incubated in the culture dish in 5% CO_2 at 37°C and the culture media was replaced once per day.

2.4. The Design of the Intelligent and Mechanically Active Bioreactor. The custom-built bioreactor mainly consists of a

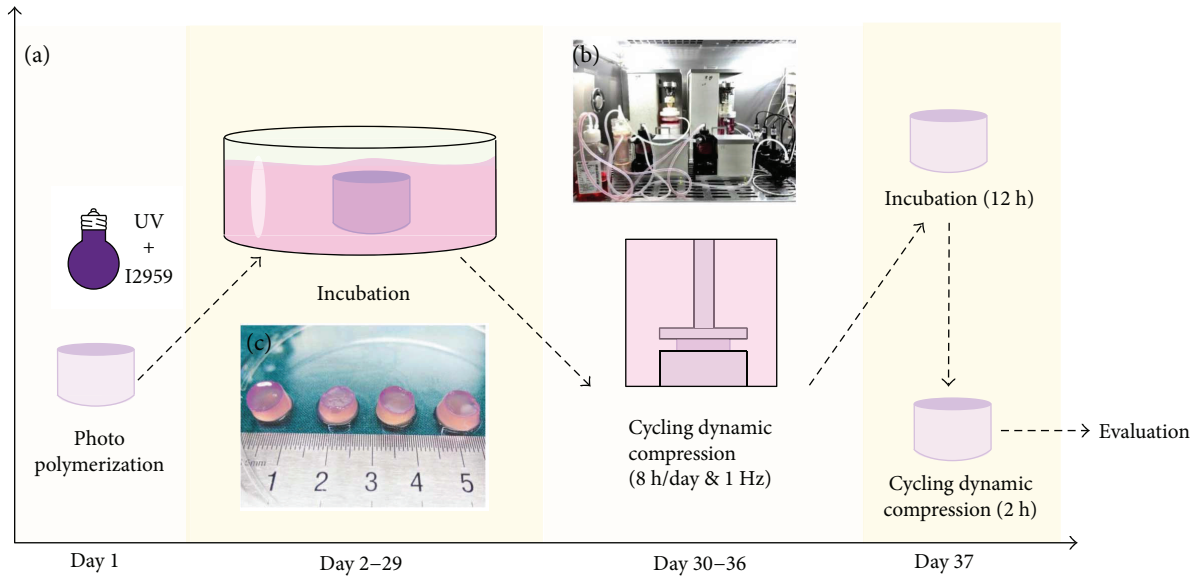

Figure 1: (a) Testing protocol of hybrid incubation and mechanical loading. The MSCs were encapsulated in the IPN hydrogel at day 1. The MSC-seeded hybrid was discogenesis induced and incubated for 28 days. Then, the composite hydrogel was treated with cyclic compressive loading for 7 days (5%, 10%, and 20% at the frequency of 1.0 Hz for 8 hours) and then evaluated at day 36. (b) Overview image of the bioreactor platform and primary units of the bioreactor. (c) Gross observation of the MSC-encapsulated hydrogels after compressive loading.

mechanical loading element, culture chamber, circulating perfusion equipment, biochemical composition monitoring platform, nutrient exchange equipment, and other attachments (Figure 1(b)). Mechanical loading is axially applied with an integrated servomotor integrated within the culture chamber. The magnitude of compression could be adjusted in real time based on feedback from a central controller. More details about the bioreactor could refer to our previous study [15].

2.5. Mechanical Loading Profile. Mechanical loading profile were illustrated in Figure 1(a). After 28 days of incubation, the cell-seeded hydrogels were transferred to the mechanically active bioreactor to conduct compressive loading. The hydrogels were randomly compressed with different magnitudes (5%, 10%, and 20%) at the frequency of 1 Hz for 8 hours per day. The compression durations (8 h) were chosen because it is the human physiological condition. The free swelling hydrogels were used as control. The bioreactor was perfused with fresh complete culture media at a rate of 15 mL/min for promoting nutrition supply and subsequently tissue remodeling. After 7 days of dynamic compression, the loaded hydrogels (Figure 1(c)) were transferred to the culture dishes to relax for 12 hours, followed by mechanical loading for 2 hours before sample evaluation.

To regulate TRPV4 channel activity under dynamic compression, media was supplemented with 10 μM GSK205, a TRPV4-selective antagonist or 1 nM GSK101, a TRPV4-selective agonist (Sigma-Aldrich, USA), during the compression stage as the experimental groups. The control group received the same amount of vehicle (0.1–0.2% DMSO) at the same time. During the static culture, all the samples were treated with fresh media without the TRPV4 antagonist or agonist.

2.6. Live/Dead Assay. The cell viability with different magnitudes of compression was investigated with the LIVE/DEAD Viability Assay Kit (Invitrogen, USA), according to the manufacturer's instructions. Briefly, the hybrids were washed with PBS for 3 times and incubated with 1 mL of PBS containing 4 mM EthD-1 and 2 mM calcein AM for 30 min at 37°C ($n = 3$). Then, the washed hybrids were visualized by a laser scanning confocal microscopy (LSCM. Zeiss 780, Germany). Living cell/dead cell ratio was calculated by ImageJ software (Wayne Rasband, National Institute of Health, USA).

2.7. Biochemistry Assays. MSC hydrogel hybrids in each group were lyophilized ($n = 3$). Cellular DNA content, cell-associated glycosaminoglycan (GAG), and hydroxyproline (HYP) were measured. Double-stranded DNA content was determined via a Quant-iT™ PicoGreen® assay kit (Invitrogen, USA) in accordance with manufacturer's protocol. Total double-stranded DNA content in each sample was determined from a standard curve developed from serial dilutions of DNA stock provided. Total sulfated GAG content was quantified using the dimethylmethylene blue assay as described before [16]. GAG content was determined via a standard curve developed from serial dilutions of known concentrations of chondroitin sulfate sodium salt. HYP content was quantified according to methods adapted from the study of Blumenkrantz and Asboe-Hansen [17]. HYP content was determined using a standard curve of known concentrations of HYP.

2.8. Histological Analysis. The collected specimens ($n = 3$) were rinsed twice with PBS and fixed in 4% paraformaldehyde for 24 h. Then, they were then embedded in paraffin

Table 1: Real-time polymerase chain reaction primers.

Gene		Sequence	Size
Aggrecan	Forward	5′ ATTTCCACACGCTACACCCTG 3′	164 bp
	Reverse	5′ TGGATGGGGTATCTGACTGTC 3′	
Type II	Forward	5′ CAGGATGCCCGAAAATTAGGG 3′	132 bp
Collagen α1	Reverse	5′ ACCACGATCACCTCTGGGT 3′	
Sox-9	Forward	5′ TCAACGGCTCCAGCAAGAACAAG 3′	194 bp
	Reverse	5′ CTCCGCCTCCTCCACGAAGG 3′	
GAPDH	Forward	5′ GGAGTTGCTGTTGAAGTCGCA 3′	532 bp
	Reverse	5′ GGAGTTGCTGTTGAAGTCGCA 3′	

Primers for aggrecan, type II collagen α1, Sox-9, and GAPDH were designed from *Mus musculus* gene sequences obtained from the NCBI GenBank and RefSeq databases using Primer 5.0 software.

and sectioned in 4 μm thickness. Serial sections were stained with Masson trichrome.

2.9. Immunohistochemical Analysis. For visualizing analysis of ECM deposition, collected hybrids were moved into paraffin and sectioned in 4 μm thickness ($n = 3$). Thereafter, the sections were immunostained with aggrecan following a standard immunohistochemistry staining procedure. The aggrecan (1 : 400, sc-16492, Santa Cruz Biotechnology, USA) and goat anti-mouse horseradish peroxidase-conjugated secondary antibody (1 : 1000, CW0102, Cwbiotech, USA) were applied in the analysis.

2.10. Real-Time PCR Assay. To determine the sensing and responding pattern of the MSCs under different magnitudes of compression, the specific gene expressions of discogenesis including aggrecan, type II collagen, and Sox-9 were assessed using real-time polymerase chain reaction (RT-PCR) and GAPDH was used as the internal reference. The MSC hydrogel-seeded hybrids were treated with TRIzol (Geno Technology Inc., USA) and fully grounded. RNA was extracted and cDNA was generated by applying cDNA reverse transcription kit (Life Technologies, USA) and diluted to 5 ng/μL. Gene expression was analyzed by quantitative RT-PCR (Applied Biosystems 7500, Thermo Fisher Scientific, USA). Data were calculated by the $2^{-\Delta\Delta Ct}$ method ($n = 3$). The primers used in this study are shown in Table 1.

2.11. Western Blotting Analysis. A semiquantitative analysis of differentiation was performed on cell-seeded hydrogels via Western blotting as described previously using the following antibodies that were diluted in 3% BSA in TBST buffer: aggrecan (1 : 1000, sc-16492, Santa Cruz Biotechnology, USA), Col II (1 : 5000, ab34712, Abcam, USA), and Sox-9 (1 : 1000, sc-20095, Santa Cruz Biotechnology, USA) antibodies and goat anti-mouse horseradish peroxidase-conjugated secondary antibody (1 : 2000, CW0102, Cwbiotech). And the protein level was quantified and normalized to GAPDH bands by densitometry in Quantity One software (version 4.6.2, Bio-Rad, $n = 3$).

2.12. Statistical Analysis. All of the quantitative data are presented as the mean ± standard deviation. One-way ANOVA was used to assess the statistical significance of results between groups by SPSS software (version 15.0, IBM, USA). Differences were considered significant when $p < 0.05$.

3. Results

3.1. Cell Viability of Encapsulated MSCs in the IPN Hydrogel under Dynamic Compression. A fluorescent Live/Dead staining was used to visualize the cell viability within the hydrogels. Living cells are stained by calcium AM, which yields a green fluorescence. Membranes of dead cells comprise EthD-1, yielding a red fluorescence. Fluorescent images of MSC hydrogel hybrids were obtained after mechanical exposure (Figures 2(a)–2(d)). In the hybrids copied with no compression (free swelling (FS) group) or lower magnitude of compression (5% magnitude of compression (5%) group), the retentive cells were almost living and very few dead cells could be found. However, in the hybrids treated with moderate compression (10% magnitude of compression (10%) group) or high compression (20% magnitude of compression (20%) group), much more dead cells were presented although the living cells still accounted for the majority. Quantitative analysis of the data (Figure 2(e)) showed that the proportion of viable cells in the FS or 5% groups was significantly higher than those in the 10% or 20% groups ($p < 0.05$). Interestingly, there is no significant difference between the FS and 5% groups ($p > 0.05$). The data from DNA content analysis were in good agreement with the Live/Dead assay (Figure 2(f)). The results demonstrated that our 3D culture system exhibited good cytocompatibility and cell viability of MSCs under the absence of stress or low-magnitude compressive stress. In contrast, the viability of MSCs was declined when treated with moderate- or high-magnitude compressive stress. Low-magnitude mechanical environment is possible to be favorable to the compressed MSCs.

3.2. ECM Deposition under Different Magnitudes of Compressive Stress. In order to study the effect of different magnitudes of compressive stress on the biosynthesis of

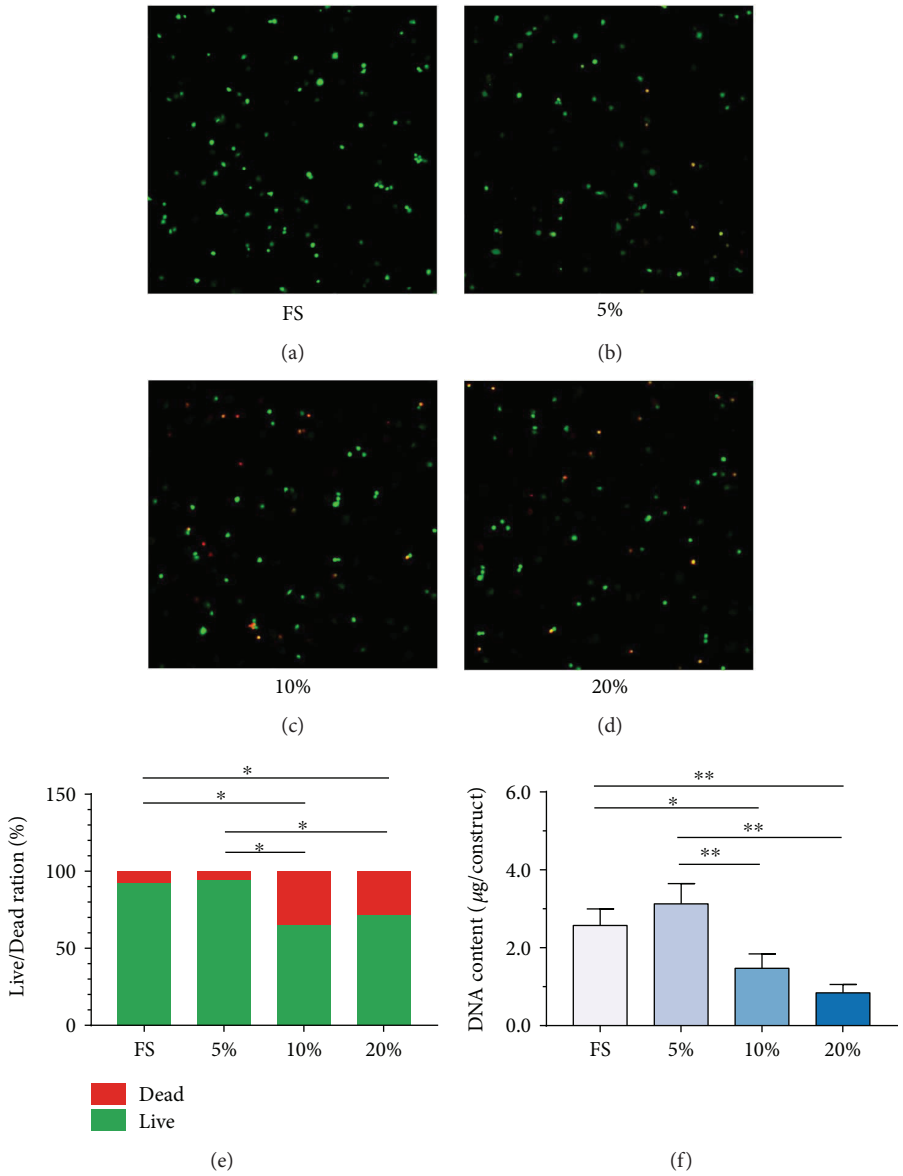

Figure 2: Cell viability of encapsulated MSCs in the IPN hydrogel. (a–d) A fluorescent Live/Dead staining for the MSC-encapsulated hybrids treated with free swelling (FS), compressive loading at magnitude of 5% (5%), compressive loading at magnitude of 10% (10%), and compressive loading at magnitude of 20% (20%) (magnification: 40x). (e) Quantification of NPC percent (Live/Dead) for the fluorescent Live/Dead staining. (f) Measurement of the DNA content of MSC-seeded hybrids treated with free swelling and compressive loading at magnitudes of 5%, 10%, and 20%. Data were expressed as means ± SD ($n = 3$). $^{*}p < 0.05$ and $^{**}p < 0.01$.

MSCs encapsulated in the hydrogels, the ECM deposition was quantitatively analyzed by biochemical composition assay, RT-PCR, and Western blot. As shown in Figures 3(a) and 3(b), MSCs treated with low-magnitude compression exhibited significantly higher GAG ($p < 0.05$) and HYP ($p < 0.01$) contents compared with those of the FS group, demonstrating elevated ECM deposition under low-magnitude compressive stimulation. However, the biochemical composition under 10% or 20% magnitude of compression was significantly decreased compared with that in the FS group ($p < 0.05$). In the gene transcription level, the discogenesis ECM-related genes, including aggrecan, type II collagen, and Sox-9, were also significantly upregulated after 7 days of 5% magnitude of compression when compared with all the other three groups (Figures 3(c)–3(e)). With increasing magnitude of compression, the gene expression exhibited an obviously declining trend and the 20% group constantly showed the lowest gene expression among all the groups. At the protein level, the results were similar to the gene expression (Figures 3(f)–3(i)). The encapsulated MSCs presented the highest expression of ECM-related proteins when treated with low magnitude of compression whereas the lowest expression suffered from the high-magnitude of compression.

The effect was further validated by histological and immunohistochemical staining (Figure 4). In the Masson trichrome staining, the chondrogenesis collagen fiber could be blue stained. As shown in Figure 4(a), the number and

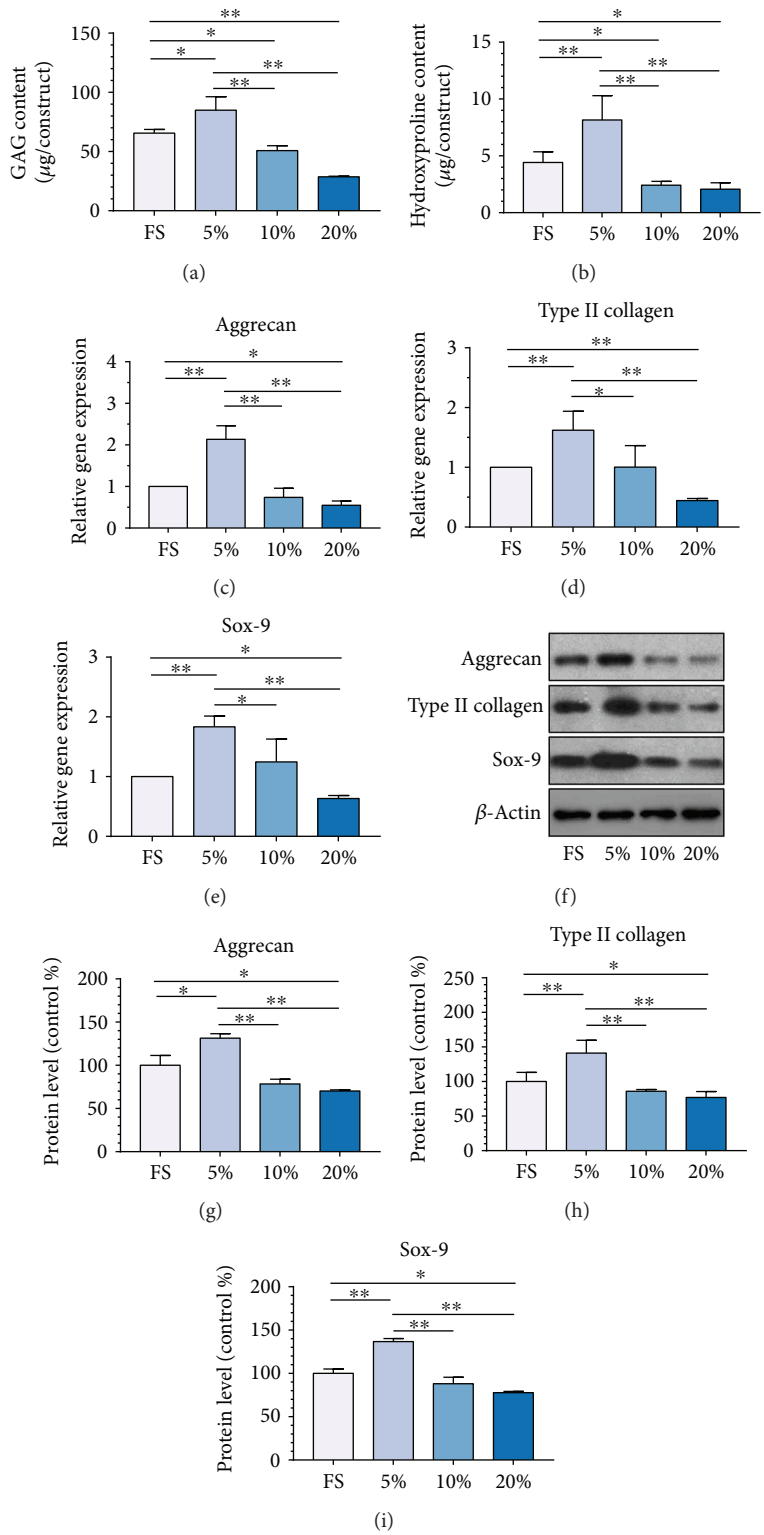

Figure 3: ECM deposition under different magnitudes of compressive stress. Measurement of the biochemical compositions, including (a) GAG content and (b) HYP content under different magnitudes of compressive stress. (c–e) The gene expressions of (c) aggrecan, (d) type II collagen, and (e) Sox-9 of MSC seeded in the hydrogel treated with free swelling and compressive loading at magnitudes of 5%, 10%, and 20%. The expression levels, quantified using real-time PCR, are normalized to those of housekeeping gene, GADPH. (f) Western blotting analysis of ECM proteins, aggrecan, type II collagen, and Sox-9 produced by MSCs cultured in the hydrogels treated with free swelling and compressive loading at magnitudes of 5%, 10%, and 20%. (g–i) The histogram of quantitative results of Western blot analysis. Data were normalized to the data obtained from MSCs cultured in the hydrogel treated with free swelling and evaluated on a relative basis for comparison between different samples. Data were expressed as means ± SD ($n = 3$). $^{*}p < 0.05$ and $^{**}p < 0.01$.

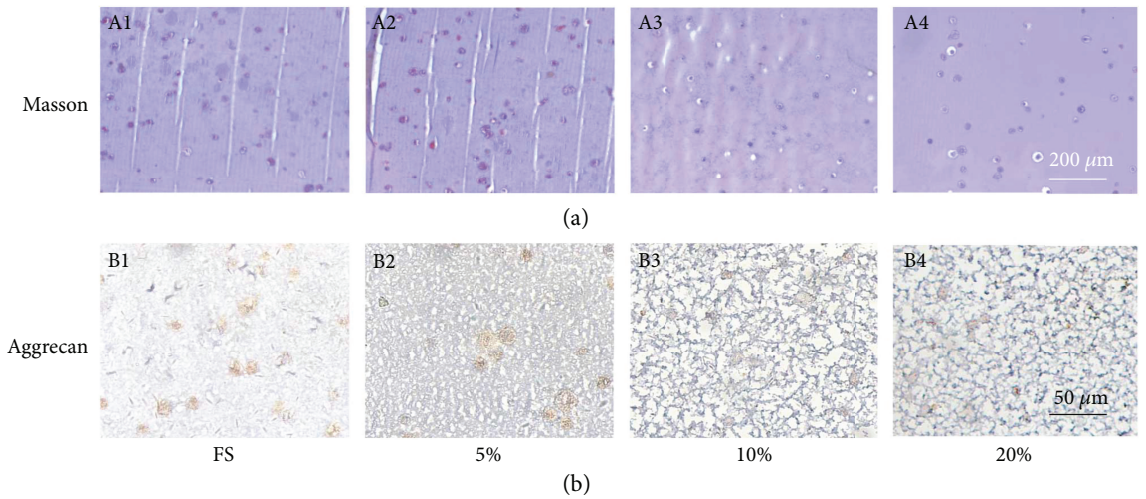

Figure 4: Histological observation of the MSC-encapsulated hybrids. (a) Photomicrographs showed Masson trichrome staining of the MSC-encapsulated hybrids treated with free swelling and compressive loading at magnitudes of 5%, 10%, and 20%. (b) The immunohistochemistry staining of the deposition of aggrecan in the MSC-encapsulated hybrids treated with free swelling and compressive loading at magnitudes of 5%, 10%, and 20%. White bar = 200 mm. Black bar = 50 mm. ($n = 3$).

intensity of blue staining MSCs in the hydrogels were also much higher in the groups of FS and 5%. With the increasing of compressive magnitude, the blue staining cell number and intensity were decreasing gradually.

The immunohistochemistry for aggrecan showed the similar situation that low-magnitude compression strongly promoted aggrecan deposition in the encapsulated MSCs. All these data demonstrated that the biosynthesis of MSCs towards nucleus pulposus appeared as an obvious dose-response relationship, namely, low-intensity compression which promoted the anabolism, while high-intensity compression enhanced the catabolism.

3.3. The Anabolic Effect of Low-Magnitude Compression Is Inhibited by Inhibiting the Transient Receptor Potential Vanilloid 4 (TRPV4) Channel. TRPV4 has been recently reported to play an important role in the mechanosensitivity of chondrocyte [18]. We further investigated whether the function of TRPV4 is related to the mechanotransduction of 3D-cultured MSCs. The cell-seeded hybrids were dynamically loaded for 7 days with low- or high-magnitude compression, both in the presence and absence of GSK205, the TRPV4 antagonists. As shown in Figures 5(a) and 5(b), the GSK205 exposure alone had no effect on the GAG and HYP content in the FS group ($p > 0.05$). When treated with low magnitude of compression, the loading-induced elevated GAG and HYP content were partially attenuated by GSK205 ($p < 0.01$). However, GSK205 had no effect on the biochemical composition of the hybrids under high-magnitude compression ($p > 0.05$). The inhibiting effect of GSK205 was further validated in protein level by Western blot analysis. The results showed that GSK205 could significantly inhibit the anabolic effect of low-magnitude compression on the expressions of aggrecan and type II collagen ($p < 0.05$). Nevertheless, the ECM-related protein expressions were not affected by GSK205 in the FS and 20% groups ($p > 0.05$), which was consistent with the above data. These results demonstrated that the anabolism of 3D-cultured MSCs induced by low-magnitude compression was possible via a TRPV4 channel-dependent manner.

3.4. Activation of TRPV4 Enhanced the Biosynthesis Analogous to Low-Magnitude Compression. In order to explore the function of the TRPV4 channel on the biosynthesis of MSCs, the MSC-encapsulated hybrids were exposed to the TRPV4 agonist GSK1016790A (GSK101) during the dynamic loading. Interestingly, as shown in Figures 6(a) and 6(b), GSK101 could significantly enhance the GAG and HYP syntheses in the hybrids in the FS group ($p < 0.05$). In contrast, the anabolic effect was not obvious when treated with dynamic loading, under neither the low magnitude of compression nor high magnitude of compression ($p > 0.05$). The result of the protein level is in good agreement with above results. The expressions of aggrecan and type II collagen are significantly upregulated by GSK101 ($p < 0.01$), and the anabolic effect of activating TRPV4 was similar to that of low-magnitude compression. GSK101 could slightly upregulate the ECM-related protein expression under low-magnitude compression but the effect was not significant ($p > 0.05$). No obvious effect of GSK101 on the protein expression could be found for the hybrids under high-magnitude compression. The above results illustrated that GSK101 processes a similar proanabolic function to low-magnitude compression by activating the TRPV4 channel.

4. Discussion

The therapy of IDD has drawn increasing attention owing to the rapidly growing number of patients with lower back pain or neck pain in recent years. Cell-based therapeutic strategy, particularly using MSC as cell source, shows promise in overcoming the self-renewal disability of NP cells, which was regarded as the difficulty to regenerate the degenerated

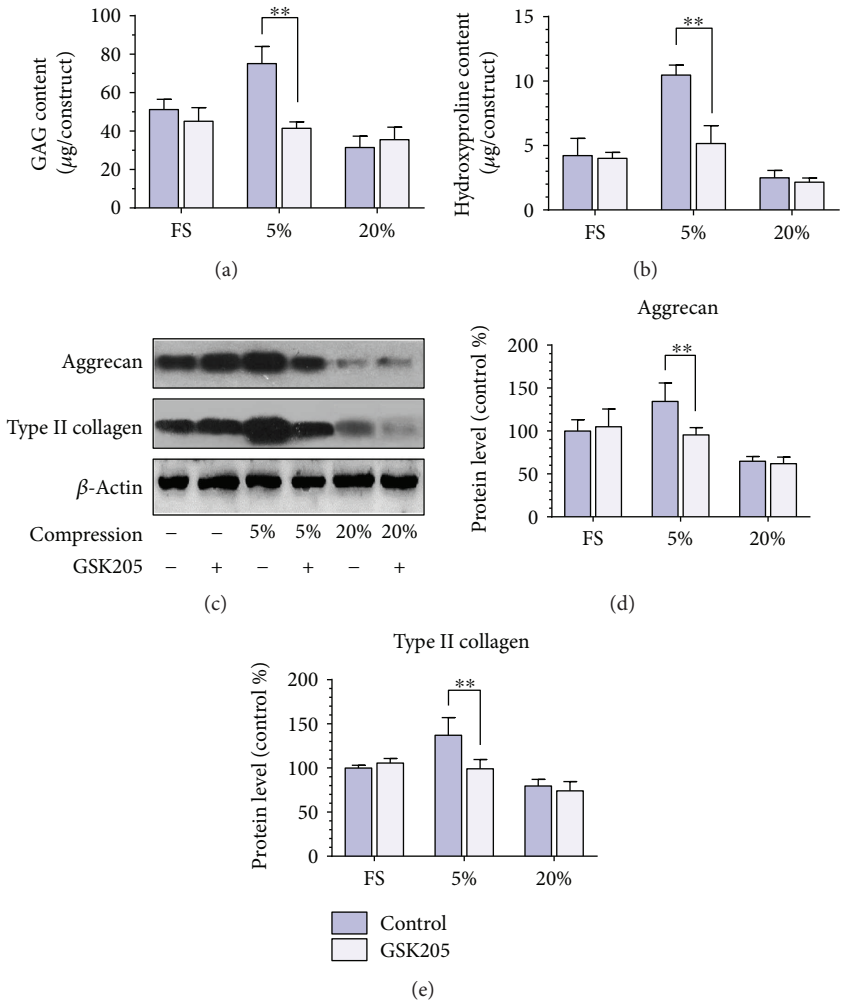

Figure 5: The anabolic effect of low-magnitude compression is inhibited by inhibiting the TRPV4 channel. Measurement of the biochemical compositions, including (a) GAG content and (b) HYP content treated with GSK205, the TRPV4 antagonists, during different magnitudes of compressive stress. The hybrids that were not treated with GSK205 were used as control. (c) Western blot analysis of ECM proteins aggrecan and type II collagen produced by MSCs cultured in the hydrogels treated with GSK205 during free swelling and compressive loading at magnitudes of 5%, 10%, and 20%. The hybrids that were not treated with GSK205 were used as control. (d–e) The histogram of quantitative results of Western blot analysis. Data were normalized to the data obtained from MSCs cultured in the hydrogel only treated with free swelling and evaluated on a relative basis for comparison between different samples. Data were expressed as means ± SD ($n = 3$). $^{**}p < 0.01$.

IVD. To promote the efficiency of discogenesis for MSCs, it is critical to develop effective stimulation in inducing oriental differentiation and biosynthesis. The aim of the study is to optimize compressive magnitude to enhance the ECM deposition of the MSCs. Therefore, we investigated the biosynthesis effect of different magnitudes of compressive stress on a tissue-engineered NP developed by MSCs and explored the related mechanism preliminarily.

In the study, we constructed the 3D culture system for MSCs by using an IPN hydrogel as scaffold. Our previous study has shown that the IPN hydrogel is tough enough to resist the extremely high magnitude of compression without structural failure [14]. Meanwhile, it exhibited as friendly to the encapsulated cell for long-term culture. The advantages of mechanical strength and bioactivity make the IPN hydrogel a suitable 3D culture scaffold to conduct the mechanical biological study. It is as biomimetic as a previous ex vivo organ model [10] while as uncomplicated as a previous single-layer 2D cell model [19]. The annulus fibrosus would be injured inevitably when hydrogel was injected into the NP cavity. Previously, our study has showed the good injectability of IPN hydrogel and an illuminating device for minimal invasion was prepared. Thus, the IPN hydrogel-based 3D culture system is suitable to be used as cell carrier for disc regeneration *in vivo*. In addition, the mechanically active bioreactor could realize the dynamic mechanical loading which is closer to the actual situation of the IVD *in vivo* than the traditional hydrostatic pressure model [15]. Simultaneously, the monitoring of the magnitude of compression and nutrition compositions in the bioreactor decreases the error caused by confound factors. All these conditions make our model a suitable model for mechanical biological study.

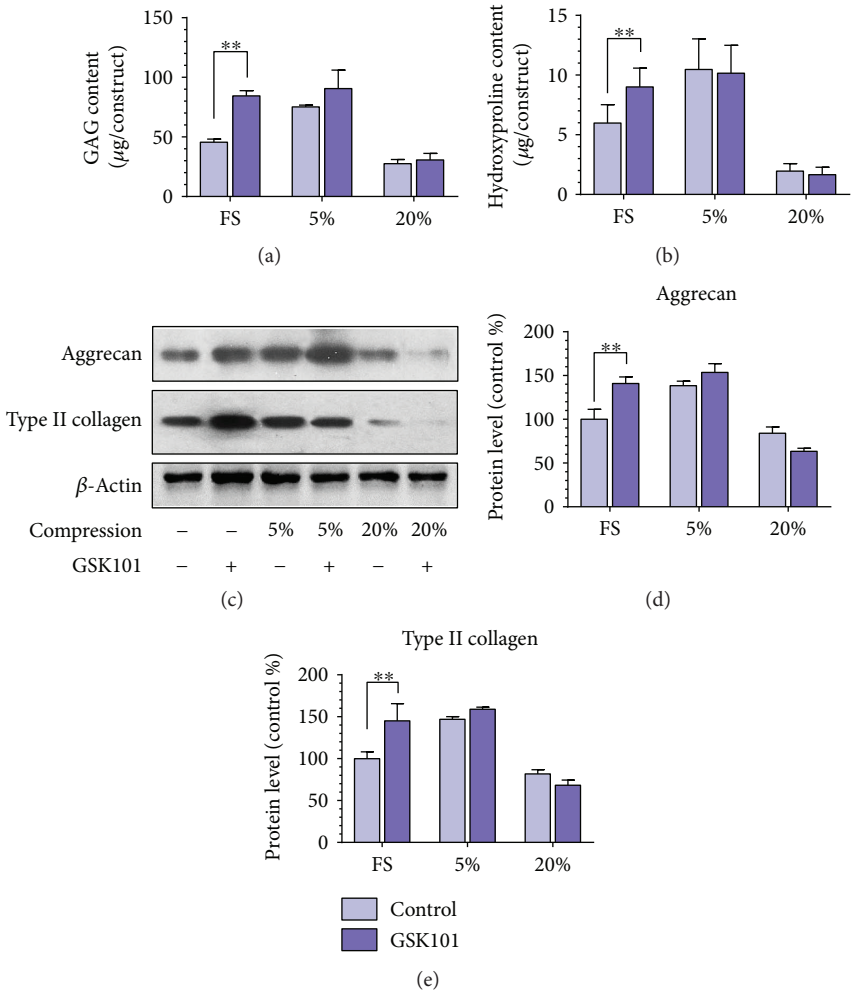

Figure 6: Activation of TRPV4 enhanced biosynthesis analogous to low-magnitude compression. Measurement of the biochemical compositions, including (a) GAG content and (b) HYP content treated with GSK101, the TRPV4 agonist, during different magnitudes of compressive stress. The hybrids that were not treated with GSK101 were used as control. (c) Western blot analysis of ECM proteins aggrecan and type II collagen produced by MSCs cultured in the hydrogels treated with GSK101 during free swelling and compressive loading at magnitude of 5%, 10%, and 20%. The hybrids that were not treated with GSK101 were used as control. (d–e) The histogram of quantitative results of Western blot analysis. Data were normalized to the data obtained from MSCs cultured in the hydrogel only treated with free swelling and evaluated on a relative basis for comparison between different samples. Data were expressed as means ± SD ($n = 3$). $^{**}p < 0.01$.

IVD *in vivo* is subject to dynamic compression during daily activities. The persistent mechanical environment is extremely important for the biological behavior of the NP [20] including the regenerated NP using cell-based therapy. If the biological effect of different mechanical environments could be understood thoroughly, the mechanical environment could be utilized to alter the biological performance of the implanted tissue-engineered NP. A previous study indicates that the biological responses of disc cells to dynamic compression are magnitude dependent in disc cell culture and animal *in vivo* studies [21]. In the present study, low-magnitude compression had little effect on the cell viability compared with free swelling. However, the cell viability was decreasing rapidly with improving the compressive magnitude. This phenomenon was in agreement with our recent study which indicated that high-magnitude compression could increase the apoptotic cells within the immature NP [10].

IVD is a load-bearing organ essentially, and NP is the central component of the mechanical behavior in the IVD. Aggrecan, one of the major ECM compositions of a NP, could absorb the water into the NP and keep the balance of external loading and internal hydrostatic pressure of the NP, which is the determinant of the load-bearing ability of the NP [22]. Thus, the ECM synthesis and secretion are core functions of natural NP cells and the key parameter of a tissue-engineered NP. Obviously, low-magnitude compression (5%) could improve the expression of aggrecan and type II collagen of the MSC-encapsulated hybrids in mRNA and protein level compared with the free swelling hybrid. Sox-9, the key regulator of ECM synthesis towards chondrogenesis [23], was also significantly elevated by low-magnitude

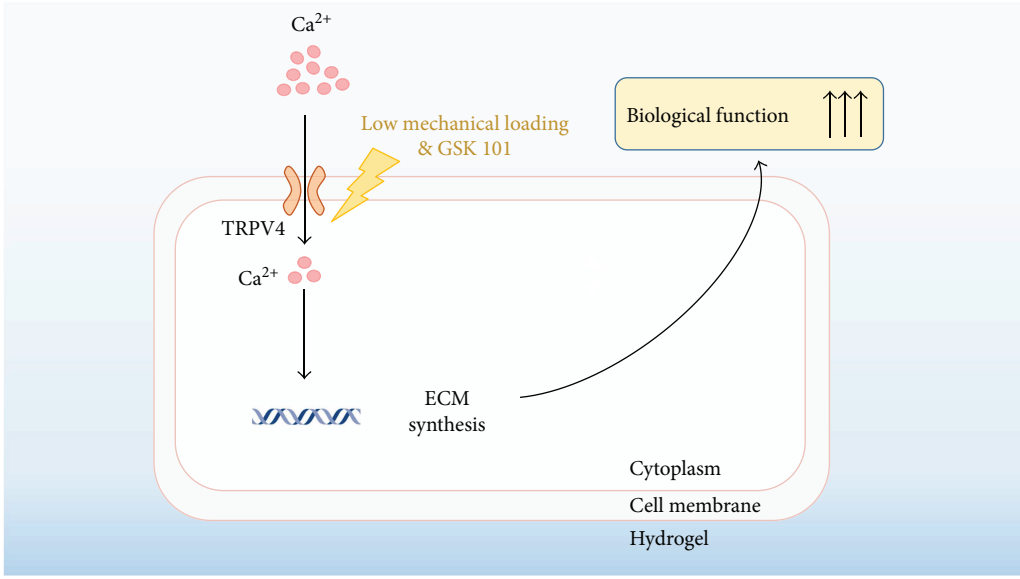

Figure 7: Schematic diagram. The low magnitude of compression and GSK101 could activate the TRPV4 channel on the cell membrane in MSCs. TRPV4, the Ca^{2+}-preferred membrane ion channel, is possible to transduce the external mechanical signals into internal response of biosynthesis expression via the generation of intracellular Ca^{2+} influx. The gene expression could result in ECM synthesis and secretion at last, improving the biosynthesis capability of MSCs towards discogenesis.

compression. In theory, low-magnitude compression is beneficial to the cell status because the persistent fluctuations of compression and relaxing lead to a pumping effect of the fluid exchange of the disc matrix [24]. The hydrogel scaffold is also a matrix full of retentive water. The phenomenon in this study should attribute to the dynamic compression could make the culture media movement into and out of the disc matrix, which is supportive to improve cell biological function as previous study [25]. In the study, low-magnitude compression could not influence the cell viability yet, but the biosynthesis was effectively changed. However, it is noteworthy that the high magnitude of compression had a negative effect on the biosynthesis of 3D-cultured MSCs, which is consistent with the pathology of IDD [26]. Our previous study also reported that a relatively high compressive magnitude can decrease matrix deposition within the immature NP [10].

TRPV4 is a Ca^{2+}-preferred membrane ion channel which extensively participated in transducing external physical and chemical signals into internal biological responses via the generation of intracellular Ca^{2+} transients [27, 28]. O'Conor et al. recently reported the TRPV4-dependent anabolic response of chondrocytes to the mechanical stimulation, suggesting that TRPV4 plays a key role in the maintenance of matrix homeostasis under mechanical loading [18]. The upregulated biosynthesis under the low-magnitude of compression in MSCs made us hypothesize that TRPV4 might be implicated in the process of mechanotransduction. In the study, the inhibition of TRPV4 made mechanically induced elevated ECM biosynthesis and matrix accumulation totally compromised. The surprising result indicated that TRPV4 plays a critical role in transducing mechanical signals of MSCs, especially for low-magnitude compression. We also found that the activation of TRPV4 by a chemical agonist could induce analogous anabolic effect on ECM with the low magnitude of compression, further confirming that these anabolic responses of MSCs were transduced via TRPV4. It has been reported that Ca^{2+} transient signaling is one of the earliest events in response to mechanical loading [29, 30]. In the process of low-magnitude compression on the MSC-encapsulated hybrids, TRPV4 could lead the Ca^{2+} influx and subsequently transduce a diverse set of biosynthesis responses (Figure 7). However, it is confusing why the ECM expressions under the high magnitude of compression were not influenced by TRPV4. Maybe, the dominant mechanotransduction mechanism is different for MSCs under different magnitudes of compression. The mechanism of the TRPV4 channel during MSC compressive stress remains to be studied further.

Previously, researchers had used growth factors or phytochemicals to enhance ECM synthesis [30–32]. However, the establishment of a long-term controlled release system is the hindrance for these drugs' application [33]. Toh et al. also reported that the relative softer scaffold with lower crosslinking density could also promote matrix deposition of MSCs towards chondrogenesis [34]. But the rapid degradation of soft hydrogel with low crosslink density might influence the effect in long term. We focused on mechanical loading owing to its long-term effect. A recent study has shown that the dynamic fixation system for treatment of IDD could reduce the mechanical bearing of the target disc [35]. What is more, the degenerated disc could be rehydrated after reducing the loading by the kind of treatment in some cases [36]. It could be a promising strategy to combine implantation with MSC-based hydrogel and fixation with the precise mechanical control system to make the NP regeneration into reality. There are some limitations in this study. The biological response of murine MSCs to mechanical loading is probably different from that of *Homo*

sapiens although a recent study has shown similar effects under mechanical loading [37]. Another limitation was that the status of MSCs *in vitro* is possible to be different from those *in vivo* because the microenvironment of the NP *in vivo* is of high acidity and low nutrient supply. In the future, an *in vivo* study should be conducted to explore the mechanical biological mechanism of MSCs by hydrogel injection in upright animals.

5. Conclusion

In summary, in this study, we investigated the ECM biosynthesis of a MSC-encapsulated hydrogel 3D culture system under different magnitudes of compression using an intelligent and mechanically active bioreactor. The findings from this study demonstrate that the biosynthesis of MSCs to dynamic compression is magnitude dependent. Low-magnitude compression promoted the anabolic response of ECM deposition towards discogenesis where high-magnitude compression induced the catabolic response for the 3D-cultured MSCs. The study further revealed the profound effects of mechanotransduction pathways that TRPV4 channel plays a key role on mechanical signal transduction of the low-magnitude compressive loading. Further understanding of this mechanism may provide insights into the development of new therapies for MSC-based NP regeneration.

Conflicts of Interest

The authors declare that there is no conflict of interests regarding the publication of this paper.

Acknowledgments

The authors thank Xue Yang for the excellent technical support. This study was funded by the NSFC of China (Grant nos. 81272029 and 81772378), Key Project of Military Logistics (BWS13C014-1), and Key Project of Military Medical Technology Innovation Program (SWH2016JSZD-01 and SWH2017JCZD-02).

References

[1] M. Juniper, T. K. Le, and D. Mladsi, "The epidemiology, economic burden, and pharmacological treatment of chronic low back pain in France, Germany, Italy, Spain and the UK: a literature-based review," *Expert Opinion on Pharmacotherapy*, vol. 10, no. 16, pp. 2581–2592, 2009.

[2] A. Di Martino, A. R. Vaccaro, J. Y. Lee, V. Denaro, and M. R. Lim, "Nucleus pulposus replacement: basic science and indications for clinical use," *Spine*, vol. 30, Supplement 16, pp. S16–S22, 2005.

[3] W. Johannessen and D. M. Elliott, "Effects of degeneration on the biphasic material properties of human nucleus pulposus in confined compression," *Spine*, vol. 30, no. 24, article E724, E729 pages, 2005.

[4] D. Oehme, T. Goldschlager, P. Ghosh, J. V. Rosenfeld, and G. Jenkin, "Cell-based therapies used to treat lumbar degenerative disc disease: a systematic review of animal studies and human clinical trials," *Stem Cells International*, vol. 2015, Article ID 946031, 16 pages, 2015.

[5] E. K. Shim, J. S. Lee, D. E. Kim et al., "Autogenous mesenchymal stem cells from the vertebral body enhance intervertebral disc regeneration via paracrine interaction: an in vitro pilot study," *Cell Transplantation*, vol. 25, no. 10, pp. 1819–1832, 2016.

[6] Y. Gan, S. Li, P. Li et al., "A controlled release codelivery system of MSCs encapsulated in dextran/gelatin hydrogel with TGF-β3-loaded nanoparticles for nucleus pulposus regeneration," *Stem Cells International*, vol. 2016, Article ID 9042019, 14 pages, 2016.

[7] A. Hiyama, J. Mochida, T. Iwashina et al., "Transplantation of mesenchymal stem cells in a canine disc degeneration model," *Journal of Orthopaedic Research*, vol. 26, no. 5, pp. 589–600, 2008.

[8] S. M. Richardson, G. Kalamegam, P. N. Pushparaj et al., "Mesenchymal stem cells in regenerative medicine: focus on articular cartilage and intervertebral disc regeneration," *Methods*, vol. 99, pp. 69–80, 2016.

[9] A. Wall and T. BoardP. Banaszkiewicz and D. Kader, "Biosynthetic response of cartilage explants to dynamic compression," in *Classic Papers in Orthopaedics*, Springer, London, 2014.

[10] P. Li, Y. Gan, H. Wang et al., "Dynamic compression effects on immature nucleus pulposus: a study using a novel intelligent and mechanically active bioreactor," *International Journal of Medical Sciences*, vol. 13, no. 3, pp. 225–234, 2016.

[11] Z. Wang, J. Leng, Y. Zhao et al., "N-cadherin maintains the healthy biology of nucleus pulposus cells under high-magnitude compression," *Cellular Physiology and Biochemistry*, vol. 43, no. 6, pp. 2327–2337, 2017.

[12] G. Yoshimatsu, N. Sakata, H. Tsuchiya et al., "Development of polyvinyl alcohol bioartificial pancreas with rat islets and mesenchymal stem cells," *Transplantation Proceedings*, vol. 45, no. 5, pp. 1875–1880, 2013.

[13] X. Geng, X. Mo, L. Fan, A. Yin, and J. Fang, "Hierarchically designed injectable hydrogel from oxidized dextran, amino gelatin and 4-arm poly(ethylene glycol)-acrylate for tissue engineering application," *Journal of Materials Chemistry*, vol. 22, no. 48, pp. 25130–25139, 2012.

[14] Y. Gan, P. Li, L. Wang et al., "An interpenetrating network-strengthened and toughened hydrogel that supports cell-based nucleus pulposus regeneration," *Biomaterials*, vol. 136, pp. 12–28, 2017.

[15] S.-T. Li, Y. Liu, Q. Zhou et al., "A novel axial-stress bioreactor system combined with a substance exchanger for tissue engineering of 3D constructs," *Tissue Engineering Part C: Methods*, vol. 20, no. 3, pp. 205–214, 2014.

[16] B. J. DeKosky, N. H. Dormer, G. C. Ingavle et al., "Hierarchically designed agarose and poly(ethylene glycol) interpenetrating network hydrogels for cartilage tissue engineering," *Tissue Engineering Part C Methods*, vol. 16, no. 6, pp. 1533–1542, 2010.

[17] N. Blumenkrantz and G. Asboe-Hansen, "An assay for hydroxyproline and proline on one sample and a simplified method for hydroxyproline," *Analytical Biochemistry*, vol. 63, no. 2, pp. 331–340, 1975.

[18] C. J. O'Conor, H. A. Leddy, H. C. Benefield, W. B. Liedtke, and F. Guilak, "TRPV4-mediated mechanotransduction regulates the metabolic response of chondrocytes to dynamic loading," *Proceedings of the National Academy of Sciences of*

the United States of America, vol. 111, no. 4, pp. 1316–1321, 2014.

[19] G. A. Sowa, J. P. Coelho, K. M. Bell et al., "Alterations in gene expression in response to compression of nucleus pulposus cells," *The Spine Journal*, vol. 11, no. 1, pp. 36–43, 2011.

[20] M. A. Adams, B. J. C. Freeman, H. P. Morrison, I. W. Nelson, and P. Dolan, "Mechanical initiation of intervertebral disc degeneration," *Spine*, vol. 25, no. 13, pp. 1625–1636, 2000.

[21] S. C. W. Chan, S. J. Ferguson, and B. Gantenbein-Ritter, "The effects of dynamic loading on the intervertebral disc," *European Spine Journal*, vol. 20, no. 11, pp. 1796–1812, 2011.

[22] P. J. Roughley, L. I. Melching, T. F. Heathfield, R. H. Pearce, and J. S. Mort, "The structure and degradation of aggrecan in human intervertebral disc," *European Spine Journal*, vol. 15, no. S3, pp. 326–332, 2006.

[23] H. J. Kim and G. I. Im, "Electroporation-mediated transfer of *SOX trio* genes (*SOX-5*, *SOX-6*, and *SOX-9*) to enhance the chondrogenesis of mesenchymal stem cells," *Stem Cells and Development*, vol. 20, no. 12, pp. 2103–2114, 2011.

[24] H.–. J. Wilke, P. Neef, M. Caimi, T. Hoogland, and L. E. Claes, "New *in vivo* measurements of pressures in the intervertebral disc in daily life," *Spine*, vol. 24, no. 8, pp. 755–762, 1999.

[25] J. C. Iatridis, M. Weidenbaum, L. A. Setton, and V. C. Mow, "Is the nucleus pulposus a solid or a fluid? Mechanical behaviors of the nucleus pulposus of the human intervertebral disc," *Spine*, vol. 21, no. 10, pp. 1174–1184, 1996.

[26] J. C. Lotz and J. R. Chin, "Intervertebral disc cell death is dependent on the magnitude and duration of spinal loading," *Spine*, vol. 25, no. 12, pp. 1477–1483, 2000.

[27] W. Everaerts, B. Nilius, and G. Owsianik, "The vanilloid transient receptor potential channel TRPV4: from structure to disease," *Progress in Biophysics and Molecular biology*, vol. 103, no. 1, pp. 2–17, 2010.

[28] C. Moore, F. Cevikbas, H. A. Pasolli et al., "UVB radiation generates sunburn pain and affects skin by activating epidermal TRPV4 ion channels and triggering endothelin-1 signaling," *Proceedings of the National Academy of Sciences of the United States of America*, vol. 110, no. 34, pp. E3225–E3234, 2013.

[29] S. K. Han, W. Wouters, A. Clark, and W. Herzog, "Mechanically induced calcium signaling in chondrocytes in situ," *Journal of Orthopaedic Research*, vol. 30, no. 3, pp. 475–481, 2012.

[30] I. Raizman, J. N. Amritha de Croos, R. Pilliar, and R. A. Kandel, "Calcium regulates cyclic compression-induced early changes in chondrocytes during in vitro cartilage tissue formation," *Cell Calcium*, vol. 48, no. 4, pp. 232–242, 2010.

[31] W. H. Chen, W. C. Lo, J. J. Lee et al., "Tissue-engineered intervertebral disc and chondrogenesis using human nucleus pulposus regulated through TGF-β1 in platelet-rich plasma," *Journal of Cellular Physiology*, vol. 209, no. 3, pp. 744–754, 2006.

[32] X. Han, X. Leng, M. Zhao, A. Chen, M. Wu, and H. Guoju, "Resveratrol increases nucleus pulposus matrix synthesis through activating the PI3K/Akt signaling pathway under mechanical compression in a disc organ culture," *Bioscience Reports*, vol. 37, no. 6, article BSR20171319, 2017.

[33] S. M. Richardson, J. A. Hoyland, R. Mobasheri, C. Csaki, M. Shakibaei, and A. Mobasheri, "Mesenchymal stem cells in regenerative medicine: opportunities and challenges for articular cartilage and intervertebral disc tissue engineering," *Journal of Cellular Physiology*, vol. 222, no. 1, pp. 23–32, 2010.

[34] W. S. Toh, T. C. Lim, M. Kurisawa, and M. Spector, "Modulation of mesenchymal stem cell chondrogenesis in a tunable hyaluronic acid hydrogel microenvironment," *Biomaterials*, vol. 33, no. 15, pp. 3835–3845, 2012.

[35] J. Gao, W. Zhao, X. Zhang et al., "MRI analysis of the ISOBAR TTL internal fixation system for the dynamic fixation of intervertebral discs: a comparison with rigid internal fixation," *Journal of Orthopaedic Surgery and Research*, vol. 9, no. 1, p. 43, 2014.

[36] L. Y. Fay, J. C. Wu, T. Y. Tsai, T. H. Tu, C. L. Wu, W. C. Huang et al., "Intervertebral disc rehydration after lumbar dynamic stabilization: magnetic resonance image evaluation with a mean followup of four years," *Advances in Orthopedics*, vol. 2013, Article ID 437570, 8 pages, 2013.

[37] P. Li, Z. Liang, G. Hou et al., "N-cadherin-mediated activation of PI3K/Akt-GSK-3β signaling attenuates nucleus pulposus cell apoptosis under high-magnitude compression," *Cellular Physiology and Biochemistry*, vol. 44, no. 1, pp. 229–239, 2017.

Hindawi
Stem Cells International
Volume 2018, Article ID 4686259, 14 pages
https://doi.org/10.1155/2018/4686259

Research Article

Human Urine-Derived Stem Cells: Potential for Cell-Based Therapy of Cartilage Defects

Long Chen,[1,2] Lang Li,[1] Fei Xing,[1] Jing Peng,[1] Kun Peng,[3] Yuanzheng Wang,[2] and Zhou Xiang[1]

[1]*Department of Orthopedics, West China Hospital, Sichuan University, Chengdu, Sichuan, China*
[2]*Department of Orthopedics, Guizhou Provincial People's Hospital, Guiyang, Guizhou, China*
[3]*Department of Orthopedics, The Second Affiliated Hospital of Nanchang University, Nanchang, China*

Correspondence should be addressed to Zhou Xiang; xiangzhou5@hotmail.com

Received 3 December 2017; Revised 25 February 2018; Accepted 19 March 2018; Published 17 April 2018

Academic Editor: Hui Bin Sun

Stem cell therapy is considered an optimistic approach to replace current treatments for cartilage defects. Recently, human urine-derived stem cells (hUSCs), which are isolated from the urine, are studied as a promising candidate for many tissue engineering therapies due to their multipotency and sufficient proliferation activities. However, it has not yet been reported whether hUSCs can be employed in cartilage defects. In this study, we revealed that induced hUSCs expressed chondrogenic-related proteins, including aggrecan and collagen II, and their gene expression levels were upregulated *in vitro*. Moreover, we combined hUSCs with hyaluronic acid (HA) and injected hUSCs-HA into a rabbit knee joint with cartilage defect. Twelve weeks after the injection, the histologic analyses (HE, toluidine blue, and Masson trichrome staining), immunohistochemistry (aggrecan and collagen II), and histologic grade of the sample indicated that hUSCs-HA could stimulate much more neocartilage formation compared with hUSCs alone, pure HA, and saline, which only induced the modest cartilage regeneration. In this study, we demonstrated that hUSCs could be a potential cell source for stem cell therapies to treat cartilage-related defects in the future.

1. Introduction

Cartilage defects caused by trauma injury and osteoarthritis (OA) are a major public health threat worldwide [1]. Cartilage defects lead to the restriction of joint activities, resulting in pain and a poor quality of life. Currently, treatment options for cartilage defects include physiotherapy, external medication, intra-articular irrigation, chondroplasty, microfracture, and mosaicplasty. However, these treatments cannot consistently stimulate the production of hyaline cartilage for tissue repair, completely fill the empty of the defect, or integrate repaired tissue with adjacent native tissue [2]. To address the issues, tissue engineering is considered to be a promising alternative strategy for the regeneration of cartilage.

Autologous chondrocyte implantation (ACI) is a type of cell therapy, in which healthy chondrocytes are harvested from nonlesion areas and transplanted back into lesion areas [3]. Recently, the Food and Drug Administration (FDA) in the United States approved the usage of autologous chondrocytes cultured on porcine collagen membrane (Maci) for repairing full-thickness cartilage defects in adult patients. For both ACI and Maci procedures, it is technically challenging to obtain a high density of chondrocytes and maintain their differentiation state [3–5]. Therefore, other cell sources need to be explored for tissue engineering. Previous studies demonstrated that mesenchymal stem cells (MSCs), such as human adipose tissue-derived stem cells (hASCs) and human bone marrow mesenchymal stem cells (hBMSCs), were potential stem cell sources for the applications of cartilage tissue engineering approaches [6, 7]. However, the sources of hBMSCs are limited and the procedure of obtaining hASCs is invasive, which urges the demand for more practical and suitable cell sources for tissue engineering of cartilage.

Since Zhang et al. initially described the isolation of MSCs from the human urine [8], hUSCs have received significant attention, and several advantages of hUSCs have been

identified. Firstly, hUSCs show robust proliferation ability and have the capacity for multipotent differentiation [9]. Secondly, hUSCs can be accessed via a simple, noninvasive, and low-cost approach, and thus surgical procedures are avoided [10]. More importantly, hUSCs that are isolated from autologous urine do not induce immune responses or rejection. In addition, since no invasive and painful procedures are involved during urine collection, there are fewer ethical issues. In previous studies [9, 11, 12], hUSCs were shown to differentiate into neuron-like cells, urothelial cells, smooth muscle cells, and osteoblasts, which have been successfully applied in studies involving neural, urinary, and bone tissue regeneration [9, 11, 12]. However, it has not yet been reported whether hUSCs can be applied to tissue regeneration of cartilage.

A novel strategy for the regeneration of cartilage defects involves seeding cells into/onto biomaterials [13]. Biomaterials provide a suitable microenvironment for cells, including mechanical support for engineered tissues [14]. Hyaluronic acid (HA) is an important component of synovial fluid, which protects joint cartilage by lubricating and absorbing shock [15]. Hence, HA is able to offer a suitable platform for cartilage repairing and is commonly used.

Therefore, in this study, we obtained hUSCs according to the previously described procedure of isolation and culture [8, 10] and assessed their capacity for chondrogenesis. We also investigated whether hUSCs could serve as a potential cell source for cartilage tissue engineering via comparing the therapeutic effects of hUSCs plus HA, hUSCs alone, HA alone, and normal saline after injections into cartilage defects of a rabbit knee joint. The therapeutic outcome was evaluated by gross appearance and histological and immunohistochemical analyses.

2. Materials and Methods

This study was conducted under the Guide for the Care and Use of Laboratory Animals of the National Institutes of Health. The Research Ethics Board for both human samples and animal protocols was approved by the Ethics Committee of West China Hospital, Sichuan University, Chengdu, China.

2.1. Isolation and Proliferation of Human Urine-Derived Stem Cells. Primary hUSCs were obtained from five healthy male adult donors, who were between 23 and 27 years old (mean age: 25 years) without urinary system disease, using the methods that were described previously [8, 10]. A total of 200 mL of the sterile urine sample was collected from each person, and subsequent steps were performed separately. Each sample was added with 1% penicillin and streptomycin and centrifuged for 10 minutes at 1500 rpm. The cell pellet was resuspended in 25 mL of phosphate-buffered saline (PBS) and centrifuged again for 10 minutes at 1500 rpm. Then, cells were seeded in 24-well plates with culture medium comprised of keratinocyte serum-free medium (KSFM) and embryonic fibroblast medium (EFM) at a ratio of 1 : 1 as well as 5% fetal calf serum (FBS) [8, 10]. The medium was changed every three days, and cells were passaged by using trypsin after reaching subconfluency.

To evaluate cell proliferation, hUSCs were seeded into a 96-well plate and incubated in 100 μL of cell culture medium at 37°C and 5% CO_2. Cell viability was assessed at days 0, 1, 3, 5, 7, and 9 using the Cell Counting Kit-8 (CCK-8; Life Technologies, USA). At each time point, 10 μL of CCK-8 reagent was added to each well and the optical density was measured using a spectrophotometer at a wavelength of 490 nm with a background correction at 630 nm.

2.2. Flow Cytometry Analysis. When at passage 4 (P4), hUSCs were harvested using trypsin-EDTA, and 1×10^6 hUSCs were resuspended in Hank's Balance Salt Solution (HBSS) supplemented with 1% (*v*/*v*) bovine serum albumin (BSA). Cells were incubated for 30 min at 4°C in the dark and followed by the following monoclonal antibodies: CD34-APC (BD, USA), CD45-PE (BD, USA), HLA-DR-PE (BD, USA), CD29-PE (BD, USA), CD73-PE (BD, USA), CD90-FITC (BD, USA), CD105 (Abcam, UK), and CD166 (Abcam, UK). Next, cells were washed with PBS and incubated with the appropriate secondary antibodies. Cells were analyzed using the Beckman Cytomics FC500 Flow Cytometry Analyzer (Beckman Coulter, USA).

2.3. Multilineage Differentiation Potential of Human Urine-Derived Stem Cells

2.3.1. Osteogenic Induction. To induce osteogenic differentiation, hUSCs were cultured at a density of 5×10^3 cells/well in a 6-well plate for 21 days under the condition of 37°C and 5% CO_2 in osteogenic medium (Cyagen Biosciences Inc., USA). The medium was replaced every 3 days. After induction, cells were fixed with 75% ethanol for 20 min and stained with Alizarin red solution (Sigma, USA) for 30 min.

2.3.2. Adipogenic Induction. hUSCs (4th passage) were cultured at a density of 5×10^3 cells/well in a 6-well plate and induced using adipogenic medium (Cyagen Biosciences Inc., USA). The medium was replaced every 3 days. After a total of 14 days, cells were fixed using 10% formalin and stained with Oil red O solution (Sigma, USA) for 30 min to visualize lipid vacuoles.

2.3.3. Chondrogenic Differentiation. To induce chondrogenic differentiation, 1×10^6 hUSCs were centrifuged for 5 min at 1500 rpm after which the pellet was resuspended in chondrogenic medium (Cyagen Biosciences Inc., USA). After the 21-day induction, toluidine blue solution was used to visualize extracellular matrix-bound proteoglycans. For immunofluorescence purposes, the pellet was embedding in optimum cutting temperature (OTC) compound after chondrogenic differentiation. Cells were subsequently incubated with anti-type II collagen (1 : 100; Novus, USA) and anti-aggrecan (1 : 100; Novus, USA) antibodies for 2 h, washed twice in PBS, and stained with anti-mouse Alexa Fluor 594 IgG (1 : 200; Jackson, USA). Nuclei were stained with DAPI. Cells were observed using a fluorescence microscope (Olympus IX50, Japan).

2.4. Quantitative Reverse Transcriptase Polymerase Chain Reaction (RT-PCR). After chondrogenic induction for 21

Table 1: Primer sequences (5′-3′) used for RT-PCR.

Gene	Primer sequences (5′ → 3′)	Amplification size (bp)
hCOL2A1F	GCTCCCAGAACATCACCTACC	192 bp
hCOL2A1R	CAGTCTTGCCCCACTTACCG	
hSox9F	CTCCTACCCGCCCATCAC	114 bp
hSox9R	TAGGTGAAGGTGGAGTAGAGGC	
hACANF	GCCTATCAGGACAAGGTCTCAC	185 bp
hACANR	ATGGCTCTGTAATGGAACACGA	
h-Actin r	CTGGAAGGTGGACAGCGAGG	205 bp
h-Actin f	TGACGTGGACATCCGCAAAG	

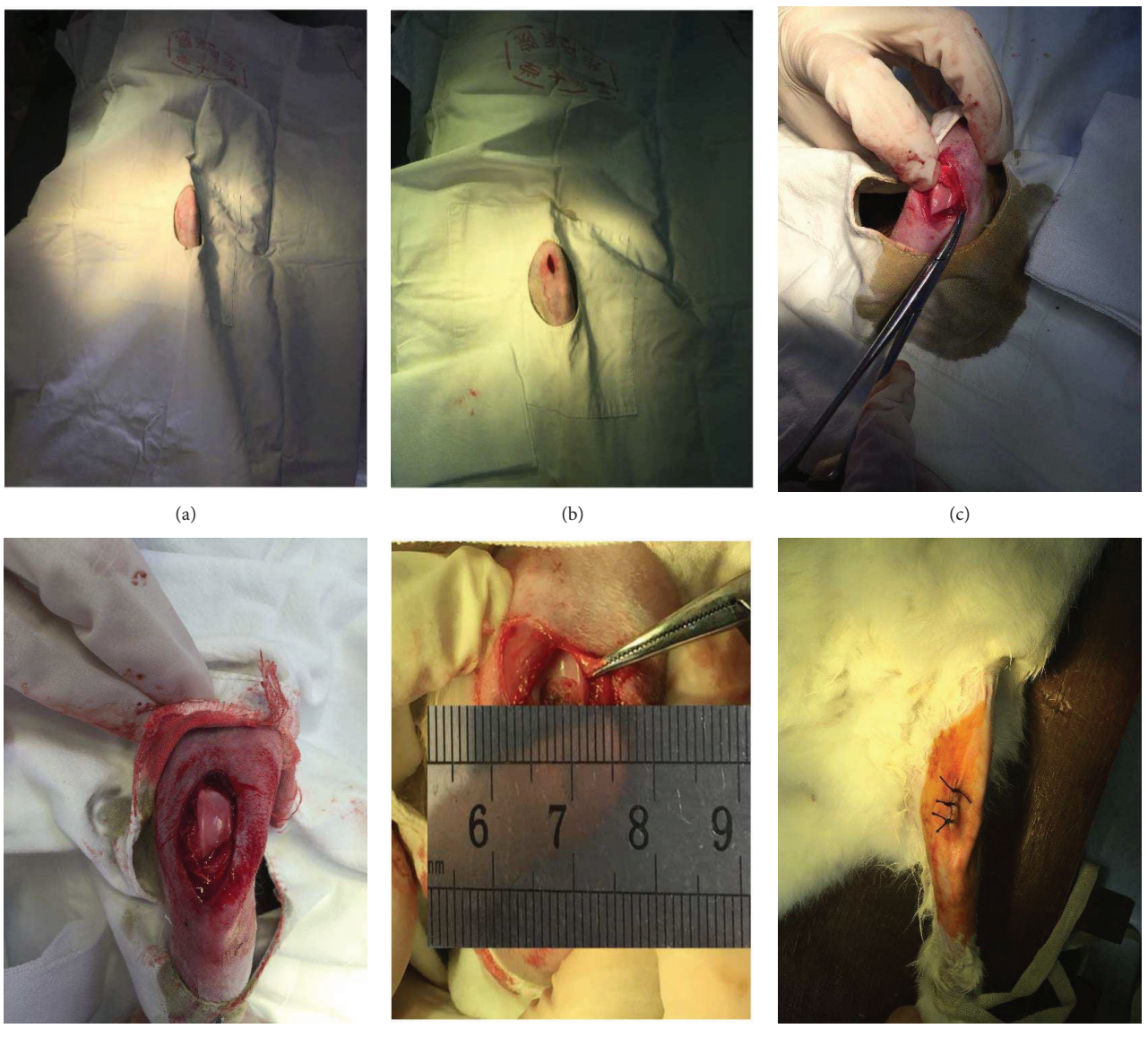

(a) (b) (c)

(d) (e) (f)

Figure 1: The process of the establishment of cartilage defect model. (a) General disinfection of the knee. (b) An incision was made on the medial joint of the knee. (c, d) After the joint capsule was opened, the patella was dislocated laterally and exposed femoral condyles. (e) A corneal trephine with a diameter of 5 mm was used to outline the cartilage defect site. (f) Wound closure.

Table 2: The semiquantitative scale for grading the natural healing articular cartilage: subcategories and their individual respective scores.

Feature	Score
Filling of defect	
100%	0
75%	1
50%	2
25%	3
0%	4
Reconstitution of osteochondral junction	
Yes	0
Almost	1
Not close	2
Matrix staining	
Normal	0
Reduced staining	1
Significantly reduced staining	2
Faint staining	3
No stain	4
Cell morphology	
Normal	0
Mostly hyaline and fibrocartilage	1
Mostly fibrocartilage	2
Some fibrocartilage but mostly nonchondrocytic cell	3
Nonchondrocytic cell only	4

days, cellular RNA was extracted using TRIzol reagent (Life Technologies, USA) and reverse-transcribed into cDNA using a PrimeScript RT reagent Kit (Takara, Japan). The expression of specific genes was quantified using an SYBR Premix Ex Taq II kit (Takara, Japan) in an IQ5 real-time system (Bio-Rad, USA). Primer sequences used for qPCR are presented in Table 1. The target gene expression was analyzed and compared to h-actin, which served as a reference gene.

2.5. Human Urine-Derived Stem Cells for Cartilage Tissue Engineering: In Vivo Study

2.5.1. Establishing the Mixture of hUSCs-Hyaluronic Acid for Injection. Hyaluronic acid (HA) was purchased from Furuida Biosciences (the concentration of HA solution was 1%). hUSCs and HA were mixed at a ratio of $1 \times 10^7 : 1$ mL. The mixture was supplied with the hUSC culture medium.

2.5.2. Cell Morphology, Viability, and Proliferation in hUSCs-HA. Cell morphology of hUSCs in HA was compared with that of hUSCs in PBS to assess the cell state. The viability of the cells in HA was determined using an annexin V-FITC/PI apoptosis detection kit [16]. Twenty-four hours after establishing the hUSCs-HA solution system, hUSCs were retrieved from the hUSCs-HA solution by centrifugation. The cell suspension was stained with 5 μL of FITC-conjugated annexin V and 10 μL of PI. Cells were analyzed by FACS Calibur (BD, USA).

Cell proliferation of hUSCs-HA and hUSCs-PBS was assessed at days 0, 1, 3, 5, and 7 using a CCK-8 kit (Life Technologies, USA) in the hUSC culture medium with HA or PBS. At each time point, 10 μL of CCK-8 reagent was added to each well, and the optical density was measured using a spectrophotometer at a wavelength of 490 nm with a background correction at 630 nm.

2.5.3. Animal Model. All surgeries were performed under general sodium pentobarbital anesthesia, and efforts were made to minimize the suffering of the animals. In this study, a total of twenty-four 12-week-old New Zealand white rabbits (2–2.5 kg, no gender limitation) were purchased from Chengdu Dashuo Laboratory Animal Limited Company. All the surgeries were conducted on both sides.

To establish a cartilage defect, rabbits were anesthetized with an intravenous injection of sodium pentobarbital (20 mg/kg). After general disinfection of the knee, an incision was made on the medial joint of the knee. After the joint capsule was opened, the patella was dislocated laterally and exposed femoral condyles. A corneal trephine with a diameter of 5 mm was used to outline the cartilage defect site. Noncalcified cartilage was scraped away using loupe visualization. The objective of modeling was to remove cartilage as much as possible without damaging the subchondral bone (Figure 1). After surgery, animals received antibiotics (penicillin for three consecutive days) and analgesics (buprenorphine for two days). Rabbits were monitored for the signs of activity, joint movement, local infection, and other complications.

Three weeks after surgery, rabbits were randomly divided into four groups for later injecting different therapeutic substances. We chose the lower and lateral edge of the patella for the injection of the substances and removed joint fluid by suction to confirm an accurate injection point. The following four groups were established: (i) group A (hUSCs plus HA, $n = 6$), 1×10^7 cells and 1 mL 1% HA (pH 6.7, 1000 kDa, Furuida, China) were injected into the knee joint cavity; (ii) group B (hUSCs, $n = 6$), 1×10^7 cells and 1 mL of normal saline were injected into knee joints; (iii) group C (HA group, $n = 6$), only 1 mL 1% HA was injected into knee joints; and (iv) group D is the control group with normal saline injected ($n = 6$).

2.5.4. Gross Appearance. Twelve weeks after injection, 24 rabbits were sacrificed and 48 knees were harvested. Surrounding soft tissues were removed, and defective cartilage tissue was obtained. Afterward, two investigators evaluated the gross appearance of the cartilage tissue, including the degree of repair, integration to the border zone, and macroscopic appearance on the surface.

2.5.5. Histological Analysis. Samples were washed twice with PBS, fixed in 4.0% paraformaldehyde for 7 days at 25–30°C, and decalcified in 10% formic acid for 3 months. After decalcification, the femoral condyles were cut into three pieces from lateral to medial condyle along the sagittal plane. All

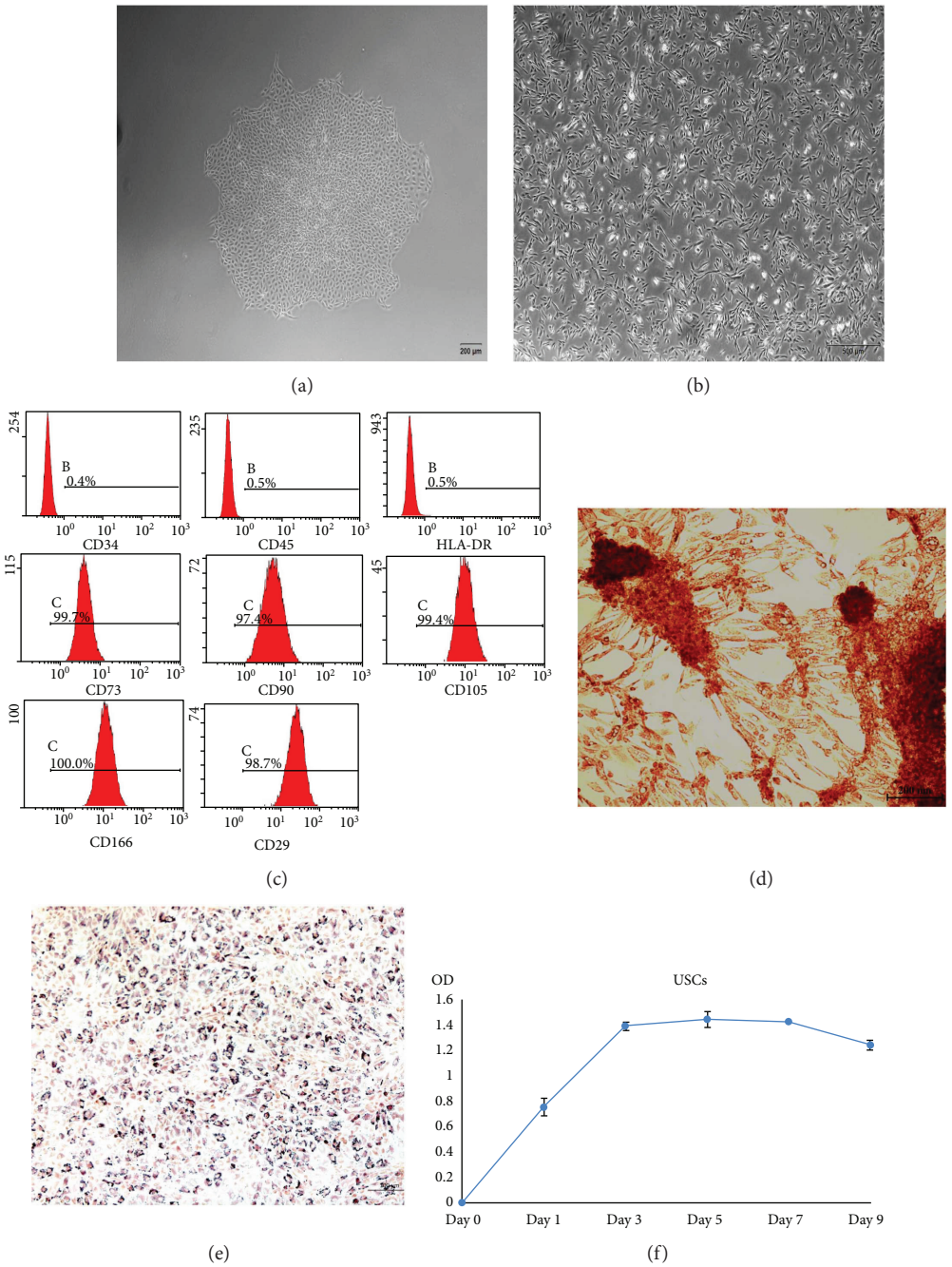

Figure 2: The morphology and characterization of hUSCs. (a) "Rice grain"-like appearance of hUSCs after initial plating. (b) Elongated morphology of hUSCs after several passages. (c) Flow cytometry results of hUSCs. (d) Osteogenic differentiation of hUSCs with Alizarin Red. (e) Adipogenic differentiation of hUSCs with Oil Red O. (f) Growth curves of hUSCs.

samples were embedded in paraffin and cut into 5 μm thick sections that were stained with hematoxylin-eosin (HE), Masson, and toluidine blue. The cell morphology, color of the matrix, intactness of the surface, and thickness and integration of cartilage with adjacent host cartilage were evaluated.

2.5.6. Immunohistochemical Analysis. Paraffin-embedded tissues were dewaxed with xylene, and endogenous peroxidase was blocked using 3% hydrogen peroxide. Sections were rinsed with PBS and blocked with goat serum (Sichuan University Ltd., China), followed by incubation with the primary antibodies: mouse anti-type II collagen and mouse anti-aggrecan (Novus, USA) for 12 h at 4°C. After washing three times for 5 min with PBS, sections were incubated with goat anti-mouse IgG (H + L) secondary antibodies (Peroxidase Affinipure, 115-035-003, Jackson, USA) for 30 min at room temperature as well as with peroxidase-conjugated streptavidin (Sichuan University Ltd., China). Next, sections were washed three times with PBS for 5 min. Finally, 3,3-diaminobenzidine (DAB) solution containing 0.01% hydrogen peroxide was added, and sections were counterstained with hematoxylin.

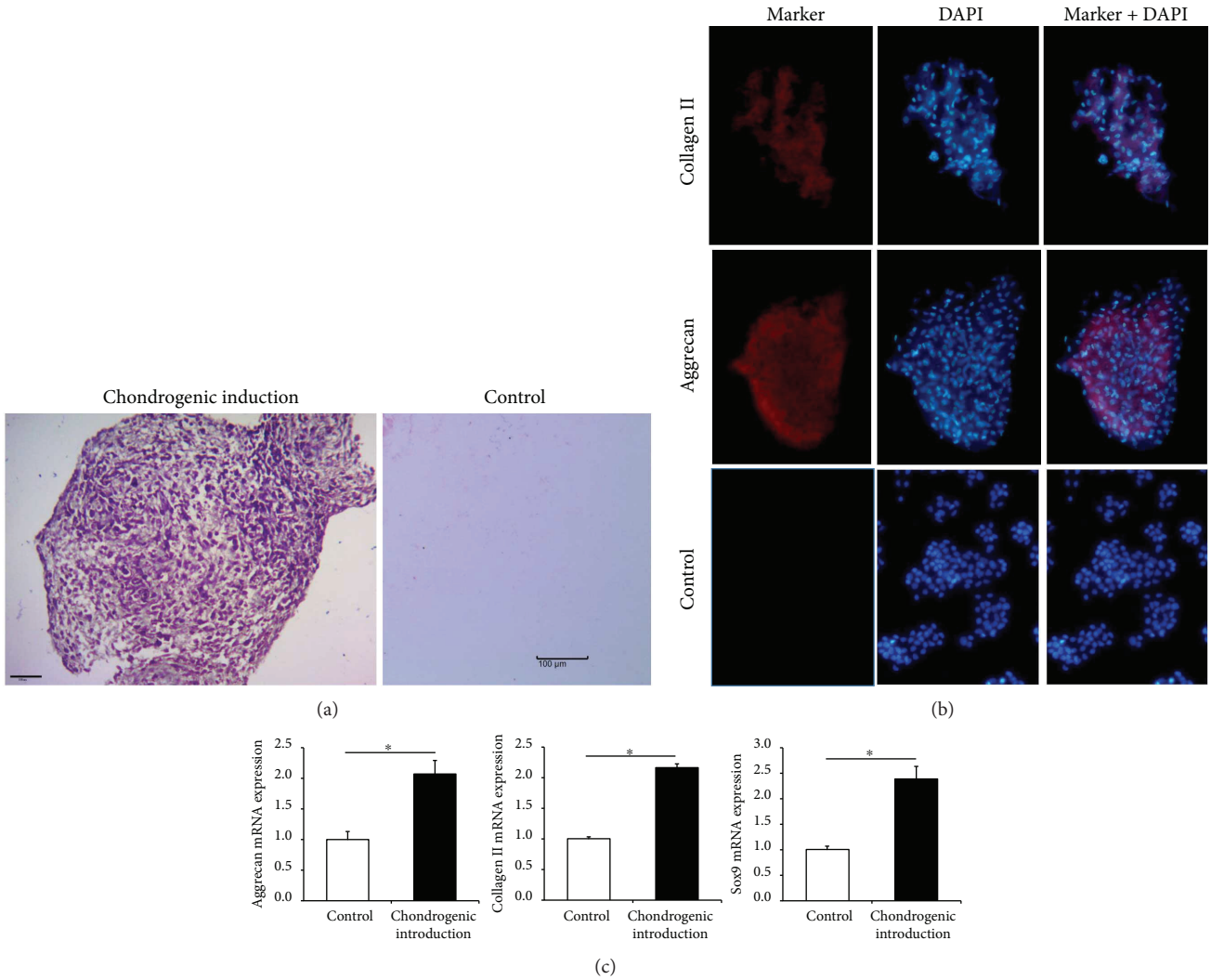

FIGURE 3: The chondrogenic differentiation potential of hUSCs *in vitro*. (a) Polysaccharides and proteoglycans were observed by toluidine blue staining after chondrogenic induction. (b) Immunofluorescence assay of chondrogenic-related markers (aggrecan and collagen II). (c) The mRNA expression of chondrogenesis-related genes (aggrecan, Sox9, and collagen II) was quantitated in hUSCs after 21 days of induction.

2.5.7. Histological Score. To quantify the differences of treatment results in histological and immunohistochemical staining, a histological score was given according to the method described by Pineda et al. [17]. In brief, a scale from 0 (good) to 14 (severe) was given. In our study, filling of the defect, reconstitution of the osteochondral junction, matrix staining, and cell morphology were scored (Table 2).

2.6. Statistical Analysis. All values are expressed as the mean ± standard deviation (SD). Statistical analyses were performed using SPSS 17.0 software (SPSS, USA). Results were analyzed using Student's t-test, and $P < 0.05$ was considered statistically significant.

3. Results

3.1. Morphology and Characterization of hUSCs. Cell colonies of hUSCs were observed 7–10 days after initial plating, in which the cells had "rice grain"-like appearance (Figure 2(a)). After several passages, hUSCs always exhibited an elongated morphology (Figure 2(b)). In addition, flow cytometry results showed that hUSCs had a positive staining for CD29, CD73, CD90, CD105, and CD166, but were negative for CD34, CD45, and MHC-II HLA-DR (Figure 2(c)). Figures 2(d) and 2(e) reveal that after culturing in specific induction media, hUSCs demonstrated to differentiate into an osteogenic or adipogenic lineage as indicated by the positive staining for Alizarin Red and Oil Red O, respectively. Moreover, the CCK-8 assay showed that the cells underwent a rapid growth phase from day 1 to day 3. After day 3, the growth slowed down (Figure 2(f)). The data indicated that cells isolated from human urine and maintained under specific culture conditions were classified as MSC.

3.2. In Vitro Chondrogenic Differentiation Potential of hUSCs. After 21 days of chondrogenic induction, toluidine blue staining of hUSCs indicated the presence of

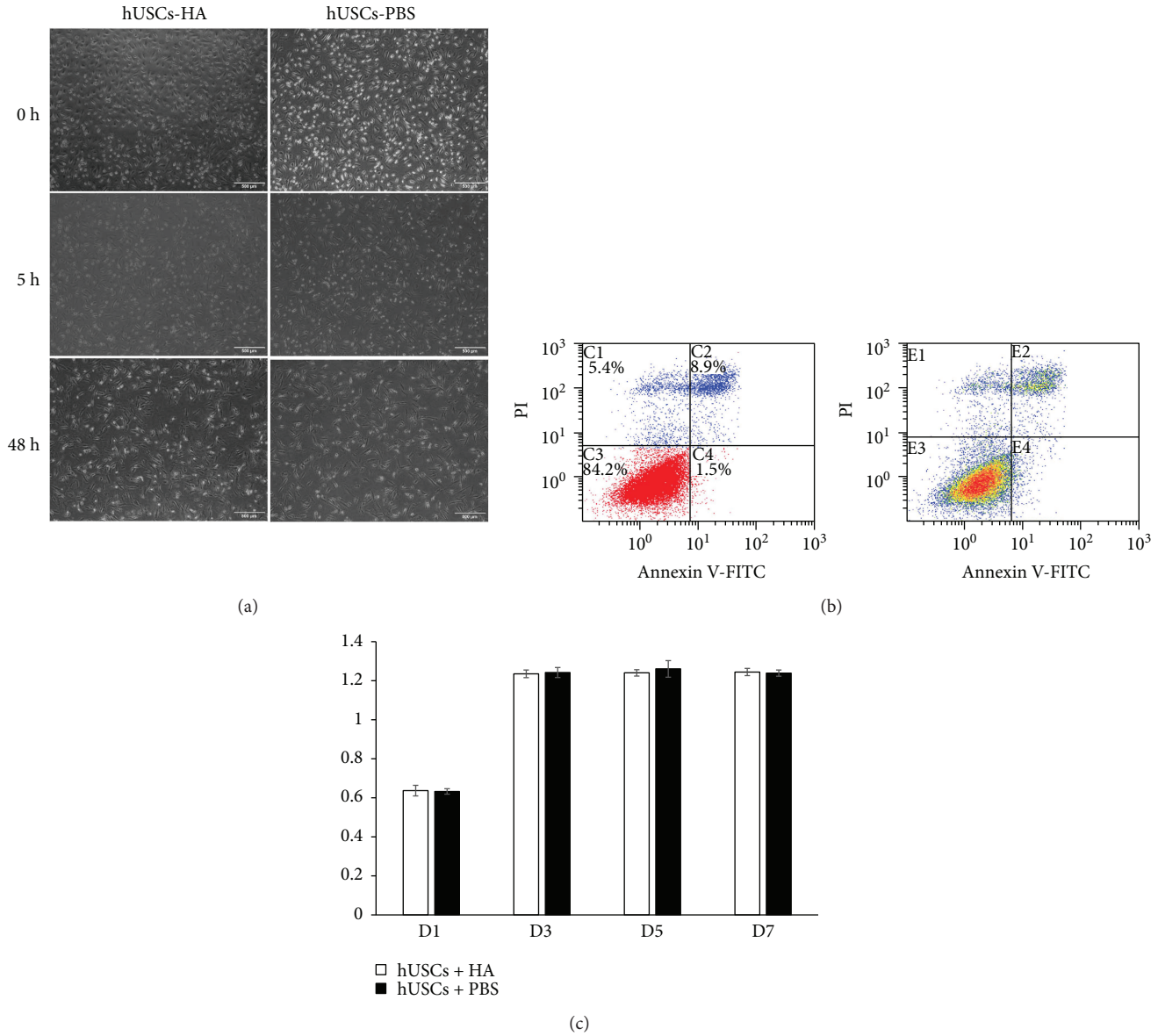

Figure 4: Cell morphology, viability, and proliferation about the hUSCs-HA system. (a) The comparison of morphology for hUSCs-HA and hUSCs-PBS at 0 h, 5 h, and 48 h. (b) Annexin V/PI assay of hUSCs seeded in HA. (c) Proliferation ability of cells in hUSCs-HA compared with those in hUSCs-PBS.

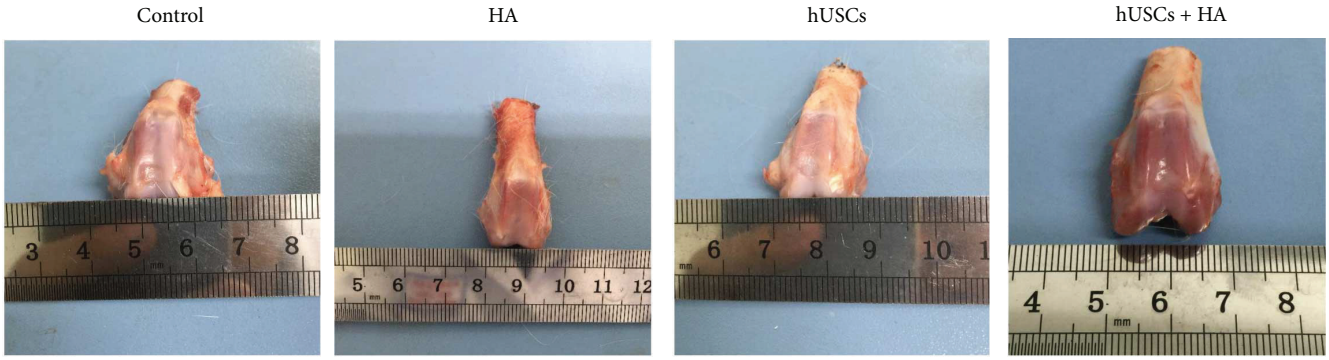

Figure 5: The gross appearance of the cartilage 12 weeks after injection.

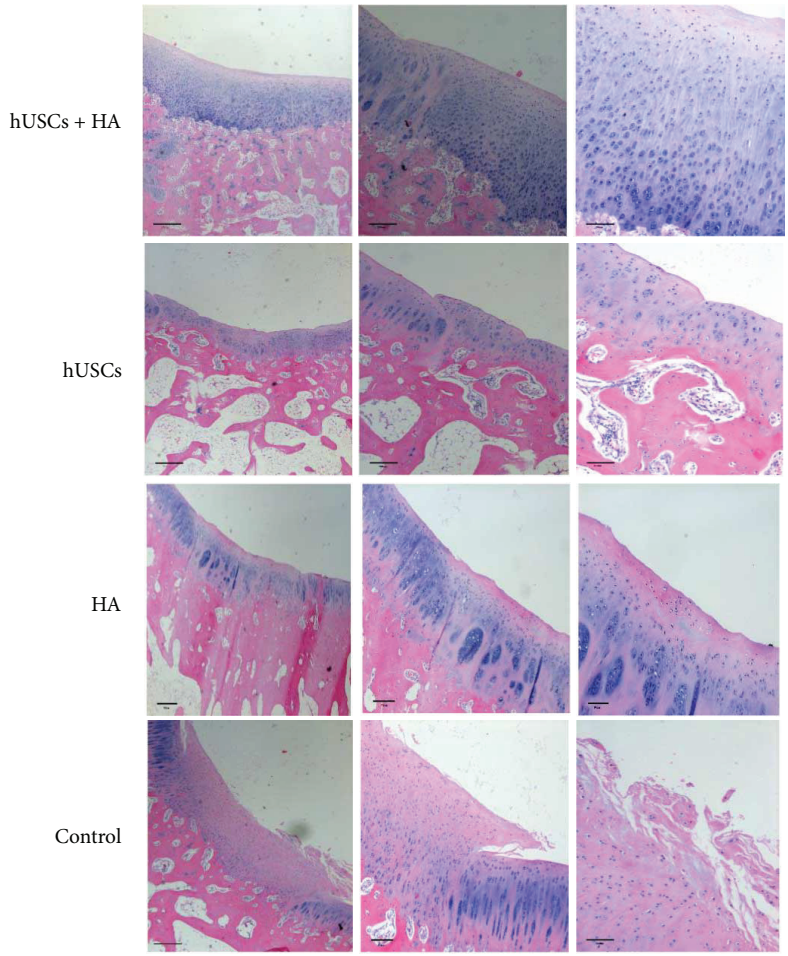

Figure 6: The HE staining of the cartilage 12 weeks after injection (scale bar = 500 μm, 200 μm, and 100 μm).

polysaccharides and proteoglycans (Figure 3(a)). The expression of chondrogenic-related markers, such as aggrecan and collagen II, was determined by immunofluorescence assay (Figure 3(b)). Furthermore, real-time PCR showed that the expression of chondrogenesis-related genes, aggrecan, Sox9, and collagen II was upregulated in induced hUSCs (Figure 3(c)).

3.3. Cell Morphology, Viability, and Proliferation in hUSCs-HA. The morphology of hUSCs in HA was similar to hUSCs in PBS at 0 h, 5 h, and 48 h after the seeding (Figure 4(a)). The annexin V/PI assay demonstrated that after 24 h, 84.2% of hUSCs seeded in HA were still alive (Figure 4(b)). Besides, CCK-8 assay showed that the proliferation ability of the cells in the hUSCs-HA group was similar to that in the hUSCs-PBS group on days 0, 1, 3, 5, and 7 (Figure 4(c)).

3.4. Gross Appearance of Cartilage. Various degrees of cartilage damage were maintained 12 weeks after injection. The representative gross appearance of cartilage is shown in Figure 5. No significant change in degeneration was observed in knee joint cartilage, except for the defect in cartilage. For group A (hUSCs plus HA), newly formed cartilage-like tissue was frequently observed on the defect site, the surface color was relatively normal, and the newly formed cartilage-like tissue connected well with the surrounding cartilage tissue. Group B (hUSCs) also showed newly formed cartilage-like tissue. However, a scratch was noticed on the junction between the defect sites and normal sites. For group C (HA), some newly formed cartilage-like tissue was observed. An obvious scratch however was present on the junction between the defect sites and normal sites. In group D (the control group with normal saline injected), the cartilage defect was not recovered and newly formed cartilage-like tissue was hardly observed.

3.5. Histological Assessment of New Cartilage Formation in an In Vivo Cartilage Defect Model. HE staining, Masson staining, and toluidine blue staining were performed. Representative images of HE staining of newly formed cartilage in groups A, B, C, and D are shown in Figure 6. In group A, the defect site was covered by tissues similar to neocartilage, in which chondrocytes were present. The matrix staining had a normal appearance. In group B, sign tissues similar to cartilage and fibrous tissue were observed. In contrast, neocartilage-like tissue was seldom seen on the defect sites in groups C and D.

Representative images of Masson staining are shown in Figure 7. In group A, many chondrocytes were present. Tissues similar to cartilage fibers were observed regularly, and

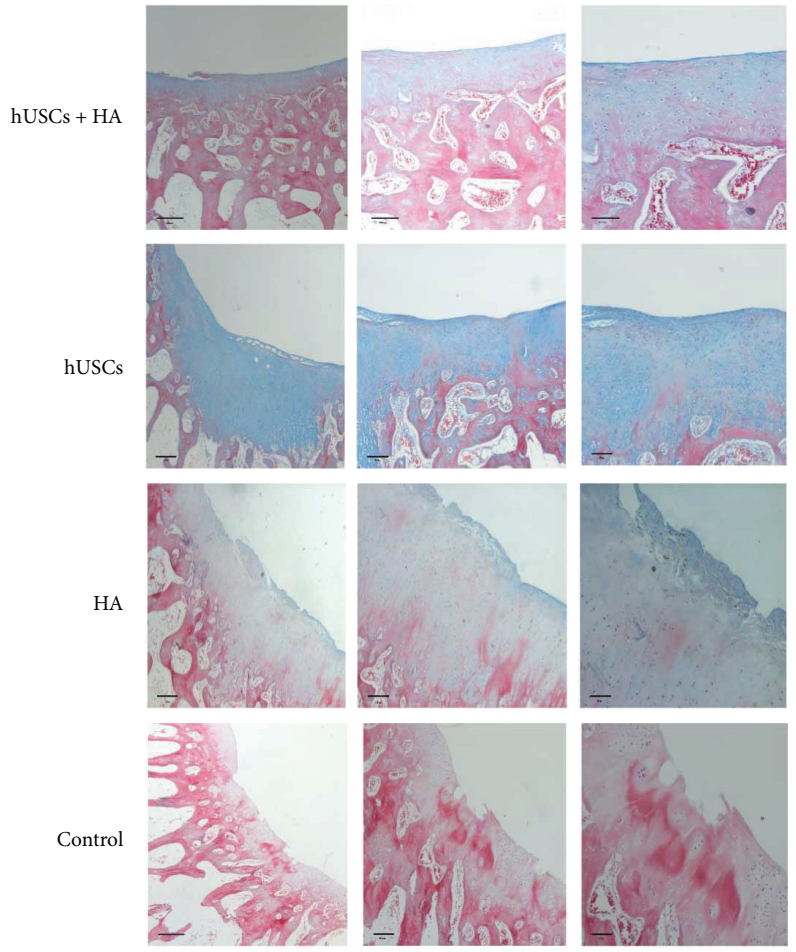

Figure 7: The Masson staining of the cartilage 12 weeks after injection (scale bar = 500 μm, 200 μm, and 100 μm).

the color of the matrix was close to that in normal cartilage tissue. In group B, chondrocytes were hardly observed, while most cells were nonchondrocytes. The color of the matrix was pale when compared to that of normal cartilage. In groups C and D, no cartilage was observed at defective sites.

Representative images of toluidine blue staining are shown in Figure 8. The staining in group A showed a darker blue staining at defect sites with a uniform layer of cartilage cells and clear tidemarks. In contrast, only a pale blue staining, few cartilage cells, a mass of fibrotic cells, and fiber tissue were observed in group B. No neocartilage tissue was observed in groups C and D.

Representative images of the immunohistochemical analysis of the neocartilage from all four groups are presented in Figures 9 and 10. Group A exhibited a large number of chondrocyte cells. Moreover, the color of the defect sites in group A was similar to that of the surrounding tissue, which indicated that a significant amount of type II collagen and aggrecan protein was secreted. In group B, few cells similar to chondrocytes were observed and the color was light at the defect sites. In groups C and D, no newly formed tissue was detected. The data indicated the presence of increased collagen fibers and aggrecan protein in group A compared to groups B, C, and D. The histochemical analysis and immunohistochemistry implied that hUSCs in combination with HA stimulated the regeneration of cartilage more effectively than hUSCs alone or HA alone.

3.6. Histological Score. The histological score for group A (2.75 ± 0.62) was significantly higher than the scores of group B (6 ± 0.74, $P < 0.001$), group C (9.58 ± 0.79, $P < 0.001$), and group D (12.41 ± 0.79, $P < 0.001$). These findings suggested that hUSCs-HA rather than hUSCs alone and HA alone was the most effective treatment in promoting the formation of neocartilage (Figure 11).

4. Discussion

In our study, we explored the cellular properties of hUSCs and compared their chondrogenic potency to differentiate into chondrocytes. After injection into cartilage defect knee joints in rabbits with or without HA, the deposition of aggrecan and collagen II was studied as a characteristic for neocartilage formation *in vivo*. The ability of hUSCs to self-renew and their differentiation potential were examined *in vitro*, whereas their ability to support novel cartilage formation in the cartilage defect model was assessed through histological assessments. These findings suggested that hUSCs could be a potential alternative therapeutic cell source for cartilage tissue engineering, especially when combined with HA.

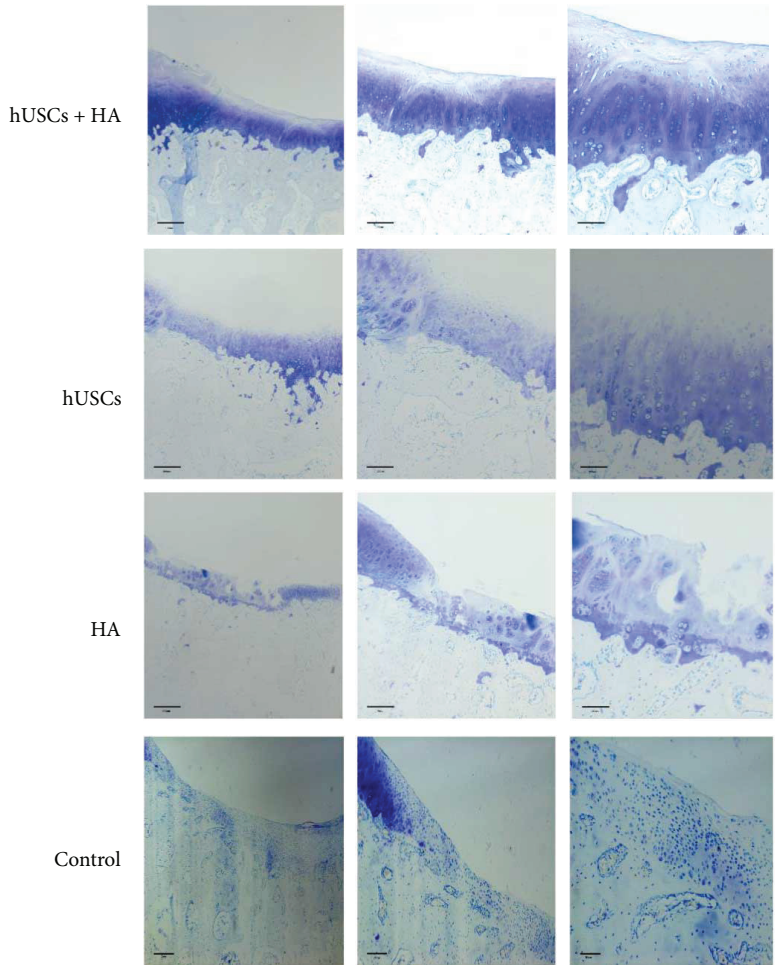

Figure 8: The toluidine blue staining of the cartilage 12 weeks after injection (scale bar = 500 μm, 200 μm, and 100 μm).

Previous studies reported that stem cells appropriately seeded onto biomaterials could promote the regeneration of cartilage at defective sites [13, 18]. MSCs could be derived from a variety of human tissues, including bone marrow, skeletal muscle, adipose tissue, cord blood, skin, dental pulp, and endometrium, which have been reported in numerous studies previously [19–22]. The viable cell types with MSC characteristics in urine have recently been discovered [8, 10, 23]. In our study, we confirmed that hUSCs, when cultured under appropriate conditions as described above, possessed the properties belonging to MSCs. Although Pei et al. [24] reported that hUSCs did not show the ability to differentiate into chondrocytes in a 5% O_2 and 5% CO_2 incubator up to 14 days, Guan et al. [9], Bharadwaj et al. [10], and Gao et al. [25] have shown that hUSCs could differentiate toward the chondrogenic lineages after chondrogenic induction for 28 days. Kang et al. [26] reported that hUSCs could differentiate into chondrocytes but showed relatively lower chondrogenic differentiation rate compared to hASCs. Guan et al. [9] also demonstrated that hUSCs possessed biological characteristics similar to hASCs and had multilineage differentiation potential. Here, we successfully isolated hUSCs from human urine samples and demonstrated the capacity of hUSCs to differentiate into chondrocytes in a 20% O_2 and 5% CO_2 incubator for 21 days, based on the evidence of cell morphology, protein expression, and chondrogenesis-related gene expression. Ample evidence has validated that three-dimensional cultures are better than a monolayer culture for stabilizing the chondrocyte phenotype *in vitro* [27], which matches the method that we used to successfully induce hUSCs to differentiate into chondrocytes. Therefore, the culture environment and the incubation time may influence the result of chondrogenic induction of hUSCs. In addition, when compared with the autologous cell transplantation that relied on expensive and invasive surgery, our study revealed that hUSCs could potentially provide a low-cost and harmless way to cure cartilage defects caused by trauma injury and OA.

As reported by Venable et al. [28], HA may be associated with cartilage damage in early pathologic changes of OA. The treatment of OA by intra-articular HA injection has been commonly used to promote cartilage repair, and the mechanisms contributing to this function are proposed to include the suppression of proinflammatory cytokines and chemokines, the promotion of the anabolism, and the relief of pain [29, 30]. Nevertheless, the effects are controversial [31–33]. The discrepancy may be due to improper position of injection [34], suboptimal dosage of HA, or a prolonged interval between induction of OA and injection of HA. In this study,

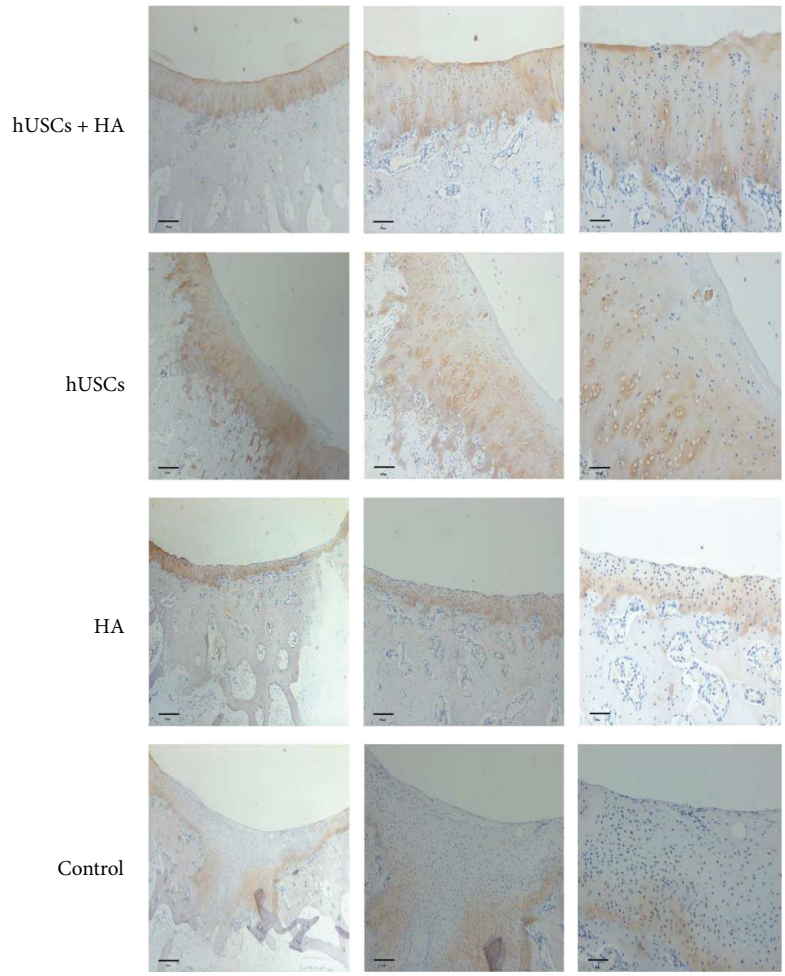

Figure 9: The type II collagen staining of the cartilage 12 weeks after injection (scale bar = 500 μm, 200 μm, and 100 μm).

we injected HA, hUSCs, or a mixture thereof into knee joints of rabbits with cartilage defects and compared the recovery levels of articular cartilage. When compared with other groups, cartilage regeneration in the hUSCs + HA group was found as the best and the corresponding histological score was the highest. Besides, in the hUSCs + HA group, neocartilage-like tissue covered the defect site, chondrocytes were found in the recovered tissue, and matrix staining was normal. In contrast, only a few neocartilage-like tissues were found in other groups. Our results are in line with the findings of several earlier studies. Neocartilage was also reported by Grigolo et al., who demonstrated that after 24 weeks of treatment with chondrocytes and HA derivatives, cartilage defects in the rabbit knee were repaired [18]. Researchers in South Korea demonstrated positive treatment effects when using a similar approach [35]. A possible explanation may be that chondrocytes seeded onto appropriately configured synthetic biodegradable polymers adhere and perform different functions *in vitro*, as demonstrated by matrix formation [18]. Surgical implantation of the hUSCs + HA cell-polymer mixture in animals resulted in the formation of new cartilage that matures over time and showed the expression of collagen type II and synthesized proteoglycans [18].

Although the findings of this study are promising, several limitations need to be addressed before clinical applications and further studies are warranted to reveal: (1) how to improve chondrogenic capacity of hUSCs because the expression levels of all chondrogenic genes were relatively low [24, 26]; (2) the advantages of hUSCs over other MSCs by comparing the chondrogenic ability of hUSCs with those of other MSC types, such as hBMSCs and hASCs; and (3) the molecular mechanisms involved in the interactions between hUSCs and HA.

Based on the results of our previous study and the measured values of the pH, osmotic pressure, and the survival rate of stem cells in solution, we chose 1% HA physiological saline solution as our intervention means. The ability of cell proliferation was tested using CCK-8 assay, which showed that the proliferation ability of the cells in the hUSCs-HA group was similar to that of the cells in the hUSCs-PBS groups at days 0, 1, 3, 5, and 7. Noticeably, the HA physiological saline solution only showed minor side effects on hUSC activity. In a study by Shapiro et al. [36], it was implied that cartilage defects in rabbits could be repaired by the animal itself in 6 weeks. But it could be achieved only if the diameter of the defect is smaller than 3 mm, the depth of the defect touched the subchondral bone, and intervention is absent.

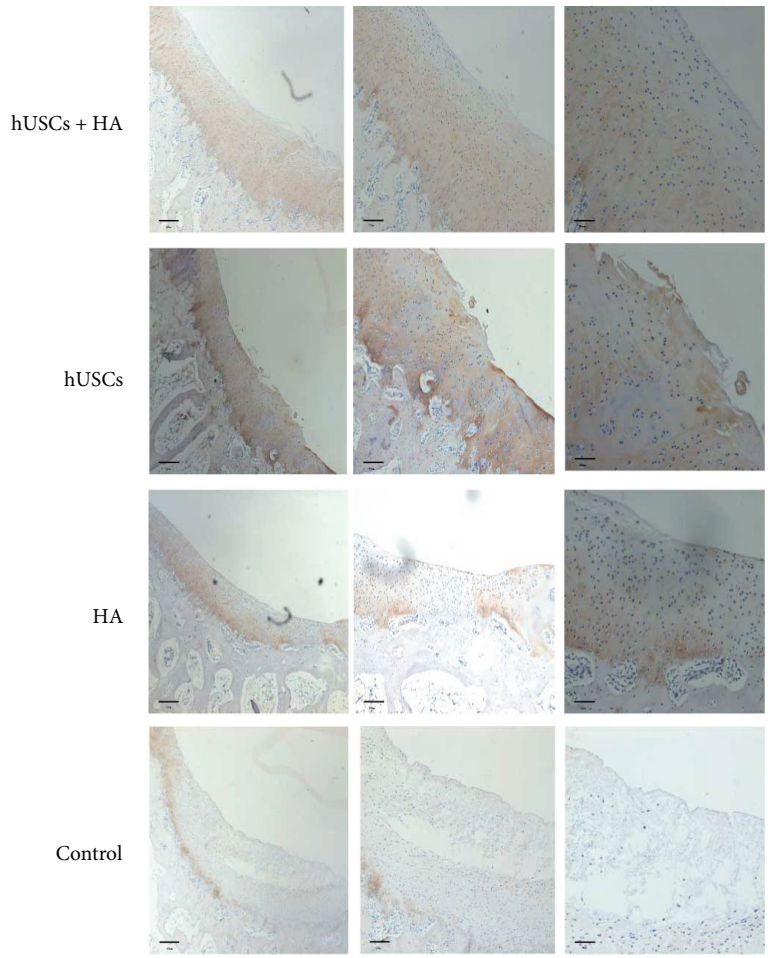

Figure 10: The aggrecan protein staining of the cartilage 12 weeks after injection (scale bar = 500 μm, 200 μm, and 100 μm).

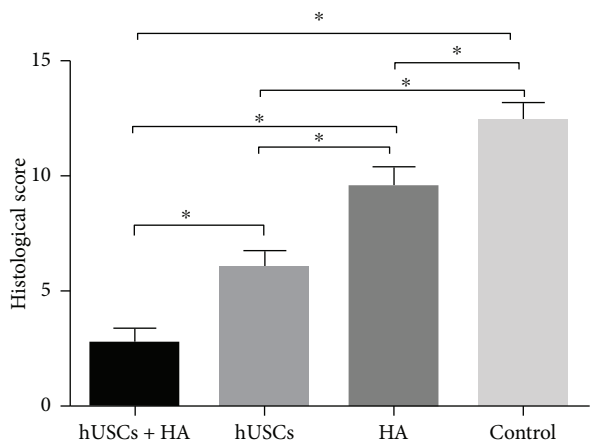

Figure 11: The histological score assessment 12 weeks after injection ($^*P < 0.05$).

To ensure the reliability of our experiments and solve the doubt about self-healing, we expanded the diameter of the defect to 5 mm and removed all cartilage without damaging the subchondral bone to avoid any interference from bone marrow-derived MSCs.

5. Conclusion

In summary, the findings of our study indicated that, according to the stem cell characteristics, hUSCs can be classified into the MSC family. hUSCs are able to differentiate into chondrocytes with characteristic deposition of aggrecan and collagen II *in vitro*. Furthermore, hUSCs-HA can stimulate significantly more neocartilage formation compared with hUSCs, HA, and saline. These results, along with the findings of our previous study, indicated that hUSCs could be an alternative therapeutic cell source for cartilage tissue engineering and a promising candidate for, especially when combined with HA.

Conflicts of Interest

The authors declare no potential conflicts of interest with respect to the research, authorship, and/or publication of this article.

Acknowledgments

This work was supported by the National Natural Science Foundation of China (no. 31370984).

References

[1] E. B. Hunziker, "Articular cartilage repair: are the intrinsic biological constraints undermining this process insuperable?," *Osteoarthritis and Cartilage*, vol. 7, no. 1, pp. 15–28, 1999.

[2] B. J. Huang, J. C. Hu, and K. A. Athanasiou, "Cell-based tissue engineering strategies used in the clinical repair of articular cartilage," *Biomaterials*, vol. 98, pp. 1–22, 2016.

[3] D. Kazemi, K. Shams Asenjan, N. Dehdilani, and H. Parsa, "Canine articular cartilage regeneration using mesenchymal stem cells seeded on platelet rich fibrin: macroscopic and histological assessments," *Bone & Joint Research*, vol. 6, no. 2, pp. 98–107, 2017.

[4] J. C. Bernhard and G. Vunjak-Novakovic, "Should we use cells, biomaterials, or tissue engineering for cartilage regeneration?," *Stem Cell Research & Therapy*, vol. 7, no. 1, p. 56, 2016.

[5] C. Madeira, A. Santhagunam, J. B. Salgueiro, and J. M. S. Cabral, "Advanced cell therapies for articular cartilage regeneration," *Trends in Biotechnology*, vol. 33, no. 1, pp. 35–42, 2015.

[6] J. Pak, J. H. Lee, W. A. Kartolo, and S. H. Lee, "Cartilage regeneration in human with adipose tissue-derived stem cells: current status in clinical implications," *BioMed Research International*, vol. 2016, Article ID 4702674, 12 pages, 2016.

[7] J. Hu, K. Feng, X. Liu, and P. X. Ma, "Chondrogenic and osteogenic differentiations of human bone marrow-derived mesenchymal stem cells on a nanofibrous scaffold with designed pore network," *Biomaterials*, vol. 30, no. 28, pp. 5061–5067, 2009.

[8] Y. Zhang, E. McNeill, H. Tian et al., "Urine derived cells are a potential source for urological tissue reconstruction," *The Journal of Urology*, vol. 180, no. 5, pp. 2226–2233, 2008.

[9] J. J. Guan, X. Niu, F. X. Gong et al., "Biological characteristics of human-urine-derived stem cells: potential for cell-based therapy in neurology," *Tissue Engineering Part A*, vol. 20, no. 13-14, pp. 1794–1806, 2014.

[10] S. Bharadwaj, G. Liu, Y. Shi et al., "Multipotential differentiation of human urine-derived stem cells: potential for therapeutic applications in urology," *Stem Cells*, vol. 31, no. 9, pp. 1840–1856, 2013.

[11] J. Guan, J. Zhang, H. Li et al., "Human urine derived stem cells in combination with β-TCP can be applied for bone regeneration," *PLoS One*, vol. 10, no. 5, article e0125253, 2015.

[12] S. Wu, Z. Wang, S. Bharadwaj, S. J. Hodges, A. Atala, and Y. Zhang, "Implantation of autologous urine derived stem cells expressing vascular endothelial growth factor for potential use in genitourinary reconstruction," *The Journal of Urology*, vol. 186, no. 2, pp. 640–647, 2011.

[13] E. Filová, M. Rampichová, A. Litvinec et al., "A cell-free nanofiber composite scaffold regenerated osteochondral defects in miniature pigs," *International Journal of Pharmaceutics*, vol. 447, no. 1-2, pp. 139–149, 2013.

[14] S. Kazemnejad, M. Khanmohammadi, N. Baheiraei, and S. Arasteh, "Current state of cartilage tissue engineering using nanofibrous scaffolds and stem cells," *Avicenna Journal of Medical Biotechnology*, vol. 9, no. 2, pp. 50–65, 2017.

[15] J. R. Watterson and J. M. Esdaile, "Viscosupplementation: therapeutic mechanisms and clinical potential in osteoarthritis of the knee," *Journal of the American Academy of Orthopaedic Surgeons*, vol. 8, no. 5, pp. 277–284, 2000.

[16] T. Tian, J. Li, B. Li et al., "Genistein exhibits anti-cancer effects via down-regulating FoxM1 in H446 small-cell lung cancer cells," *Tumour Biology*, vol. 35, no. 5, pp. 4137–4145, 2014.

[17] S. Pineda, A. Pollack, S. Stevenson, V. Goldberg, and A. Caplan, "A semiquantitative scale or histologic grading of articular cartilage repair," *Cells Tissues Organs*, vol. 143, no. 4, pp. 335–340, 1992.

[18] B. Grigolo, L. Roseti, M. Fiorini et al., "Transplantation of chondrocytes seeded on a hyaluronan derivative (Hyaff®-11) into cartilage defects in rabbits," *Biomaterials*, vol. 22, no. 17, pp. 2417–2424, 2001.

[19] K. Bieback and H. Klüter, "Mesenchymal stromal cells from umbilical cord blood," *Current Stem Cell Research & Therapy*, vol. 2, no. 4, pp. 310–323, 2007.

[20] M. Gnecchi and L. G. Melo, *Bone Marrow-Derived Mesenchymal Stem Cells: Isolation, Expansion, Characterization, Viral Transduction, and Production of Conditioned Medium*, pp. 281–294, Humana Press, Totowa, NJ, USA, 2009.

[21] H. E. Gruber, R. Deepe, G. L. Hoelscher et al., "Human adipose-derived mesenchymal stem cells: direction to a phenotype sharing similarities with the disc, gene expression profiling, and coculture with human annulus cells," *Tissue Engineering Part A*, vol. 16, no. 9, pp. 2843–2860, 2010.

[22] I. Ishige, T. Nagamura-Inoue, M. J. Honda et al., "Comparison of mesenchymal stem cells derived from arterial, venous, and Wharton's jelly explants of human umbilical cord," *International Journal of Hematology*, vol. 90, no. 2, pp. 261–269, 2009.

[23] S. Bharadwaj, G. Liu, Y. Shi et al., "Characterization of urine-derived stem cells obtained from upper urinary tract for use in cell-based urological tissue engineering," *Tissue Engineering Part A*, vol. 17, no. 15-16, pp. 2123–2132, 2011.

[24] M. Pei, J. Li, Y. Zhang, G. Liu, L. Wei, and Y. Zhang, "Expansion on a matrix deposited by nonchondrogenic urine stem cells strengthens the chondrogenic capacity of repeated-passage bone marrow stromal cells," *Cell and Tissue Research*, vol. 356, no. 2, pp. 391–403, 2014.

[25] P. Gao, P. Han, D. Jiang, S. Yang, Q. Cui, and Z. Li, "Effects of the donor age on proliferation, senescence and osteogenic capacity of human urine-derived stem cells," *Cytotechnology*, vol. 69, no. 5, pp. 751–763, 2017.

[26] H. S. Kang, S. H. Choi, B. S. Kim et al., "Advanced properties of urine derived stem cells compared to adipose tissue derived stem cells in terms of cell proliferation, immune modulation and multi differentiation," *Journal of Korean Medical Science*, vol. 30, no. 12, pp. 1764–1776, 2015.

[27] P. D. Benya and J. D. Shaffer, "Dedifferentiated chondrocytes reexpress the differentiated collagen phenotype when cultured in agarose gels," *Cell*, vol. 30, no. 1, pp. 215–224, 1982.

[28] R. O. Venable, A. M. Stoker, C. R. Cook, M. K. Cockrell, and J. L. Cook, "Examination of synovial fluid hyaluronan quantity and quality in stifle joints of dogs with osteoarthritis," *American Journal of Veterinary Research*, vol. 69, no. 12, pp. 1569–1573, 2008.

[29] M. N. Collins and C. Birkinshaw, "Hyaluronic acid based scaffolds for tissue engineering–a review," *Carbohydrate Polymers*, vol. 92, no. 2, pp. 1262–1279, 2013.

[30] R. Altman, A. Bedi, A. Manjoo, F. Niazi, P. Shaw, and P. Mease, "Anti-inflammatory effects of intra-articular hyaluronic acid: a systematic review," *Cartilage*, vol. I-10, 2018.

[31] S. Armstrong, R. Read, and P. Ghosh, "The effects of intraarticular hyaluronan on cartilage and subchondral bone changes in an ovine model of early osteoarthritis," *Journal of Rheumatology*, vol. 21, no. 4, pp. 680–688, 1994.

[32] G. N. Smith, S. L. Myers, K. D. Brandt, and E. A. Mickler, "Effect of intraarticular hyaluronan injection in experimental canine osteoarthritis," *Arthritis & Rheumatism*, vol. 41, no. 6, pp. 976–985, 1998.

[33] R. D. Altman, C. Akermark, A. D. Beaulieu, T. Schnitzer, and Durolane International Study Group, "Efficacy and safety of a single intra-articular injection of non-animal stabilized hyaluronic acid (NASHA) in patients with osteoarthritis of the knee," *Osteoarthritis and Cartilage*, vol. 12, no. 8, pp. 642–649, 2004.

[34] M. Abate, C. Schiavone, and V. Salini, "Hyaluronic acid in ankle osteoarthritis: why evidence of efficacy is still lacking?," *Clinical and Experimental Rheumatology*, vol. 30, no. 2, pp. 277–281, 2012.

[35] Foundation, B.C., *Evaluation of Safety and Exploratory Efficacy of CARTISTEM®, a Cell Therapy Product for Articular Cartilage Defects*, Bone & Cancer Foundation, 2015.

[36] F. Shapiro, S. Koide, and M. J. Glimcher, "Cell origin and differentiation in the repair of full-thickness defects of articular cartilage," *The Journal of Bone & Joint Surgery*, vol. 75, no. 4, pp. 532–553, 1993.

Hindawi
Stem Cells International
Volume 2018, Article ID 8947548, 9 pages
https://doi.org/10.1155/2018/8947548

Review Article

Adipose-Derived Mesenchymal Stem Cells in the Use of Cartilage Tissue Engineering: The Need for a Rapid Isolation Procedure

Sam L. Francis,[1,2] **Serena Duchi**,[1,2] **Carmine Onofrillo**,[1,2] **Claudia Di Bella**,[1,2] **and Peter F. M. Choong**[1,2]

[1]*Department of Surgery, The University of Melbourne, Melbourne, VIC, Australia*
[2]*Department of Orthopaedics, St. Vincent's Hospital, Melbourne, VIC, Australia*

Correspondence should be addressed to Sam L. Francis; sfrancis1@student.unimelb.edu.au

Received 19 December 2017; Accepted 1 March 2018; Published 3 April 2018

Academic Editor: Jianying Zhang

Mesenchymal stem cells (MSCs) have shown much promise with respect to their use in cartilage tissue engineering. MSCs can be obtained from many different tissue sources. Among these, adipose tissue can provide an abundant source of adipose-derived mesenchymal stem cells (ADMSCs). The infrapatellar fat pad (IFP) is a promising source of ADMSCs with respect to producing a cartilage lineage. Cell isolation protocols to date are time-consuming and follow conservative approaches that rely on a long incubation period of 24–48 hours. The different types of ADMSC isolation techniques used for cartilage repair will be reviewed and compared with the view of developing a rapid one-step isolation protocol that can be applied in the context of a surgical procedure.

1. Introduction

Cartilage tissue engineering has become a major research interest in the past few decades, primarily due to the inability of native human cartilage to self-repair [1, 2]. There is no reliable long-term joint preserving management option for early onset arthritis secondary to cartilage defects, and this may potentially lead to joint replacement (arthroplasty) and associated short- and long-term risks and sequelae [3, 4]. Fibrocartilage formation is the major barrier in the long-term viability of currently used clinical methods and is detrimental to joint function [5, 6].

The diamond concept [7] embodies the 4 major strategies that underpin tissue engineering, namely, cells, scaffolds, growth factor/cytokines, and environmental stimulation.

This review will focus specifically on ADMSC isolation techniques and their efficiency with respect to driving cartilage formation.

Current isolation procedures in cartilage tissue engineering are in vitro and laboratory-based. These are primarily complex two-step procedures that also raise ethical concerns with respect to human tissue culture in a laboratory setting [8].

Translating these techniques into the clinical setting will require the development of a rapid, sterile, one-step technique that could fit into a day surgery timeframe. To date, rapid isolation of bone marrow-derived MSCs [9, 10] and their therapeutical potential has been studied [11], but an important barrier to adoption has been the low number of stem cells requiring a period of cell expansion in the laboratory. There is only one published study assessing a rapid isolation protocol (<30 minutes) for ADMSCs from abdominal lipoaspirate [12], but even this technique relies on a minimum of 24 hours for plastic adherence.

2. Adipose-Derived Mesenchymal Stem Cells

ADMSCs have the ability to differentiate into mesodermal tissue lineages, that is, bone, cartilage, muscle, and adipose [6, 13–16]. They have been incorporated into many different scaffold-based systems and have an established role in cartilage tissue engineering [17, 18].

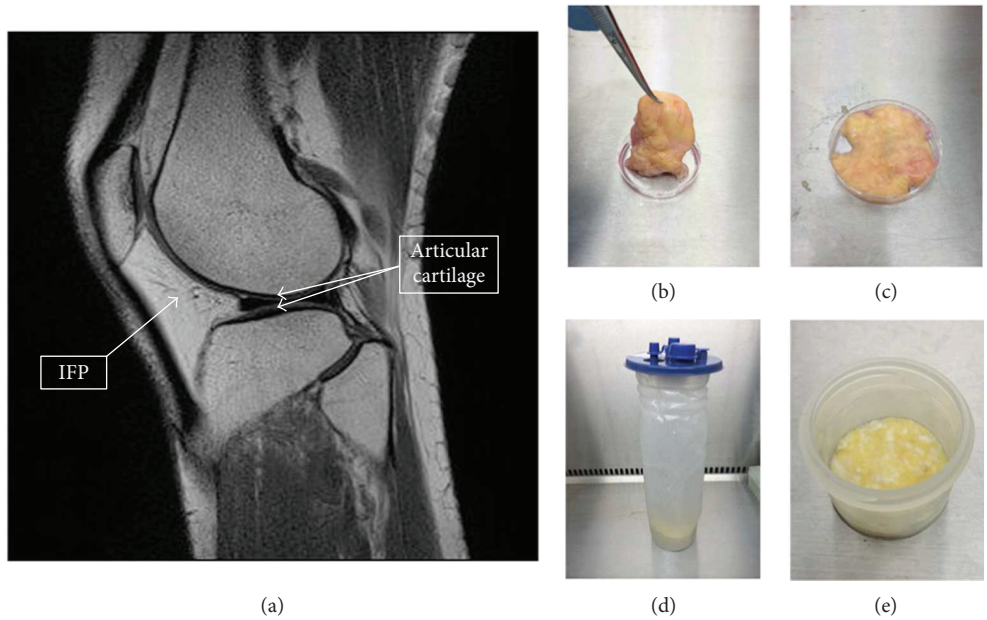

Figure 1: (Modified and used with permission from Wiley under CC BL). Infrapatellar fat pad (IFP) location and harvested tissue. (a) Sagittal magnetic resonance imaging scan of the knee showing the relationship of the IFP (arrow) to the articular cartilage (double arrow). (b, c) Excised IFP from a patient undergoing knee arthroplasty (b) has the fat removed from the fibrous tissue (c). (d, e) The arthroscopically harvested fat pad (d) was separated from the irrigation fluid before enzymatic digestion (e).

Initially, bone marrow (BM) was the most commonly used source of MSCs. Like ADMSCs, BM-derived MSCs are multipotent in nature and can produce tissue of mesodermal lineage [19]. Tissue can be harvested autologously and does not pose the ethical, tumorigenic, or immunogenic risk as presented by pluripotent stem cells. The disadvantages of using BM include low tissue volume and low cell volume [13, 20, 21]. BM-derived MSCs are comparable [22], if not inferior, in respect to chondrogenic potential when compared to ADMSCs [22, 23]. These factors, in addition to less invasive tissue harvesting techniques, make adipose tissue a more desirable source.

3. Tissue Sources and Harvesting Techniques

ADMSCs can be obtained from different sources and by different techniques. The two major sources are abdominal fat and infrapatellar fat pad (IFP). Techniques and protocols for ADMSC harvest and isolation vary based on different laboratory groups. Abdominal fat can be harvested from subcutaneous tissue via abdominoplasty or arthroscopy.

The IFP (Figure 1(a)) is an emerging source of MSCs for cartilage tissue engineering [24, 25]. IFP can be opportunistically harvested (Figure 1(a)) during routine surgical procedures such as knee arthroplasty (Figures 1(b) and 1(c)) or arthroscopy (Figures 1(d) and 1(e)) and is known to have high chondrogenic potential [26]. Although there is less fat volume in the IFP compared to abdominal fat, chondrogenic potential has been shown to higher in ADMSCs sourced from the IFP [27, 28]. The proximity of the IFP to the knee joint may account for this higher potential.

These results could pave the way for future novel advances in minimally invasive arthroscopy or techniques for pure fat pad harvesting as opposed to opportunistic harvest and, better yet, the possible establishment of a single-step surgical repair technique using stem cell technology.

4. Cell Isolation Procedure

Obtaining a stem cell population requires several sequential steps, including harvest, mechanical breakdown, chemical breakdown, purification, and plastic adherence. After these steps, it is important to count and characterise cells and their stemness potential with appropriate investigations.

Cell expansion plays a crucial role to allow adequate cell numbers required for in vitro studies. However, when considering an in situ one-step regenerative procedure for chondral defects, initial cell harvest numbers will need to be adequate for repairing variably sized lesions. Approximately one million cells are needed for a 1 cm^3 lesion [29]. Therefore, studies into cell numbers per tissue unit harvested will be crucial. Recently, cell aggregates have demonstrated increased proliferative ability. This may be due to direct cell-cell contact, allowing better intracellular communication [30–32]. It will be important to now study the number of aggregated cells needed to repair variably sized lesions; if less than one million cells are needed per 1 cm^3 lesion, this could prove to be a major breakthrough.

The steps involved and respective timeframes when using standard protocols are shown below (Figure 2). With both sources, current techniques take >1 hour for cell isolation and subsequently require incubation for up to 24–48 hours to allow for plastic adherence [33]. This was proven to be a lengthy procedure which is not a major concern if only applied to in vitro studies.

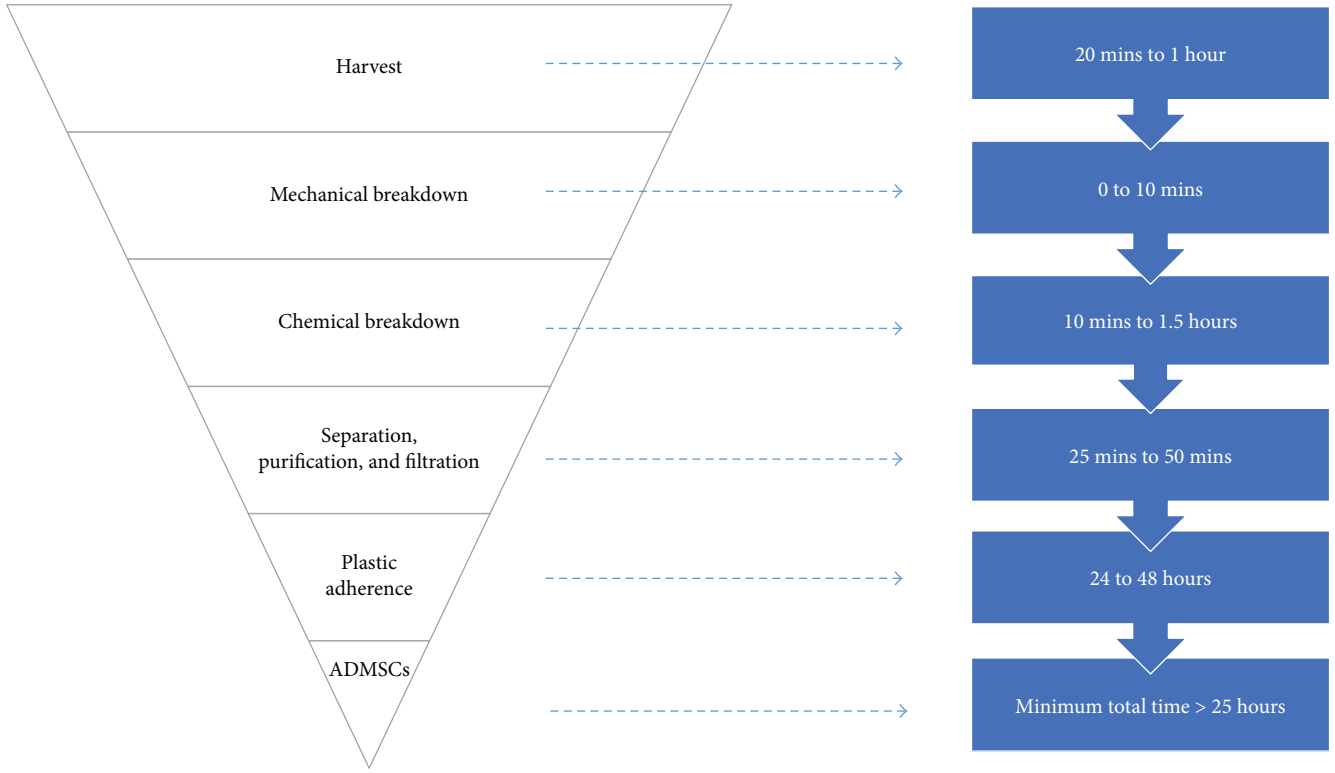

Figure 2: Adipose-derived mesenchymal stem cell (ADMSC) isolation protocol including timeframes.

4.1. Harvest. Abdominal fat can be harvested endoscopically or via abdominoplasty with no significant difference in cell structure and the number of cells yielded per unit of volume [34]. Both take minimal procedural time of <20 minutes; however, the intended abdominoplasty procedure may take much longer. Minimal comparisons are present in the literature. Two studies showed the comparable morphology of cells harvested from endoscopic (liposuction) and abdominoplasty (resection) techniques; however, inadequate phenotyping and characterisation of isolated cells were undertaken in both studies [35–37].

Infrapatellar fat pad (IFP) can be harvested via arthroscopy and opportunistically from arthroplasty. While both tissue harvesting techniques only require the minimal procedural time of <20 minutes, the overall arthroplasty procedure may take up to 2 hours. Additionally, isolated ADMSCs from IFP have been shown to have higher chondrogenic potential compared to cells isolated from bone marrow [26] and abdominal adipose tissue [27], making them a superior source.

4.2. Mechanical Breakdown. Abdominal fat harvested via liposuction is obtained in lipoaspirate form and does not require any further mechanical breakdown. IFP tissue requires separation of fat from the fibrous pad via a scalpel which takes roughly 10 minutes [38].

4.3. Chemical Breakdown. Once fat particles have been isolated from both sources, collagenase is added to the samples to allow chemical breakdown of the tissue. While a number of collagenases are available for ADMSC isolation (Table 1), type 1 collagenase is the preferred agent for isolation prior to chondrogenic lineage induction. Research shown using collagenase type 1 at 0.2% for 10 minutes of chemical/enzymatic breakdown can obtain a stromal vascular fraction [39]. Increased time > 30 minutes using collagenase digestion has been shown to reduce the number of viable adipocytes [40]. Adding trypsin to pure collagenase allows for maximal digestion [41]. Further study is warranted to find the optimal type and concentration of collagenase to enable rapid, effective, and efficient disaggregation of AMDSCs.

After the addition of collagenase, the samples are incubated and agitated with a rotating platform (≥100 revolutions per minute). During incubation on the platform, both chemical and mild mechanical agitations occur synergistically.

4.4. Purification. Purification refers to the separation of material, the removal of unrequired product, and filtration. Following mechanical and chemical breakdowns, the sample undergoes a universal step of centrifugation for 10 minutes [34, 38]. Next, the supernatant is removed, and the pellet is washed with phosphate buffer solution before being filtered through a sterile 100 μm filter. After another round of centrifugation for 5 minutes, the supernatant is discarded and the remaining pellet is then resuspended in 5 millilitres of red cell lysis buffer [28] for 10 minutes before being filtered through a sterile 40 μm filter [38]. After a final 5-minute round of centrifugation, the resulting supernatant is removed, leaving a cell pellet. This total purification procedure is reported to take anywhere between 25 and 50 minutes. Postpurification

Table 1: Comparison of human studies using enzymatic breakdown with collagenase for ADMSC isolation from subcutaneous tissue. Phosphate buffer solution (PBS), Hank's balanced salt solution (HBSS), bovine serum albumin (BSA), and Dulbecco's modified eagle's medium (DMEM).

Author	Collagenase	Concentration	Dilution media	Enzymatic duration
Cheng et al. [42]	Type 1	0.1%	PBS	60 minutes
Choudhery et al. [43]	Type 4	0.2%	PBS	20 minutes
Satish et al. [44]	Type 2	0.1%	HBSS/BSA	40 minutes
Kinoshita et al. [45]	Type 1	0.075%	PBS	30 minutes
Al-Saqi et al. [46]	Type 2	0.1%	Unspecified	45 minutes
Koellensperger et al. [47]	Type 1	0.15%	BSA	45 minutes
Najar et al. [48]	Type 1	0.1%	BSA	45 minutes
Cervelli et al. [49]	Type 1	0.1%	Unspecified	60 minutes
Wu et al. [50]	Type 1	0.1%	DMEM	90 minutes
Yang et al. [51]	Type 1	0.1%	PBS	60 minutes
Yu et al. [52]	Type 1	0.1%	DMEM	60 minutes
Tan et al. [53]	Type 2	1.0%	HBSS/BSA	50 minutes
Kilroy et al. [54]	Type 1	0.1%	PBS/BSA	60 minutes
Jeon et al. [55]	Type 1	0.1%	HBSS/BSA	60 minutes
Rodriguez et al. [39]	Unspecified	0.2%	DMEM/BSA	10 minutes
Devireddy et al. [56]	Type 1	0.1%	PBS/BSA	60 minutes

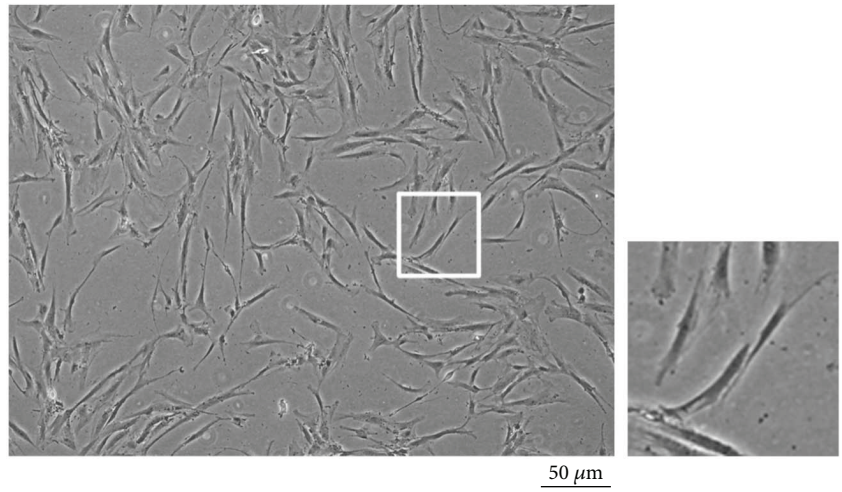

Figure 3: Plastic adherence and morphology of mesenchymal stem cells isolated from the infrapatellar fat pad, representative view using bright field microscopy.

cells are resuspended in culture media and then counted prior to being plated in flasks.

4.5. Plastic Adherence. Once cells are plated in appropriate flasks based on cell counts, they are incubated usually for 24–48 hours. Cell attachment to plastic is a key step for identifying and isolating cells with stem cell characteristics. Unattached cells are discarded. At this stage, the attached cells can be expanded and passaged or frozen in liquid nitrogen for later use. This plastic adherence step requires a minimum of 24 hours of incubation. Cell sorting using marker selection (flow sorting) is an alternative to plastic adherence with respect to isolating a pure ADMSC population [57]. The drawback to this technique is the time requirement and lack of exact phenotypic characterisation of ADMSCs.

4.6. Phenotype. As per the International Society for Cellular Therapy [58, 59], three criteria must be fulfilled for the MSC phenotype: adherence to plastic, appropriate surface antigens, and expression of multipotent differentiation potential.

Plastic adherence is a hallmark property of all MSC groups [60, 61]. Furthermore, typical morphology and colony formation can be observed under a microscope as seen in Figure 3.

To confirm the phenotype of cells isolated as MSCs, specific surface antigens are tested through immunophenotyping and can be done via flow cytometry [46]. MSCs generally express (≥95%) CD73, CD90, and CD105, while lacking expression (≤2%) of CD 11b, CD14, CD34, CD45, and CD79a [47].

Table 2: Mesenchymal stem cell differentiation testing. COL: collagen; OCN: osteocalcin; ALP: alkaline phosphatase; PPARG: peroxisome proliferator-activated receptor gamma; C/EBP: CCAAT/enhancer-binding protein; ACAN: aggrecan.

Lineage	Histological staining	qPCR gene expression
Osteoblasts	Alizarin Red, Von Kossa	COL 1A1, OCN, runx 2, ALP
Adipocytes	Oil Red O	PPARG 1 and 2, C/EBP a and d
Chondroblasts	Alcian blue	COL 2A1, SOX-9, ACAN

However, exact characterisation is still in development [57, 62], and surface phenotyping should be used in conjunction with other criteria to help best identify MSC.

Biologically, MSCs should display three lines of differentiation potential: osteoblasts, adipocytes, and chondroblasts [58]. Multipotent potential can be evidenced by differentiation into various lineages using different induction paths [16] and can be tested with staining and qPCR (Table 2).

5. Rapid Isolation Procedures in Literature

Over the past decade, several commercially available enzymatic and nonenzymatic adipose tissue cell isolation systems [63, 64] have achieved sterile processing and high yields of cells. However, these systems only isolate a stromal vascular fraction (SVF), implying that a plastic adherence step is still required for pure ADMSC isolation.

One published attempt at a rapid protocol using abdominal lipoaspirates achieved an SVF isolation within 30 minutes [12]. 2.5×10^5 ADMSCs were isolated using the 30-minute approach compared to 2.0×10^6 from the standard approach. The final step of plastic adherence to isolate a pure ADMSC population still required 24–48 hours of further incubation. Furthermore, the number of ADMSCs yielded was nearly 10 times less when compared to the standard procedure.

A purely nonenzymatic breakdown approach with blender mixing and sonication has been used to obtain an SVF within 25 minutes [65]. On average, 2.6×10^5 cells were isolated in the SVF, resulting in a very low average of 2.4×10^4 ADMSCs. Although SVF isolation is rapid, overnight (>24 hours) plastic adherence is once again still required to obtain a pure ADMSC population.

It is evident from these two approaches that a low number of cells are obtained, possibly due to toxicity from the methodology. Moreover, only an SVF was rapidly isolated as opposed to a pure ADMSC population, which still takes >24 hours.

The use of SVF alone, without the use of a pure ADMSC population, may be another therapeutic option. As mentioned earlier, given the superior chondrogenic potential of ADMSCs isolated from the IFP [27, 28], SVF populations from abdominal fat should be compared to IFP before trialling SVF as a direct one-step therapeutic option. However, the lack of cell-cell contact within an SVF due to scattered ADMSCs will lead to inferior cartilage repair as a result of reduced paracrine stimulation [30].

6. Where Can We Save Time?

There are three procedural steps where time could be saved. These are discussed below and also represented in Figure 4.

6.1. Mechanical Breakdown. The initial mechanical breakdown could be further enhanced by adding mechanical agitation through shaking, vortexing, and possibly adding sterile solid materials during chemical breakdown to synergistically assist the breakdown of tissue. Sterile beads have been used commercially in liposuction kits to help emulsify tissue [66]. If such materials were to be used, they need to be sterilisable and nontoxic and show a consistent and predictable effect on tissue breakdown based on morphology and weight. These factors will need proper investigation prior incorporation into isolation techniques. The risk of these more vigorous approaches is cell damage and death; therefore, it will be important to assess cell viability in such intended studies.

Although it currently only takes 0–10 minutes to break tissue down depending on the source, the more vigorous breakdown of tissue earlier, particularly of IFP tissue, may help reduce the total time needed for the subsequent step of chemical breakdown.

6.2. Chemical Breakdown. The chemical breakdown shows varying timeframes with reports of 10 minutes for the breakdown of tissue into an SVF [39]. Higher concentrations of collagenase with the addition of trypsin may allow for the maximal breakdown, while higher rpm use on rotating platforms may enable synergistic breakdown. Once again, the possibility of cell toxicity will need to be investigated [40].

6.3. Plastic Adherence. Plastic adherence forms the major time barrier (minimum of 24 hours). A new rapid technique needs to be established in this step as this timeframe is not clinically feasible.

Recent literature has reported the high affinity of articular progenitor cells (APCs) to fibronectin, with research showing APC adherence to fibronectin-coated wells in 20 minutes [67]. Although lacking clearly defined markers, these APCs, also known as chondrogenic progenitor cells, have shown stem cell potential and are similar to and possibly more differentiated forms of ADMSCs [68].

This is a major finding supporting the use of fibronectin-coated wells or plates to isolate ADMSCs if it can be demonstrated through immunophenotyping that stem cells are attaching selectively to the coating.

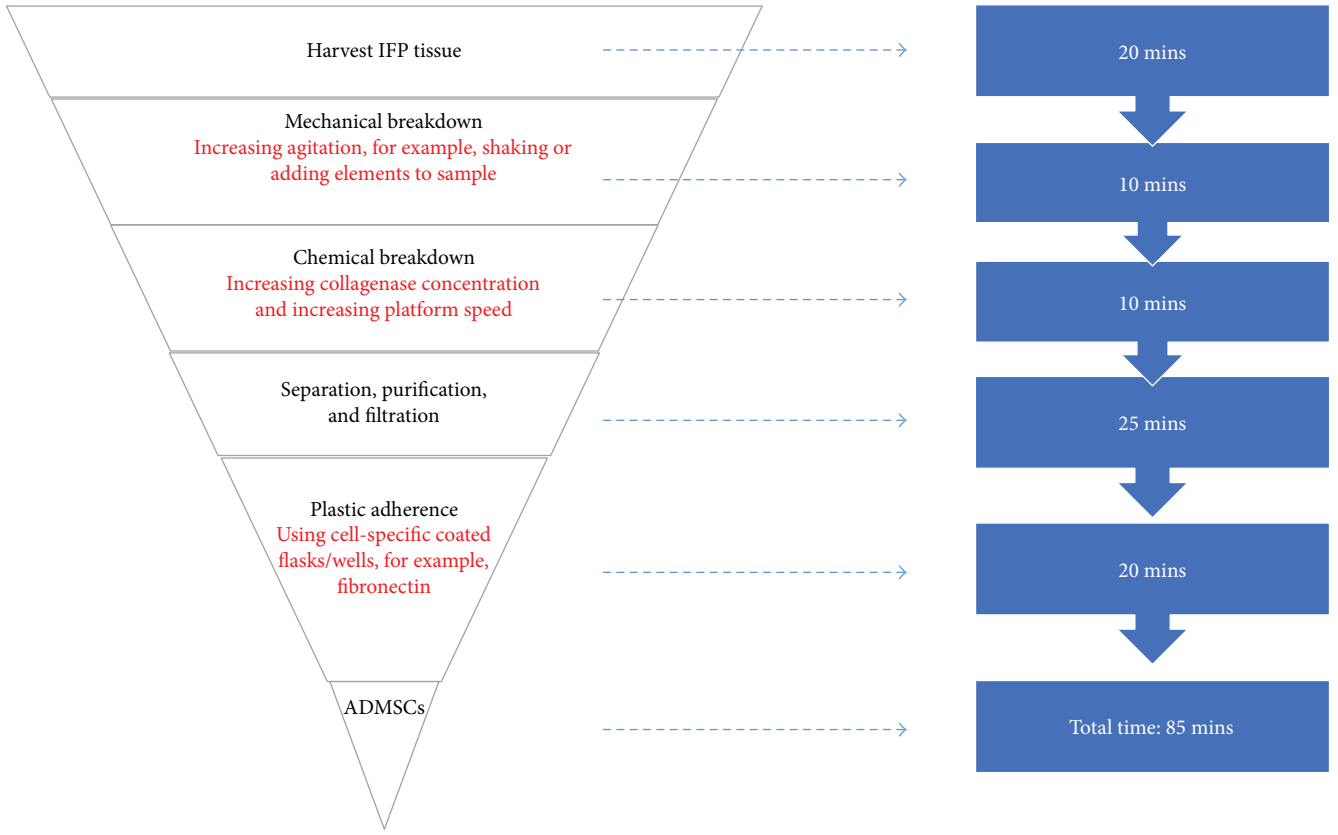

Figure 4: Proposed rapid adipose-derived mesenchymal stem cell (ADMSC) isolation procedure from the infrapatellar fat pad (IFP). The three major changes proposed are highlighted in red.

7. Conclusion and Future Clinical Applicability

A rapid ADMSC isolation technique is necessary for a single-step, tissue engineering-based surgical repair of cartilage tissue. Literature to date suggests IFP-harvested ADMSCs to be the most promising in chondrogenic potential. If a procedure can isolate ADMSCs using an approach such as that described in Figure 4, then incorporating the cells into a matrix and implanting them into a defect using handheld bioprinters [69–71] may pave the way for a single-step intraoperative cartilage repair technique. When leveraging the advantages of a day-only minimal incision surgery, such as arthroscopy, there may be significant clinical outcome and health care cost gains.

The future of cartilage repair is promising. By speeding up cell isolation techniques, a major time barrier can be overcome, translating a clinically to a nonlaboratory-based procedure, shorter surgical time, quicker recovery for the patient, and a smaller burden on the health care system. Younger patients can now hope for a simple, low-risk treatment option that aids in preventing the onset of osteoarthritis.

Abbreviations

MSCs: Mesenchymal stem cells
ADMSCs: Adipose-derived mesenchymal stem cells
IFP: Infrapatellar fat pad
BM: Bone marrow
SVF: Stromal vascular fraction
APC: Articular progenitor cells.

Conflicts of Interest

The authors declare that there is no conflict of interest regarding the publication of this paper.

References

[1] J. E. Jeon, K. Schrobback, D. W. Hutmacher, and T. J. Klein, "Dynamic compression improves biosynthesis of human zonal chondrocytes from osteoarthritis patients," *Osteoarthritis and Cartilage*, vol. 20, no. 8, pp. 906–915, 2012.

[2] A. P. Hollander, S. C. Dickinson, and W. Kafienah, "Stem cells and cartilage development: complexities of a simple tissue," *Stem Cells*, vol. 28, no. 11, pp. 1992–1996, 2010.

[3] O. Robertsson, A. Stefánsdòttir, L. Lidgren, and J. Ranstam, "Increased long-term mortality in patients less than 55 years old who have undergone knee replacement for osteoarthritis," *The Journal of Bone and Joint Surgery*, vol. 89-B, no. 5, pp. 599–603, 2007.

[4] J. Julin, E. Jämsen, T. Puolakka, Y. T. Konttinen, and T. Moilanen, "Younger age increases the risk of early prosthesis failure following primary total knee replacement for osteoarthritis," *Acta Orthopaedica*, vol. 81, no. 4, pp. 413–419, 2010.

[5] CITER (Cardiff Institute of Tissue Engineering and Repair), Cardiff School of Biosciences, Museum Avenue, Cardiff, CF10 3US, Wales, UK, S. N. Redman, S. F. Oldfield, and

C. W. Archer, "Current strategies for articular cartilage repair," *European Cells & Materials*, vol. 9, pp. 23–32, 2005.

[6] B. Bunnell, M. Flaat, C. Gagliardi, B. Patel, and C. Ripoll, "Adipose-derived stem cells: isolation, expansion and differentiation," *Methods*, vol. 45, no. 2, pp. 115–120, 2008.

[7] P. V. Giannoudis, T. A. Einhorn, and D. Marsh, "Fracture healing: the diamond concept," *Injury*, vol. 38, pp. S3–S6, 2007.

[8] M. L. Torre, E. Lucarelli, S. Guidi et al., "Ex vivo expanded mesenchymal stromal cell minimal quality requirements for clinical application," *Stem Cells and Development*, vol. 24, no. 6, pp. 677–685, 2015.

[9] K. Beitzel, M. B. McCarthy, M. P. Cote et al., "Rapid isolation of human stem cells (connective progenitor cells) from the distal femur during arthroscopic knee surgery," *Arthroscopy*, vol. 28, no. 1, pp. 74–84, 2012.

[10] A. D. Mazzocca, M. B. R. McCarthy, D. M. Chowaniec, M. P. Cote, R. A. Arciero, and H. Drissi, "Rapid isolation of human stem cells (connective tissue progenitor cells) from the proximal humerus during arthroscopic rotator cuff surgery," *The American Journal of Sports Medicine*, vol. 38, no. 7, pp. 1438–1447, 2010.

[11] B. Dozza, G. Gobbi, E. Lucarelli et al., "A rapid method for obtaining mesenchymal stem cells and platelets from bone marrow aspirate," *Journal of Tissue Engineering and Regenerative Medicine*, vol. 8, no. 6, pp. 483–492, 2014.

[12] M. P. Francis, P. C. Sachs, L. W. Elmore, and S. E. Holt, "Isolating adipose-derived mesenchymal stem cells from lipoaspirate blood and saline fraction," *Organogenesis*, vol. 6, no. 1, pp. 11–14, 2014.

[13] P. A. Zuk, M. Zhu, H. Mizuno et al., "Multilineage cells from human adipose tissue: implications for cell-based therapies," *Tissue Engineering*, vol. 7, no. 2, pp. 211–228, 2001.

[14] A. J. Becker, E. A. Mcculloch, and J. E. Till, "Cytological demonstration of the clonal nature of spleen colonies derived from transplanted mouse marrow cells," *Nature*, vol. 197, no. 4866, pp. 452–454, 1963.

[15] A. J. Friedenstein, U. F. Deriglasova, N. N. Kulagina et al., "Precursors for fibroblasts in different populations of hematopoietic cells as detected by the in vitro colony assay method," *Experimental Hematology*, vol. 2, no. 2, pp. 83–92, 1974.

[16] M. F. Pittenger, A. M. Mackay, S. C. Beck et al., "Multilineage potential of adult human mesenchymal stem cells," *Science*, vol. 284, no. 5411, pp. 143–147, 1999.

[17] T. Rada, R. L. Reis, and M. E. Gomes, "Adipose tissue-derived stem cells and their application in bone and cartilage tissue engineering," *Tissue Engineering Part B: Reviews*, vol. 15, no. 2, pp. 113–125, 2009.

[18] F. Veronesi, M. Maglio, M. Tschon, N. N. Aldini, and M. Fini, "Adipose-derived mesenchymal stem cells for cartilage tissue engineering: state-of-the-art in in vivo studies," *Journal of Biomedical Materials Research Part A*, vol. 102, no. 7, pp. 2448–2466, 2014.

[19] G. Sheng, "The developmental basis of mesenchymal stem/stromal cells (MSCs)," *BMC Developmental Biology*, vol. 15, no. 1, p. 44, 2015.

[20] M.-C. Kastrinaki, I. Andreakou, P. Charbord, and H. A. Papadaki, "Isolation of human bone marrow mesenchymal stem cells using different membrane markers: comparison of colony/cloning efficiency, differentiation potential, and molecular profile," *Tissue Engineering Part C: Methods*, vol. 14, no. 4, pp. 333–339, 2008.

[21] M. C. Ronzière, E. Perrier, F. Mallein-Gerin, and A. M. Freyria, "Chondrogenic potential of bone marrow- and adipose tissue-derived adult human mesenchymal stem cells," *Biomedical Materials and Engineering*, vol. 20, no. 3, pp. 145–158, 2010.

[22] M. Strioga, S. Viswanathan, A. Darinskas, O. Slaby, and J. Michalek, "Same or not the same? Comparison of adipose tissue-derived versus bone marrow-derived mesenchymal stem and stromal cells," *Stem Cells and Development*, vol. 21, no. 14, pp. 2724–2752, 2012.

[23] Y. Jang, Y. G. Koh, Y. J. Choi et al., "Characterization of adipose tissue-derived stromal vascular fraction for clinical application to cartilage regeneration," *In Vitro Cellular & Developmental Biology. Animal*, vol. 51, no. 2, pp. 142–150, 2015.

[24] J. L. Dragoo, B. Samimi, M. Zhu et al., "Tissue-engineered cartilage and bone using stem cells from human infrapatellar fat pads," *The Journal of Bone and Joint Surgery, British Volume*, vol. 85-B, no. 5, pp. 740–747, 2003.

[25] C. T. Buckley, T. Vinardell, S. D. Thorpe et al., "Functional properties of cartilaginous tissues engineered from infrapatellar fat pad-derived mesenchymal stem cells," *Journal of Biomechanics*, vol. 43, no. 5, pp. 920–926, 2010.

[26] P. Hindle, N. Khan, L. Biant, and B. Péault, "The Infrapatellar fat pad as a source of perivascular stem cells with increased chondrogenic potential for regenerative medicine," *Stem Cells Translational Medicine*, vol. 6, no. 1, pp. 77–87, 2017.

[27] S. Lopa, A. Colombini, D. Stanco, L. de Girolamo, V. Sansone, and M. Moretti, "Donor-matched mesenchymal stem cells from knee infrapatellar and subcutaneous adipose tissue of osteoarthritic donors display differential chondrogenic and osteogenic commitment," *European Cells & Materials*, vol. 27, pp. 298–311, 2014.

[28] R. Felimban, K. Ye, K. Traianedes et al., "Differentiation of stem cells from human infrapatellar fat pad: characterization of cells undergoing chondrogenesis," *Tissue Engineering Part A*, vol. 20, no. 15-16, pp. 2213–2223, 2014.

[29] A. Singh, S. C. Goel, K. K. Gupta et al., "The role of stem cells in osteoarthritis: an experimental study in rabbits," *Bone & Joint Research*, vol. 3, no. 2, pp. 32–37, 2014.

[30] B. Sridharan, S. M. Lin, A. T. Hwu, A. D. Laflin, and M. S. Detamore, "Stem cells in aggregate form to enhance chondrogenesis in hydrogels," *PLoS One*, vol. 10, no. 12, article e0141479, 2015.

[31] G. M. van Buul, E. Villafuertes, P. K. Bos et al., "Mesenchymal stem cells secrete factors that inhibit inflammatory processes in short-term osteoarthritic synovium and cartilage explant culture," *Osteoarthritis and Cartilage*, vol. 20, no. 10, pp. 1186–1196, 2012.

[32] I. Linero and O. Chaparro, "Paracrine effect of mesenchymal stem cells derived from human adipose tissue in bone regeneration," *PLoS One*, vol. 9, no. 9, article e107001, 2014.

[33] S. Nae, I. Bordeianu, A. T. Stăncioiu, and N. Antohi, "Human adipose-derived stem cells: definition, isolation, tissue-engineering applications," *Romanian Journal of Morphology and Embryology*, vol. 54, no. 4, pp. 919–924, 2013.

[34] S. Schneider, M. Unger, M. van Griensven, and E. R. Balmayor, "Adipose-derived mesenchymal stem cells from liposuction and resected fat are feasible sources for regenerative medicine," *European Journal of Medical Research*, vol. 22, no. 1, p. 17, 2017.

[35] H. Busser, M. Najar, G. Raicevic et al., "Isolation and characterization of human mesenchymal stromal cell subpopulations: comparison of bone marrow and adipose tissue," *Stem Cells and Development*, vol. 24, no. 18, pp. 2142–2157, 2015.

[36] H. Eto, H. Suga, D. Matsumoto et al., "Characterization of structure and cellular components of aspirated and excised adipose tissue," *Plastic and Reconstructive Surgery*, vol. 124, no. 4, pp. 1087–1097, 2009.

[37] M. Faustini, M. Bucco, T. Chlapanidas et al., "Nonexpanded mesenchymal stem cells for regenerative medicine: yield in stromal vascular fraction from adipose tissues," *Tissue Engineering Part C: Methods*, vol. 16, no. 6, pp. 1515–1521, 2010.

[38] P. Tangchitphisut, N. Srikaew, S. Numhom et al., "Infrapatellar fat pad: an alternative source of adipose-derived mesenchymal stem cells," *Arthritis*, vol. 2016, Article ID 4019873, 10 pages, 2016.

[39] A. M. Rodriguez, D. Pisani, C. A. Dechesne et al., "Transplantation of a multipotent cell population from human adipose tissue induces dystrophin expression in the immunocompetent mdx mouse," *The Journal of Experimental Medicine*, vol. 201, no. 9, pp. 1397–1405, 2005.

[40] S. A. Seaman, S. C. Tannan, Y. Cao, S. M. Peirce, and K. Y. Lin, "Differential effects of processing time and duration of collagenase digestion on human and murine fat grafts," *Plastic and Reconstructive Surgery*, vol. 136, no. 2, pp. 189e–199e, 2015.

[41] S. K. Williams, S. Mckenney, and B. E. Jarrell, "Collagenase lot selection and purification for adipose tissue digestion," *Cell Transplantation*, vol. 4, no. 3, pp. 281–289, 2017.

[42] N. C. Cheng, T. Y. Hsieh, H. S. Lai, and T. H. Young, "High glucose-induced reactive oxygen species generation promotes stemness in human adipose-derived stem cells," *Cytotherapy*, vol. 18, no. 3, pp. 371–383, 2016.

[43] M. S. Choudhery, M. Badowski, A. Muise, and D. T. Harris, "Effect of mild heat stress on the proliferative and differentiative ability of human mesenchymal stromal cells," *Cytotherapy*, vol. 17, no. 4, pp. 359–368, 2015.

[44] L. Satish, J. M. Krill-Burger, P. H. Gallo et al., "Expression analysis of human adipose-derived stem cells during in vitro differentiation to an adipocyte lineage," *BMC Medical Genomics*, vol. 8, no. 1, p. 41, 2015.

[45] K. Kinoshita, S. Kuno, H. Ishimine et al., "Therapeutic potential of adipose-derived SSEA-3-positive muse cells for treating diabetic skin ulcers," *Stem Cells Translational Medicine*, vol. 4, no. 2, pp. 146–155, 2015.

[46] S. H. Al-Saqi, M. Saliem, S. Asikainen et al., "Defined serum-free media for in vitro expansion of adipose-derived mesenchymal stem cells," *Cytotherapy*, vol. 16, no. 7, pp. 915–926, 2014.

[47] E. Koellensperger, N. Bollinger, V. Dexheimer, F. Gramley, G. Germann, and U. Leimer, "Choosing the right type of serum for different applications of human adipose tissue-derived stem cells: influence on proliferation and differentiation abilities," *Cytotherapy*, vol. 16, no. 6, pp. 789–799, 2014.

[48] M. Najar, R. M. Rodrigues, K. Buyl et al., "Proliferative and phenotypical characteristics of human adipose tissue-derived stem cells: comparison of Ficoll gradient centrifugation and red blood cell lysis buffer treatment purification methods," *Cytotherapy*, vol. 16, no. 9, pp. 1220–1228, 2014.

[49] V. Cervelli, M. G. Scioli, P. Gentile et al., "Platelet-rich plasma greatly potentiates insulin-induced adipogenic differentiation of human adipose-derived stem cells through a serine/threonine kinase Akt-dependent mechanism and promotes clinical fat graft maintenance," *Stem Cells Translational Medicine*, vol. 1, no. 3, pp. 206–220, 2012.

[50] I. Wu, Z. Nahas, K. A. Kimmerling, G. D. Rosson, and J. H. Elisseeff, "An injectable adipose matrix for soft-tissue reconstruction," *Plastic and Reconstructive Surgery*, vol. 129, no. 6, pp. 1247–1257, 2012.

[51] X. F. Yang, X. He, J. He et al., "High efficient isolation and systematic identification of human adipose-derived mesenchymal stem cells," *Journal of Biomedical Science*, vol. 18, no. 1, p. 59, 2011.

[52] G. Yu, Z. E. Floyd, X. Wu, Y.-D. C. Halvorsen, and J. M. Gimble, "Isolation of human adipose-derived stem cells from lipoaspirates," *Methods in Molecular Biology*, vol. 702, pp. 17–27, 2011.

[53] H. Tan, A. J. DeFail, J. P. Rubin, C. R. Chu, and K. G. Marra, "Novel multiarm PEG-based hydrogels for tissue engineering," *Journal of Biomedical Materials Research Part A*, vol. 92A, no. 3, pp. 979–987, 2009.

[54] G. E. Kilroy, S. J. Foster, X. Wu et al., "Cytokine profile of human adipose-derived stem cells: expression of angiogenic, hematopoietic, and pro-inflammatory factors," *Journal of Cellular Physiology*, vol. 212, no. 3, pp. 702–709, 2007.

[55] E. S. Jeon, H. Y. Song, M. R. Kim et al., "Sphingosylphosphorylcholine induces proliferation of human adipose tissue-derived mesenchymal stem cells via activation of JNK," *Journal of Lipid Research*, vol. 47, no. 3, pp. 653–664, 2006.

[56] R. Devireddy, S. Thirumala, and J. Gimble, "Cellular response of adipose derived passage-4 adult stem cells to freezing stress," *Journal of Biomechanical Engineering*, vol. 127, no. 7, pp. 1081–1086, 2005.

[57] U. D. Wankhade, M. Shen, R. Kolhe, and S. Fulzele, "Advances in adipose-derived stem cells isolation, characterization, and application in regenerative tissue engineering," *Stem Cells International*, vol. 2016, Article ID 3206807, 9 pages, 2016.

[58] M. Dominici, K. le Blanc, I. Mueller et al., "Minimal criteria for defining multipotent mesenchymal stromal cells. The International Society for Cellular Therapy position statement," *Cytotherapy*, vol. 8, no. 4, pp. 315–317, 2006.

[59] M. Krampera, J. Galipeau, Y. Shi, K. Tarte, L. Sensebe, and MSC Committee of the International Society for Cellular Therapy (ISCT), "Immunological characterization of multipotent mesenchymal stromal cells—The International Society for Cellular Therapy (ISCT) working proposal," *Cytotherapy*, vol. 15, no. 9, pp. 1054–1061, 2013.

[60] D. C. Colter, R. Class, C. M. DiGirolamo, and D. J. Prockop, "Rapid expansion of recycling stem cells in cultures of plastic-adherent cells from human bone marrow," *Proceedings of the National Academy of Sciences of the United States of America*, vol. 97, no. 7, pp. 3213–3218, 2000.

[61] Y. Jiang, B. N. Jahagirdar, R. L. Reinhardt et al., "Pluripotency of mesenchymal stem cells derived from adult marrow," *Nature*, vol. 418, no. 6893, pp. 41–49, 2002.

[62] F. Sabatini, L. Petecchia, M. Tavian, V. J. de Villeroché, G. A. Rossi, and D. Brouty-Boyé, "Human bronchial fibroblasts exhibit a mesenchymal stem cell phenotype and multilineage differentiating potentialities," *Laboratory Investigation*, vol. 85, no. 8, pp. 962–971, 2005.

[63] E. Oberbauer, C. Steffenhagen, C. Wurzer, C. Gabriel, H. Redl, and S. Wolbank, "Enzymatic and non-enzymatic isolation

systems for adipose tissue-derived cells: current state of the art," *Cell Regeneration*, vol. 4, no. 1, p. 4:7, 2015.

[64] E. Raposio, F. Simonacci, and R. E. Perrotta, "Adipose-derived stem cells: comparison between two methods of isolation for clinical applications," *Annals of Medicine and Surgery*, vol. 20, pp. 87–91, 2017.

[65] M. A. Amirkhani, R. Mohseni, M. Soleimani, A. Shoae-Hassani, and M. A. Nilforoushzadeh, "A rapid sonication based method for preparation of stromal vascular fraction and mesenchymal stem cells from fat tissue," *Bioimpacts*, vol. 6, no. 2, pp. 99–104, 2016.

[66] February 2018, http://www.lipogems.eu/lipoaspiration-procedure.html.

[67] G. P. Dowthwaite, J. C. Bishop, S. N. Redman et al., "The surface of articular cartilage contains a progenitor cell population," *Journal of Cell Science*, vol. 117, no. 6, pp. 889–897, 2004.

[68] Y. Jiang and R. S. Tuan, "Origin and function of cartilage stem/progenitor cells in osteoarthritis," *Nature Reviews Rheumatology*, vol. 11, no. 4, pp. 206–212, 2015.

[69] C. Di Bella, A. Fosang, D. M. Donati, G. G. Wallace, and P. F. M. Choong, "3D bioprinting of cartilage for orthopedic surgeons: reading between the lines," *Frontiers in Surgery*, vol. 2, 2015.

[70] C. D. O'Connell, C. Di Bella, F. Thompson et al., "Development of the Biopen: a handheld device for surgical printing of adipose stem cells at a chondral wound site," *Biofabrication*, vol. 8, no. 1, 2016.

[71] S. Duchi, C. Onofrillo, C. D. O'Connell et al., "Handheld co-axial bioprinting: application to in situ surgical cartilage repair," *Scientific Reports*, vol. 7, no. 1, p. 5837, 2017.

Hindawi
Stem Cells International
Volume 2018, Article ID 5421019, 13 pages
https://doi.org/10.1155/2018/5421019

Review Article

Combating Osteoarthritis through Stem Cell Therapies by Rejuvenating Cartilage: A Review

Navneet Kumar Dubey,[1,2] Viraj Krishna Mishra,[3] Rajni Dubey,[4] Shabbir Syed-Abdul,[5] Joseph R. Wang,[6] Peter D. Wang,[7,8] and Win-Ping Deng[2,7,9]

[1]*Ceramics and Biomaterials Research Group, Advanced Institute of Materials Science, Ton Duc Thang University, Ho Chi Minh City, Vietnam*
[2]*Faculty of Applied Sciences, Ton Duc Thang University, Ho Chi Minh City, Vietnam*
[3]*Applied Biotech Engineering Centre (ABEC), Department of Biotechnology, Ambala College of Engineering and Applied Research, Ambala, India*
[4]*Graduate Institute of Food Science and Technology, National Taiwan University, Taipei, Taiwan*
[5]*Graduate Institute of Biomedical Informatics, College of Medical Science and Technology, Taipei Medical University, Taipei, Taiwan*
[6]*Department of Periodontics, College of Dental Medicine, Columbia University, New York, NY, USA*
[7]*School of Dentistry, College of Oral Medicine, Taipei Medical University, Taipei, Taiwan*
[8]*Department of Dentistry, Taipei Medical University Hospital, Taipei, Taiwan*
[9]*Graduate Institute of Basic Medicine, Fu Jen Catholic University, Taipei, Taiwan*

Correspondence should be addressed to Win-Ping Deng; wpdeng@tmu.edu.tw

Received 29 December 2017; Accepted 5 February 2018; Published 22 March 2018

Academic Editor: Wesley Sivak

Knee osteoarthritis (OA) is a chronic degenerative disorder which could be distinguished by erosion of articular cartilage, pain, stiffness, and crepitus. Not only aging-associated alterations but also the metabolic factors such as hyperglycemia, dyslipidemia, and obesity affect articular tissues and may initiate or exacerbate the OA. The poor self-healing ability of articular cartilage due to limited regeneration in chondrocytes further adversely affects the osteoarthritic microenvironment. Traditional and current surgical treatment procedures for OA are limited and incapable to reverse the damage of articular cartilage. To overcome these limitations, cell-based therapies are currently being employed to repair and regenerate the structure and function of articular tissues. These therapies not only depend upon source and type of stem cells but also on environmental conditions, growth factors, and chemical and mechanical stimuli. Recently, the pluripotent and various multipotent mesenchymal stem cells have been employed for OA therapy, due to their differentiation potential towards chondrogenic lineage. Additionally, the stem cells have also been supplemented with growth factors to achieve higher healing response in osteoarthritic cartilage. In this review, we summarized the current status of stem cell therapies in OA pathophysiology and also highlighted the potential areas of further research needed in regenerative medicine.

1. Introduction

Osteoarthritis (OA) is a prevalent debilitating joint disorder characterized by erosion of articular cartilage, excessive stiffness pain, and crepitus [1, 2]. According to the United Nations estimates, till 2050, 130 million people will be affected by OA throughout the world, out of which 40 million will develop severe OA [3]. As a consequence, a huge economic pressure will be imposed in treatment and management of OA leading to stressed and decreased quality of life [1, 4]. OA is classified as primary and secondary OA; primary OA is associated with aging, whereas secondary OA is pertinent to disease or other factors [5]. Further, the degradation of network of collagen and proteoglycan in OA cartilage leads to a loss in tensile strength and shear properties of cartilage [6]. Interestingly, though OA manifests as

loss of the articular cartilage, it also includes all tissues of the joint, particularly the subchondral bone [5, 7] Besides aging, the increase in level of accumulation of advanced glycation end products (AGEs), oxidative stress, and senescence-related secretory phenotypes are few reported factors associated with pathogenesis of OA [8]. The elevated senescent phenotypes in OA reduces healing properties of cartilage in an aging individual [9, 10], which might be attributed to oxidative damage and telomere shortening [10]. Aging also severely affects extracellular matrix (ECM) and proteoglycans synthesizing capacity of chondrocytes in OA leading to thinning of the cartilage and decreased water content [11–14]. Synthesis of irregular and small aggrecans disrupts the structural integrity of aging cartilage and reduces the chondrocytes' response to cytokines [15].

Currently, the awareness, prevention, diagnosis, and nonpharmacological and pharmacological treatments are used to manage the OA. If these initial nonpharmaceutical interventions fail, the pharmaceutical interventions such as NSAIDs, opioids, and surgery are considered as next level of treatment [16]. However, success of these therapeutic approaches is limited due to related complication and their efficiency. Besides, the autologous chondrocyte implantation (ACI) is one of the most preferred therapeutic approaches for treatment of damaged OA cartilage. Still, the complication related to harvesting chondrocytes had compelled to focus on other cell-based therapies [17]. Recent progresses in tissue engineering have highlighted the regenerative potential of stem cells for therapeutic purposes. The multilineage potential of stem cells, suitable scaffolds, and appropriate chondrogenic agent (chemical and mechanical stimuli) has been implicated to regenerate damaged cartilage [18, 19]. Stem cells could be the unlimited source of chondrocytes and expected to control iatrogenic effects of ACI treatments [18]. Mesenchymal stem cell- (MSC-) based therapy is also emerging as alternative to joint replacement with prostheses, due to its long-lasting effect [20]. The potential of stem cells to differentiate into osteoblasts, chondroblasts, and adipocytes [21], if stimulated properly, can regenerate cartilage both *in vivo* and *in vitro* too [17]. Bone marrow-derived MSC (BMSCs) and the MSCs derived from other cell sources such as synovium, umbilical cord blood, periosteum, peripheral blood, adipose tissue, and muscle have extensively been induced to differentiate into specialized tissues and organs [22]. Moreover, the coculture system of chondrocytes and MSCs have been investigated for cartilage regeneration [17]. Embryonic stem cells (ESCs) are considered as a better source of chondrocytes; however, the ethical concerns and other safety-related complications had impeded the utilization of these cells in regenerative therapy [22]. So, the current researches have more focused towards establishing adult stem cells as therapeutic progenitor for cartilage regeneration. The stem cell-based therapy offers various opportunities such as resurfacing whole joint surface, selection of personalized stem cells, mimicking the environmental conditions to develop the desired phenotype, and increase in level and rate of matrix synthesis, intra-articular stem cell injections, and exogenous wangling of stem cells to regenerate articular cartilage. However, the retention of the chondrogenic phenotype of differentiated stem cells, their integration with native tissue, and mimicking the natural physical strength is posing a challenge to adopt stem cell therapy for OA [18]. Therefore, in this review article, we summarized the current status of stem cell therapies in OA pathophysiology and also discussed the potential areas of further research needed in regenerative medicine.

2. Cartilage Injury and Stem Cells

The proper balance of aggrecan and collagen contents establishes the cartilage homeostasis and develops a characteristic physiochemical structure for distribution of loads and mobility [23]. The proteolytic enzymes are associated with synthesis, restructuring and repair of connective tissues, and any cartilage injury or genetic incongruity in association with irregular loading, which promote imbalance in metabolic activity through enhancing proteolytic activity, resulting in degradation of cartilage [24, 25]. Chondrocytes express these proteins under various stimulations such as mechanical stress, oxidative stress, growth factor response, and aging [26]. The cartilage injury leads to disintegration and degradation of cartilage and finally leads to release of aggrecan fragments, chondroitin sulfate, keratin sulfate, and type II collagen along with other catabolic and anabolic products such as disintegrin, the collagenase matrix metalloproteinase 13 (MMP-13), tumor necrosis factor-inducible gene 6 protein (TSG-6), tissue inhibitor of metalloproteinases-1 (TIMP-1), and activin A [27]. Monoclonal antibodies have also been produced to detect the presence of these compounds in body samples such as sera, urine, and synovial fluids of arthritis patients [28–31]. Cartilage is a nonvascular tissue and eludes vascularization by secreting antiangiogenic compounds (thrombospondin-1, chondromodulin-1, and SPARC (secreted protein acidic and rich in cysteine)), collagen type II derived N-terminal propeptide (PIIBNP), and the type XVIII derived endostatin [32]. Along with these factors, presence of tidemarks and calcific nature of the cartilage also resists vascularization of cartilage [33]. It has been established that injured cartilage activates kinases, resulting in activation of growth factors such as fibroblast growth factor 2 (FGF-2) [34, 35] and expression of chemokines and cytokines [27]. FGF-2 plays a critical role in degradation and protection of cartilage depending on its interaction with FGF receptor (FGFR)-1 or FGFR-3, respectively [36]. Molecular signaling pathways such as WNT and BMP have been reported for their role in promoting cartilage repair [37]. It has been reported that cartilage regeneration in OA is promoted by an increase in matrix synthesis and cellular growth, where chondrocytes clumps are generated in middle and deep zones of the cartilage [38, 39]. However, these processes are not capable enough to fully regenerate damaged cartilage [40].

Multilineage potential of stem cells is progressively exploited to regenerate cartilage and to provide cellular therapy for other related arthritis disorders. The current developments in tissue engineering have been made feasible to mimic the process of cartilage synthesis both *in vivo* and *in vitro*. Embryonic stem cells (ESCs), induced pluripotent stem cells

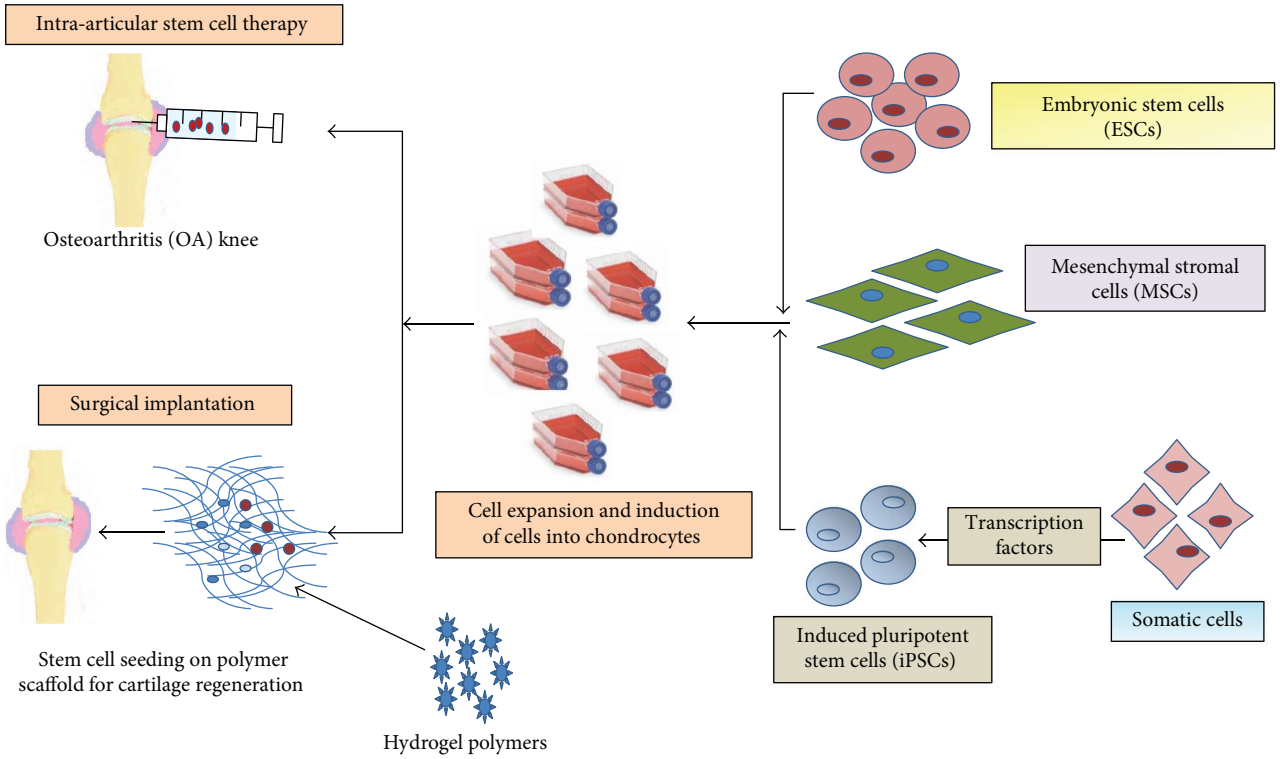

Figure 1: Schematic of stem cell-based therapy in osteoarthritis (OA).

(iPSCs), mesenchymal stem cells (MSCs), bone marrow-derived stem cells (BMSCs), adipose-derived stem cells (ADSCs), and synovium-derived stem cells (SMSCs) have been widely explored for regenerating cartilage (Figure 1). In the further section of this article, we will discuss the various stem cells for cartilage regeneration for the treatment of OA.

3. MSCs and Cartilage Regeneration

Owing to multipotency and less problematic with regard to ethical issues, the adult MSCs are the natural choice for cartilage regeneration (Figure 2). The bone marrow, adipose tissues, peripheral blood, umbilical cord blood (UCB), synovium, and skeletal and cardiac muscles are well-known sources of MSCs [41]. Notably, the low concentration of MSCs in bone marrow (BM) aspirate made it compulsory to isolate MSCs which is primarily done by Ficoll gradient centrifugation and further expanded to acquire the sufficient number for quicker recovery of injury after transplantation [42, 43]. The isolated stem cells reduce the chance of cross-contamination and increase the efficacy of stem cell-based therapy. However, the isolation and expansion of MSCs need expertise and also make regenerative therapy expensive. Hence, if the isolation and expansion steps are skipped, it will save significant amount of cost and time in providing cell-based regenerative therapy at less equipped hospitals [44]. To accomplish this goal, volume of BM may be reduced by closed centrifuge to achieve higher concentration of MSCs as compared to Ficoll gradient, which seems a prospective method to provide instant stem cell therapy. Further, the adipose tissue, synovial fluid, and Wharton's jelly of the umbilical cord are considered as potential source of MSCs for cartilage regeneration; however, the source of MSCs depends upon the factors such as feasibility in harvesting, expansion potential, hypoimmunogenicity, and establish procedures [45]. These MSCs are positive for CD73, CD 90, and CD 105 cell markers, whereas they do not express hematopoietic markers such as CD11b, CD14, CD19, CD34, CD45, and HLA-DR [21, 41]. Further, various studies have been carried out to evaluate the potential of human and animal MSCs to regenerate cartilage tissue *in vitro* [46] with reduced immunogenic response [47, 48], thus making feasibility of allogenic MSC transplantation without HLA matching [49]. The other approach for chondrocyte differentiation and cartilage regeneration includes coculturing of MSCs with chondron or other chondrogenesis-promoting cells. Coculturing provides more natural environment and biomechanical stress to promote cartilage regeneration [50, 51]. Various studies have also established an improved chondrogenesis and ECM synthesis when MSCs were cocultured with chondrocytes [52–54].

Cellular contact, secretion of signals (growth factors, cytokines, etc.), and mechanical stress are factors demonstrated to promote cartilage formation and increase in ECM content [55, 56]. Chondrocytes and MSCs in ratio of 1 : 1 and 1 : 4 have been used to explore the advantage of coculture for development of functional cartilage [53, 55, 57]. However, in a study, the coculture of human infrapatellar fat pad-derived stem cells (IPF-ASCs) and chondrons was unable to promote chondrogenic differentiation [58]. BMSCs and articular chondrocytes were cocultured in 1 : 1 ratio in different models and injected in OA-induced rats; as a

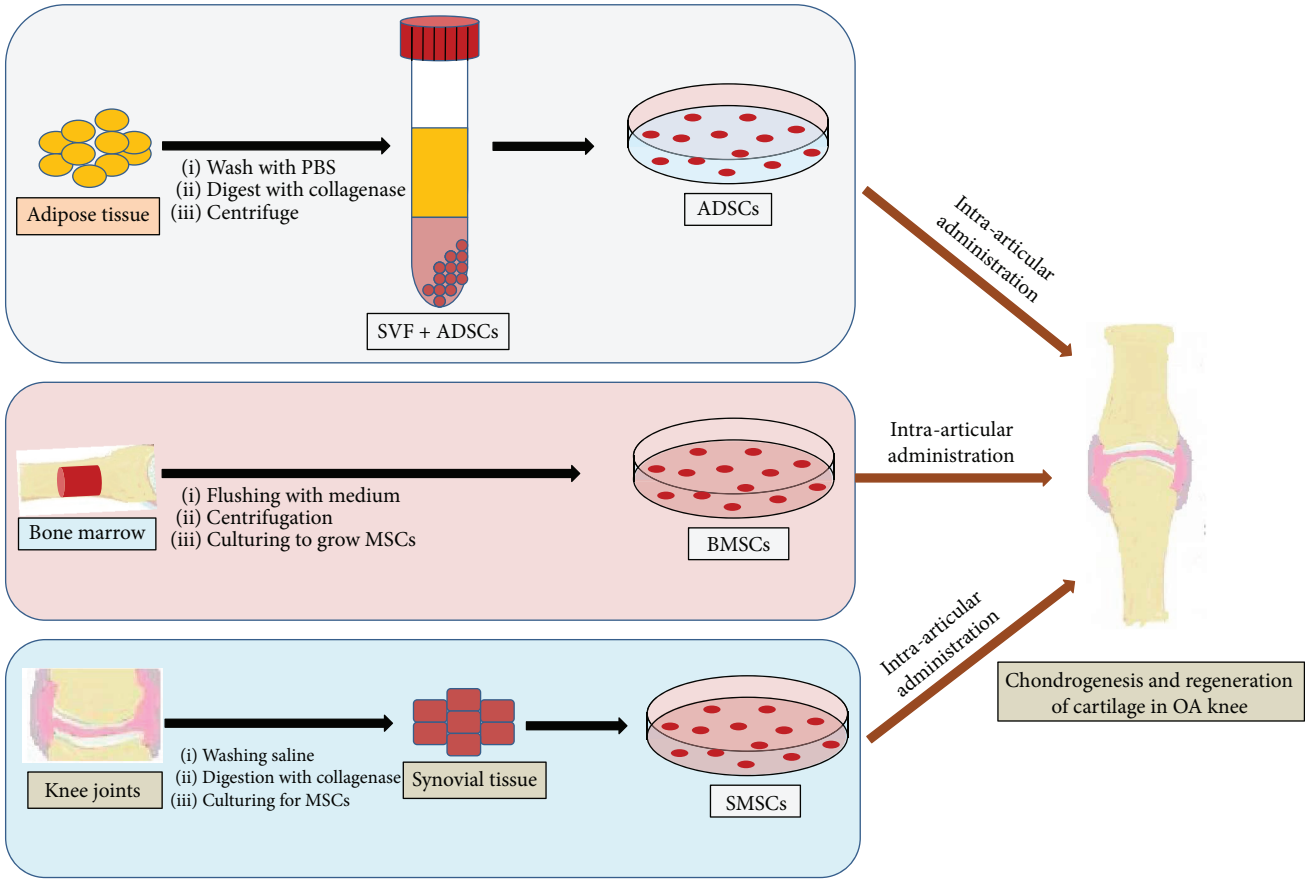

Figure 2: An overview of isolation procedure of various stem cells and their administration in the OA knee joint. OA: osteoarthritis; MSC: mesenchymal stem cells; SVF: stromal vascular fraction; ADSCs: adipose-derived stem cells; BMSCs: bone marrow-derived stem cells.

consequence, the reduced vascularization and hypertrophy along with increased expression of chondrogenic gene was found [59]. Further, in an interesting study, the suspension coculture of hMSCs and hACs was used, which yielded 4.74-fold increase in 3-dimensional aggregates of chondrocytes till 16 days [60]. On the other hand, the hypoxia and transactivation of stable hypoxia-inducible factors (HIF) also promote chondrogenesis [61]. It has also been reported that the proper concentration of hyaluronic acid (HA) also boosts chondrogenesis [62]. Furthermore, the factors including TGF-β and insulin growth factor- (IGF-) 1 have been reported to regulate MSC proliferation and chondrocyte differentiation, whereas BMP controls the development of skeletal muscle [63, 64]. Taken together, the MSC-based OA treatment procedures seem promising which has also been shown in various clinical studies (Figure 3). However, some obstacle like control of differentiation, characterization of MSC, and lack of established procedures for chondrogenesis hinders the progress in the therapeutic exploitation of MSCs [65].

4. Rejuvenating Cartilage through ADSCs

Stromal vascular fraction (SVF) of adipose tissue contains stem cells, known as adipose-derived stem cells (ADSCs), has the potential to differentiate into chondrocytes, adipocyte, osteoblasts, and myocytes [66, 67]. Currently, the ADSCs are considered as a promising source of chondrocytes due to ease of harvest, their abundance in adipose tissue, and low morbidity rate and side effect, as well as a noninvasive procedure. Various studies have already implicated the significance of ADSC in cartilage regeneration for the treatment of OA [68–71]. Specifically, the intra-articular and surgical implantations of ADSCs combined with biomaterials have been carried out to assess the magnitude of cartilage regeneration in OA-induced animal models [72]. Additionally, the autologous platelet-rich plasma induces cartilage regeneration by secreting growth factors such as TGF-β, epidermal growth factor (EGF), and fibroblast growth factor (FGF) to promote the growth and differentiation of stem cells and their adherence to cartilage lesions [73]. In an important study by Tang et al., the intra-articularly injected subcutaneous ADSCs were found to be more effective than visceral ADSC in a rat model of OA [69]. The paracrine effect of ADSCs is considered as one of the paramount factors for cartilage regeneration in OA [74]. Further, the scaffolds seeded with ADSCs in presence of growth factors, stimuli, and compressive stress promote regeneration of cartilage ex vivo. A 3-dimensional scaffold of collagen type I was developed to study the effect of PRP and human recombinant insulin on differentiation of ADSCs into chondrocytes and osteocytes [68]. The study showed that through this approach, it promoted ADSC-mediated chondro- and osteogenesis, and the

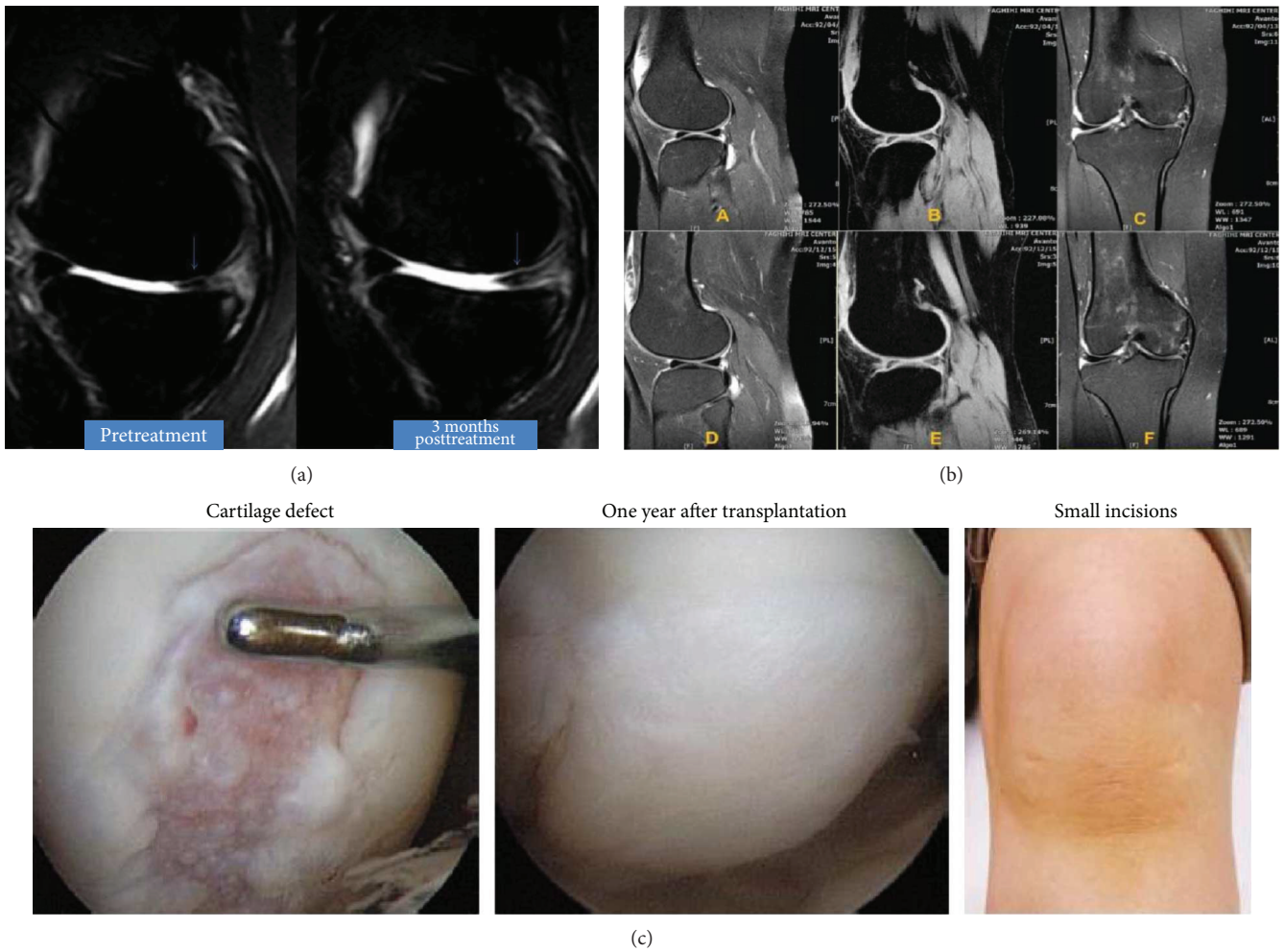

Figure 3: Clinical efficacy of various stem cells-treated OA knee joint: (a) ADSC, (b) BMSC, and (c) SMSC. ADSC: adipose-derived stem cells; BMSC: bone marrow-derived stem cells; SMSC: synovium-derived stem cells; OA: osteoarthritis. Figure 3 is reproduced from Pak [159], Mehrabani et al. [160], and Sekiya et al. [161] [under the Creative Commons Attribution License/public domain].

PRP/insulin-induced differentiation was independent of IGF-1R signaling. In another study, it was reported that xanthan gum significantly improved the chondrogenic potential of intra-articularly implanted ADSC in a rat OA model [70]. Based on the above evidence, ADSC seems highly promising for therapeutic treatment of OA; however, limited knowledge of differentiation mechanism and lack of established procedures are hindering the progress of this therapy to exploit clinically. Issues related to the safety of ADSC-based therapy have been addressed in various clinical trials [75–79]. A report including 70 systematic studies documented that approximately 20% patients developed antibodies during allogeneic cellular therapy, and one case of breast cancer out of 121 patients was also found [75]. Therefore, though the clinical trials indicate the potential of ADSCs in cell-based therapy of OA, further extensive clinical studies are needed to identify potential risks.

5. Revitalization of Cartilage by BMSCs

MSCs derived from bone marrow (BMSCs) are capable enough to differentiate into tissues such as bone and cartilage [80, 81] and mobilize at an injured cartilage site in knee joints thereby assisting in cartilage regeneration in OA [82]. In a study, the intra-articularly transplanted BMSC successfully regenerated injured cartilage in a rabbit model of OA and also improved osteoarthritic symptoms in humans without any major side effect even in the long-term [83]. This study demonstrated the possibility of intra-articular injection of MSCs for the treatment of injured articular tissue including anterior cruciate ligament, meniscus, or cartilage. Therefore, if this treatment option is well-established, it may be minimally invasive procedure compared to conventional surgeries. In a very interesting study, out of the alginate, fibrin-alginate (FA), agarose hydrogel 3D culture, and cell pellet systems, the FA hydrogels and cell pellet promoted chondrogenic differentiation of equine BMSCs, whereas no effect was found in agarose group [84]. However, FA seems a better option than pellet culture system, as the pellets require large amount of chondrocytes. Another study established an agarose hydrogel-based model for cartilage regeneration from human BMSCs in presence of TGF-β3, where the level of chondrogenesis in agarose gel was dependent on the initial density of cells [85]. Furthermore, a scaffold-free

human BMSCs-derived cartilage-like sheet matrix has also been developed in presence of FGF-2 and its efficacy was assessed by transplanting it into an OA rat model. This approach though improved OA condition, the cellular density was decreased significantly within 12 months [86]. Further, in a report by Peng et al., limited proliferation ability of the primary BMSCs was overcomed by immortalizing them by using human papillomavirus- (HPV-) 16 E6/E7 genes, which showed enhanced chondrogenic potential and long-term survival both in *in vitro* and *in vivo* OA mice model [87]. A recent study identified both the promoting as well as the inhibitory role of miR-29b factor in BMSC-based regulation of collagen expression and cartilage regeneration in OA model [88]. Further, the chondrogenically primed BMSCs have also demonstrated to promote cartilage regeneration under hypoxia in a sheep model of OA [89]. However, the effect of oxygen tension was not consistent during ex vivo cartilage regeneration. On the other hand, BMSC also showed enhanced chondrogenesis when seeded on chondrogenic fibrin/hyaluronic hydrogel with improved mechanical strength by adding methacrylic anhydride. Hence, it can also be considered as a promising delivery method for cartilage regeneration in OA therapy [90]. Besides, the intra-articular injection of MSCs may also be applied via microfracture through the cartilage and subchondral bone [91]. In a clinical trial (phase I/II), the intra-articularly injected BMSCs among OA patients showed a significant improvement; however, to assess all the clinical parameters, clinical phase III study was required [92]. In another clinical study, human BMSCs demonstrated that the optimum level of cell dose (25 million) improved the OA without any major adverse effects [93]. However, at higher doses, the knee pain and swelling were among observed as adverse effects, which suggested that more clinical studies are required to establish the therapeutic role of human BMSCs in OA treatment.

6. SMSCs and Cartilage Regeneration

SMSCs have been considered more efficient for chondrocyte differentiation than ADSCs or BMSCs [94]. Notwithstanding, in the recent years, only few human-based studies using SMSCs have been conducted compared to ADSCs and BMSC for the treatments for OA. SMSCs are also isolated from hip joints; however, those isolated from knee joints have shown a better chondrogenic potential [95]. These MSCs can also be preserved in complete human serum at 4 or 13°C without significantly affecting their viability and chondrogenic potential [96]. In an interesting research, the exosomes derived from SMSC-140s promoted chondrogenesis without affecting the quality of ECM [97]. SMSCs isolated from OA patients have also shown to be an effective alternative cell source for tissue engineering construct-based therapy for chondral defects [98]. Besides, the pretreatment of SMSCs with IL-1β also enhances the chondrogenic potential of SMSCs [99].

In a rat knee OA model, the periodically injected SMSCs migrated into the synovium and retained their undifferentiated SMSC properties with an increased genetic expression of chondroprotective proteins such as BMP-2 and an anti-inflammatory gene, TSG-6 [100]. This suggests that SMSCs not only retain their MSC characteristics but might also inhibit the advancement of OA through genetic machinery. Further, SMSCs have demonstrated the ability to enhance the repair of longitudinally torn menisci in avascular areas in a miniature pig model [59]. In 2014, Hatsushika et al. further demonstrated that intra-articularly injected MSCs in pig knee joint regenerated cartilage in resected medial meniscus [101]. Based on these abovementioned evidence, it could be concluded that the regenerative chondrogenic capabilities of SMSCs catapulted them to the forefront of cell-based OA therapy.

7. Infrapatellar Fat Pad- (IFP-) Derived Stem Cells in Cartilage Regeneration

Knee joints are surrounded by extrasynovial adipose tissue known as IFP, which not only provides energy but also releases cytokines/adipokines [102]. IFP is considered as an alternative source of autologous stem cells. MSCs isolated from these tissues of knee joints have superior chondrogenic properties than BMSCs or ADSCs [103]. The characterization of IFP-MSCs is based on the presence of cell markers such as CD9, CD10, CD13, CD29, CD44, CD49e, CD59, CD105, CD106, and CD166 [104]. These cells are also capable to differentiate in trilineages (adipo-, chondro-, and osteogenic) [104–107]. In a recent study, ADSCs were isolated from both the human suprapatellar and IFP and differentiated into trilineage cells. However, the suprapatellar-derived ASCs were found to be more effective in reducing OA symptoms, including knee inflammation and cartilage degeneration in a mouse model [108]. Besides, the IFP-MSCs have been demonstrated with higher rate of expansion compared to synovial fluid- (SF-) MSCs [109]. However, both cells can be exploited to treat the cartilage injury in OA. Further, it was reported that platelet-rich plasma and hyaluronic acid-treated IFP adipocytes promote chondrogenesis and inhibit adipocyte-mediated inflammation [110]. IFP is also a rich source of perivascular stem cells (PSCs) and homeostasis regulating the progenitor MSCs. IFP-PSCs maintain their characteristic and adherent growth properties even after multiple expansion due to their ability to retain the structural integrity of telomere [111]. Interestingly, the PSCs isolated from IFP have shown superior chondrogenic activity as compared to those derived from subcutaneous adipose tissues. In another study, the improved chondrogenic efficiency of coculture of chondrocytes and IFP-MSCs in the presence of chitosan/hyaluronic acid nanoparticles was revealed, which implied that coculture approach in presence of proper stimuli could assist in cartilage regeneration in an osteoarthritic knee [112]. The IFP-PSCs can also be engineered by manipulating the oxygen gradients and mechanical environment of hydrogels to obtain cartilage structurally and functionally similar to a natural one [113]. Though the IFP-derived stem cells appear to be a prospective alternative, further extensive studies are needed to prove their clinical efficacy towards cartilage regeneration for the treatment of OA.

8. Regeneration of Cartilage Using ESCs

ESCs are derived from inner cell mass of the blastocyst and could be indefinitely expanded and differentiated into any of the three embryonic germ cell lines including ectoderm, endoderm, and mesoderm [114]. The perpetual self-renewal potential of ESCs makes it unlimited source of stem cells and chondrocytes for cartilage regeneration. However, the major bottleneck to utilize ESCs for cartilage matrix is ethical complexity and poor survival rate of human ESCs after the disintegration of cell mass [115]. Additionally, the differentiation of ESCs into chondrocytes and regeneration of cartilage is complex as it requires complicated microenvironment along with 3-dimensional structure and specific mechanotransduction signal [116]. In a seminal study, McKee et al. showed that under compressive stress, ESCs combined with polydimethylsiloxane (PDMS) scaffolds promoted the initial expression of chondrogenic markers Sox9 and Acan, which further enhanced the expression of collagen type 2 (cartilage-specific marker) and reduced Oct4 (pluripotent marker). However, it did not promote differentiation of hypertrophic cells [116]. This study showed that a proper model is still needed to established ESC-mediated chondrogenesis. An *in vitro* study used embryoid bodies to assess the chondrogenic potential of ESCs and demonstrated that ESCs could develop into hypertrophic and calcifying cells [117]. In another study, ESC also revealed chondrogenic activity when stimulated with bone morphogenetic protein 4 (BMP-4). Further, the accumulation of cartilaginous matrix and type II collagen was recorded in the presence of transforming growth factor- (TGF-) β3. [118], and this chondrogenic activity was further promoted by the platelet-derived growth factor- (PDGF-) BB. The higher concentration of BMP-2 with other cofactors, the TGF-β-1, insulin, and ascorbic acid, also promotes the chondrogenic ability of ESC under controlled environmental conditions [119]. Transforming growth factor-β1, BMP-2, and BMP-4 have been reported to induce differentiation of mice ESCs into chondrocytes [115–120].

Besides, the exosomes have been reported to mediate cellular communication between stem cells and chondrocytes, and understanding this interaction is crucial in developing an effective protocol to regenerate the cartilage [121]. Exosomes are extracellular vesicle primarily secreted by MSCs and assist in maintaining homeostasis, repair and regeneration, and tissue function [122]. In a seminal study, Wang et al. isolated exosomes from culture media of ESC-MSCs and evaluated their effect in OA mice model. This study showed that exosomes exerted protective and regenerative effecst in the injured cartilage [121]. Likewise, various studies have established the chondroregenerative potential of ESCs; however, the major bottlenecks to utilize ESCs for cartilage matrix regeneration are ethical concerns involving the destruction of embryo and poor survival rate of human ESCs after disintegration of cell mass [115, 123].

9. iPSCs and Cartilage Regeneration

iPSCs are the reprogrammed somatic cells similar to ESCs, which seems to be a promising alternative to the ESCs [124]. Oct 4, c-Myc, Klf4, Nanog, Esrrb, Lin28, and Sox2 are some of the transcription factors which have been used to reprogram these somatic cells [125–128]. Other approaches like viral transfection and genetic engineering are used to develop iPSCs. Vector characteristics and related promoters are critical factors in gene delivery to differentiate iPSCs into specific cells. Adenoviral, adeno-associated viral, retroviral, and lentiviral vectors have been considered suitable for delivery of target genes in iPSCs [129]. Moreover, the differentiation of patient-specific somatic cell to iPSCs reduces the risk cross-reactivity and immunogenicity [130, 131]. Chondrogenesis has been induced in iPSC-derived embryonic body of mice by using growth factors such as TGF-β3, transretinoic acid, and BMP-2 [132, 133]. Another study demonstrated that human iPSCs (hiPSCs) differentiated into chondrocytes and expressed type II collagen and aggrecan similar to cartilage [134]. Zhu et al. induced embryonic body formation from hiPSCs, which were further differentiated to chondrocytes and transplanted in an OA rat to regenerate cartilage [135]. They have also shown that MSCs derived from induced pluripotent cells (iMSCs) were able to secrete exosomes which were superior to exosomes of synovial membrane MSCs (SMMSC) in regenerating cartilage in OA rat [136]. Besides, both with and without scaffold-based cartilage regeneration approaches have been explored for differentiating hiPSCs into chondrocyte for the treatment of cartilage injury [122, 137–142]. The utilization of iPSCs cannot be limited up to regeneration of cartilage but also in the discovery of agents promoting chondrogenesis or inhibiting cartilage degeneration [143]. These studies showed the immense potential of iPSCs to regenerate cartilage in OA. However, the low efficiency and variations in requirement of transcription factors in somatic cells are the major limitation for iPSC generation. Moreover, the undifferentiated iPSC contaminates differentiated MSCs causing tumorigenicity, which limits the use of heterogeneous-differentiated MSCs in cell-based regenerative therapy [144]. Furthermore, over and unregulated expression of *Oct4*, *Sox2*, *Klf4*, and *c–Myc* develops cell dysplasia, serrated polyps and mucinous colon carcinomas, breast tumors, and cancers, respectively [145–150]. Moreover, the clinical application is limited due to lack of a proper model for large-scale and economic differentiation of iPSCs.

10. Conclusion and Future Prospects

The self-renewing and multidifferentiation abilities have rendered stem cells, an attractive alternative for the treatment of osteoarthritic pathology. Considering the complexity and efficiency of currently available therapies in long-term, the cell-based regenerative therapy has widely been explored to treat the OA and proven to hold a promising future. The MSCs obtained from adults offer a considerable therapeutic approach in translational medicine. The therapeutic efficacy of stem cells can also be magnified through supplementing growth factors. One of the major limitations of therapies for cartilage repair is that they employ autologous cells and therefore, the development of a universal donor cell is still lacking.

Current reprogrammable approaches to induce stem cell differentiation into cartilage tissues seem inefficient. Further, it seems that genetic modification and gene editing techniques will assist to overcome the current limitations of stem cell-based therapy. The localized delivery of gene therapeutic agents provides more effective and safe recovery in OA. Recombinant adeno-associated viral vector (rAAV) is also used as a genetic vector to deliver genetic sequence in situ to promote the cartilage regeneration [151]. Various animal model studies and clinical trials were carried to out to develop a comprehensive approach for effective gene therapy and encourage to extended clinical trial to develop gene transfer technique to regenerate injured cartilage in situ [152]. microRNAs (miRNAs) such as miR-29a, miR-140-3p, miR-140-5p, miR-145, miR-146a, miR146b, miR-193b, miR-194, miR-221, miR-495 are known to be involved in the differentiation of stem cells into chondrocytes; and their regulated expression enhance chondrogenesis and thus repair cartilage injury [153, 154]. Besides, the development of gene editing technique, the CRISPR/Cas 9 seems promising to regulate chondrogenesis [155]. This technique was exploited in the development of stem cells that controlled interleukin-1 (IL-1) and tumor necrosis factor-α- (TNF-α-) mediated inflammatory response [156]. Further, the 3-dimensional scaffold promotes the development of cartilage tissue structurally similar to native cartilage by providing conducive microenvironment and essential mechanical stimuli [152, 157]. The recent advances in 3D printing will also improve the scaffold design, which might support chondrocytic growth to overcome osteoarthritic symptoms [158]. It is of note that though multiple studies have sorted out the most effective stem cells, scaffold materials, genetic approach, and other procedures for cartilage regeneration in OA knee and the rigorous randomized and blinded trials, with large sample sizes and long-term follow-up, is needed to reach a consensus.

Conflicts of Interest

The authors declare that there are no conflicts of interest regarding the publication of this paper.

References

[1] M. J. Elders, "The increasing impact of arthritis on public health," *The Journal of Rheumatology Supplement*, vol. 60, pp. 6–8, 2000.

[2] U. Nöth, A. F. Steinert, and R. S. Tuan, "Technology insight: adult mesenchymal stem cells for osteoarthritis therapy," *Nature Clinical Practice Rheumatology*, vol. 4, pp. 371–380, 2008.

[3] United Nations, "World population to 2300," http://www.un.org/esa/population/publications/longrange2/WorldPop2300final.pdf.

[4] J.-Y. Reginster, "The prevalence and burden of arthritis," *Rheumatology*, vol. 41, Supplement 1, pp. 3–6, 2002.

[5] L. S. Rachel Wittenauer and K. Aden, "Priority medicines for Europe and the world "a public health approach to innovation"- update on 2004 background paper, BP 6.12 osteoarthritis," http://www.who.int/medicines/areas/priority_medicines/BP6_12Osteo.pdf.

[6] L. A. Setton, D. M. Elliott, and V. C. Mow, "Altered mechanics of cartilage with osteoarthritis: human osteoarthritis and an experimental model of joint degeneration," *Osteoarthritis and Cartilage*, vol. 7, no. 1, pp. 2–14, 1999.

[7] D. M. Findlay and J. S. Kuliwaba, "Bone–cartilage crosstalk: a conversation for understanding osteoarthritis," *Bone Research*, vol. 4, no. 1, article 16028, 2016.

[8] Y. Li, X. Wei, J. Zhou, and L. Wei, "The age-related changes in cartilage and osteoarthritis," *BioMed Research International*, vol. 2013, Article ID 916530, 12 pages, 2013.

[9] J. A. Martin and J. A. Buckwalter, "The role of chondrocyte senescence in the pathogenesis of osteoarthritis and in limiting cartilage repair," *The Journal of Bone & Joint Surgery*, vol. 85, pp. 106–110, 2003.

[10] J. A. Martin and J. A. Buckwalter, "Aging, articular cartilage chondrocyte senescence and osteoarthritis," *Biogerontology*, vol. 3, no. 5, pp. 257–264, 2002.

[11] J. A. Buckwalter, P. J. Roughley, and L. C. Rosenberg, "Age-related changes in cartilage proteoglycans: quantitative electron microscopic studies," *Microscopy Research & Technique*, vol. 28, no. 5, pp. 398–408, 1994.

[12] M. C. Bolton, J. Dudhia, and M. T. Bayliss, "Age-related changes in the synthesis of link protein and aggrecan in human articular cartilage: implications for aggregate stability," *Biochemical Journal*, vol. 337, no. 1, pp. 77–82, 1999.

[13] J. Buckwalter and H. Mankin, "Instructional course lectures, the American Academy of Orthopaedic Surgeons - articular cartilage. Part II: degeneration and osteoarthrosis, repair, regeneration, and transplantation," *The Journal of Bone & Joint Surgery*, vol. 79, no. 4, pp. 612–632, 1997.

[14] J. Buckwalter, J. Martin, and H. Mankin, "Synovial joint degeneration and the syndrome of osteoarthritis," *Instructional Course Lectures*, vol. 49, pp. 481–489, 2000.

[15] J. Martin and J. Buckwalter, "The role of chondrocyte–matrix interactions in maintaining and repairing articular cartilage," *Biorheology*, vol. 37, no. 1-2, pp. 129–140, 2000.

[16] D. J. Hunter and D. T. Felson, "Osteoarthritis," *BMJ*, vol. 332, no. 7542, pp. 639–642, 2006.

[17] T. S. de Windt, J. A. A. Hendriks, X. Zhao et al., "Concise review: unraveling stem cell cocultures in regenerative medicine: which cell interactions steer cartilage regeneration and how?," *Stem Cells Translational Medicine*, vol. 3, no. 6, pp. 723–733, 2014.

[18] B. O. Diekman and F. Guilak, "Stem cell-based therapies for osteoarthritis: challenges and opportunities," *Current Opinion in Rheumatology*, vol. 25, no. 1, pp. 119–126, 2013.

[19] R. C. Lawrence, D. T. Felson, C. G. Helmick et al., "Estimates of the prevalence of arthritis and other rheumatic conditions in the United States: part II," *Arthritis & Rheumatism*, vol. 58, no. 1, pp. 26–35, 2008.

[20] S. Kurtz, K. Ong, E. Lau, F. Mowat, and M. Halpern, "Projections of primary and revision hip and knee arthroplasty in the United States from 2005 to 2030," *The Journal of Bone & Joint Surgery*, vol. 89, no. 4, pp. 780–785, 2007.

[21] M. Dominici, K. Le Blanc, I. Mueller et al., "Minimal criteria for defining multipotent mesenchymal stromal cells. The International Society for Cellular Therapy position statement," *Cytotherapy*, vol. 8, no. 4, pp. 315–317, 2006.

[22] P. Orth, A. Rey-Rico, J. K. Venkatesan, H. Madry, and M. Cucchiarini, "Current perspectives in stem cell research for knee cartilage repair," *Stem Cells and Cloning: Advances and Applications*, vol. 7, pp. 1–17, 2014.

[23] W. J. Koopman and L. W. Moreland, Eds., *Arthritis & Allied Conditions: A Textbook of Rheumatology*, Lippincott Williams, Wilkins, Philadelphia, PA, USA, 2005.

[24] M. Benito, D. Veale, O. FitzGerald, W. B. van den Berg, and B. Bresnihan, "Synovial tissue inflammation in early and late osteoarthritis," *Annals of the Rheumatic Diseases*, vol. 64, no. 9, pp. 1263–1267, 2005.

[25] A. D. Pearle, C. R. Scanzello, S. George et al., "Elevated high-sensitivity C-reactive protein levels are associated with local inflammatory findings in patients with osteoarthritis," *Osteoarthritis and Cartilage*, vol. 15, no. 5, pp. 516–523, 2007.

[26] M. B. Goldring and K. B. Marcu, "Cartilage homeostasis in health and rheumatic diseases," *Arthritis Research & Therapy*, vol. 11, no. 3, p. 224, 2009.

[27] A. Burleigh, A. Chanalaris, M. D. Gardiner et al., "Joint immobilization prevents murine osteoarthritis and reveals the highly mechanosensitive nature of protease expression in vivo," *Arthritis & Rheumatism*, vol. 64, no. 7, pp. 2278–2288, 2012.

[28] N. C.-B. Tabassi and P. Garnero, "Monitoring cartilage turnover," *Current Rheumatology Reports*, vol. 9, no. 1, pp. 16–24, 2007.

[29] J. C. Rousseau and P. D. Delmas, "Biological markers in osteoarthritis," *Nature Clinical Practice Rheumatology*, vol. 3, no. 6, pp. 346–356, 2007.

[30] E. Dayer, J. M. Dayer, and P. Roux-Lombard, "Primer: the practical use of biological markers of rheumatic and systemic inflammatory diseases," *Nature Clinical Practice Rheumatology*, vol. 3, no. 9, pp. 512–520, 2007.

[31] Y. Henrotin, S. Addison, V. Kraus, and M. Deberg, "Type II collagen markers in osteoarthritis: what do they indicate?," *Current Opinion in Rheumatology*, vol. 19, no. 5, pp. 444–450, 2007.

[32] D. Patra and L. J. Sandell, "Antiangiogenic and anticancer molecules in cartilage," *Expert Reviews in Molecular Medicine*, vol. 14, article e10, 2012.

[33] A. Ludin, J. J. Sela, A. Schroeder, Y. Samuni, D. W. Nitzan, and G. Amir, "Injection of vascular endothelial growth factor into knee joints induces osteoarthritis in mice," *Osteoarthritis and Cartilage*, vol. 21, no. 3, pp. 491–497, 2013.

[34] K.-W. Chong, A. Chanalaris, A. Burleigh et al., "Fibroblast growth factor 2 drives changes in gene expression following injury to murine cartilage in vitro and in vivo," *Arthritis & Rheumatism*, vol. 65, no. 9, pp. 2346–2355, 2013.

[35] F. E. Watt, H. M. Ismail, A. Didangelos et al., "Src and fibroblast growth factor 2 independently regulate signaling and gene expression induced by experimental injury to intact articular cartilage," *Arthritis & Rheumatism*, vol. 65, no. 2, pp. 397–407, 2013.

[36] M. B. Ellman, D. Yan, K. Ahmadinia, D. Chen, H. S. An, and H. J. Im, "Fibroblast growth factor control of cartilage homeostasis," *Journal of Cellular Biochemistry*, vol. 114, no. 4, pp. 735–742, 2013.

[37] F. Dell'Accio, C. de Bari, N. M. F. el Tawil et al., "Activation of WNT and BMP signaling in adult human articular cartilage following mechanical injury," *Arthritis Research & Therapy*, vol. 8, no. 5, p. R139, 2006.

[38] K. D. Brandt, P. Dieppe, and E. L. Radin, "Etiopathogenesis of osteoarthritis," *Rheumatic Disease Clinics of North America*, vol. 34, no. 3, pp. 531–559, 2008.

[39] M. K. Lotz, S. Otsuki, S. P. Grogan, R. Sah, R. Terkeltaub, and D. D'Lima, "Cartilage Cell Clusters," *Arthritis & Rheumatism*, vol. 62, no. 8, pp. 2206–2218, 2010.

[40] M. L. Tiku and H. E. Sabaawy, "Cartilage regeneration for treatment of osteoarthritis: a paradigm for nonsurgical intervention," *Therapeutic Advances in Musculoskeletal Disease*, vol. 7, no. 3, pp. 76–87, 2015.

[41] A. Keating, "Mesenchymal stromal cells," *Current Opinion in Hematology*, vol. 13, no. 6, pp. 419–425, 2006.

[42] S. P. Bruder, D. J. Fink, and A. I. Caplan, "Mesenchymal stem cells in bone development, bone repair, and skeletal regenaration therapy," *Journal of Cellular Biochemistry*, vol. 56, no. 3, pp. 283–294, 1994.

[43] R. Quarto, M. Mastrogiacomo, R. Cancedda et al., "Repair of large bone defects with the use of autologous bone marrow stromal cells," *The New England Journal of Medicine*, vol. 344, no. 5, pp. 385-386, 2001.

[44] P. Kasten, I. Beyen, M. Egermann et al., "Instant stem cell therapy: characterization and concentration of human mesenchymal stem cells in vitro," *European Cells and Materials*, vol. 16, pp. 47–55, 2008.

[45] A. Mobasheri, G. Kalamegam, G. Musumeci, and M. E. Batt, "Chondrocyte and mesenchymal stem cell-based therapies for cartilage repair in osteoarthritis and related orthopaedic conditions," *Maturitas*, vol. 78, no. 3, pp. 188–198, 2014.

[46] A. Goldberg, K. Mitchell, J. Soans, L. Kim, and R. Zaidi, "The use of mesenchymal stem cells for cartilage repair and regeneration: a systematic review," *Journal of Orthopaedic Surgery and Research*, vol. 12, no. 1, article 39, 2017.

[47] K. Le Blanc, C. Tammik, K. Rosendahl, E. Zetterberg, and O. Ringdén, "HLA expression and immunologic propertiesof differentiated and undifferentiated mesenchymal stem cells," *Experimental Hematology*, vol. 31, no. 10, pp. 890–896, 2003.

[48] X. Zhang, T. Tang, Q. Shi, J. C. Fernandes, and K. Dai, "The immunologic properties of undifferentiated and osteogenic differentiated mouse mesenchymal stem cells and its potential application in bone regeneration," *Immunobiology*, vol. 214, no. 3, pp. 179–186, 2009.

[49] M. K. Mamidi, A. K. Das, Z. Zakaria, and R. Bhonde, "Mesenchymal stromal cells for cartilage repair in osteoarthritis," *Osteoarthritis and Cartilage*, vol. 24, no. 8, pp. 1307–1316, 2016.

[50] Y. Zhang, W. Guo, M. Wang et al., "Co-culture systems-based strategies for articular cartilage tissue engineering," *Journal of Cellular Physiology*, vol. 233, no. 3, pp. 1940–1951, 2018.

[51] E. J. Levorson, M. Santoro, F. Kurtis Kasper, and A. G. Mikos, "Direct and indirect co-culture of chondrocytes and mesenchymal stem cells for the generation of polymer/extracellular matrix hybrid constructs," *Acta Biomaterialia*, vol. 10, no. 5, pp. 1824–1835, 2014.

[52] J. Hendriks, J. Riesle, and C. A. van Blitterswijk, "Co-culture in cartilage tissue engineering," *Journal of Tissue Engineering and Regenerative Medicine*, vol. 1, no. 3, pp. 170–178, 2007.

[53] L. Bian, D. Y. Zhai, R. L. Mauck, and J. A. Burdick, "Coculture of human mesenchymal stem cells and articular chondrocytes reduces hypertrophy and enhances functional properties of

engineered cartilage," *Tissue Engineering Part A*, vol. 17, no. 7-8, pp. 1137–1145, 2011.

[54] J. Fischer, A. Dickhut, M. Rickert, and W. Richter, "Human articular chondrocytes secrete parathyroid hormone–related protein and inhibit hypertrophy of mesenchymal stem cells in coculture during chondrogenesis," *Arthritis & Rheumatism*, vol. 62, no. 9, pp. 2696–2706, 2010.

[55] E. J. Levorson, P. M. Mountziaris, O. Hu, F. K. Kasper, and A. G. Mikos, "Cell-derived polymer/extracellular matrix composite scaffolds for cartilage regeneration, part 1: investigation of cocultures and seeding densities for improved extracellular matrix deposition," *Tissue Engineering Part C: Methods*, vol. 20, no. 4, pp. 340–357, 2014.

[56] N. S. Hwang, S. Varghese, C. Puleo, Z. Zhang, and J. Elisseeff, "Morphogenetic signals from chondrocytes promote chondrogenic and osteogenic differentiation of mesenchymal stem cells," *Journal of Cellular Physiology*, vol. 212, no. 2, pp. 281–284, 2007.

[57] E. J. Levorson, O. Hu, P. M. Mountziaris, F. K. Kasper, and A. G. Mikos, "Cell-derived polymer/extracellular matrix composite scaffolds for cartilage regeneration, part 2: construct devitalization and determination of chondroinductive capacity," *Tissue Engineering Part C: Methods*, vol. 20, no. 4, pp. 358–372, 2014.

[58] P. Nikpou, D. M. Nejad, H. Shafaei et al., "Study of chondrogenic potential of stem cells in co-culture with chondrons," *Iranian Journal of Basic Medical Sciences*, vol. 19, no. 6, pp. 638–645, 2016.

[59] I. Prasadam, A. Akuien, T. E. Friis et al., "Mixed cell therapy of bone marrow-derived mesenchymal stem cells and articular cartilage chondrocytes ameliorates osteoarthritis development," *Laboratory Investigation*, vol. 98, no. 1, pp. 106–116, 2017.

[60] M. Khurshid, A. Mulet-Sierra, A. Adesida, and A. Sen, "Osteoarthritic human chondrocytes proliferate in 3D co-culture with mesenchymal stem cells in suspension bioreactors," *Journal of Tissue Engineering and Regenerative Medicine*, 2017.

[61] J. Shang, H. Liu, J. Li, and Y. Zhou, "Roles of hypoxia during the chondrogenic differentiation of mesenchymal stem cells," *Current Stem Cell Research & Therapy*, vol. 9, no. 2, pp. 141–147, 2014.

[62] E. Amann, P. Wolff, E. Breel, M. van Griensven, and E. R. Balmayor, "Hyaluronic acid facilitates chondrogenesis and matrix deposition of human adipose derived mesenchymal stem cells and human chondrocytes co-cultures," *Acta Biomaterialia*, vol. 52, pp. 130–144, 2017.

[63] D.-A. Yu, J. Han, and B.-S. Kim, "Stimulation of chondrogenic differentiation of mesenchymal stem cells," *International Journal of Stem Cells*, vol. 5, no. 1, pp. 16–22, 2012.

[64] J. L. Puetzer, J. N. Petitte, and E. G. Loboa, "Comparative review of growth factors for induction of three-dimensional in vitro chondrogenesis in human mesenchymal stem cells isolated from bone marrow and adipose tissue," *Tissue Engineering Part B: Reviews*, vol. 16, no. 4, pp. 435–444, 2010.

[65] W. Y.-W. Lee and B. Wang, "Cartilage repair by mesenchymal stem cells: clinical trial update and perspectives," *Journal of Orthopaedic Translation*, vol. 9, pp. 76–88, 2017.

[66] P. A. Zuk, M. Zhu, H. Mizuno et al., "Multilineage cells from human adipose tissue: implications for cell-based therapies," *Tissue Engineering*, vol. 7, no. 2, pp. 211–228, 2001.

[67] P. A. Zuk, M. Zhu, P. Ashjian et al., "Human adipose tissue is a source of multipotent stem cells," *Molecular Biology of the Cell*, vol. 13, no. 12, pp. 4279–4295, 2002.

[68] M. G. Scioli, A. Bielli, P. Gentile, V. Cervelli, and A. Orlandi, "Combined treatment with platelet-rich plasma and insulin favours chondrogenic and osteogenic differentiation of human adipose-derived stem cells in three-dimensional collagen scaffolds," *Journal of Tissue Engineering and Regenerative Medicine*, vol. 11, no. 8, pp. 2398–2410, 2017.

[69] Y. Tang, Z. Y. Pan, Y. Zou et al., "A comparative assessment of adipose-derived stem cells from subcutaneous and visceral fat as a potential cell source for knee osteoarthritis treatment," *Journal of Cellular and Molecular Medicine*, vol. 21, no. 9, pp. 2153–2162, 2017.

[70] L. Mei, B. Shen, J. Xue et al., "Adipose tissue–derived stem cells in combination with xanthan gum attenuate osteoarthritis progression in an experimental rat model," *Biochemical and Biophysical Research Communications*, vol. 494, no. 1-2, pp. 285–291, 2017.

[71] K. L. Burrow, J. A. Hoyland, and S. M. Richardson, "Human adipose-derived stem cells exhibit enhanced proliferative capacity and retain multipotency longer than donor-matched bone marrow mesenchymal stem cells during expansion in vitro," *Stem Cells International*, vol. 2017, Article ID 2541275, 15 pages, 2017.

[72] F. Perdisa, N. Gostyńska, A. Roffi, G. Filardo, M. Marcacci, and E. Kon, "Adipose-derived mesenchymal stem cells for the treatment of articular cartilage: a systematic review on preclinical and clinical evidence," *Stem Cells International*, vol. 2015, Article ID 597652, 13 pages, 2015.

[73] J. Pak, J. H. Lee, W. A. Kartolo, and S. H. Lee, "Cartilage regeneration in human with adipose tissue-derived stem cells: current status in clinical implications," *BioMed Research International*, vol. 2016, Article ID 4702674, 12 pages, 2016.

[74] L. Mei, B. Shen, P. Ling et al., "Culture-expanded allogenic adipose tissue-derived stem cells attenuate cartilage degeneration in an experimental rat osteoarthritis model," *PLoS One*, vol. 12, no. 4, article e0176107, 2017.

[75] N. M. Toyserkani, M. G. Jørgensen, S. Tabatabaeifar, C. H. Jensen, S. P. Sheikh, and J. A. Sørensen, "Concise review: a safety assessment of adipose-derived cell therapy in clinical trials: a systematic review of reported adverse events," *Stem Cells Translational Medicine*, vol. 6, no. 9, pp. 1786–1794, 2017.

[76] J. Freitag, K. Shah, J. Wickham, R. Boyd, and A. Tenen, "The effect of autologous adipose derived mesenchymal stem cell therapy in the treatment of a large osteochondral defect of the knee following unsuccessful surgical intervention of osteochondritis dissecans – a case study," *BMC Musculoskeletal Disorders*, vol. 18, no. 1, p. 298, 2017.

[77] M. Berman and E. Lander, "A prospective safety study of autologous adipose-derived stromal vascular fraction using a specialized surgical processing system," *The American Journal of Cosmetic Surgery*, vol. 34, no. 3, pp. 129–142, 2017.

[78] Z. Arshad, C.-L. Halioua-Haubold, M. Roberts et al., "Adipose-derived stem cells in aesthetic surgery: a mixed methods evaluation of the current clinical trial, intellectual property, and regulatory landscape," *Aesthetic Surgery Journal*, vol. 38, no. 2, pp. 199–210, 2018.

[79] Y.-B. Park, C.-W. Ha, J. H. Rhim, and H.-J. Lee, "Stem cell therapy for articular cartilage repair: review of the entity of cell populations used and the result of the clinical application

of each entity," *The American Journal of Sports Medicine*, no. - article 0363546517729152, 2017.

[80] B. A. Ashton, T. D. Allen, C. R. Howlett, C. C. Eaglesom, A. Hattori, and M. Owen, "Formation of bone and cartilage by marrow stromal cells in diffusion chambers in vivo," *Clinical Orthopaedics and Related Research*, vol. 151, pp. 294–307, 1980.

[81] J. Goshima, V. M. Goldberg, and A. I. Caplan, "The osteogenic potential of culture-expanded rat marrow mesenchymal cells assayed in vivo in calcium phosphate ceramic blocks," *Clinical Orthopaedics and Related Research*, vol. 262, pp. 298–311, 1991.

[82] M. Agung, M. Ochi, S. Yanada et al., "Mobilization of bone marrow-derived mesenchymal stem cells into the injured tissues after intraarticular injection and their contribution to tissue regeneration," *Knee Surgery, Sports Traumatology, Arthroscopy*, vol. 14, no. 12, pp. 1307–1314, 2006.

[83] S. Yamasaki, H. Mera, M. Itokazu, Y. Hashimoto, and S. Wakitani, "Cartilage repair with autologous bone marrow mesenchymal stem cell transplantation: review of preclinical and clinical studies," *Cartilage*, vol. 5, no. 4, pp. 196–202, 2014.

[84] A. E. Watts, J. C. Ackerman-Yost, and A. J. Nixon, "A comparison of three-dimensional culture systems to evaluate in vitro chondrogenesis of equine bone marrow-derived mesenchymal stem cells," *Tissue Engineering Part A*, vol. 19, no. 19-20, pp. 2275–2283, 2013.

[85] C.-Y. C. Huang, P. M. Reuben, G. D'Ippolito, P. C. Schiller, and H. S. Cheung, "Chondrogenesis of human bone marrow-derived mesenchymal stem cells in agarose culture," *The Anatomical Record*, vol. 278A, no. 1, pp. 428–436, 2004.

[86] M. Itokazu, S. Wakitani, H. Mera et al., "Transplantation of scaffold-free cartilage-like cell-sheets made from human bone marrow mesenchymal stem cells for cartilage repair: a preclinical study," *Cartilage*, vol. 7, no. 4, pp. 361–372, 2016.

[87] B.-Y. Peng, C. S. Chiou, N. K. Dubey et al., "Non-invasive in vivo molecular imaging of intra-articularly transplanted immortalized bone marrow stem cells for osteoarthritis treatment," *Oncotarget*, vol. 8, no. 57, pp. 97153–97164, 2017.

[88] U. Mayer, A. Benditz, and S. Grässel, "miR-29b regulates expression of collagens I and III in chondrogenically differentiating BMSC in an osteoarthritic environment," *Scientific Reports*, vol. 7, no. 1, article 13297, 2017.

[89] T. D. Bornes, A. B. Adesida, and N. M. Jomha, "Articular cartilage repair with mesenchymal stem cells after chondrogenic priming: a pilot study," *Tissue Engineering Part A*, 2017.

[90] T. N. Snyder, K. Madhavan, M. Intrator, R. C. Dregalla, and D. Park, "A fibrin/hyaluronic acid hydrogel for the delivery of mesenchymal stem cells and potential for articular cartilage repair," *Journal of Biological Engineering*, vol. 8, no. 1, p. 10, 2014.

[91] B. Kristjánsson and S. Honsawek, "Mesenchymal stem cells for cartilage regeneration in osteoarthritis," *World Journal of Orthopedics*, vol. 8, no. 9, pp. 674–680, 2017.

[92] J. M. Lamo-Espinosa, G. Mora, J. F. Blanco et al., "Intra-articular injection of two different doses of autologous bone marrow mesenchymal stem cells versus hyaluronic acid in the treatment of knee osteoarthritis: multicenter randomized controlled clinical trial (phase I/II)," *Journal of Translational Medicine*, vol. 14, no. 1, p. 246, 2016.

[93] P. K. Gupta, A. Chullikana, M. Rengasamy et al., "Efficacy and safety of adult human bone marrow-derived, cultured, pooled, allogeneic mesenchymal stromal cells (Stempeucel®): preclinical and clinical trial in osteoarthritis of the knee joint," *Arthritis Research & Therapy*, vol. 18, no. 1, article 301, 2016.

[94] Y. Sakaguchi, I. Sekiya, K. Yagishita, and T. Muneta, "Comparison of human stem cells derived from various mesenchymal tissues: superiority of synovium as a cell source," *Arthritis & Rheumatism*, vol. 52, no. 8, pp. 2521–2529, 2005.

[95] A. Hatakeyama, S. Uchida, H. Utsunomiya et al., "Isolation and characterization of synovial mesenchymal stem cell derived from hip joints: a comparative analysis with a matched control knee group," *Stem Cells International*, vol. 2017, Article ID 9312329, 13 pages, 2017.

[96] M. Mizuno, H. Katano, K. Otabe et al., "Complete human serum maintains viability and chondrogenic potential of human synovial stem cells: suitable conditions for transplantation," *Stem Cell Research & Therapy*, vol. 8, no. 1, p. 144, 2017.

[97] S.-C. Tao, T. Yuan, Y.-L. Zhang, W.-J. Yin, S.-C. Guo, and C.-Q. Zhang, "Exosomes derived from miR-140-5p-overexpressing human synovial mesenchymal stem cells enhance cartilage tissue regeneration and prevent osteoarthritis of the knee in a rat model," *Theranostics*, vol. 7, no. 1, pp. 180–195, 2017.

[98] K. Koizumi, K. Ebina, D. A. Hart et al., "Synovial mesenchymal stem cells from osteo- or rheumatoid arthritis joints exhibit good potential for cartilage repair using a scaffold-free tissue engineering approach," *Osteoarthritis and Cartilage*, vol. 24, no. 8, pp. 1413–1422, 2016.

[99] E. Matsumura, K. Tsuji, K. Komori, H. Koga, I. Sekiya, and T. Muneta, "Pretreatment with IL-1β enhances proliferation and chondrogenic potential of synovium-derived mesenchymal stem cells," *Cytotherapy*, vol. 19, no. 2, pp. 181–193, 2017.

[100] N. Ozeki, T. Muneta, H. Koga et al., "Not single but periodic injections of synovial mesenchymal stem cells maintain viable cells in knees and inhibit osteoarthritis progression in rats," *Osteoarthritis and Cartilage*, vol. 24, no. 6, pp. 1061–1070, 2016.

[101] D. Hatsushika, T. Muneta, T. Nakamura et al., "Repetitive allogeneic intraarticular injections of synovial mesenchymal stem cells promote meniscus regeneration in a porcine massive meniscus defect model," *Osteoarthritis and Cartilage*, vol. 22, no. 7, pp. 941–950, 2014.

[102] A. Ioan-Facsinay and M. Kloppenburg, "An emerging player in knee osteoarthritis: the infrapatellar fat pad," *Arthritis Research & Therapy*, vol. 15, no. 6, p. 225, 2013.

[103] H. Koga, T. Muneta, T. Nagase et al., "Comparison of mesenchymal tissues-derived stem cells for in vivo chondrogenesis: suitable conditions for cell therapy of cartilage defects in rabbit," *Cell and Tissue Research*, vol. 333, no. 2, pp. 207–215, 2008.

[104] M. Q. Wickham, G. R. Erickson, J. M. Gimble, T. P. Vail, and F. Guilak, "Multipotent stromal cells derived from the infrapatellar fat pad of the knee," *Clinical Orthopaedics and Related Research*, vol. 412, pp. 196–212, 2003.

[105] K. Ye, R. Felimban, K. Traianedes et al., "Chondrogenesis of infrapatellar fat pad derived adipose stem cells in 3D printed chitosan scaffold," *PLoS One*, vol. 9, no. 6, article e99410, 2014.

[106] C. T. Buckley, T. Vinardell, S. D. Thorpe et al., "Functional properties of cartilaginous tissues engineered from

infrapatellar fat pad-derived mesenchymal stem cells," *Journal of Biomechanics*, vol. 43, no. 5, pp. 920–926, 2010.

[107] F. S. Toghraie, N. Chenari, M. A. Gholipour et al., "Treatment of osteoarthritis with infrapatellar fat pad derived mesenchymal stem cells in rabbit," *The Knee*, vol. 18, no. 2, pp. 71–75, 2011.

[108] I. Muñoz-Criado, J. Meseguer-Ripolles, M. Mellado-López et al., "Human suprapatellar fat pad-derived mesenchymal stem cells induce chondrogenesis and cartilage repair in a model of severe osteoarthritis," *Stem Cells International*, vol. 2017, Article ID 4758930, 12 pages, 2017.

[109] J. Garcia, K. Wright, S. Roberts et al., "Characterisation of synovial fluid and infrapatellar fat pad derived mesenchymal stromal cells: the influence of tissue source and inflammatory stimulus," *Scientific Reports*, vol. 6, no. 1, article 24295, 2016.

[110] W.-H. Chen, C.-M. Lin, C.-F. Huang et al., "Functional recovery in osteoarthritic chondrocytes through hyaluronic acid and platelet-rich plasma–inhibited infrapatellar fat pad adipocytes," *The American Journal of Sports Medicine*, vol. 44, no. 10, pp. 2696–2705, 2016.

[111] S. Neri, S. Guidotti, N. L. Lilli, L. Cattini, and E. Mariani, "Infrapatellar fat pad-derived mesenchymal stromal cells from osteoarthritis patients: in vitro genetic stability and replicative senescence," *Journal of Orthopaedic Research*, vol. 35, no. 5, pp. 1029–1037, 2017.

[112] S. Huang, X. Song, T. Li et al., "Pellet coculture of osteoarthritic chondrocytes and infrapatellar fat pad-derived mesenchymal stem cells with chitosan/hyaluronic acid nanoparticles promotes chondrogenic differentiation," *Stem Cell Research & Therapy*, vol. 8, no. 1, p. 264, 2017.

[113] L. Luo, A. R. O'Reilly, S. D. Thorpe, C. T. Buckley, and D. J. Kelly, "Engineering zonal cartilaginous tissue by modulating oxygen levels and mechanical cues through the depth of infrapatellar fat pad stem cell laden hydrogels," *Journal of Tissue Engineering and Regenerative Medicine*, vol. 11, no. 9, pp. 2613–2628, 2017.

[114] J. Yu and J. A. Thomson, "Embryonic stem cells 2006," December 2017, https://stemcells.nih.gov/info/Regenerative_Medicine/2006Chapter1.htm.

[115] K. Watanabe, M. Ueno, D. Kamiya et al., "A ROCK inhibitor permits survival of dissociated human embryonic stem cells," *Nature Biotechnology*, vol. 25, no. 6, pp. 681–686, 2007.

[116] C. McKee, Y. Hong, D. Yao, and G. R. Chaudhry, "Compression induced chondrogenic differentiation of embryonic stem cells in three-dimensional polydimethylsiloxane scaffolds," *Tissue Engineering Part A*, vol. 23, no. 9-10, pp. 426–435, 2017.

[117] C. Hegert, J. Kramer, G. Hargus et al., "Differentiation plasticity of chondrocytes derived from mouse embryonic stem cells," *Journal of Cell Science*, vol. 115, no. 23, pp. 4617–4628, 2002.

[118] N. Nakayama, D. Duryea, R. Manoukian, G. Chow, and C. Y. Han, "Macroscopic cartilage formation with embryonic stem-cell-derived mesodermal progenitor cells," *Journal of Cell Science*, vol. 116, no. 10, pp. 2015–2028, 2003.

[119] N. I. Zur Nieden, G. Kempka, D. E. Rancourt, and H.-J. Ahr, "Induction of chondro-, osteo- and adipogenesis in embryonic stem cells by bone morphogenetic protein-2: effect of cofactors on differentiating lineages," *BMC Developmental Biology*, vol. 5, no. 1, p. 1, 2005.

[120] J. Kramer, C. Hegert, K. Guan, A. M. Wobus, P. K. Müller, and J. Rohwedel, "Embryonic stem cell-derived chondrogenic differentiation in vitro: activation by BMP-2 and BMP-4," *Mechanisms of Development*, vol. 92, no. 2, pp. 193–205, 2000.

[121] Y. Wang, D. Yu, Z. Liu et al., "Exosomes from embryonic mesenchymal stem cells alleviate osteoarthritis through balancing synthesis and degradation of cartilage extracellular matrix," *Stem Cell Research & Therapy*, vol. 8, no. 1, article 189, 2017.

[122] J. Lee, S. E. B. Taylor, P. Smeriglio et al., "Early induction of a prechondrogenic population allows efficient generation of stable chondrocytes from human induced pluripotent stem cells," *The FASEB Journal*, vol. 29, no. 8, pp. 3399–3410, 2015.

[123] B. Lo and L. Parham, "Ethical issues in stem cell research," *Endocrine Reviews*, vol. 30, no. 3, pp. 204–213, 2009.

[124] C. A. Goldthwaite Jr., "The promise of induced pluripotent stem cells (iPSCs)," 2006, https://stemcells.nih.gov/info/Regenerative_Medicine/2006Chapter10.htm.

[125] N. Maherali, R. Sridharan, W. Xie et al., "Directly reprogrammed fibroblasts show global epigenetic remodeling and widespread tissue contribution," *Cell Stem Cell*, vol. 1, no. 1, pp. 55–70, 2007.

[126] K. Takahashi and S. Yamanaka, "Induction of pluripotent stem cells from mouse embryonic and adult fibroblast cultures by defined factors," *Cell*, vol. 126, no. 4, pp. 663–676, 2006.

[127] J. Yu, M. A. Vodyanik, K. Smuga-Otto et al., "Induced pluripotent stem cell lines derived from human somatic cells," *Science*, vol. 318, no. 5858, pp. 1917–1920, 2007.

[128] B. Feng, J. Jiang, P. Kraus et al., "Reprogramming of fibroblasts into induced pluripotent stem cells with orphan nuclear receptor Esrrb," *Nature Cell Biology*, vol. 11, no. 2, pp. 197–203, 2009.

[129] M. Zhang, K. Niibe, T. Kondo, Y. Kamano, M. Saeki, and H. Egusa, "Gene delivery and expression systems in induced pluripotent stem cells," in *Interface Oral Health Science 2016: Innovative Research on Biosis–Abiosis Intelligent Interface*, K. Sasaki, O. Suzuki, and N. Takahashi, Eds., pp. 121–133, Springer, Singapore, 2017.

[130] C. Murphy, A. Mobasheri, Z. Táncos, J. Kobolák, and A. Dinnyés, "The potency of induced pluripotent stem cells in cartilage regeneration and osteoarthritis treatment," in *Advances in Experimental Medicine and Biology*, pp. 1–14, Springer, Boston, MA, USA, 2017.

[131] T. Saito, F. Yano, D. Mori et al., "Generation of Col2a1-EGFP iPS cells for monitoring chondrogenic differentiation," *PLoS One*, vol. 8, no. 9, article e74137, 2013.

[132] T. Teramura, Y. Onodera, T. Mihara, Y. Hosoi, C. Hamanishi, and K. Fukuda, "Induction of mesenchymal progenitor cells with chondrogenic property from mouse-induced pluripotent stem cells," *Cellular Reprogramming*, vol. 12, no. 3, pp. 249–261, 2010.

[133] G. Bilousova, D. H. Jun, K. B. King et al., "Osteoblasts derived from induced pluripotent stem cells form calcified structures in scaffolds both in vitro and in vivo," *Stem Cells*, vol. 29, no. 2, pp. 206–216, 2011.

[134] N. Koyama, M. Miura, K. Nakao et al., "Human induced pluripotent stem cells differentiated into chondrogenic lineage via generation of mesenchymal progenitor cells," *Stem Cells and Development*, vol. 22, no. 1, pp. 102–113, 2012.

[135] Y. Zhu, X. Wu, Y. Liang et al., "Repair of cartilage defects in osteoarthritis rats with induced pluripotent stem cell derived chondrocytes," *BMC Biotechnology*, vol. 16, no. 1, p. 78, 2016.

[136] Y. Zhu, Y. Wang, B. Zhao et al., "Comparison of exosomes secreted by induced pluripotent stem cell-derived mesenchymal stem cells and synovial membrane-derived mesenchymal stem cells for the treatment of osteoarthritis," *Stem Cell Research & Therapy*, vol. 8, no. 1, p. 64, 2017.

[137] A. Yamashita, M. Morioka, Y. Yahara et al., "Generation of scaffoldless hyaline cartilaginous tissue from human iPSCs," *Stem Cell Reports*, vol. 4, no. 3, pp. 404–418, 2015.

[138] H. Nejadnik, S. Diecke, O. D. Lenkov et al., "Improved approach for chondrogenic differentiation of human induced pluripotent stem cells," *Stem Cell Reviews and Reports*, vol. 11, no. 2, pp. 242–253, 2015.

[139] J.-Y. Ko, K.-I. Kim, S. Park, and G.-I. Im, "In vitro chondrogenesis and in vivo repair of osteochondral defect with human induced pluripotent stem cells," *Biomaterials*, vol. 35, no. 11, pp. 3571–3581, 2014.

[140] J. Liu, H. Nie, Z. Xu et al., "The effect of 3D nanofibrous scaffolds on the chondrogenesis of induced pluripotent stem cells and their application in restoration of cartilage defects," *PLoS One*, vol. 9, no. 11, article e111566, 2014.

[141] B. O. Diekman, N. Christoforou, V. P. Willard et al., "Cartilage tissue engineering using differentiated and purified induced pluripotent stem cells," *Proceedings of the National Academy of Sciences*, vol. 109, no. 47, pp. 19172–19177, 2012.

[142] T. Saito, F. Yano, D. Mori et al., "Hyaline cartilage formation and tumorigenesis of implanted tissues derived from human induced pluripotent stem cells," *Biomedical Research*, vol. 36, no. 3, pp. 179–186, 2015.

[143] R. M. Guzzo and M. B. O'Sullivan, "Human pluripotent stem cells: advances in chondrogenic differentiation and articular cartilage regeneration," *Current Molecular Biology Reports*, vol. 2, no. 3, pp. 113–122, 2016.

[144] T. Kuroda, S. Yasuda, S. Kusakawa et al., "Highly sensitive in vitro methods for detection of residual undifferentiated cells in retinal pigment epithelial cells derived from human iPS cells," *PLoS One*, vol. 7, no. 5, article e37342, 2012.

[145] K. Okita, T. Ichisaka, and S. Yamanaka, "Generation of germline-competent induced pluripotent stem cells," *Nature*, vol. 448, no. 7151, pp. 313–317, 2007.

[146] I. Ben-Porath, M. W. Thomson, V. J. Carey et al., "An embryonic stem cell–like gene expression signature in poorly differentiated aggressive human tumors," *Nature Genetics*, vol. 40, no. 5, pp. 499–507, 2008.

[147] K. Hochedlinger, Y. Yamada, C. Beard, and R. Jaenisch, "Ectopic expression of *Oct-4* blocks progenitor-cell differentiation and causes dysplasia in epithelial tissues," *Cell*, vol. 121, no. 3, pp. 465–477, 2005.

[148] E. T. Park, J. R. Gum, S. Kakar, S. W. Kwon, G. Deng, and Y. S. Kim, "Aberrant expression of SOX2 upregulates MUC5AC gastric foveolar mucin in mucinous cancers of the colorectum and related lesions," *International Journal of Cancer*, vol. 122, no. 6, pp. 1253–1260, 2008.

[149] F. Kuttler and S. Mai, "c-Myc, genomic instability and disease," *Genome Dynamics*, vol. 1, pp. 171–190, 2006.

[150] A. M. Ghaleb, M. O. Nandan, S. Chanchevalap, W. B. Dalton, I. M. Hisamuddin, and V. W. Yang, "Krüppel-like factors 4 and 5: the yin and yang regulators of cellular proliferation," *Cell Research*, vol. 15, no. 2, pp. 92–96, 2005.

[151] H. Madry and M. Cucchiarini, "Gene therapy for human osteoarthritis: principles and clinical translation," *Expert Opinion on Biological Therapy*, vol. 16, no. 3, pp. 331–346, 2016.

[152] V. Rai, M. F. Dilisio, N. E. Dietz, and D. K. Agrawal, "Recent strategies in cartilage repair: a systemic review of the scaffold development and tissue engineering," *Journal of Biomedical Materials Research Part A*, vol. 105, no. 8, pp. 2343–2354, 2017.

[153] E. Budd, S. Waddell, M. C. de Andrés, and R. O. C. Oreffo, "The potential of microRNAs for stem cell-based therapy for degenerative skeletal diseases," *Current Molecular Biology Reports*, vol. 3, no. 4, pp. 263–275, 2017.

[154] X.-M. Yu, H.-Y. Meng, X.-L. Yuan et al., "MicroRNAs' involvement in osteoarthritis and the prospects for treatments," *Evidence-Based Complementary and Alternative Medicine*, vol. 2015, Article ID 236179, 13 pages, 2015.

[155] G. van den Akker, H. van Beuningen, E. Blaney Davidson, and P. van der Kraan, "CRISPR/CAS9 mediated genome engineering of human mesenchymal stem cells," *Osteoarthritis and Cartilage*, vol. 24, article S231, 2016.

[156] J. M. Brunger, A. Zutshi, V. P. Willard, C. A. Gersbach, and F. Guilak, "Genome engineering of stem cells for autonomously regulated, closed-loop delivery of biologic drugs," *Stem Cell Reports*, vol. 8, no. 5, pp. 1202–1213, 2017.

[157] E. Kon, G. Filardo, A. Roffi, L. Andriolo, and M. Marcacci, "New trends for knee cartilage regeneration: from cell-free scaffolds to mesenchymal stem cells," *Current Reviews in Musculoskeletal Medicine*, vol. 5, no. 3, pp. 236–243, 2012.

[158] D. F. Duarte Campos, W. Drescher, B. Rath, M. Tingart, and H. Fischer, "Supporting biomaterials for articular cartilage repair," *Cartilage*, vol. 3, no. 3, pp. 205–221, 2012.

[159] J. Pak, "Regeneration of human bones in hip osteonecrosis and human cartilage in knee osteoarthritis with autologous adipose-tissue-derived stem cells: a case series," *Journal of Medical Case Reports*, vol. 5, no. 1, article 296, 2011.

[160] D. Mehrabani, F. Mojtahed Jaberi, M. Zakerinia et al., "The healing effect of bone marrow-derived stem cells in knee osteoarthritis: a case report," *World Journal of Plastic Surgery*, vol. 5, no. 2, pp. 168–174, 2016.

[161] I. Sekiya, T. Muneta, M. Horie, and H. Koga, "Arthroscopic transplantation of synovial stem cells improves clinical outcomes in knees with cartilage defects," *Clinical Orthopaedics and Related Research*, vol. 473, no. 7, pp. 2316–2326, 2015.

Hindawi
Stem Cells International
Volume 2018, Article ID 3237253, 9 pages
https://doi.org/10.1155/2018/3237253

Research Article

The Hypoxia-Mimetic Agent Cobalt Chloride Differently Affects Human Mesenchymal Stem Cells in Their Chondrogenic Potential

Gabriella Teti,[1] **Stefano Focaroli**,[1] **Viviana Salvatore**,[2] **Eleonora Mazzotti**,[3] **Laura Ingra'**,[1] **Antonio Mazzotti**,[4] **and Mirella Falconi**[1]

[1]*Department of Biomedical and Neuromotor Sciences, University of Bologna, Bologna, Italy*
[2]*An2H Discovery Limited, National Institute of Cellular Biotechnology (NICB), Dublin City University Campus, Dublin, Ireland*
[3]*Faculty of Comparative Biomedical Sciences, University of Teramo, Teramo, Italy*
[4]*First Orthopaedic and Traumatologic Clinic, Istituto Ortopedico Rizzoli, University of Bologna, Bologna, Italy*

Correspondence should be addressed to Mirella Falconi; mirella.falconi@unibo.it

Received 28 August 2017; Revised 10 December 2017; Accepted 1 January 2018; Published 13 March 2018

Academic Editor: Wesley Sivak

Adult stem cells are a promising cell source for cartilage regeneration. They resided in a special microenvironment known as the stem-cell niche, characterized by the presence of low oxygen concentration. Cobalt chloride ($CoCl_2$) imitates hypoxia in vitro by stabilizing hypoxia-inducible factor-alpha (HIF-1α), which is the master regulator in the cellular adaptive response to hypoxia. In this study, the influence of $CoCl_2$ on the chondrogenic potential of human MSCs, isolated from dental pulp, umbilical cord, and adipose tissue, was investigated. Cells were treated with concentrations of $CoCl_2$ ranging from 50 to 400 μM. Cell viability, HIF-1α protein synthesis, and the expression of the chondrogenic markers were analyzed. The results showed that the $CoCl_2$ supplementation had no effect on cell viability, while the upregulation of chondrogenic markers such as SOX9, COL2A1, VCAN, and ACAN was dependent on the cellular source. This study shows that hypoxia, induced by $CoCl_2$ treatment, can differently influence the behavior of MSCs, isolated from different sources, in their chondrogenic potential. These findings should be taken into consideration in the treatment of cartilage repair and regeneration based on stem cell therapies.

1. Introduction

Hyaline articular cartilage has a very limited or no intrinsic capacity for repair and minor traumatic lesions or pathological injuries may trigger progressive damage and joint degeneration [1]. Early intervention is needed to avoid growth of traumatic chondral and osteochondral defects and to delay cartilage degeneration and osteoarthritis.

Novel cell-based tissue engineering techniques have been proposed with the aim to repair cartilage defects and reconstitute the properties of hyaline cartilage. The mesenchymal stromal cells (MSCs), due to the high proliferative capacity, self-renewal, and potential to differentiate into different lineages, represent a promising strategy in regenerative medicine [2]. The MSCs are separated from several human tissues such as the bone marrow [3], the synovial tissue [4], the adipose tissue [5, 6], the periosteum [7, 8], the dental pulp [9] and Wharton's jelly umbilical cord [10].

The microenvironment of MSCs is characterized by a low oxygen tension, demonstrating that MSCs might be quite resistant to oxygen limitation [11]. Changes in the oxygen concentration activate intracellular mechanisms responsible either for cell death or for cell adaptation to new environmental conditions [11, 12]. The key adaptive response to hypoxic conditions is the stabilization of hypoxia-inducible factor- (HIF) 1 [13]. As a transcription factor, it plays a vital role in the functional expression of a number of genes involved in the adaptation and survival of cells, tissues, and organs. The transcription factor HIF-1 is composed of two subunits, HIF-1α and HIF-β or aryl hydrocarbon receptor nuclear translocator (ARNT) [14]. In both normoxic and hypoxic conditions, the HIF-β is constantly biosynthesised, degraded, and recycled [15]. HIF-1α in normal oxygen

condition, despite being biosynthesised, is subjected to the instantaneous decomposition [16]. In normoxic conditions, HIF-1α is polyhydroxylated by oxygen-dependent prolyl (P4HS) and arginyl hydroxylases (FIH). Once hydroxylated, HIF-1α protein binds to von Hippel–Lindau (VHL) tumor suppressor protein—the recognition component of E3 ubiquitin-protein ligases—and is rapidly degraded by the proteasome. In hypoxic condition, hydroxylation is inhibited, which leads to the stabilization of HIF-1α and its accumulation in the nucleus [14, 17]. All P4Hs are 2-oxoglutarate dioxygenases and require Fe^{2+}, 2-oxoglutarate, O_2, and ascorbate. Thus, even small decreases in the O_2 concentration will inhibit the activities of the HIF-P4Hs so that HIF-1α escape degradation [17].

Recent evidences suggested that hypoxia is involved in the chondrogenic differentiation of MSCs [18]. Expansion and chondrogenic induction of the bone marrow-derived MSCs under hypoxia generally result in enhanced chondrogenic differentiation, while they showed a reduced capacity in differentiating into adipogenic and osteogenic lineage [19–21].

In in vitro studies, hypoxia is generally induced by decreasing atmospheric oxygen concentrations or by utilization of mimetic chemical agents such as cobalt chloride ($CoCl_2$) and desferrioxamine (DFO). Chemical agents are more attractive in experimental laboratories because they are cheap, they maintain steady oxygen tension, and they are more stable compared to hypoxic chamber. They artificially induce hypoxia through blocking the degradation of HIF-1α [22]. Cobalt chloride has been reported to inhibit the activities of HIF-P4Hs and FIH, suggesting that it may occupy their Fe^{2+} binding site and block the degradation of HIF-1α [17]. It is demonstrated that the effects of hypoxia-mimetic agents are comparable to those resulting from reduced atmospheric oxygen levels [17].

Despite several studies on the impact of hypoxia preconditioning on MSC differentiation, the influence of hypoxia on MSC behavior is still a matter of discussion. The data on their response to hypoxic conditions are rather controversial, demonstrating both damaging and ameliorating effects. The present study was aimed to compare the effects of hypoxia, induced by $CoCl_2$, among the human MSCs derived from human dental pulp, adipose tissue, and Wharton's jelly umbilical cord, and their response to chondrogenic induction under hypoxic conditions.

2. Materials and Methods

2.1. Mesenchymal Stem Cells. The human adipose mesenchymal stem cells (ADMSCs) were purchased from Invitrogen (Life Technologies, Monza, Italy). The human dental pulp mesenchymal stem cells (DPMSCs) were obtained from healthy permanent premolars extracted during orthodontic treatment, under informed consent [9]. The human umbilical cord mesenchymal stem cells (UBMSCs) were obtained from the tissue of umbilical cords of full-term pregnancies. Informed consent was obtained from each patient according to the guidelines of the National Bioethics Committee, and the samples were treated following a protocol approved by the University of Bologna. All the cells were maintained at 37°C and 5% CO_2 in DMEM/F12 Glutamax® medium (Gibco, Thermo Fisher, Monza, Italy) supplemented with 10% FBS (*v*/*v*) and 1% (*v*/*v*) penicillin and streptomycin (Gibco, Thermo Fisher, Monza, Italy). In this study, all the cells were used between passages 4 and 7.

2.2. Immunophenotyping. The DPMSCs, UCMSCs, and ADMSCs were checked for their surface marker profile by FACSCalibur flow cytometry system (Becton Dickinson, CA, USA) as already described [8, 9, 23]. Briefly, the MSCs were detached from the surface of the flask with enzyme digestion for 3 minutes at room temperature, collected, and centrifuged at 300*g* for 5 minutes. The pellets were resuspended in stain buffer and the cells were counted by hemocytometer. Then, 2.5×10^5 cells were incubated for 45 min, in the dark at 4°C, with the following antibodies: fluorescein isothiocyanate- (FITC-) labeled mouse antihuman CD90 (Stem-Cell Technologies, Milan, Italy), CD105, CD14, and CD19 (Diaclone, France); R-phycoerythrin- (PE-) labeled mouse antihuman CD34, CD44, CD45 (Diaclone, France), and CD73 (Becton Dickinson, CA, USA); and anti-HLA-DR (Diaclone, France). The control for FITC- or PE-coupled antibodies was isotypic mouse IgG1. The data were evaluated using CellQuest software (Becton Dickinson, CA, USA).

2.3. Cobalt Chloride Treatment and MTT Assay. The cells were seeded in 96-well culture plates at a density of 1×10^4 cells/well for 24 h. The culture medium was changed to fresh MEM containing 2% FBS and 1% antibiotics and treated with different concentrations of $CoCl_2$ ranging from 50 to 400 μM. After 24 h and 48 h, the medium was changed with a new one supplemented with 0.5 mg/mL of 3-(4,5-dimethylthiazol-2-yl)-2,5-diphenyltetrazolium bromide (MTT) for 3 h at 37°C. The formazan produced was dissolved by solvent solution (0.1 N HCl in isopropanol), and the optical density was read at 570 nm by microplate reader (Model 680, Bio-Rad Lab Inc., CA, USA).

2.4. HIF-1α Protein Expression. The MSCs were treated with 100 μM $CoCl_2$ for 6 h, 12 h, 24 h, and 48 h, and cytosolic extract was obtained by using RIPA lysis buffer (Pierce, Thermo Fisher Scientific, Monza, Italy) supplemented with 25 μmol/L protease inhibitor cocktail (Pierce, Thermo Fisher Scientific, Monza, Italy) and 1 μL of β-mercapto-ethanol (Sigma-Aldrich, St. Louis, Missouri, USA). Total proteins were resolved on 4–12% SDS polyacrylamide gel electrophoresis (SDS–PAGE) and electrophoretically transferred into a nitrocellulose membrane using a wet blotting apparatus (Invitrogen, Thermo Fisher Scientific, Monza, Italy). The membranes were blocked with dry milk (Invitrogen, Thermo Fisher Scientific, Monza, Italy) for 30 minutes at room temperature and were then incubated with antihuman HIF-1α, diluted 1 : 400 (Invitrogen, Thermo Fisher Scientific, Monza, Italy), and antihuman actin, diluted 1 : 1000 (Cell Signaling Technology, Leiden, The Netherlands) at 4°C over night. After washing with transfer buffer (TBS-T), each blot was incubated with antirabbit secondary antibody (1 : 5,000 dilution; Cell Signaling Technology, Leiden, The Netherlands) for 1 h and 30 minutes at room temperature.

The antibody signal was visualized with the enhancement chemiluminescence system (Pierce, Thermo Fisher Scientific, Monza, Italy). Images were obtained by using Image Station 2000R (Kodak, NY, USA).

Band densitometry was measured using ImageJ software (National Institutes of Health), and the intensities of the specific protein bands were corrected for equal actin loading; they were expressed as relative to the intensity of the control sample. Data showed the average of triplicates ± SD and were representative from three independent experiments.

2.5. Chondrogenic Differentiation. The MSCs, in micromass culture, were stimulated with MEM supplemented with 2% FBS and 100 μM $CoCl_2$ for 48 h and then were cultured in chondrogenic medium consisting in MEM supplemented with 2% FBS, 10 ng/mL of TGF-β3 (Millipore, Milan, Italy), 100 nm dexamethasone (Sigma-Aldrich, St. Louis, Missouri, USA), 100 μg/mL ascorbate-2-phosphate (Sigma-Aldrich, St. Louis, Missouri, USA), ITS (6.25 μg/mL insulin, 6.25 μg/mL transferrin, 6.25 μg/mL selenous acid) (Gibco, Thermo Fisher Scientific, Monza, Italy) for 7, 14, 21, and 28 days. The chondrogenic medium was replaced every 3 days. Control samples consisted in MSCs cultured in micromass system in MEM supplemented with 10% FBS up to 28 days.

At the end of each treatment, the cells were collected and RNA extraction and quantitative real time PCR (qRT-PCR) was performed.

2.6. mRNA Extraction and qRT-PCR. RNeasy Mini Kit (Invitrogen, Thermo Fisher Scientific, Monza, Italy) was used for the extraction of RNA from cellular pellets, and 200 ng of total RNA was reverse transcribed into first-strand cDNA using SuperScript™ III One-Step RT-PCR System (Invitrogen, Thermo Fisher Scientific, Monza, Italy). Chondrogenic mRNA marker expression levels were analyzed via real-time PCR by 7500 real-time PCR machine (Applied Biosystems, Life Technologies, Monza, Italy). For mRNA quantification, TaqMan assays (Life Technologies, Thermo Fischer Scientific, Monza Italy) were used specific for collagen type II (COL2A1; Hs00264051_m1), collagen type 10 (COL10A1; Hs00166657_m1), Sox9 (SOX9; Hs01001343_g1), versican (VCAN; Hs00171642_m1), and aggrecan (ACAN; Hs00153936_m1). Relative gene expression levels were normalized to that of glyceraldehyde 3-phosphate dehydrogenase (GAPDH; Hs99999905_m1). Data are presented as fold changes relative to levels in control samples by using formula $2^{-\Delta\Delta CT}$, as recommended by the manufacturer (User Bulletin number 2 P/N 4303859; Applied Biosystems).

2.7. Alcian Blue and Safranin O Staining. The MSCs were stimulated with MEM supplemented with 2% FBS and 100 μM $CoCl_2$ for 48 h in micromass culture, and then they were cultured in chondrogenic medium as previously described. At the end of each experimental point, the MSCs were immediately fixed in 4% formaldehyde (Sigma-Aldrich, St. Louis, Missouri, USA) in phosphate buffer (PBS) for 24 h at 4°C. Then, they were dehydrated in a graded series of ethanol and embedded in paraffin wax (Fluka, Sigma-Aldrich). Paraffin sections of 6 μm were obtained with an automated rotary microtome (Leica Microsystems Srl, Cambridge, United Kingdom) and collected on Superfrost glass slides (Carl Roth, Karlshure, Germany). Samples were subsequently processed for alcian blue staining by using alcian blue and safranin O staining kits (Bio-Optica, Milan, Italy). Images utilized are representative from three independent experiments.

2.8. Statistical Analysis. MTT and real-time PCR values were presented as the mean ± standard deviation, and each type of experiment was replicated three times. One way ANOVA followed by Dunnett's multiple comparison test was used to evaluate the differences between the samples. Statistical analysis was performed by GraphPad Prism 5.0 software (GraphPad Software Inc., San Diego, CA, USA). P values of <0.05 were considered statistically significant.

3. Results

3.1. Immunophenotyping. The MSCs utilized for all the experiments were characterized for CD105, CD14, CD19, CD34, CD45, CD73, CD90, and HLADR using flow cytometric analysis. It was found that these cells were highly positive for CD105, CD73, and CD90 (>95%) and negative for CD34, CD19, CD45, CD14, and HLA-DR (<3%) (data not showed) [8, 9, 23]. Moreover, they were able to differentiate into all the mesenchymal lineages (data not showed) [8, 9, 23].

3.2. MTT Assay. To evaluate the potential toxicity of $CoCl_2$ on MSCs cells, an MTT assay testing different concentration of $CoCl_2$, ranging from 50 μM to 400 μM, was carried out, for 24 h and 48 h. Results showed a high cell viability in all the three MSCs tested for 24 h and 48 h (Figures 1(a) and 1(b)). A light reduction of viability was observed after 48 h with the concentration of 400 μM (Figure 1(b)). The concentration of 100 μM showed the highest cell viability both at 24 h and 48 h; therefore, this concentration was used for all the following experiments.

3.3. HIF-1α Expression. To determine if the treatment with $CoCl_2$ was responsible of an upregulation of the transcription factor HIF1α, the expression of the protein after 6 h, 12 h, 24 h, and 48 h of $CoCl_2$ exposition was evaluated by western blotting analysis (Figure 2).

Apparently, no difference between control and treated samples was observed by western blot, in the entire MSCs tested (Figures 2(a)–2(c)). Densitometric analysis of protein bands showed a time-dependent upregulation of HIF-1α in DPMSCs and UCMSCs, while no significant difference was evaluated in ADMSCs (Figure 2(d)). After 48 h of $CoCl_2$ incubation, the expression of HIF-1α was increased at about 4.4-fold in DPMSCs and UCMSCs (Figure 2(d)) compared to that in each control sample.

3.4. Chondrogenic Differentiation of DPMSCs, UCMSCs, and ADMSCs in Hypoxia. To determine if hypoxia, induced by $CoCl_2$, enhances chondrogenic differentiation, DPMSCs, UCMSCs, and ADMSCs were preincubated with 100 μM $CoCl_2$ for 48 h, and then they were induced to chondrogenic differentiation by chondrogenic medium up to 28 days. At

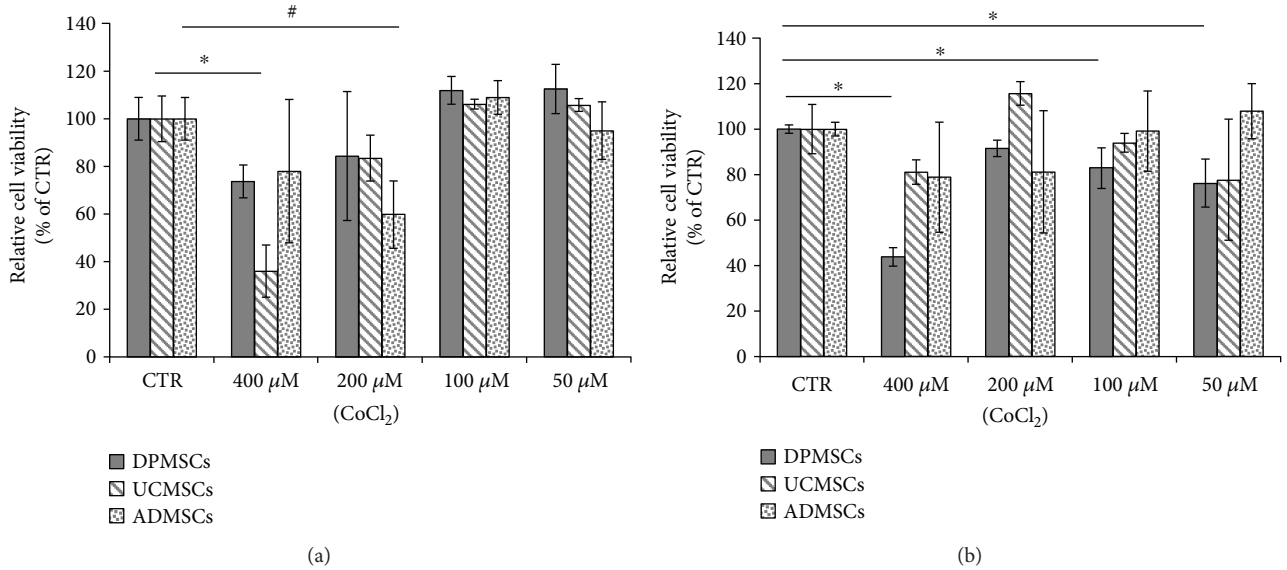

Figure 1: Effects of different concentration of $CoCl_2$ on the DPMSCs, UCMSCs, and ADMSCs. (a) Cells treated for 24 h; (b) cells treated for 48 h. Cell viability was determined by MTT assay and the results were expressed as relative cell viability compared to each control sample. Each value is the mean ± SD of triplicate independent experiments. $^{*}p < 0.05$, as compared to control DPMSCs; $^{\#}p < 0.05$, as compared to control UCMSCs; $^{\S}p < 0.05$, as compared to control ADMSCs.

each experimental point, the gene expression of the chondrogenic markers SRY-box containing gene 9 (SOX9), a key transcription factor for chondrocyte differentiation, type II collagen (COL2A1), versican (VCAN), and aggrecan (ACAN), downstream targets of SOX9, was assessed by qRT-PCR (Figure 3).

The DPMSCs showed an upregulation of about 3-fold of the transcription factor SOX9 after 7 days of chondrogenic differentiation, followed by a reduction of expression after 14, 21, and 28 days of induction (Figure 3(a)). An upregulation of VCAN was also observed after 7, 14, 21, and 28 days of chondrogenic stimulation (Figure 3(a)), while no amplification was detected for mRNA corresponding to COL2A1 and ACAN (Figure 3(a)).

The UCMSCs showed a time-dependent upregulation of all the chondrogenic markers tested (Figure 3(b)). The SOX9 mRNA level reached the highest level after 21 days of differentiation, while COL2A1 mRNA expression was observed after 14 days of differentiation and increased about 5-fold after 28 days (Figure 3(b)). VCAN mRNA showed a light time-dependent upregulation, while the expression of ACAN mRNA was significantly increased up to 21 and 28 days of chondrogenic differentiation (Figure 3(b)).

On the contrary, the ADMSCs showed a constant expression of SOX9 and ACAN compared to control samples (Figure 3(c)), while an upregulation of expression was detected for COL2A1 and ACAN mRNA at the end of the chondrogenic induction (Figure 3(c)).

To demonstrate the absence of hypertrophic chondrogenesis, a qRT-PCR to evaluate the expression of the hypertrophic chondrogenic marker, collagen type 10, was carried out. Results showed a low signal of collagen type 10 in the UCMSCs and DPMSCs after 28 days of differentiation (Figure 4), while the ADMSCs showed a light but statistically significant upregulation of collagen type 10 compared to the control samples (Figure 4).

3.5. Alcian Blue and Safranin O Staining. To demonstrate the presence of proteoglycans in the extracellular matrix produced by the MSCs stimulated to chondrogenic differentiation up to 28 days, alcian blue and safranin O stainings were carried out. Alcian blue results showed an intense blue color on extracellular matrix produced by the UCMSCs and ADMSCs (Figure 5), while a very light signal was detected in the DPMSCs. These data are supported by safranin O staining, which demonstrated a clear red color, corresponding to proteoglycan deposition, in the UCMSCs and ADMSCs, while no red signal was detected in the DPMSCs (Figure 5).

4. Discussion

Articular cartilage damage caused by sports injuries, accidental trauma, and aging generally progresses to more serious joint disorders, including osteoarthritis (OA), necrosis of subchondral bone, or arthritis [1, 2]. The hyaline articular cartilage has a very limited or no intrinsic capacity for repair, and even minor lesions or injuries may trigger progressive damage and joint degeneration [1]. Current treatments, based on surgical interventions, are still not satisfactory, often followed by the development of fibrocartilage [2]. Nowadays, repair and regeneration of hyaline cartilage are still a challenge. Novel cell-based tissue engineering techniques have been proposed with the aim to repair defects with bioengineered tissue that mimics the properties of hyaline cartilage and helps in the integration into native tissue. Transplantation of MSCs is a promising strategy based on their high proliferative capacity, self-renewal, and potential to differentiate into cartilage-producing cells. However, still

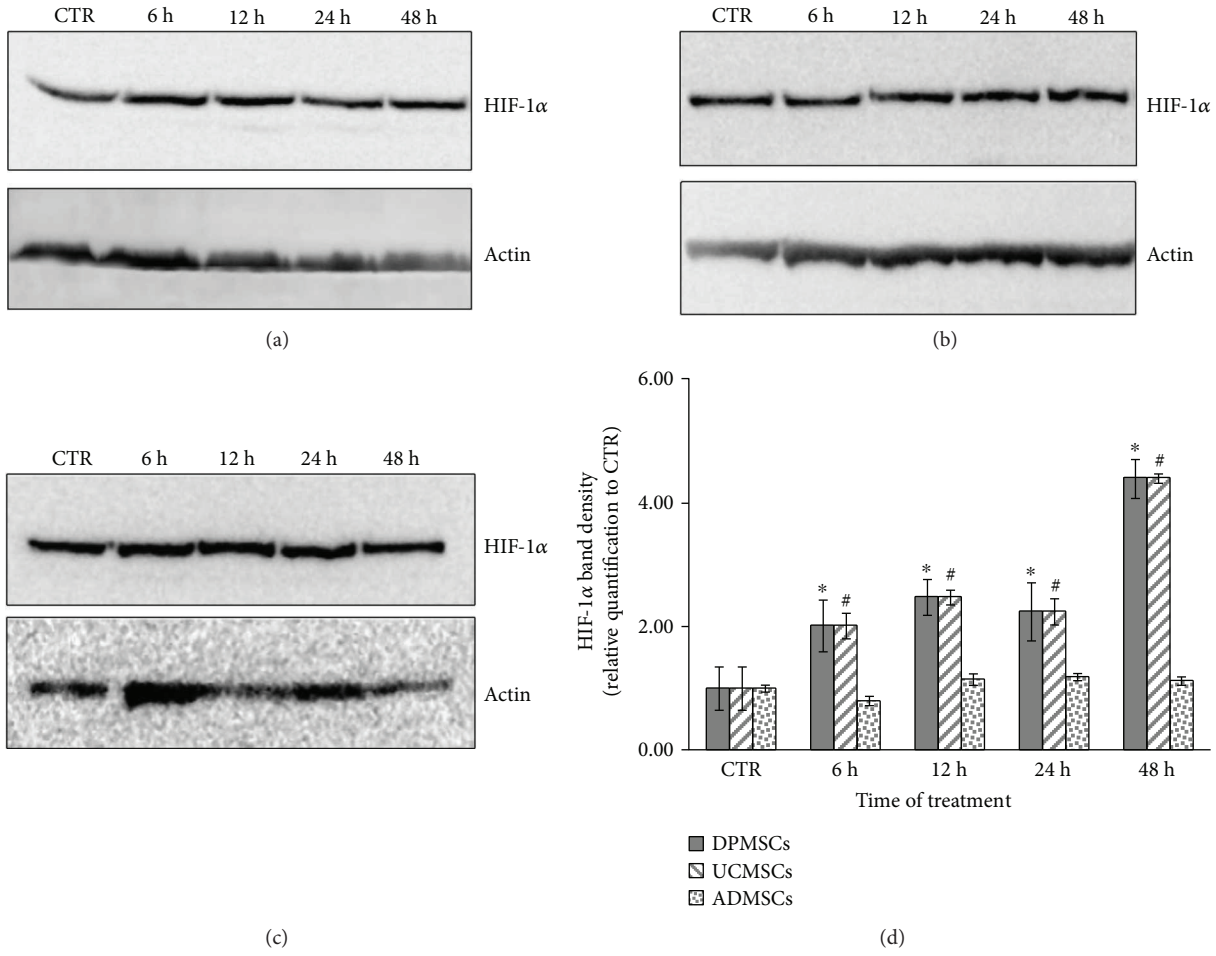

Figure 2: Effect of $CoCl_2$ in the expression of HIF-1α. The MSCs were incubated with 100 μM of $CoCl_2$ in cell medium supplemented with 2% of FCS for 6 h, 12 h, 24 h, and 48 h. (a) HIF-1α expression in the DPMSCs; (b) HIF-1α expression in the UCMSCs; (c) HIF-1α expression in the ADMSCs; (d) densitometric analysis of western blot bands. Control samples consist in the MSCs cultured with cell medium supplemented with 10% FCS for 48 h. The value was normalized to each corresponding β-actin level and represented as a relative expression compared to the control sample. Each value is the mean ± SD of triplicate independent experiments. $^{*}p < 0.05$, as compared to control DPMSCs; $^{\#}p < 0.05$, as compared to control UCMSCs; $^{\S}p < 0.05$, as compared to control ADMSCs.

biological obstacles persist in the MSC-based regeneration of articular cartilage [1]. Mechanical properties of the reconstructed cartilage are inferior to the native tissue, and heterogeneity of initial cell population and poor matrix deposition contribute to functional limitation of the MSCs [1].

Increasing evidence indicates that environmental preconditioning is a powerful approach in promoting stem cell proliferation and chondrogenic potential [24]. In the native cartilage, cells are exposed to very low oxygen tension which promotes MSC survival, proliferation, and differentiation capacity [24]. However, the data regarding the effect of hypoxia on MSC behavior are still contradictory and the role of hypoxia is still unclear.

The aim of this study was to compare the behavior of three human MSCs, separated from dental pulp, Wharton's jelly umbilical cord, and adipose tissues, induced to chondrogenic phenotype under hypoxic environment.

The choice of DPMSCs, UCMSCs, and ADMSCs for this study reflects their readily accessible source, easy protocols for isolation, and easy availability without ethical concerns. They represent the ideal source for stem cell-based therapy and regenerative medicine. Although the DPMSCs, UCMSCs, and ADMSCs seem very similar, they show specific characteristic of the tissue of origin which diversifies their response to hypoxia and tissue regeneration.

Cobalt chloride, a chemical hypoxia-mimetic agent, is an attractive alternative to creating physical hypoxic agents [25–27]. The potential toxicity of $CoCl_2$ on the different MSCs utilized in this study was investigated by MTT analysis. The highest cell viability was obtained at 100 μM of $CoCl_2$, after 24 h and 48 h in all the three MSCs tested. Therefore, 100 μM was the concentration of cobalt chloride utilized in the study, in agreement with previous investigations on murine stem cells [21]. A pretreatment of 100 μM $CoCl_2$ was performed on DPMSCs, UCMSCs, and ADMSCs for 48 h, as a hypoxic preconditioning approach, with the aim to promote chondrogenic differentiation [24]. The mechanism by which hypoxia exerts its effect on cells is mainly regulated by HIF-1α, which upregulates several genes involved in glucose metabolism, erythropoiesis, iron

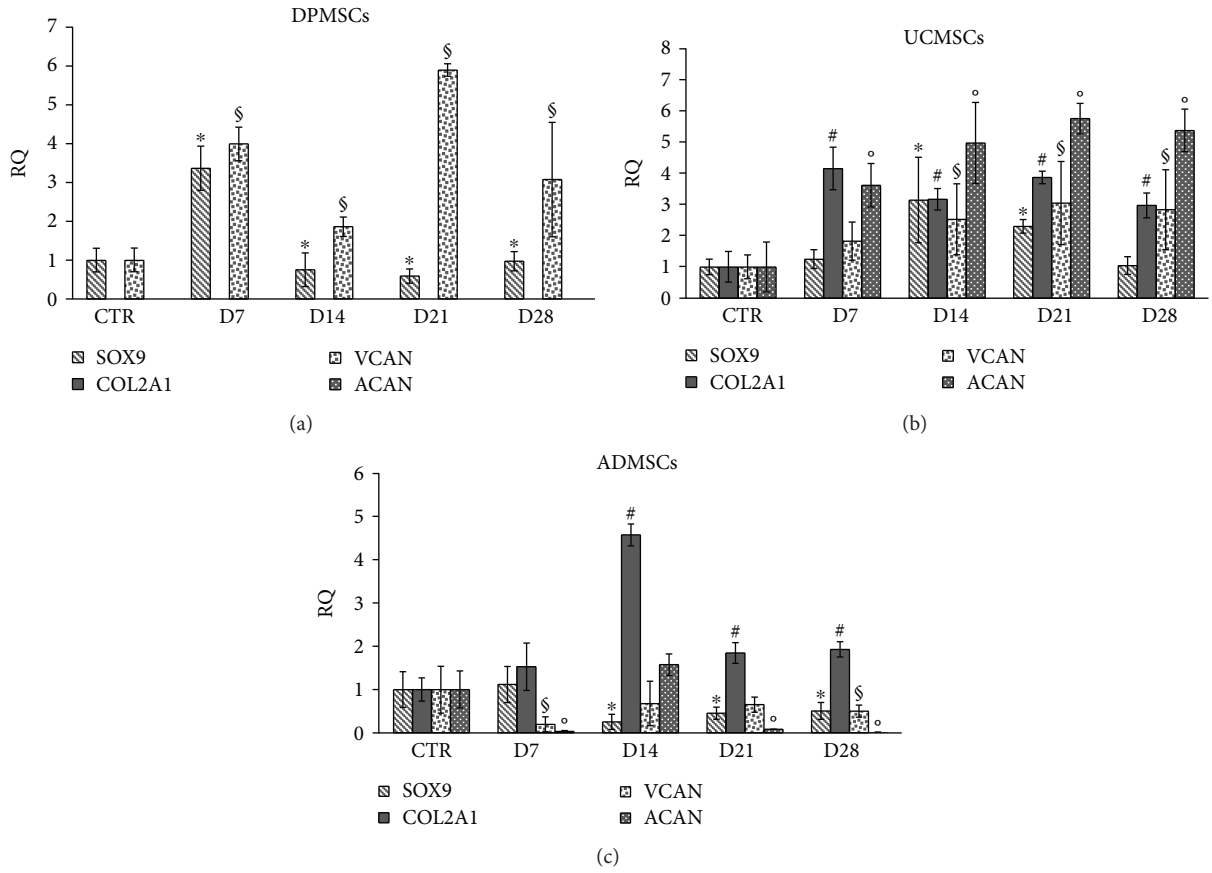

Figure 3: Effects of $CoCl_2$ on the MSCs induced to chondrogenic phenotype for 7, 14, 21, and 28 days. mRNA expression of SOX9, COL2A1, VCAN, and ACAN in (a) DPMSCs, (b) UCMSCs, and (c) ADMSCs. Gene expression was normalized to the corresponding GAPDH and calculated as relative expression compared to control cells for the DPMSCs and UCMSCs and to D14 for the ADMSCs. The experiments were performed three times. Data were expressed as mean ± SD. $^{*}p < 0.05$, as compared to control SOX9 mRNA; $^{\#}p < 0.05$, as compared to control COL2A1 mRNA; $^{\S}p < 0.05$, as compared to control VCAN; $^{\circ}p < 0.05$, as compared to control ACAN.

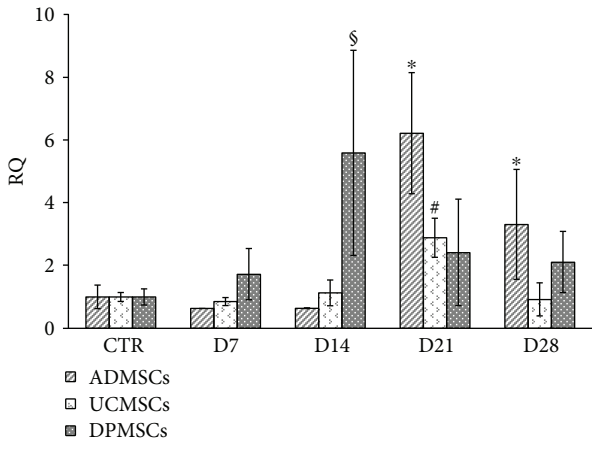

Figure 4: mRNA expression of COL10A in the ADMSCs, UCMSCs, and DPMSCs induced to chondrogenic differentiation up to 28 days. The experiments were performed three times. Data were expressed as mean ± SD. $^{*}p < 0.05$, as compared to control ADMSCs; $^{\S}p < 0.05$, as compared to control DPMSCs. $^{\#}p < 0.05$, as compared to control UCMSCs.

transport, angiogenesis, and chondrogenesis [11, 13, 24]. To confirm the hypoxic condition induced by $CoCl_2$, the presence of HIF-1α protein was evaluated. Results showed a time-dependent upregulation of HIF-1α, in the DPMSCs and UCMSCs, compared to untreated control, while no increase of expression of HIF-1α was detected in the ADMSCs, compared to control sample. Therefore, $CoCl_2$ successfully mimicked the hypoxic condition in DPMSCs and UCMSCs but failed in inducing hypoxic microenvironment in ADMSCs. Our data are in agreement with previous results on murine bone marrow mesenchymal stem cells [21], human periodontal ligament MSCs [26], and DPMSCs [25] where the hypoxic induction by $CoCl_2$ triggered the HIF-1α pathway.

The influence of hypoxia, induced by $CoCl_2$, was subsequently investigated on the chondrogenic potential of DPMSCs, UCMSCs, and ADMSCs. The cell previously treated with $CoCl_2$ for 48 h and then induced to chondrogenic differentiation up to 28 days showed different results regarding the mRNA expression of the chondrogenic markers analyzed. In the DPMSCs, while the transcription factor SOX9 and VCAN had an increase of expression, there was no expression of COL2A1 and ACAN. These findings

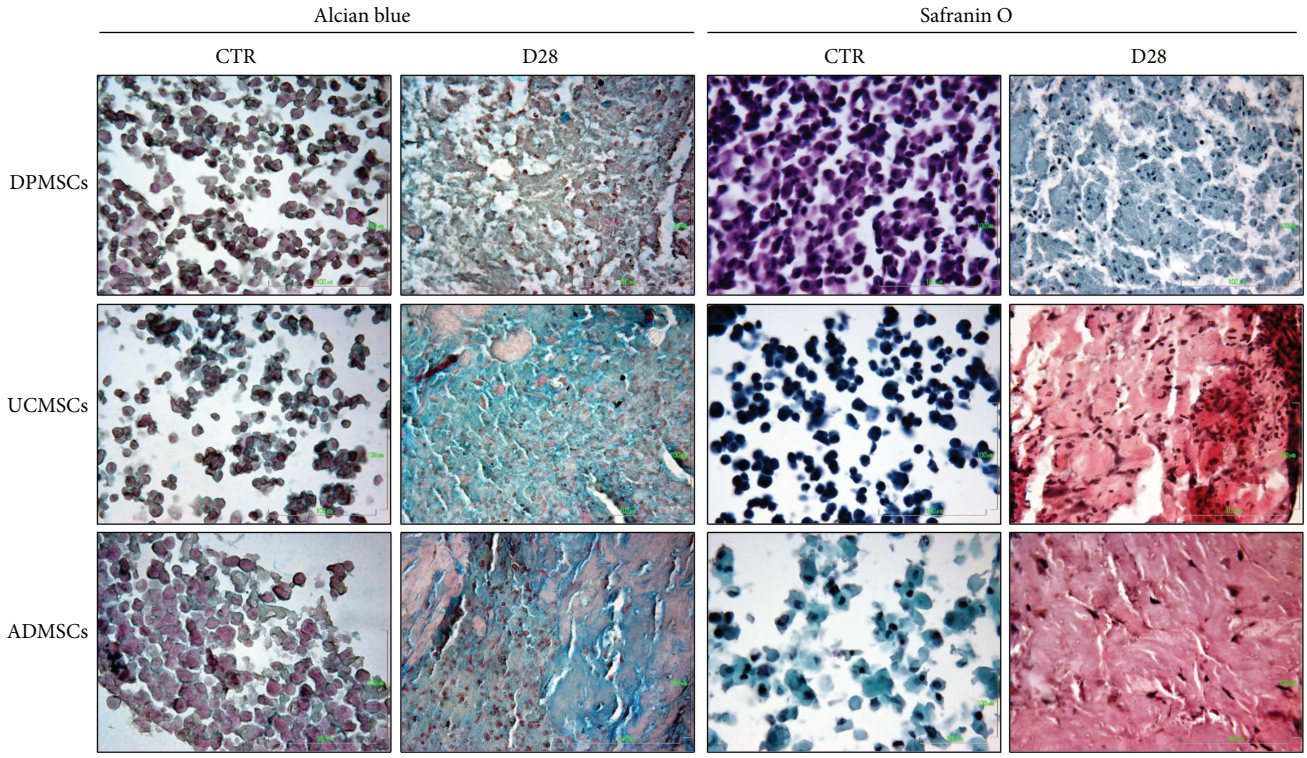

Figure 5: Alcian blue and safranin O staining on MSC micromasses, previously treated with 100 μM $CoCl_2$ and subsequently stimulated to chondrogenic differentiation up to 28 days. The images are representative of three different experiments (magnification 400x; bar: 100 μM).

suggest an inhibitory effect of hypoxia, on chondrogenic differentiation, in agreement with previous data on human periodontal ligament MSCs and human DPMSCs in which hypoxia induced by $CoCl_2$ exposition inhibited osteogenic differentiation and enhanced the upregulation of the stem cell markers REX1 and OCT4, responsible for maintaining stemness [26].

Similar results were obtained in the ADMSCs, in which hypoxia induced by $CoCl_2$ treatment induced a weak chondrogenic induction, as expected due to the lack of upregulation of HIF-1α protein observed by western blot. Few studies investigated the impact of hypoxia on differentiation of the ADMSCs yielded inconsistent and contrasting results [28]. It was found that oxygen tension at 2–5% significantly affected the differentiation capacity of ADMSCs, while oxygen tension at 1 and 1.5% maintained adipogenic, osteogenic, and chondrogenic differentiation [29]. Fotia and colleagues [29] reported that hypoxia enhances ADMSC proliferation and maintains the multipotency status, allowing the differentiation in specific lineages in the presence of proper factors. However, they demonstrated chondrogenic differentiation by alcian blue staining without any quantitative data on the mRNA expression of the chondrogenic markers. Other studies have demonstrated that low oxygen tension increased the ADMSC stemness marker expression and proliferation rate without altering their morphology and surface markers [30, 31]. Low oxygen tension further enhances the chondrogenic differentiation ability but reduces both adipogenic and osteogenic differentiation potential [32–34]. On the contrary, Pilgaard and colleagues [34] demonstrated that hypoxic pretreatment did not exhibit an enhanced chondrogenic differentiation in human ADMSCs, in agreement with our results. We hypothesize that higher concentration of $CoCl_2$ or a longer duration of $CoCl_2$ supplementation might be required to induce hypoxic effect on ADMSCs.

In our study, the UCMSCs demonstrated the best chondrogenic phenotype after a hypoxic pretreatment and chondrogenic induction up to 28 days. All the chondrogenic markers showed an upregulation of their expression compared to untreated control samples, supported by alcian blue and safranin O stainings, and a high expression of the transcription factor HIF-1α, responsible for the upregulation of the downstream chondrogenic genes. Previous studies demonstrated that chemical hypoxia, induced by 100 μM $CoCl_2$, induced proliferation and mitochondrial protection and did not alter the differentiation capacity of the human UCMSCs [35]. Reppel and colleagues [36] reported an increase in chondrogenic differentiation when Wharton's jelly-derived human MSCs were expanded under hypoxia, in agreement with our results.

5. Conclusion

Our data demonstrated that the effect of hypoxia on chondrogenic differentiation of MSCs was dependent on cell source. The UCMSCs are more prone to chondrogenic differentiation and to nonhypertrophic chondrogenesis, compared to the DPMSCs and ADMSCs, and these features could be correlated to the nature of the donor tissue and the different hypoxic environment of the umbilical cord compared to the

adipose tissue and dental pulp [37–39]. These findings should be taken in great consideration in the choice of stem cells for prospective regenerative strategies.

Conflicts of Interest

The authors declare that they have no conflicts of interest.

References

[1] Y. Wang, M. Yuan, Q. Y. Guo, S. B. Lu, and J. Peng, "Mesenchymal stem cells for treating articular cartilage defects and osteoarthritis," *Cell Transplantation*, vol. 24, no. 9, pp. 1661–1678, 2015.

[2] T. D. Bornes, A. B. Adesida, and N. M. Jomha, "Mesenchymal stem cells in the treatment of traumatic articular cartilage defects: a comprehensive review," *Arthritis Research & Therapy*, vol. 16, no. 5, p. 432, 2014.

[3] A. Polymeri, W. V. Giannobile, and D. Kaigler, "Bone marrow stromal stem cells in tissue engineering and regenerative medicine," *Hormone and Metabolic Research*, vol. 48, no. 11, pp. 700–713, 2016.

[4] Y. Z. Huang, H. Q. Xie, A. Silini et al., "Mesenchymal stem/progenitor cells derived from articular cartilage, synovial membrane and synovial fluid for cartilage regeneration: current status and future perspectives," *Stem Cell Reviews and Reports*, vol. 13, no. 5, pp. 575–586, 2017.

[5] B. Bunnell, M. Flaat, C. Gagliardi, B. Patel, and C. Ripoll, "Adipose-derived stem cells: isolation, expansion and differentiation," *Methods*, vol. 45, no. 2, pp. 115–120, 2008.

[6] S. Focaroli, G. Teti, V. Salvatore, I. Orienti, and M. Falconi, "Calcium/cobalt alginate beads as functional scaffolds for cartilage tissue engineering," *Stem Cells International*, vol. 2016, Article ID 2030478, 12 pages, 2016.

[7] C. Ferretti and M. Mattioli-Belmonte, "Periosteum derived stem cells for regenerative medicine proposals: boosting current knowledge," *World Journal of Stem Cells*, vol. 6, no. 3, pp. 266–277, 2014.

[8] M. Mattioli-Belmonte, G. Teti, V. Salvatore et al., "Stem cell origin differently affects bone tissue engineering strategies," *Frontiers in Physiology*, vol. 6, p. 266, 2015.

[9] G. Teti, V. Salvatore, S. Focaroli et al., "*In vitro* osteogenic and odontogenic differentiation of human dental pulp stem cells seeded on carboxymethyl cellulose-hydroxyapatite hybrid hydrogel," *Frontiers in Physiology*, vol. 6, p. 297, 2015.

[10] A. K. Batsali, M.-C. Kastrinaki, H. A. Papadaki, and C. Pontikoglou, "Mesenchymal stem cells derived from Wharton's jelly of the umbilical cord: biological properties and emerging clinical applications," *Current Stem Cell Research & Therapy*, vol. 8, no. 2, pp. 144–155, 2013.

[11] L. B. Buravkova, E. R. Andreeva, V. Gogvadze, and B. Zhivotovsky, "Mesenchymal stem cells and hypoxia: where are we?," *Mitochondrion*, vol. 19, Part A, pp. 105–112, 2014.

[12] L. B. Buravkova, E. R. Andreeva, and A. I. Grigor'ev, "The impact of oxygen tension in physiological regulation of human multipotent mesenchymal stromal cell functions," *Fiziologiia Cheloveka*, vol. 38, no. 4, pp. 121–130, 2012.

[13] G. L. Wang and G. L. Semenza, "General involvement of hypoxia-inducible factor 1 in transcriptional response to hypoxia," *Proceedings of the National Academy of Sciences of the United States of America*, vol. 90, no. 9, pp. 4304–4308, 1993.

[14] M. Eskandani, S. Vandghanooni, J. Barar, H. Nazemiyeh, and Y. Omidi, "Cell physiology regulation by hypoxia inducible factor-1: targeting oxygen-related nanomachineries of hypoxic cells," *International Journal of Biological Macromolecules*, vol. 99, pp. 46–62, 2017.

[15] J. M. Gleadle and P. J. Ratcliffe, "Hypoxia and the regulation of gene expression," *Molecular Medicine Today*, vol. 4, no. 3, pp. 122–129, 1998.

[16] H. M. Sowter, R. R. Raval, J. W. Moore, P. J. Ratcliffe, and A. L. Harris, "Predominant role of hypoxia-inducible transcription factor (Hif)-1α versus Hif-2α in regulation of the transcriptional response to hypoxia," *Cancer Research*, vol. 63, no. 19, pp. 6130–6134, 2003.

[17] M. Hirsilä, P. Koivunen, L. Xu, T. Seeley, K. I. Kivirikko, and J. Myllyharju, "Effect of desferrioxamine and metals on the hydroxylases in the oxygen sensing pathway," *The FASEB Journal*, vol. 19, no. 10, pp. 1308–1310, 2005.

[18] J. Shang, H. Liu, J. Li, and Y. Zhou, "Roles of hypoxia during the chondrogenic differentiation of mesenchymal stem cells," *Current Stem Cell Research & Therapy*, vol. 9, no. 2, pp. 141–147, 2014.

[19] A. B. Adesida, A. Mulet-Sierra, and N. M. Jomha, "Hypoxia mediated isolation and expansion enhances the chondrogenic capacity of bone marrow mesenchymal stromal cells," *Stem Cell Research & Therapy*, vol. 3, no. 2, p. 9, 2012.

[20] M. Ejtehadifar, K. Shamsasenjan, A. Movassaghpour et al., "The effect of hypoxia on mesenchymal stem cell biology," *Advanced Pharmaceutical Bulletin*, vol. 5, no. 2, pp. 141–149, 2015.

[21] H. I. Yoo, Y. H. Moon, and M. S. Kim, "Effects of $CoCl_2$ on multi-lineage differentiation of C3H/10T1/2 mesenchymal stem cells," *The Korean Journal of Physiology & Pharmacology*, vol. 20, no. 1, pp. 53–62, 2016.

[22] Y. Huang, K. M. Du, Z. H. Xue et al., "Cobalt chloride and low oxygen tension trigger differentiation of acute myeloid leukemic cells: possible mediation of hypoxia-inducible factor-1α," *Leukemia*, vol. 17, no. 11, pp. 2065–2073, 2003.

[23] S. Durante, G. Teti, V. Salvatore et al., "Matricellular protein expression and cell ultrastructure as parameters to test in vitro cytotoxicity of a biomimetic scaffold," *Journal of Cytology & Histology*, vol. 5, no. 5, 2014.

[24] M. Pei, "Environmental preconditioning rejuvenates adult stem cells' proliferation and chondrogenic potential," *Biomaterials*, vol. 117, pp. 10–23, 2017.

[25] K. Laksana, S. Sooampon, P. Pavasant, and W. Sriarj, "Cobalt chloride enhances the stemness of human dental pulp cells," *Journal of Endodontics*, vol. 43, no. 5, pp. 760–765, 2017.

[26] T. Osathanon, P. Vivatbutsiri, W. Sukarawan, W. Sriarj, P. Pavasant, and S. Sooampon, "Cobalt chloride supplementation induces stem-cell marker expression and inhibits osteoblastic differentiation in human periodontal ligament cells," *Archives of Oral Biology*, vol. 60, no. 1, pp. 29–36, 2015.

[27] H.-L. Zeng, Q. Zhong, Y.-L. Qin et al., "Hypoxia-mimetic agents inhibit proliferation and alter the morphology of human umbilical cord-derived mesenchymal stem cells," *BMC Cell Biology*, vol. 12, no. 1, p. 32, 2011.

[28] J. R. Choi, K. W. Yong, and W. K. Z. Wan Safwani, "Effect of hypoxia on human adipose-derived mesenchymal stem cells and its potential clinical applications," *Cellular and Molecular Life Sciences*, vol. 74, no. 14, pp. 2587–2600, 2017.

[29] C. Fotia, A. Massa, F. Boriani, N. Baldini, and D. Granchi, "Hypoxia enhances proliferation and stemness of human adipose-derived mesenchymal stem cells," *Cytotechnology*, vol. 67, no. 6, pp. 1073–1084, 2015.

[30] J. R. Choi, B. Pingguan-Murphy, W. A. B. W. Abas et al., "In situ normoxia enhances survival and proliferation rate of human adipose tissue-derived stromal cells without increasing the risk of tumourigenesis," *PLoS One*, vol. 10, no. 1, article e0115034, 2015.

[31] W. K. Z. W. Safwani, J. R. Choi, K. W. Yong, I. Ting, N. A. M. Adenan, and B. Pingguan-Murphy, "Hypoxia enhances the viability, growth and chondrogenic potential of cryopreserved human adipose-derived stem cells," *Cryobiology*, vol. 75, pp. 91–99, 2017.

[32] J. R. Choi, B. Pingguan-Murphy, W. A. B. W. Abas et al., "Impact of low oxygen tension on stemness, proliferation and differentiation potential of human adipose-derived stem cells," *Biochemical and Biophysical Research Communications*, vol. 448, no. 2, pp. 218–224, 2014.

[33] S. Portron, C. Merceron, O. Gauthier et al., "Effects of in vitro low oxygen tension preconditioning of adipose stromal cells on their in vivo chondrogenic potential: application in cartilage tissue repair," *PLoS One*, vol. 8, no. 4, article e62368, 2013.

[34] L. Pilgaard, P. Lund, M. Duroux et al., "Transcriptional signature of human adipose tissue-derived stem cells (hASCs) preconditioned for chondrogenesis in hypoxic conditions," *Experimental Cell Research*, vol. 315, no. 11, pp. 1937–1952, 2009.

[35] L. Zhang, J. Yang, Y. M. Tian, H. Guo, and Y. Zhang, "Beneficial effects of hypoxic preconditioning on human umbilical cord mesenchymal stem cells," *Chinese Journal of Physiology*, vol. 58, no. 5, pp. 343–353, 2015.

[36] L. Reppel, T. Margossian, L. Yaghi et al., "Hypoxic culture conditions for mesenchymal stromal/stem cells from Wharton's jelly: a critical parameter to consider in a therapeutic context," *Current Stem Cell Research & Therapy*, vol. 9, no. 4, pp. 306–318, 2014.

[37] S. M. Richardson, G. Kalamegam, P. N. Pushparaj et al., "Mesenchymal stem cells in regenerative medicine: focus on articular cartilage and intervertebral disc regeneration," *Methods*, vol. 99, pp. 69–80, 2016.

[38] U. Nekanti, S. Dastidar, P. Venugopal, S. Totey, and M. Ta, "Increased proliferation and analysis of differential gene expression in human Wharton's jelly-derived mesenchymal stromal cells under hypoxia," *International Journal of Biological Sciences*, vol. 6, no. 5, pp. 499–512, 2010.

[39] B. Dionigi, A. Ahmed, E. C. Pennington, D. Zurakowski, and D. O. Fauza, "A comparative analysis of human mesenchymal stem cell response to hypoxia *in vitro*: implications to translational strategies," *Journal of Pediatric Surgery*, vol. 49, no. 6, pp. 915–918, 2014.

Hindawi
Stem Cells International
Volume 2018, Article ID 3217895, 11 pages
https://doi.org/10.1155/2018/3217895

Research Article

Link Protein N-Terminal Peptide as a Potential Stimulating Factor for Stem Cell-Based Cartilage Regeneration

Ruijun He,[1] **Baichuan Wang**,[1] **Min Cui**,[1] **Zekang Xiong**,[1] **Hui Lin**,[1] **Lei Zhao**,[1] **Zhiliang Li**,[1] **Zhe Wang**,[1] **Shaun Peggrem**,[2] **Zhidao Xia**,[2] **and Zengwu Shao**[1]

[1]*Department of Orthopaedics, Union Hospital, Tongji Medical College, Huazhong University of Science and Technology, Wuhan 430022, China*
[2]*Centre for NanoHealth, College of Medicine, Swansea University, Singleton Park, Swansea SA2 8PP, UK*

Correspondence should be addressed to Baichuan Wang; wangbaichuan-112@163.com and Zengwu Shao; szwpro@163.com

Received 18 October 2017; Accepted 13 December 2017; Published 30 January 2018

Academic Editor: Shiwu Dong

Background. Link protein N-terminal peptide (LPP) in extracellular matrix (ECM) of cartilage could induce synthesis of proteoglycans and collagen type II in cartilaginous cells. Cartilage stem/progenitor cells (CSPCs), the endogenous stem cells in cartilage, are important in cartilage degeneration and regeneration. We hypothesized that LPP could be a stimulator for stem cell-based cartilage regeneration by affecting biological behaviors of CSPC. *Methods*. CSPCs were isolated from rat knee cartilage. We evaluated the promoting effect of LPP on proliferation, migration, and chondrogenic differentiation of CSPCs. The chondrogenic differentiation-related genes and proteins were quantitated. Three-dimensional culture of CSPC was conducted in the presence of TGF-β3 or LPP, and the harvested pellets were analyzed to assess the function of LPP on cartilage regeneration. *Results*. LPP stimulated the proliferation of CSPC and accelerated the site-directional migration. Higher expression of SOX9, collagen II, and aggrecan were demonstrated in CSPCs treated with LPP. The pellets treated with LPP showed more distinct characteristics of chondroid differentiation than those with TGF-β3. *Conclusion*. LPP showed application prospect in cartilage regeneration medicine by stimulating proliferation, migration, and chondrogenic differentiation of cartilage stem/progenitor cells.

1. Introduction

Articular cartilage is insufficient with intrinsic repairing ability because of its avascular and nerveless structure. Either sizable trauma or accumulated injury can impair articular cartilage, leading to degeneration diseases that cause symptoms and impact living quality [1].

For more efficient repair of the cartilage, the regenerative medicine provides a variety of trials. While the ability in forming autologous cartilage is the gold standard for seed cells in the cartilage tissue engineering, cartilage stem/progenitor cell (CSPC), a subpopulation located in both normal and degenerated human joints [2–4], inspired high hopes for its in situ repairing potency. It participates in the maintenance of homeostasis in the process of cartilage degeneration [5] and meets the requirement of seed cells for cartilage regeneration.

Intra-articular injection of growth factor is thought to be useful in cartilage repair. Bone morphogenetic proteins (BMPs) [6], transforming growth factor-β3 (TGF-β3) [7], insulin-like growth factor-1 (IGF-1) [8], and so on have been investigated in previous researches. But these growth factors have also shown osteoinductive activity on cartilage tissue [9, 10], which is harmful for long-term effect. As the most common growth factor applied in cartilage tissue engineering, TGF-β3 has a short half-life, which results in a dilemma that when it existed in the joint for too long, TGF-β3 would enhance inflammation [9], but a short-term application may not be sufficient for cartilage regeneration. The potential oncogenicity is also a disadvantage for the clinical application of TGF-β3 [11]. Link protein, a glycoprotein that exists in human intervertebral discs as well as in the articular cartilage [12], plays an important role in strengthening the binding between aggrecan and hyaluronan [13]. Link

protein N-terminal peptide (LPP) is the cleaved N-terminal 16 amino peptide (DHLSDNYTLDHDRAIH) of link protein. LPP was thought to be the functional fragment of link protein as the cross-linker [14, 15]. Both native and biochemistry-synthesized form of LPP have an effect on promoting the production of collagen type II and proteoglycans in human intervertebral disc [16] and other cartilaginous cells in vitro [17, 18], which make it an alternative for cartilage regeneration medicine.

In this study, we focused on the effects of LPP on proliferation, migration, and chondrogenic differentiation of rat cartilage stem/progenitor cells to see if LPP can act as a stimulating factor for the CSPC-based cartilage regeneration.

2. Materials and Methods

2.1. Peptide Synthesis. Peptide LPP (DHLSDNYTLDHDRAIH) representing the consensus sequence of human N-terminal link protein was synthesized following the standard solid phase peptide synthesis method by Zhejiang ONTORES Biotechnologies Co. Ltd (Hangzhou, China). The peptide was characterized by electrospray ionization mass spectroscopy and the purity was higher than 92%. The quality report was shown in Supplementary 1.

2.2. Isolation and Culture of CSPCs. All animal studies were conducted in accordance with approved protocols of the Huazhong University of Science and Technology animal experimentation committee. Cells were collected from surface cartilage of female Sprague-Dawley rats (aged 8 weeks, 200 g~250 g) after 8 hours of digestion with 0.25% type II collagenase at 37°C and filtration with a 150 μm strainer. Then, the cells were resuspended in DMEM/F12 (HyClone, USA) and diluted to a density of 4000 mL^{-1}. CSPCs were isolated through a fibronectin adhesion assay as described previously [2, 19]. Briefly, 10 cm dishes were coated with 10 μg/mL fibronectin (Sigma, UK) in 0.1 M phosphate-buffered saline (PBS) containing 1 mM $MgCl_2$ and 1 mM $CaCl_2$ (PBS+) overnight at 4°C. 2 × 10^4 cells were seeded onto the coated plates for 10 min adhesion at 37°C. Then, medium and nonadherent cells were removed. Low glucose DMEM/F12 (HyClone, USA) containing 10% fetal bovine serum (FBS) and 1% penicillin/streptomycin, the complete culture medium, was added into the dishes and renewed every other day for further culture. When it reached 80%~90% confluence, cells were digested by 0.25% trypsin plus 0.02% EDTA (Gibco, USA) for analysis or expanding culture.

2.3. Flow Cytometry. Passage 1 of cartilage stem/progenitor cells that resuspended in PBS at a concentration of 1.0×10^6 mL^{-1} were aliquoted into 200 μL in test tubes (BD352052, USA) and centrifuged at 1500 rpm, 5 minutes to remove the trypsin and EDTA. The resulting cells were incubated with a solution of antibody CD90, CD73, CD105, CD44, CD34, or HLA-DR at 37°C for 30 min. Besides, another sample was resuspended with PBS and set as calibration. The labeled cells were rinsed and then marked by secondary antibodies at 37°C for 15 minutes. The information of antibodies used in this study was shown. Cells were washed twice and resuspended in 200 μL FACS-Buffer prior to their flow cytometry analyses with FACS Calibur (Becton Dickinson and Company, USA). The information on antibodies is shown in Table 1.

Table 1: Anti-rat antibodies used in flow cytometry analysis.

Antibodies	Code number
Primary antibody	
CD90	Abcam, ab3105
CD73	BD, 551123
CD105	Abcam, ab11414
CD34	Abcam, ab81289
HLA-DR	Abcam, ab92511
Secondary antibody	
Alexa Fluor® 488	Abcam, ab150113
Alexa Fluor 647	Abcam, ab150075

2.4. Multilineage Differentiation Potential Assay. CSPCs were seeded onto 24-well plates at a concentration of 2 × 10^4 per well. For osteogenic differentiation, when the cells reached 80%~90% confluence, the culture media was replaced by 0.5 mL osteogenic differentiation induction medium (Cyagen Biosciences Inc., USA) containing 10% FBS, 10 nM dexamethasone, 10 mM β-glycerophosphate, and 0.1 mM L-ascorbic acid-2-phosphate. Induction medium was replaced each other day. After four weeks, the cells were rinsed and fixed by 4% formaldehyde. Alizarin red staining was performed following the instruction of the manufacturer.

For adipogenic differentiation, medium was changed into adipogenic differential medium A (purchased from Cyagen Biosciences Inc., USA) for induction when the cultures reached full confluence. Three days later, adipogenic differential media B (Cyagen Biosciences Inc., USA) was used for 24-hour maintaining. Four cycles later, cells were incubated with adipogenic differential media B for 6 more days. Oil Red O (Beyotime, China) staining was used for lipid detecting, which would show lipid droplets in reddish-brown.

2.5. Cytotoxicity and Proliferation Assay of LPP. Cell Counting Kit-8 (Dojindo, Japan) assay was performed in 96-well plates with different CSPC seeding density to decide optimal protocols for the following experiments. For cytotoxicity test, CSPCs were seeded on 96-well plate at a density of 1 × 10^4 per well and incubated in 10% FBS culture medium overnight. After adhesion, cells were then treated with various concentrations of LPP in serum-free medium. For proliferation assay, however, 1 × 10^3 cells were seeded into each well and cultured in 10% FBS medium containing LPP. In both experiments, medium was changed every other day. Cell Counting Kit-8 assays were performed at 1st, 3rd, and 5th day after the cell seeding.

2.6. Scratch Assay. CSPCs were seeded onto six-well plates and cultured to a confluent monolayer. After making a

"scratch" in the middle of cell layer with a 200 μL pipette tip, the cultures were rinsed gently with PBS to discard debris. The cells were cultivated in serum-free medium with or without LPP for 48 hours. Migration was documented by phase contrast microscopy and the photos were analyzed with a computer program.

2.7. Chemotaxis Tests. Effect of LPP as chemokine was analyzed via a 24-well microchemotaxis chamber (Corning, USA) with 8 μm-pore polycarbonate filters. LPP was added into the lower compartment of the chemotaxis chamber at a concentration of 10 ng/mL or 100 ng/mL in serum-free medium. In another group, medium was supplemented with 10 ng/mL TGF-β3 (PeproTech Inc., USA) to provide comparison. DMEM/F12 in the lower well served as a negative control (basal migration) for each experiment. The upper chambers were loaded with 100 μL cell suspension ($2 \times 10\text{^}4$ cells) and incubated at 37°C, 5% CO2 in 95% humidity. After 24 hours, the filters were taken out and washed gently with PBS. The nonmigrated cells on the upper chamber were removed by cotton swabs. Those on the lower side, which were regarded as migrated cells, were fixed with 4% formaldehyde and stained with crystal violet. The number of migrated cells were counted under an inverted microscope.

2.8. Real-Time PCR Analysis. Different concentration of LPP was added into the culture medium for 7 days of incubation. Total RNA in different groups was extracted with TRIzol (Invitrogen, USA). The cDNA was obtained with Revert Aid Reverse Transcriptase (Fermenta, EP0442) according to manufacturer's instructions. The expression levels of chondrogenic genes (aggrecan, collagen II, and SOX9) as well as osteogenic markers (Runx2 and collagen X) were quantified. Real-time polymerase chain reactions (RT-PCRs) were performed using the ABI StepOnePlus Real-Time PCR System (Applied Biosystems, Foster City, CA) and KAPA SYBR® FAST qPCR Kit (Kapa Biosystems, USA). Relative RNA quantities were normalized to the amounts of the endogenous control gene, β-actin. The results are represented as a ratio to control group using the comparative Ct method of relative quantification. The sequences of primers used in qPCR are presented in Table 2.

2.9. Western Blot Analysis. CSPCs were treated with different concentration of LPP for 7 days. Protein from the culture medium as well as cell lysates in each group was collected after preparation with lysis buffer (RIPA Lysis Buffer, Beyotime, China) on ice. Lysate proteins were separated with SDS-PAGE and transferred to PVDF membranes following the routine mentioned before [20]. Primary antibodies against SOX9 (Abcam, USA), collagen type II (Novus Biologicals, USA), aggrecan (Novus Biologicals, USA), or β-actin (Tianjin Sungene Biotech Co., China) were applied to blots labeling at 4°C overnight. The blots were then incubated with secondary antibodies (Boster Biological Technology Co. LTD., China) for 1 h. The bands were visualized by the enhanced chemiluminescence (ECL) procedure (Amersham Biosciences, Piscataway, NJ, USA) and integrated density was quantified using Image J software.

Table 2: The primer sequences used for the amplification of CSPC cDNA.

Gene	Primer sequence	Product length
SOX9	Forward: 5′AAGAAAGACCA CCCCGATTACA3′ Reverse: 5′ GCCTTGAAGAT GGCGTTAGGA3′	122 bp
Aggrecan	Forward: 5′ATCCAGAACCT TCGCTCCAA3′ Reverse: 5′ GGGCTCGGTCA AAGTCCAGT3′	157 bp
Col2a1	Forward: 5′ ATTGCCTACCT GGACGAAGC3′ Reverse: 5′ TGATGGTCTTG CCCCACTTAC3′	160 bp
Runx2	Forward: 5′ TTCCTGTGCTCCGTGCTG3′ Reverse: 5′AAAGTGAAACT CTTGCCTCGTC3′	236 bp
Col10a1	Forward: 5′ TTTGGATAGGG CAGTGCTTCA3′ Reverse: 5′ CACCCCATCAT CAGAGTTCATT3′	239 bp
β-Actin	Forward: 5′ CGTTGACATCC GTAAAGACCTC3′ Reverse: 5′ TAGGAGCCAGG GCAGTAATCT3′	110 bp

2.10. Chondrogenic Differentiation Assay. CSPCs were aliquoted into 500 μL DMEM/F12 of $2.5 \times 10\text{^}5$ cells. Suspensions were centrifuged at 1500 rpm, 5 minutes in 15 mL tubes to form spherical pellets which were then immersed by 0.5 mL incomplete culture medium (Cyagen Biosciences Inc., USA) containing ITS (10 mg/mL insulin, 5.5 mg/mL transferrin, and 5 ng/mL selenium), 100 mg/mL gentamicin, 50 mg/mL L-ascorbic acid, 2 mM L-glutamine, 10 mM HEPES, $10\text{^}-7$ M dexamethasone, and 2% FBS. To evaluate the effect of LPP on chondrogenic differentiation of CSPC, groups were set as control (no LPP neither TGF-β3), LPP (50 ng/mL), TGF-β3 (10 ng/mL), and LPP (50 ng/mL) + TGF-β3 (10 ng/mL). During the 14 days of induction, the medium was changed every other day. Pellets were photographed for general observation and then subjected to histology and immunohistochemistry analysis after formalin fixation and paraffin embedding.

2.11. Pellet Analysis. The sections of each pellet were dewaxed with xylene, hydrated in a decreasing graded alcohol series, and then washed three times with dH_2O. Toluidine blue

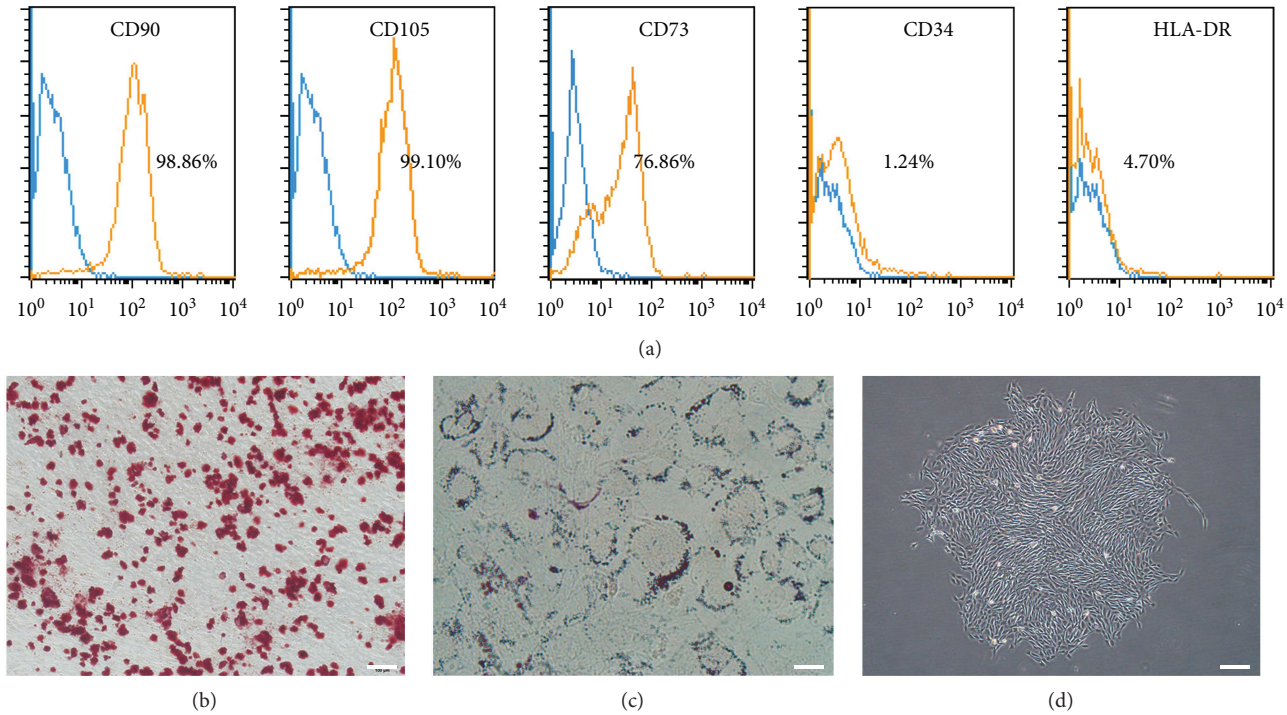

Figure 1: Identification of CSPCs. (a) Flow cytometric analysis for CSPC surface markers. Data were shown as percentage of deviation from the unlabeled groups (blue curve). (b) The alizarin red staining showed calcium nodes after osteogenic differentiation. Bar = 100 μm. (c) The Oil Red O staining showed lipid droplets after adipogenic differentiation. Bar = 20 μm. (d) Morphology of the cartilage stem/progenitor cells under an inverted microscope. Bar = 200 μm.

staining and safranin O staining were conducted for proteoglycan detection and extracellular matrix assessment following conventional methods.

For immunohistochemistry tests, antigen retrieval was conducted and the endogenous peroxidase and heterogenetic antigen were blocked by 3% H_2O_2 and 10% goat serum, respectively. Sections were incubated with antibody of collagen II (Abcam, USA) and SOX9 (Abcam, USA) at 4°C overnight. The labeled sections were submitted to Dako REALTM EnVision Detection System following the instruction of the manufacturer. The secondary antibody was set as negative control. Haematoxylin was used for nuclear staining. After coloration, sections were observed with inversion microscope.

2.12. Statistical Analysis. All data are reported as mean ± standard deviation (SD) from at least three independent technical replicates. Statistical analysis was performed using SPSS 18.0. The differences between the two groups were analyzed with Student's *t*-tests. Multiple data were analyzed by one-way analysis of variance (ANOVA) followed by the least significant difference (LSD). Statistically significant differences were considered when $p < 0.05$.

3. Results

3.1. Identification of Cartilage Stem/Progenitor Cells. The cell surface markers of CSPCs were analyzed by FACS. High levels of CD90 and CD105 (both > 90%) were detected. CD73 was also positive (>75%) while almost no expression of CD34 or HLA-DR was observed (Figure 1(a)). The multilineage differentiation potency was tested with osteogenic and adipogenic induction. Safranin O staining displayed the calcium nodes in red (Figure 1(b)) and the Oil Red staining showed lipid droplets that distributed around the edge of cytoplasm (Figure 1(c)). CSPCs grew in a fibroblast cell-like shape and were able to form colonies from one single cell, for the culture density was extremely low (Figure 1(d)). While CSPC was a subpopulation isolated from articular cartilage and represented progenitor status of chondrocytes, we thought that chondrogenic differentiation test was helpless to stem cell identification and the results were not shown. Comparing with the experiment conducted by other researchers [21, 22], we confirmed that the characteristics of these cells conform to the criteria of International Society for Cellular Therapy (ISCT) [23].

3.2. The Effect of LPP on Cell Viability of CSPCs. The growth of CSPCs which were seeded in 96-well plates in various densities was analyzed with CCK-8 assays after the 1, 2, and 3 days of culturing. Briefly, the CSPCs were grown slowly at 100, 500, and 1000 cells per well but proliferated distinctly when seeded 5000 or 10,000 cells per well. Results were shown in Fig supp 1. Therefore, we seeded 10,000 cells per well to see if LPP would impair the cell viability or suppress the proliferation for toxicity test. In order to investigate the promoting effect of LPP on the proliferation of CSPC, 1000 cells were seeded per well for the following tests. During the 5 days of culture, cell viability was not influenced by LPP (Figure 2(a)). Meanwhile, the proliferation of CSPCs

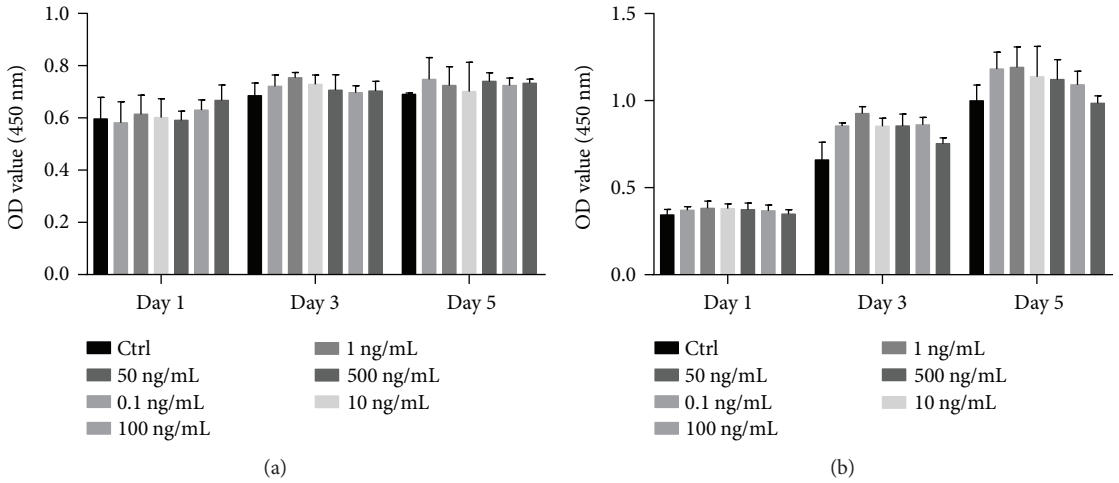

Figure 2: Toxicity tests (a) and proliferation test (b) were performed with CCK-8 kit. OD value at 450 nm was analyzed at the 1st, 3rd, and 5th days, respectively. Results were shown as means ± SD. The data of experimental groups were compared with each associated control group. $^{*}p < 0.05$; $^{**}p < 0.01$.

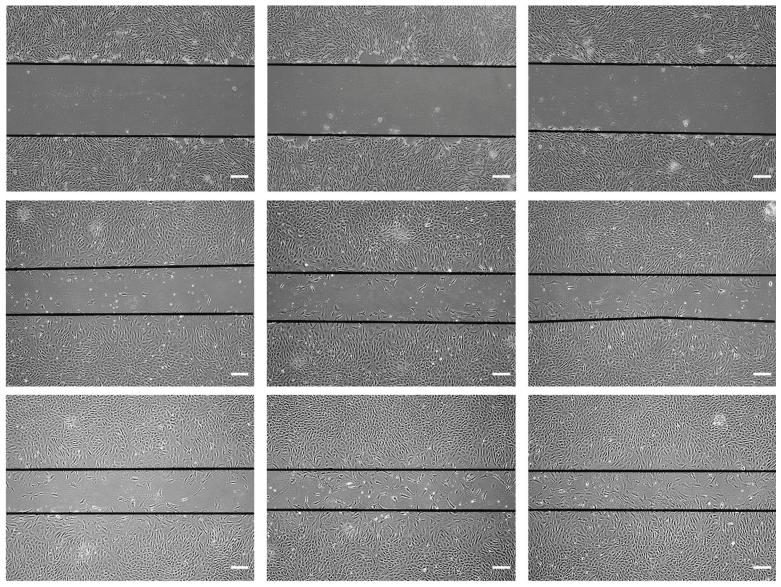

Figure 3: Scratch assays. The migration of CSPCs was documented with an inverted microscope at 0 hour, 24 hours, and 48 hours after the "scratch." The black lines indicate the baseline from which the cells migrated. Bar = 50 μm.

was promoted by LPP at a concentration of 0.1 ng/mL and 1 ng/mL in the third day, $p < 0.05$ (Figure 2(b)). The promoting effect with 0.1 ng/mL and 1 ng/mL LPP was sustained on the fifth day ($p < 0.01$), indicating that LPP accelerates the proliferation of CSPCs continuously. In the fifth day, 10 ng/mL LPP also showed a stimulation effect, $p < 0.05$. Although the OD value in the LPP groups at third day and fifth day implied an upgoing trend when compared to the control group, the *t*-tests showed no significant difference between groups of higher concentration LPP and the control.

3.3. LPP Promoted the Migration of CSPCs. Confluent CSPCs were scratched and incubated in serum-free culture medium for 48 hours. LPP was added at a concentration of 10 ng/mL and 100 ng/mL. The migration of each group at 0 hour, 24 hours, and 48 hours after scratch is depicted in Figure 3. The black lines indicate the starting line from which the cells crawled during the 48 hours of incubation. In the control group, few cells existed between the black lines. However, when the medium was supplemented with LPP, CSPCs infiltrated the gap and LPP at 100 ng/mL accelerated this process comparing to 10 ng/mL. It is notable that 48 hrs later, the scratch in 100 ng/mL LPP was almost closed with an indistinctive shrinking in the control group.

We then performed transwell test to compare site-directional chemotaxis effect of TGF-β3 and LPP. After 48 hours incubation, the chambers were taken out and cells were stained with crystal violet. The lower side of the filtration

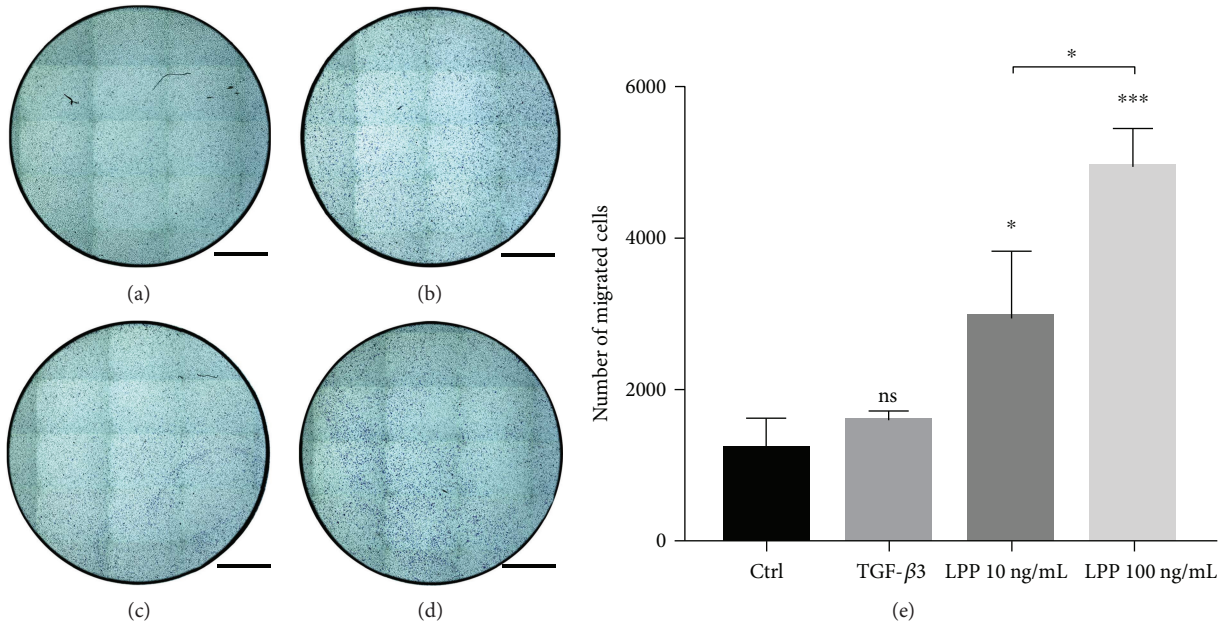

Figure 4: Transwell assay. Image synthesis was performed with EVOS™ FL Auto 2 Imaging System. (a) Control group, (b) TGF-β3, (c) LPP 10 ng/mL, and (d) LPP 100 ng/mL. Bar = 1 mm. (e) Number of migrated cells. Cells were counted with a computer program and analyzed with t-tests. $^{*}p < 0.05$; $^{***}p < 0.001$.

membrane was photographed and montaged into a panorama (Figure 4). The violet spots represent cells that crossed through the micropore, displaying a tendency of numbers of migrated cells, A < B < C < D. Numbers of migrated CSPC were calculated and analyzed with the method mentioned above, Figure 4(e). In the control group, 1219 ± 404 cells went through the filtration, while 2946 ± 882 cells in LPP (10 ng/mL) and 4931 ± 504 cells in LPP (100 ng/mL) traversed to the lower side. There were 1586 ± 129 cells in TGF-β3 group, but the difference was without significant meaning when compared to the control group, $p > 0.05$.

3.4. LPP Regulated the Expression of Chondrogenic-Related Genes and Synthesis of Matrix. To figure out if LPP can influence the chondrogenic differentiation and matrix synthesis of CSPCs, cells were treated with different concentration of LPP in monolayer culture. The qPCR tests demonstrated that the expression of SOX9, which is thought to be related with chondrogenesis, was promoted by LPP at doses of 1, 10, 50, 100, and 500 ng/mL compared to untreated cells (0 ng/mL). For aggrecan, the group of 500 ng/mL showed no significant difference while others upregulated the expression, $p < 0.001$. The mRNA ratio of collagen II was influenced by 50, 100, and 500 ng/mL LPP (Figure 5(a)). Thus, 50 ng/mL LPP was used in following experiments: fold change of SOX9 was 2.34 ± 0.15, aggrecan was 1.58 ± 0.04, and col2 was 1.32 ± 0.11. We also found that the mRNA levels of Runx2 and collagen X were not affected by LPP, indicating that LPP had no effect on osteogenic induction (Figure 5(a)). Western blot assays semiquantified the protein levels of SOX9, collagen type II, and aggrecan in cells incubated with LPP (Figure 5(b)). The integrated optical density of each banding was analyzed by setting β-actin as an internal reference (Figure 5(c)). SOX9 and aggrecan were apparently elevated by LPP, while collagen II was enhanced only in 100 and 500 ng/mL LPP.

3.5. Pellet Matrix Synthesis with LPP or TGF-β3. CSPCs were aliquoted and centrifuged to form pellets. The chondrogenic differentiation basal medium was prepared and supplemented with 50 ng/mL LPP or 10 ng/mL TGF-β3 or both. After 14 days, pellets from four groups all showed a smooth surface morphology (Figure 6(a)). The size of LPP + TGF-β3 is bigger than others and got a more spherical shape. Safranin O and toluidine blue staining of the paraffin sections of pellets demonstrated glycosaminoglycan synthesis after the induction (Figures 6(b) and 6(c)). When compared to control, the slices in LPP and LPP + TGF-β3 groups were stained in more thick jacinth in Figure 6(b), indicating stimulating effects on matrix synthesis. At the edge of pellets, the majority of aggrecan stained by toluidine blue was distributed (Figure 6(c)), and the density of CSPCs was obviously lower in TGF-β3 and LPP + TGF-β3 groups, indicating more abundant extracellular matrix synthesis (Figure 6(c)). Immunohistochemical methods were also performed to assess the synthesis and location of collagen type II (Figure 6(d)) and SOX9. Collagen II in LPP and LPP + TGF-β3 groups is more than in control. In the pellet incubated with LPP, collagen II presented in an approximately radial distribution pattern. IHC of SOX9 in Figure 6(e) showed that LPP enhanced expression of SOX9. In LPP + TGF-β3 group, however, this increase was distinctly improved when compared to TGF-β3 group, indicating that LPP have the potency of stimulating chondrogenic differentiation of CSPCs, and it can also promote the inducing effect of TGF-β3.

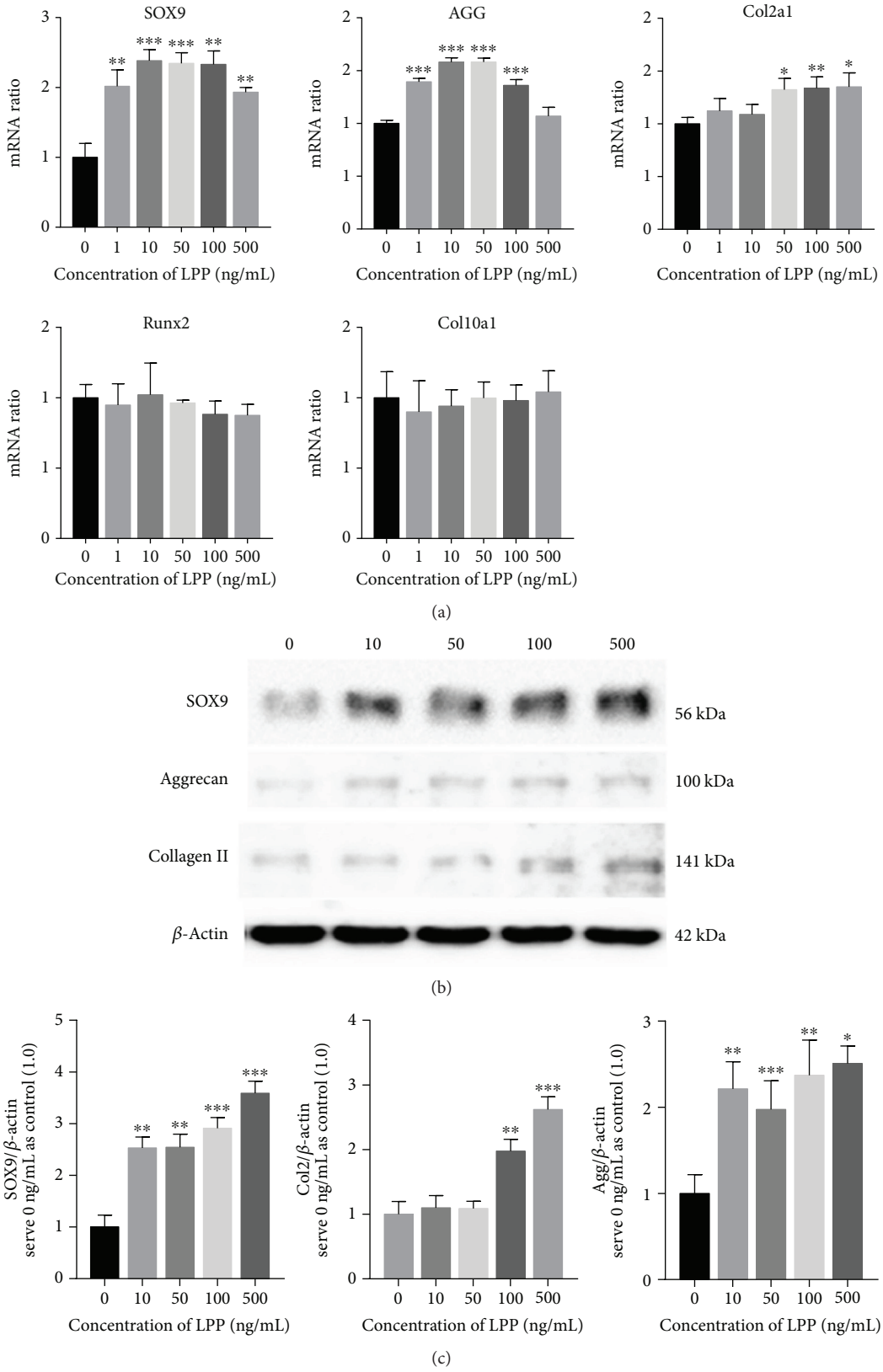

Figure 5: (a) Relative mRNA levels of SOX9, aggrecan, collagen type II, Runx2, and collagen type X in different concentration of LPP. Error bars are means ± SD. (b) Bandings of SOX9 and collagen type II represented the protein content of cells treated with different concentration of LPP. (c) Integrated density of each banding was shown in columns as means ± SD. Data of experimental groups were compared with the control group (0 ng/mL) using Student's t-test, respectively. $^{*}p < 0.05$; $^{**}p < 0.01$; $^{***}p < 0.001$.

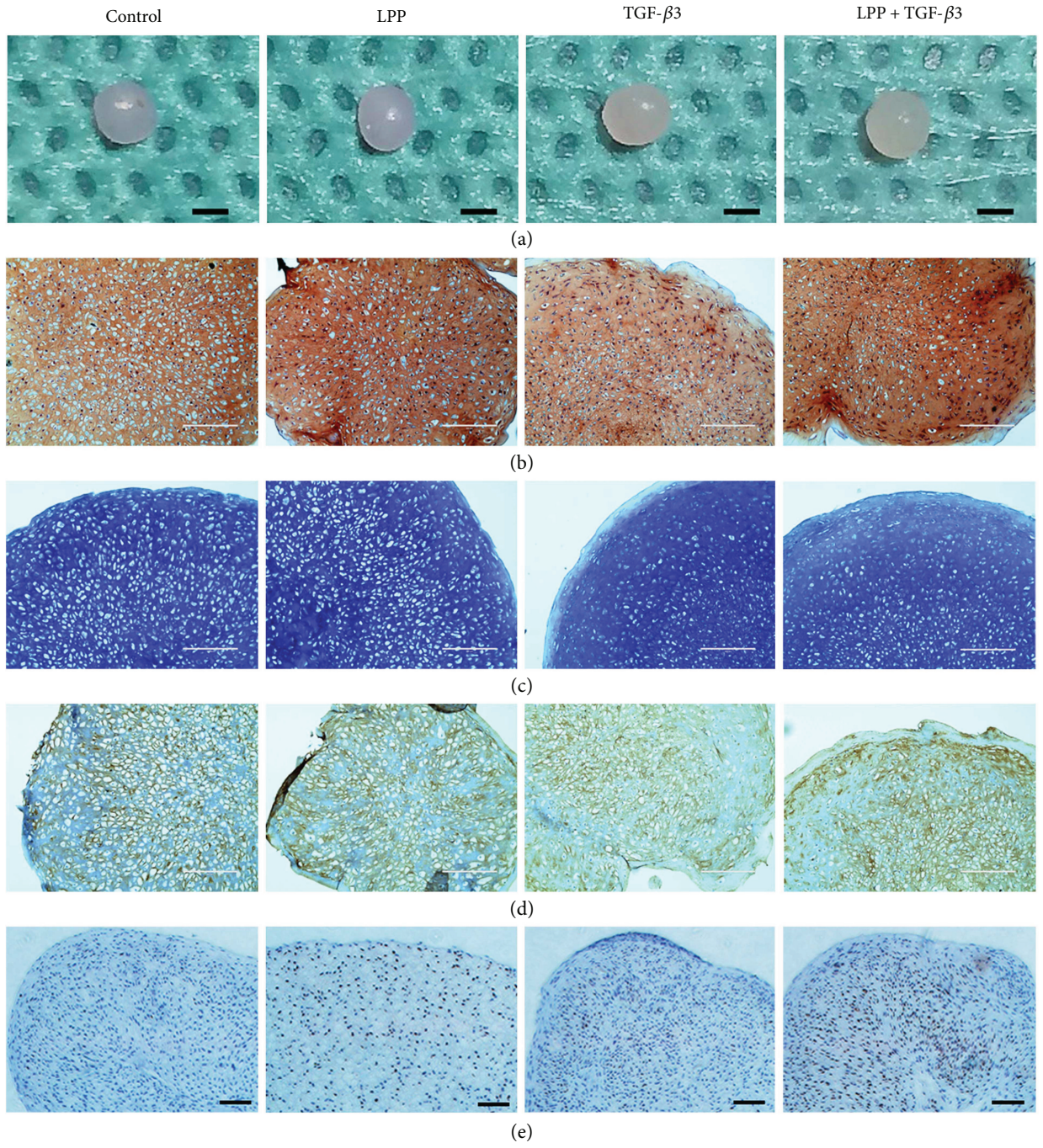

Figure 6: Pellets formed by CSPCs after 2-week chondrogenic differentiation induction. (a) General view of pellets. Bar = 1 mm. (b) Safranin O staining of sections (thickness is less than 2 μm). Bar = 200 μm. (c) Toluidine blue staining of sections. Bar = 200 μm. (d) Immunohistochemistry test of collagen type II. The collagen type II was labeled in yellow. Bar = 200 μm. (e) SOX9 was labeled in brown in IHC assays. Bar = 200 μm.

4. Discussion

CSPCs were isolated from normal and degenerative human cartilage as well as rat knee joints [24]. It was thought to participate in the renewal of chondrocytes and cartilage extracellular matrix [5, 25]. To modulate the regenerative function of CSPC, varieties of factors were tested, for instance, the fibroblast growth factor-2 (FGF-2) [26], TGF-β3, IGF [8], and BMPs [27, 28]. LPP is a peptide cleaved from link protein, which exists in cartilage, bridging the collagen type II and hyaluronic acid. It was reported that LPP promoted synthesis of collagen II and proteoglycan in nucleus pulposus cells from intervertebral discs [16, 29] and human chondrocytes [30]. However, the effect of LPP on stem cells, especially the endogenous stem cells in cartilage, remains to be illuminated. In the present study, we evaluated for the

first time the effect of LPP on biological behaviors of CSPC, which can favor the stem cell-based cartilage regeneration.

The characterization of passage 1 CSPCs isolated with differential adhesion assay was analyzed. The FACS results indicated that the surface markers of CSPC were similar to bone marrow-derived stem cells (BMSC) [31] and also in agreement with results from other researches [32]. The differentiation induction assays demonstrated the adipogenic and osteogenic potency of CSPC, similar to the results previously reported [19, 33]. Results of cell count kit-8 suggested that LPP promoted cell proliferation at a concentration of 1, 10, and 50 ng/mL. LPP also accelerated the migration of CSPC in scratch assay in 48 hours. The transwell culture showed chemotaxis effect of LPP, indicating that the directional migration of CSPC might be strengthened with higher concentration of LPP. Although TGF-β3 showed chemotaxis effect on bone marrow-derived mesenchymal stem cells [34, 35], the outcome in this experiment was the lack of statistic meaning. While cell migration is necessary for stem cell-based intrinsic repair, our study aroused a possibility that LPP could be used in bioactivity materials as a chemotactic factor to help recruitment. The expression levels of chondrogenesis genes were also promoted with LPP and the results of Western blot conformed to the qPCR, which agreed with the findings in previous researches [17, 36, 37]. LPP also showed chondrogenic induction effect on the CSPC in three-dimensional culture. During the chondrogenesis of the skeleton, the condensation of chondroprogenitor cells was vital for chondrogenic differentiation [38, 39]. The chemotaxis effect of LPP might be beneficial to the formation of cell pellet by accelerating the cell condensation, which resulted in higher histology score. Wang et al. verified that LPP upregulated the expression of SOX9 by binding to BMP-RII [29]. We speculated that cartilage stem/progenitor cells, as a transition style of skeleton stem cell during the chondrogenesis [21], had already expressed BMP-RII on the cell membrane. Besides, a hypothesis is that the BMPRII and relevant signal pathway have higher activity than TβR-II during the differentiation of CSPC, which demands further investigation.

In the present research, normal rat cartilage was obtained and the cells were isolated for function test in vitro. To figure out whether LPP can help in the recruitment or migration of CSPC in vivo, further studies were required. The difference between LPP and TGF-β3 groups in transwell assay and pellet culture requires more detailed explanation, while TGF-β3 was also thought to be a stimulating factor in cartilage tissue engineering [40].

LPP may promote the production of tissue-engineered cartilage in vitro by regulating the metabolism of CSPC, making it possible for application in transplant therapy. During the progressing process of arthritis or degeneration, LPP in cartilage is undermined by the inflammation and immunoreaction, which add up to the disbalance of ECM of cartilage [41, 42]. So, the supplement of LPP might be helpful in delaying the articular degeneration. Allowing for limits of exogenous growth factors such as TGF-β3 in the in vivo treatment of osteoarthritis, we believe that LPP would be a preferable alternation.

5. Conclusion

Collectively, LPP might be a promising stimulating factor for stem cell-based cartilage regeneration for its promoting function on migration, proliferation, and chondrogenic differentiation of cartilage stem/progenitor cell. With benefits of LPP demonstrated in this research, the CSPC-based cellular therapy gives hope to cartilage regeneration medicine, bringing a new research focus which still requires further investigation.

Conflicts of Interest

The authors declare that they have no conflicts of interests.

Authors' Contributions

Ruijun He and Baichuan Wang contributed to this research equally as the co-first authors. All listed authors made significant contributions to this manuscript through study design, data analysis, or during the process of writing and revisions. All authors have read and approved the submitted manuscript. The integrity of this work is guaranteed by Ruijun He, Baichuan Wang, and Zengwu Shao.

Acknowledgments

This study was supported by Grants 81501916 from the National Natural Science Foundation of China to Baichuan Wang and 2016YFC1100100 from the National Key Research and Development Program of China to Zengwu Shao.

Supplementary Materials

Supplementary 1. The quality report of the synthetic Link protein N-terminal peptide.

Supplementary 2. Proliferation velocity of CSPC in different density. Figure Supplement 1: the growth characteristic of CSPCs. Different numbers of CPSCs were seeded into 96-well plates and cultured in complete culture medium. OD value was detected during the 3-day culturing with CCK-8 assay.

References

[1] N. C. G. Centre, "Osteoarthritis: Care and Management in Adults," *National Institute for Health and Clinical Excellence: Clinical Guidances, No.177*, 2014.

[2] S. Alsalameh, R. Amin, T. Gemba, and M. Lotz, "Identification of mesenchymal progenitor cells in normal and osteoarthritic human articular cartilage," *Arthritis & Rheumatism*, vol. 50, no. 5, pp. 1522–1532, 2004.

[3] G. P. Dowthwaite, "The surface of articular cartilage contains a progenitor cell population," *Journal of Cell Science*, vol. 117, no. 6, pp. 889–897, 2004.

[4] S. Fickert, J. Fiedler, and R. E. Brenner, "Identification of subpopulations with characteristics of mesenchymal progenitor cells from human osteoarthritic cartilage using triple staining

for cell surface markers," *Arthritis Research & Therapy*, vol. 6, no. 5, pp. R422–R422, 2004R432, 2004.

[5] S. Koelling, J. Kruegel, M. Irmer et al., "Migratory chondrogenic progenitor cells from repair tissue during the later stages of human osteoarthritis," *Cell Stem Cell*, vol. 4, no. 4, pp. 324–335, 2009.

[6] D. Noel, D. Gazit, C. Bouquet et al., "Short-term BMP-2 expression is sufficient for in vivo osteochondral differentiation of mesenchymal stem cells," *Stem Cells*, vol. 22, no. 1, pp. 74–85, 2004.

[7] L. Bian, D. Y. Zhai, E. Tous, R. Rai, R. L. Mauck, and J. A. Burdick, "Enhanced MSC chondrogenesis following delivery of TGF-β3 from alginate microspheres within hyaluronic acid hydrogels *in vitro* and *in vivo*," *Biomaterials*, vol. 32, no. 27, pp. 6425–6434, 2011.

[8] L. O'Rear, "Signaling cross-talk between IGF-binding protein-3 and transforming growth factor-β in mesenchymal chondroprogenitor cell growth," *Journal of Molecular Endocrinology*, vol. 34, no. 3, pp. 723–737, 2005.

[9] H. M. van Beuningen, H. L. Glansbeek, P. M. van der Kraan, and W. B. van den Berg, "Osteoarthritis-like changes in the murine knee joint resulting from intra-articular transforming growth factor-β injections," *Osteoarthritis and Cartilage*, vol. 8, no. 1, pp. 25–33, 2000.

[10] H. Cheng, W. Jiang, F. M. Phillips et al., "Osteogenic activity of the fourteen types of human bone morphogenetic proteins (BMPs)," *The Journal of Bone and Joint Surgery-American Volume*, vol. 85-A, no. 8, pp. 1544–1552, 2003.

[11] D. R. Principe, J. A. Doll, J. Bauer et al., "TGF-β: duality of function between tumor prevention and carcinogenesis," *Journal of the National Cancer Institute*, vol. 106, no. 2, article djt369, 2014.

[12] Q. Nguyen, J. Liu, P. J. Roughley, and J. S. Mort, "Link protein as a monitor in situ of endogenous proteolysis in adult human articular cartilage," *Biochemical Journal*, vol. 278, no. 1, pp. 143–147, 1991.

[13] T. E. Hardingham, "The role of link-protein in the structure of cartilage proteoglycan aggregates," *Biochemical Journal*, vol. 177, no. 1, pp. 237–247, 1979.

[14] L. L. Faltz, C. B. Caputo, J. H. Kimura, J. Schrode, and V. C. Hascall, "Structure of the complex between hyaluronic acid, the hyaluronic acid-binding region, and the link protein of proteoglycan aggregates from the swarm rat chondrosarcoma," *Journal of Biological Chemistry*, vol. 254, no. 4, pp. 1381–1387, 1979.

[15] J. H. Kimura, T. E. Hardingham, and V. C. Hascall, "Assembly of newly synthesized proteoglycan and link protein into aggregates in cultures of chondrosarcoma chondrocytes," *Journal of Biological Chemistry*, vol. 255, no. 15, pp. 7134–7143, 1980.

[16] A. Petit, G. Yao, S. A. Rowas et al., "Effect of synthetic link N peptide on the expression of type I and type II collagens in human intervertebral disc cells," *Tissue Engineering Part A*, vol. 17, no. 7-8, pp. 899–904, 2011.

[17] L. A. McKenna, H. Liu, P. A. Sansom, and M. F. Dean, "An N-terminal peptide from link protein stimulates proteoglycan biosynthesis in human articular cartilage in vitro," *Arthritis & Rheumatism*, vol. 41, no. 1, pp. 157–162, 1998.

[18] H. Liu, L. A. McKenna, and M. F. Dean, "The macromolecular characteristics of cartilage proteoglycans do not change when synthesis is up-regulated by link protein peptide," *Biochimica et Biophysica Acta (BBA) - General Subjects*, vol. 1428, no. 2-3, pp. 191–200, 1999.

[19] R. Williams, I. M. Khan, K. Richardson et al., "Identification and clonal characterisation of a progenitor cell subpopulation in normal human articular cartilage," *PLoS One*, vol. 5, no. 10, pp. e13246–e13246, 2010.

[20] H. Lin, L. Zhao, X. Ma et al., "Drp1 mediates compression-induced programmed necrosis of rat nucleus pulposus cells by promoting mitochondrial translocation of p53 and nuclear translocation of AIF," *Biochemical and Biophysical Research Communications*, vol. 487, no. 1, pp. 181–188, 2017.

[21] Y. Jiang and R. S. Tuan, "Origin and function of cartilage stem/progenitor cells in osteoarthritis," *Nature Reviews Rheumatology*, vol. 11, no. 4, pp. 206–212, 2015.

[22] K. Xue, X. Zhang, L. Qi, J. Zhou, and K. Liu, "Isolation, identification, and comparison of cartilage stem progenitor/cells from auricular cartilage and perichondrium," *American Journal of Translational Research*, vol. 8, no. 2, pp. 732–741, 2016.

[23] M. Dominici, K. Le Blanc, I. Mueller et al., "Minimal criteria for defining multipotent mesenchymal stromal cells. The International Society for Cellular Therapy position statement," *Cytotherapy*, vol. 8, no. 4, pp. 315–317, 2006.

[24] M. Kim, J. Kim, S. R. Park et al., "Comparison of fetal cartilage-derived progenitor cells isolated at different developmental stages in a rat model," *Development, Growth & Differentiation*, vol. 58, no. 2, pp. 167–179, 2016.

[25] D. Seol, D. J. McCabe, H. Choe et al., "Chondrogenic progenitor cells respond to cartilage injury," *Arthritis & Rheumatism*, vol. 64, no. 11, pp. 3626–3637, 2012.

[26] M. Bianchessi, Y. Chen, S. Durgam, H. Pondenis, and M. Stewart, "Effect of fibroblast growth factor 2 on equine synovial fluid chondroprogenitor expansion and Chondrogenesis," *Stem Cells International*, vol. 2016, Article ID 9364974, 11 pages, 2016.

[27] C.-H. Lu, T.-S. Yeh, C.-L. Yeh et al., "Regenerating cartilages by engineered ASCs: prolonged TGF-β3/BMP-6 expression improved articular cartilage formation and restored zonal structure," *Molecular Therapy*, vol. 22, no. 1, pp. 186–195, 2014.

[28] A. J. Neumann, O. F. W. Gardner, R. Williams, M. Alini, C. W. Archer, and M. J. Stoddart, "Human articular cartilage progenitor cells are responsive to mechanical stimulation and adenoviral-mediated overexpression of bone-morphogenetic protein 2," *PLoS One*, vol. 10, no. 8, article e0136229, 2015.

[29] Z. Wang, M. N. Weitzmann, S. Sangadala, W. C. Hutton, and S. T. Yoon, "Link protein N-terminal peptide binds to bone morphogenetic protein (BMP) type II receptor and drives matrix protein expression in rabbit intervertebral disc cells," *Journal of Biological Chemistry*, vol. 288, no. 39, pp. 28243–28253, 2013.

[30] H. Liu, L. A. McKenna, and M. F. Dean, "An N-terminal peptide from link protein can stimulate biosynthesis of collagen by human articular cartilage," *Archives of Biochemistry and Biophysics*, vol. 378, no. 1, pp. 116–122, 2000.

[31] H. E. McCarthy, J. J. Bara, K. Brakspear, S. K. Singhrao, and C. W. Archer, "The comparison of equine articular cartilage progenitor cells and bone marrow-derived stromal cells as potential cell sources for cartilage repair in the horse," *The Veterinary Journal*, vol. 192, no. 3, pp. 345–351, 2012.

[32] P. Bernstein, I. Sperling, D. Corbeil, U. Hempel, and S. Fickert, "Progenitor cells from cartilage—no osteoarthritis-grade-specific differences in stem cell marker expression," *Biotechnology Progress*, vol. 29, no. 1, pp. 206–212, 2013.

[33] H. Joos, A. Wildner, C. Hogrefe, H. Reichel, and R. E. Brenner, "Interleukin-1β and tumor necrosis factor α inhibit migration activity of chondrogenic progenitor cells from non-fibrillated osteoarthritic cartilage," *Arthritis Research & Therapy*, vol. 15, no. 5, pp. R119–R119, 2013.

[34] S. J. Zhang, X. Y. Song, M. He, and S. B. Yu, "Effect of TGF-β1/SDF-1/CXCR4 signal on BM-MSCs homing in rat heart of ischemia/perfusion injury," *European Review for Medical and Pharmacological Sciences*, vol. 20, no. 5, pp. 899–905, 2016.

[35] M. J. Dubon, J. Yu, S. Choi, and K.-S. Park, "Transforming growth factor β induces bone marrow mesenchymal stem cell migration via noncanonical signals and N-cadherin," *Journal of Cellular Physiology*, vol. 233, no. 1, pp. 201–213, 2017.

[36] F. Mwale, C. N. Demers, A. Petit et al., "A synthetic peptide of link protein stimulates the biosynthesis of collagens II, IX and proteoglycan by cells of the intervertebral disc," *Journal of Cellular Biochemistry*, vol. 88, no. 6, pp. 1202–1213, 2003.

[37] B. Wang, C. Sun, Z. Shao et al., "Designer self-assembling peptide nanofiber scaffolds containing link protein N-terminal peptide induce chondrogenesis of rabbit bone marrow stem cells," *BioMed Research International*, vol. 2014, Article ID 421954, 10 pages, 2014.

[38] M. B. Goldring, K. Tsuchimochi, and K. Ijiri, "The control of chondrogenesis," *Journal of Cellular Biochemistry*, vol. 97, no. 1, pp. 33–44, 2006.

[39] M. Bhattacharjee, J. Coburn, M. Centola et al., "Tissue engineering strategies to study cartilage development, degeneration and regeneration," *Advanced Drug Delivery Reviews*, vol. 84, pp. 107–122, 2015.

[40] C. T. Jayasuriya, Y. Chen, W. Liu, and Q. Chen, "The influence of tissue microenvironment on stem cell–based cartilage repair," *Annals of the New York Academy of Sciences*, vol. 1383, no. 1, pp. 21–33, 2016.

[41] A. Guerassimov, Y. Zhang, A. Cartman et al., "Immune responses to cartilage link protein and the G1 domain of proteoglycan aggrecan in patients with osteoarthritis," *Arthritis & Rheumatism*, vol. 42, no. 3, pp. 527–533, 1999.

[42] A. Guerassimov, Y. Zhang, S. Banerjee et al., "Autoimmunity to cartilage link protein in patients with rheumatoid arthritis and ankylosing spondylitis," *The Journal of Rheumatology*, vol. 25, no. 8, pp. 1480–1484, 1998.